University of Alberta

Some proetids (Class Trilobita) from the Lower to Middle Devonian of southern Morocco

by

Stacey Gibb ©

A thesis submitted to the Faculty of Graduate Studies and Research in partial fulfillment of

the

requirements for the degree of *Master of Science*

Department of *Earth & Atmospheric Sciences*

Edmonton, Alberta
Spring 2005

Your file Votre référence
ISBN: 0-494-08058-2
Our file Notre référence
ISBN: 0-494-08058-2

ABSTRACT

Two genera of proetids (Order Proetida, Class Trilobita) are be discussed in this thesis – *Timsaloproetus* new genus and *Gerastos*. The species described here and assigned to these two genera are from the Lower to Middle Devonian of southern Morocco. Two new species are proposed for *Timsaloproetus*: *T. dibbanus* and *T. elguerrouji*. Along with the systematics, a cladistic analysis was undertaken of the *Gerastos* species found in the northern flank of the Tindouf Basin, the Ma'der Basin, and at one locality of the Tafilalt Basin. Eleven new species/subspecies of *Gerastos* are proposed (from oldest to youngest): *G. tuberculatus marocensis, G. aintawilus, G. lisanrasus, G. ainrasifus, G. discombobulates, G. cuiveri malisus, G. taqus, G. malisjildus, G. raribus, G. emmetus* and *G. izius*.

ACKNOWLEDGEMENTS

For answering my endless questions, I am very grateful to my supervisor, Brian Chatterton, who can still tolerate me and is actually still open to even more queries (or he is an incredible actor). His support has been outstanding and I do not think that I could ever ask for a better supervisor. All funding was provided by B.D.E. Chatterton's NSERC grants, which enabled the completion the field work, and the purchase and preparation of specimens.

I would like to thank the other members of my committee, Dr. S.G. Pemberton and Dr. M.V.H. Wilson, for their valuable comments and time.

A number of individuals provided me with invaluable support and encouragement: My parents, J. Duffy, R. McKellar, S. Hesse, B. Frizzell, my grandma and grandpa Bob (whom I neglected to visit during my thesis work – my apologies!), R. Allarie, C. Swindlehurst, P. Dasgupta, A. MacNeil, R. Wheeler, and G. Taylor and the Belmac Womens' Soccer team.

Hammi Ait Hssain was always more than willing to provide us with his superb knowledge of the trilobites and *couches* within southern Morocco. Without his assistance, knowledge and endless positivity, my work would not have progressed as well as it has.

The Department of Earth & Atmospheric Sciences has been supportive with teaching assistantships and office space, for which I am grateful. A number of individuals within the department have also provided support and assistance, including (in no particular order): P. Cavell, S. Gleeson, J. Waldron, G. Pemberton, M. Sharpe, M. Fisher, K. Sanderson, F. Metcalfe, K. Arndt, I. Hotchkiss, E. Tsang, and D. Caird.

I would also like to thank the Faculty of Graduate Studies and Research for their support when I needed it the most – for this I am most indebted.

To this day I do not understand how my husband, J. Bohun, could tolerate me throughout this whole endeavor, and still provide understanding, support and love. I will definitely try to train harder and stress less during my PhD!

TABLE OF CONTENTS

CHAPTER 3: SYSTEMATIC PALAEONTOLOGY II

LIST OF TABLES

CHAPTER 2

LIST OF FIGURES

CHAPTER 1

CHAPTER 2

2-4: *1-8, Timsaloproetus haasi* (Alberti, 1971). All specimens are from bou Dib *'Harpes/Thysanopeltis* horizon' (BD5), El Otfal Formation, lower Eifelian, Ma'der Basin, southern Morocco. *1, 4-6, 8*, almost complete exoskeleton UA13272. *1*, dorsal view of cephalon X16.9; *4*, lateral view X13.9; *5*, dorsal view X15.6; *6*, dorsal view of posterior of thorax and pygidium X15.7; *8*, dorsal view minus cephalon X15.4. *2*, dorsal view of almost complete cranidium UA13275 X11.8; *3*, dorsal view of fragmented cranidium UA13274 X11.2; *7*, dorsal view of pygidium UA13273 X21. 41

2-5: *1-2, 4-6, 8, 9, Timsaloproetus haasi* (Alberti, 1971); '*Harpes/Thysanopeltis* horizon', El Otfal Formation, lower Eifelian, from bou Dib, Ma'der, southern Morrocco. Almost complete articulated individual UA13256. *1*, dorsal view X7.2; *2*, dorsal view X7.2; *4*, lateral view X6.5; *5*, dorsal view of crandium X18.6; *6*, oblique dorsolateral view X6.9; *8*, dorsal view of pygidium X21.3; *9*, dorsal view of cranidium X16.3. *3, 7, 10*, ZGEE3 horizon, Timrhanrhart Formation, lower Eifelian, Zguilma, southern Morocco. Damaged articulated exoskeleton UA13269. *3*, dorsolateral oblique view of cehalon X10.3; *7*, dorsal view X5.7; *10*, dorsal view of partial pygidium X11.7. 42

2-6: *1-14, Timsaloproetus haasi* (Alberti, 1971), NZ10 horizon ('near Zguilma' section), Timrhanrhart Formation, lower Eifelian, near Foum Zguid, southern Morocco. *1, 3, 6*, cranidium UA13282. *1*, lateral view X15.4; *3*, dorsal view X22.2; *6*, anterior view X16.5. *2*, hypostome UA13283, ventral view X45.9; *4*, right free cheek UA13284, dorsal view, X25.4; *5*, right free cheek UA13285, dorsal view, X19.8; *7*, fragmented thoracic segment UA13286, ventral view X25.1; *8*, left free cheek UA13287, ventral view X23.1; *9, 11, 14,* pygidium UA 13288; *9,* lateral view X12.5; *11,* posterior view X16.6; *14*, dorsal view X16.8; *10,* fragmented hypostome UA13289, ventral view X30.5. *12,* fragmented thoracic segment UA13290, dorsal view X26.7; *13*, fragmented pygidium UA13291, dorsal view X18.3. 44

2-7: *1-12, Timsaloproetus dibbanus* new genus and species. ZGEE1 horizon, Timrhanrhart Formation, upper Emsian, from Zguilma, southern Morocco. *1-4*, cranidium UA13257: *1*, dorsal view X11.1; *2*, anterior view X10; *3*, lateral oblique view X10.5; *4*, dorsal view X11.2. *5-6, 8, 11-12*, pygidium UA13258: *5*, dorsal view X10.6; *6*, posterior view X10.1; *8*, dorsal view X10.3; *11*, lateral view X25.2; *12*, dorsolateral oblique view X21.5. *7, 9*, pygidium UA13259: *7*, posterior view X10.7; *9*, dorsal view X10.9. *10*, incomplete pygidium UA13281, dorsal view X22.8. 51

2-8: *1-7, Timsaloproetus elguerrouji* new genus and species. ZGEE3 horizon, Timrhanhart Formation, upper Emsian, from Zguilma, southern

CHAPTER 3

LIST OF APPENDICES

CHAPTER 1: INTRODUCTION

> The Devonian marked a further expansion in the importance of the Proetida, and the order became a major constituent of trilobite faunas for the first time since the early Ordovician, and along with the Phacopida dominated the Devonian trilobite faunas. Proetida presumably filled niches vacated by other trilobites declining at the end of the Silurian (Fortey and Owen, 1975).

Introduction

Morocco is located on the northwestern corner of Africa (Figure 1-1). It is an invaluable source of trilobites from the Devonian, when the region was part of the continental shelf of Gondwana. Specimens of extraordinary preservation, diversity and disparity can be collected from strata that are often continuously exposed for many kilometres along strike. As a result, it is a valuable research area from both a geological and palaeontological standpoint. Trilobites of the Order Proetida are found throughout Morocco. They have been addressed by a number of authors (e.g. Richter and Richter, 1943; 1956; Alberti, 1964; 1966; 1967a; 1967b; 1969; 1975; 1980; 1981a; 1981b; 1981c; 1982a; 1982b; 1988; H. Alberti, 1975a; 1975b; Feist and Orth, 2000;). Almost every publication, however, has dealt with disarticulated, and fragmented proetids. This thesis describes mainly complete articulated specimens collected in recent field work to provide definitive identifications and correct associations of different parts of the exoskeleton. Two genera, *Timsaloproetus* new genus, and *Gerastos*, are discussed, and the following new species/subspecies are introduced: *Timsaloproetus elguerrouji, T. dibbanus, Gerastos tuberculatus marocensis, G. aintawilus, G. lisanrasus, G. ainrasifus, G. discombobulatus, G. cuvieri malisus, G. malisjildus, G. taqus, G. raribus, G. emmetus,* and *G. izius.*

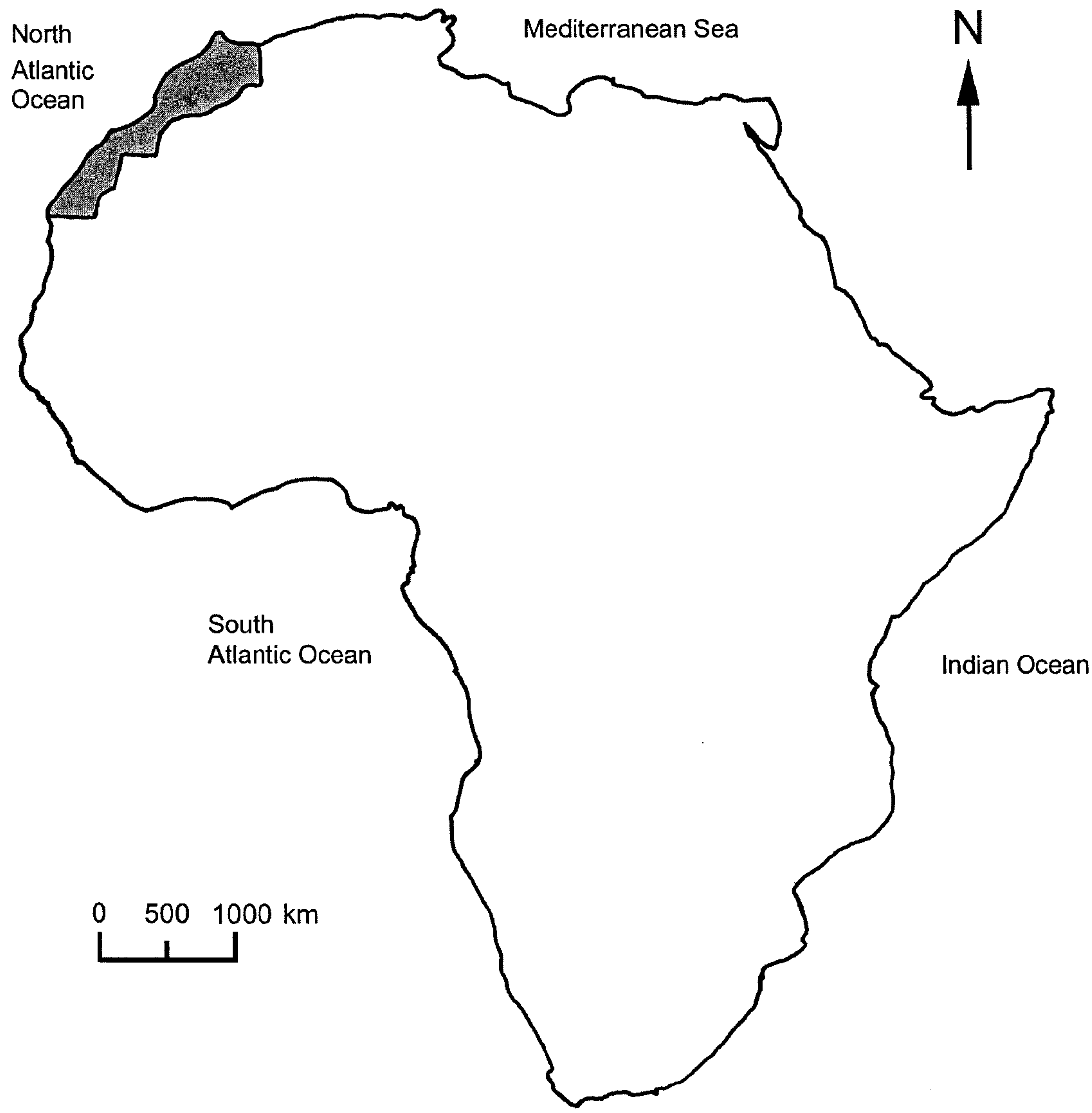

FIGURE 1-1--Map of Africa with Morocco shaded (modified from Philip, 1991).

A shallow marine continental shelf that connected Germany, France, the Czech Republic and Morocco during the Devonian (discussed in more detail in a later section) (Alberti, 1969; 1970; Šnajdr, 1980; Chlupác, 1983; Chlupác et al., 2000; Schraut, 2000; Schraut and; Scotese, 2001; Feist, 2004) allows some regional correlations to be made using trilobites, and these can be confirmed through the use of various other index fossils such as conodonts, ostracodes and/or ammonoids. Formation names have been applied to the sections studied in southern Morocco. This is sometimes a difficult task, as demonstrated by the number of authors who have published stratigraphic columns in the region without labelling them with formation names or who have exclusively used fossils to define the formation.

Location & Geology of Morocco

Morocco is bounded on the west by the North Atlantic Ocean, the north by the Mediterranean Sea, the northeast and south by Algeria and the southeast and south by Mauritania (along 'Western Sahara'). The southern region of Morocco, along the Algerian border, the primary research area, can be subdivided into three regions: the Dra Valley, Ma'der region, and Tafilalt region (Figure 1-2).

To understand the setting in which the proetids of southern Morocco existed during the Early and Middle Devonian, one must observe climatic reconstructions derived from analysis of distributions of indicator sediments and the position of the continents during this time period (Scotese, 2002). Scotese (2002) located North 'Africa' in a warm temperate region within the southern 30° to 60° latitude during the early Devonian. Contact between the Moroccan and the Bohemian faunas was proposed by

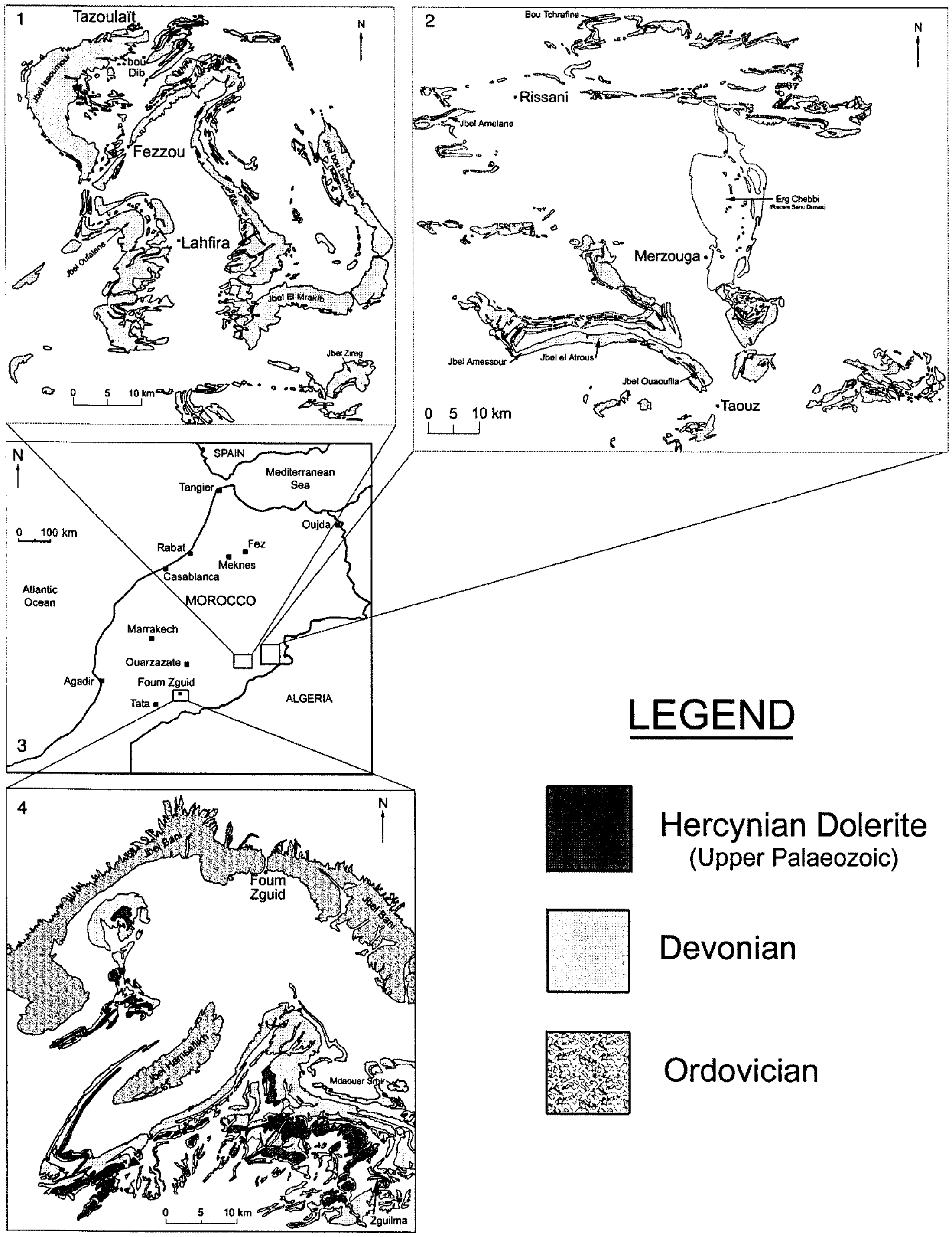

FIGURE 1-2—*1-4*, Generalized locality map for Morocco depicting the three regions of study. *1*, Ma'der region Devonian outcrop map (modified from Fetah et al., 1988); *2*, Tafilalt region Devonian outcrop map (modified from Fetah et al., 1986); *3*, Map of Morocco and surrounding areas; *4*, Dra Valley region Devonian outcrop (modified from Jaïdi et al., 1970; Jaïdi et al., 1971).

Alberti (1969; 1970), Šnajdr (1980), Chlupác (1983), Charpentier (1984), Chlupác et al. (2000), Schraut (2000), Scotese (2001), and Schraut and Feist (2004). It was made possible by a shallow continental shelf that joined the regions. This interchange would also be facilitated by the warm subtropical gyre proposed by Heckel and Wiztke (1979) circulating counterclockwise over Bohemia and into Morocco.

Another factor that should be considered is the eustatic sea levels. Dineley (1984; figure 1.4) presented a schematic of transgressive and regressive cycles throughout the Devonian, including the end Silurian and early Carboniferous for context. Dineley (1984) demonstrated that the Lochkovian began as a minor transgressive event that progressed into a major regressive event at the beginning of the Pragian. The Pragian then ends with a major transgressive event, with the Emsian peaking midway with a major regression. The Emsian concluded with a major transgression. During the Eifelian, the sea fluctuated in depth with three minor regressive events. The Givetian stated with a minor transgression. The Givetian demonstrated the same pattern as the Eifelian, though the regressive events are on a larger scale, and the stage ended with an immense transgression at the Givetian-Frasnian boundary. The regressive trend during the early Devonian can be accounted for by the vast amount of evaporites found around the world, in rocks of this age (Scotese, 2002).

The Middle Devonian began with a massive transgressive event that followed an immense regression, and this can be observed within the Dra Valley region. This event is recorded lithologically with the deposition of 'Rich 3' (Upper Member of the Mdâouer – el-Kbîr Formation defined by Hollard (1978)), a massive sandstone interval. Becker et al. (2004) had stated that "Rich 1 to 4 sandstones represent the upper part of shallowing upwards cycles with subsequent transgressions linked to global eustatic pulses and events". In the Upper Emsian of the Timrhanrhart Formation (defined by Hollard (1978)) and the horizons at Zguilma, the transgressive event is also evident. Jansen et al. (2004) also concurred that the in Upper Emsian "a transgressive tendency can be stated, with a change from neritic to rather hemipelagic conditions".

The Middle Devonian saw Morocco migrate slightly to the North on the palaeogeographic map of Scotese (2002), but remaining within the Southern Hemisphere, between the latitudes of 30-60°. The warm temperate zone within the Southern Hemisphere extended more northerly, though no other noticeable changes can be observed. Belka et al. (1997) noted in their Figure 1 that there may have been possible emerged strata between Jbel Ou Driss and to the west of the Jbel Issoumour range and that of Jbel Oufatene, therefore corresponding with Dineley's (1984) regressive cycles during the Eifelian and possibly more so into the Givetian.

Johnson and Boucot's (1973) brachiopod provinces demonstrated that the Emsian of Morocco and Bohemia (plus those of southern Europe) are all within the 'Old World Province', hence correlating these regions. During the Eifelian-Givetian, the 'Old World Province encompassed a larger area, into northern Europe and Asia, hence confirming that Heckel and Witzke's (1979) gyre could have circulated fauna throughout these regions.

Localities Studied

The Dra Valley is located on the north flank of the Devonian Tindouf Basin (Figure 1-3), and the locality that was collected from is referred to as Zguilma as it is shadowed from the southeast by Jbel Gara El Zguilma. Zguilma is situated approximately at N 29° 42' 35.2" and W 06° 42' 10.2", about 53 kilometres southeast of the town of Foum Zguid. We (the research group lead by Dr. B.D.E. Chatterton) collected from three main horizons (ZGEE1, ZGEE2 & ZGEE3) in a section through the Timrhanrhart Formation comprised of nodular to layered limestone interbedded with calcareous shales.

In the Ma'der region, our focus was the Devonian Ma'der Basin (Figure 1-4). The region approximately encompasses the following coordinates: N 31° 08' to 30° 35' and W 05° 03' to 04° 30'. Specimens were collected from the following localities: bou Dib (N 31° 05' 16.6" and W 04° 52' 32.2" [accuracy of ~6 metres]); three areas of Jbel Issoumour including, the base at N 30° 58' 15.9" and W 05° 02' 42.7" (~4 metres), a '*Koneprusites* interval' = KPE located at N 31° 0' 15.9" and W 04° 58' 39.3", and the Taboumakhloûf section with coordinates of N 30° 02' 0.8" and W 05° 00' 36" (Campbell et al., 2002); Jbel Oufatene with the '*Diademaproetus* horizon' at N 30° 50' 21.3" and W 04° 52' 58.7" (~5 metres) and a Taharajat section situated to the southwest at N 30° 47' 48.0" and W 04° 54' 20.3"; Jbel El Mrakib to the southeast at approximately N 30° 45' 48.6" and W 04° 40' 42.7" (~5 metres) on the northwestern edge of the mountain; and Zireg located south of Jbel Zireg at N 30° 36' 41.6" and W 04° 32' 22.7". Each of the localities is discussed in greater detail in the following two chapters. Sections were measured at some of these localities and are included in subsequent parts of the thesis.

The final area of study is the Tafilalt region, more specifically the Devonian Tafilalt Basin (Figure 1-5). We only collected from one locality for this thesis – Merzouga, located at N 31° 16' 28.5" and W 03° 53' 29.4" (~7 metres) to the ESE of Rissani, and is focused upon in more detail in Chapter 3.

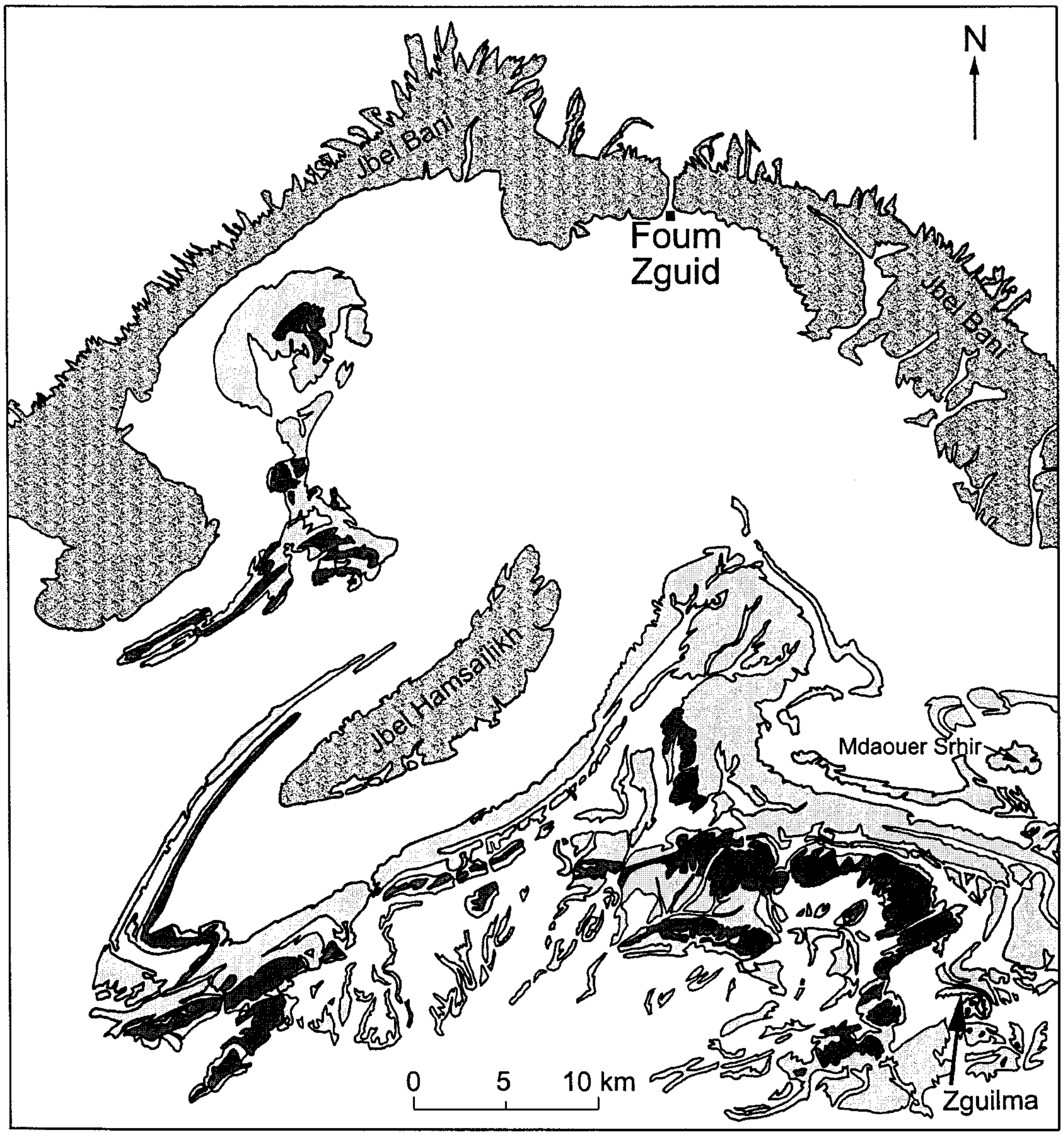

FIGURE 1-3--The Dra Valley region whereupon the locality of Zguilma was measured and collected from (See Figure 1-2 for legend) (modified from Jaïdi et al., 1970 and Jaïdi et al., 1971).

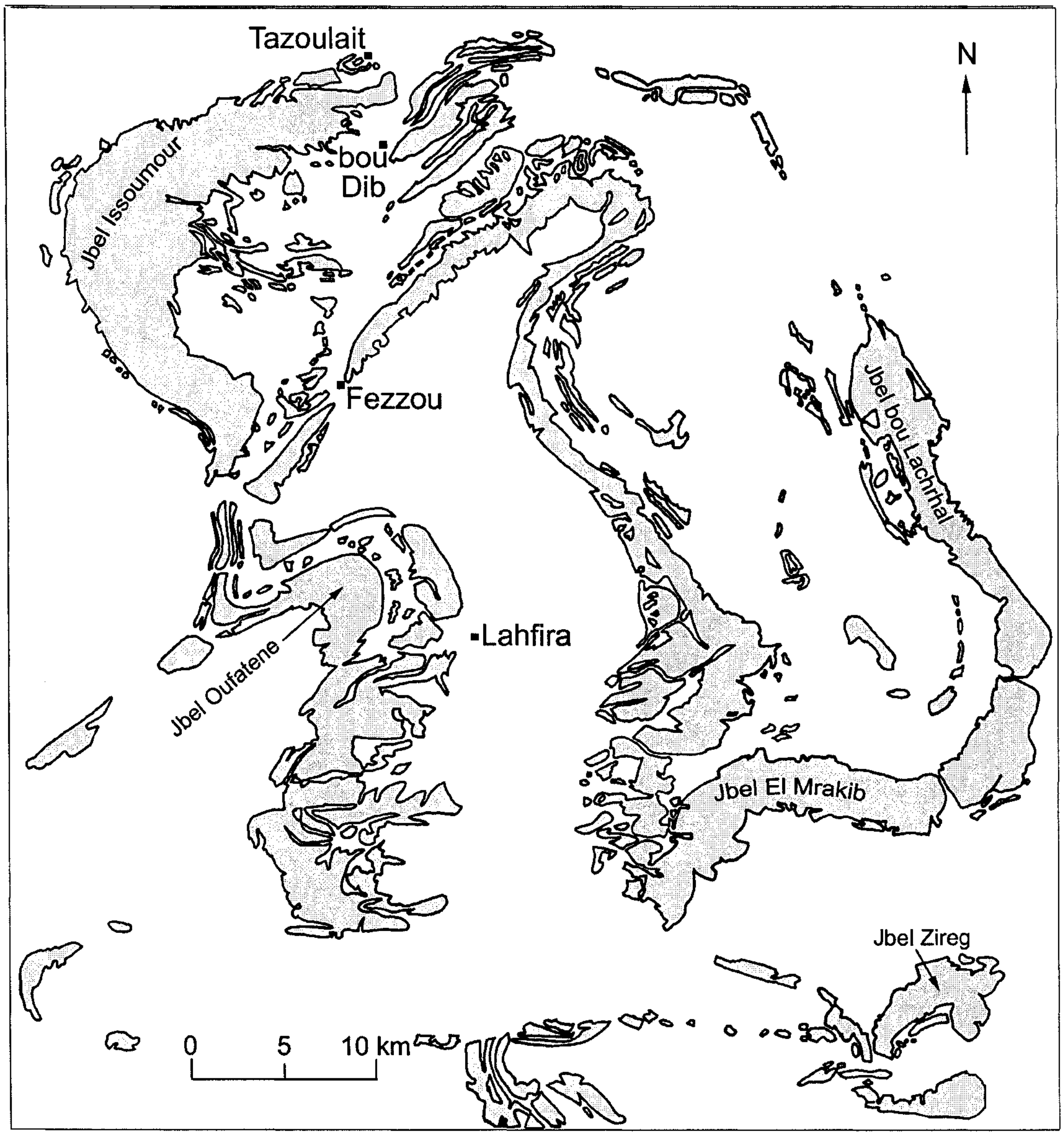

FIGURE 1-4--Ma'der Region depicting the Devonian outcrops (modified from Fetah et al., 1988).

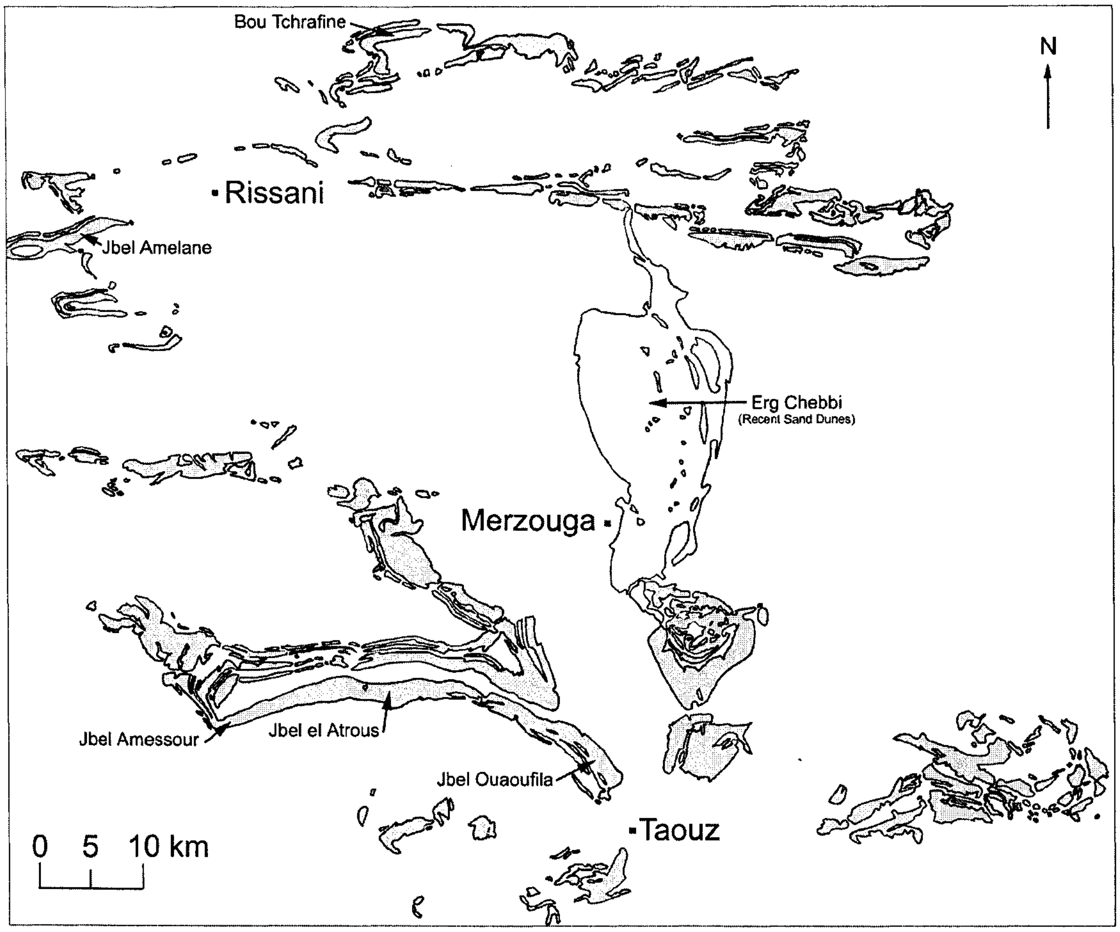

FIGURE 1-5--Tafilalt region depicting the Devonian outcrops (modified from Fetah et al., 1986).

Purpose and Scope of the Study

The purpose of this thesis is to study the systematics of some of the trilobites within the Order Proetida from the Lower to Middle Devonian of Morocco. A new genus, *Timsaloproetus*, is introduced along with the following new species: *T. elguerrouji,* and *T. dibbanus*. A phylogenetic (cladistic) analysis has been carried out for *Gerastos*, a proetid genus with a large number of Moroccan Devonian species, to determine whether relationships in that genus provide patterns or groups of species that illuminate Early and Middle Devonian biogeography and/or biostratigraphy. From the cladistic analysis and species comparisons based on thorough literature searches, the following eleven new species/subspecies of *Gerastos* are proposed: *G. tuberculatus marocensis, G. aintawilus, G. lisanrasus, G. ainrasifus, G. discombobulatus, G. cuvieri malisus, G. taqus, G. malisjildus, G. raribus, G. emmetus,* and *G. izius*. Another motivation for this research is the multitude of trilobites that are being mined, prepared and then sold on the open market. Unfortunately a number of these trilobites have been improperly identified, researched and published upon. In many cases locality information has been absent, vague or clearly incorrect (based on the town where the specimens were purchased and not the collection locality). This thesis and subsequent publications attempt to close this gap. Furthermore, much of the early work on trilobites from this region is based on disarticulated specimens, and often only cranidia, cephalons and/or pygidia are included among the described types. In some cases, more than one species name has been proposed for different sclerites of the same animal.

It was found during the course of this research that the task of correlating species to other regions throughout the world was going to be an arduous one without accurate stratigraphic columns and biostratigraphic work. An important part of the present work is to locate accurately all of the species described, both geographically and stratigraphically. This is to provide a useful framework for future biostratigraphic and biogeographic correlations. Some of the sections from which we collected have been published by various authors (e.g. Hollard, 1967; 1974; 1978; Bultynck and Hollard, 1980; Bultynck and Walliser, 2000; Morzadec, 2001). Unfortunately and surprisingly the stratigraphic positions of the beds that are mined for trilobites were not included in any of these sections (despite the fact that they can be seen for a considerable distance. In order to correlate our discoveries and the trilobite beds being actively mined for trilobites by the Moroccan collectors, it has been necessary to measure and describe the sections. Through collecting and identifying of a wide range of fossil groups (primarily ammonoids, brachiopods, conodonts, ostracodes and trilobites) we were able to correlate and date our sections. A number of localities that we are studying have not been published. Therefore the sections needed to be described, drafted and correlated to published sections.

Previous Research

Correlation of Horizons and Localities

As previously mentioned, the study of the geology of Morocco, in comparison with that of Europe and North America, is in a preliminary stage. Therefore, much more work is necessary to correlate the Devonian strata of the whole region. Hollard (1967; 1974; 1978) provided the foundation for further research by naming a number of Devonian formations in south and southeastern Morocco. However, many subsequent authors have ignored the formation names in favour of applying conodont (e.g. Muller and Bensaid, 1969; Bultynck and Hollard, 1980; Bultynck and Jacobs, 1981; Bultynck, 1985; Bultynck, 1989; Belka et al., 1997) or ammonoid zones (Töneböhn, 1991), or occurrences of ostracodes (G. Becker et al., 2003) to the sections, even when they have published stratigraphic columns. The reluctance to apply formation names to some published stratigraphic columns may be in part because most of the Lower and Middle Devonian formations are composed primarily of limestones and calcareous shale. The facies change along strike, and the proportions of carbonate and clay minerals, thicknesses and degrees of prominence in outcrop vary in subtle and complex fashions. This makes formation boundaries that are clear in one area difficult to identify in another locality only 20 kilometres away. Some researchers have applied formation names to the strata and shown the ranges of the fossils in them (e.g. Pique and Michard, 1989; Pique et al., 1991; Plodowski et al., 1999; Bultynck and Walliser, 2000; Morzadec, 2001; T. R. Becker et al., 2004; Jansen et al., 2004;). The correlation of the horizons using only *conodont zones/ammonoid zones/* or *event markers* (ignoring formation names) may be justified by facies changes and the large geographic region that is being researched, but a more clear outline of the formation boundaries is desirable. Therefore, the original formation descriptions must be analyzed and the type sections revisited in order to establish a clear sense of lithological features that define the boundaries of the formations. This knowledge will allow more extensive and useful applications of formation terminology to the sections of southern Morocco. Unfortunately, this work is beyond the scope to the present thesis.

The formations discussed in this thesis, the authors of the formations, and any unique defining features will follow in stratigraphic order as to the region.

The Dra Valley in the southern region of Morocco includes the Zguilma locality within the Timrhanrhart Formation. This formation was named by Hollard (1978), with the type locality approximately 6.5 kilometers southeast of Agadir Tissint, located on the map sheet, scale of 1/100 000, Agadir Tissint 1969 at the coordinates x=318.4 and y=318.7 (Hollard, 1978). Only the Timrhanrhart Formation is recognized in the section at Zguilma (it is overlain by Hercynian dolerites and at the base extends into a flat desert plain) (Figures 2-2 or 3-3). The most recent literature provides an accurate formation description (T. R. Becker et al., 2004; Jansen et al., 2004) complementing the original description by Hollard (1967;1978).

To the east of the Dra Valley region, is the Ma'der Basin, from which the following localities are addressed: Jbel Issoumour (west side and dip slope of Taboumakhloûf section (Figure 3-6)), Oufatene, bou Dib (Figures 2-2 or 3-7), Mrakib (Figure 3-8) and Zireg. A number of Devonian formations are omitted from this study due to the fact that neither *Gerastos* nor *Timsaloproetus* were found in them, leaving the following formations for discussion: Tazoulaït, El Otfal, Taboumakhloûf and Bou Dib.

The Tazoulaït Formation was named by Henri Hollard for the town of Tazoulaït (the town is located at approximately N 31° 06' 00" and W 04° 52' 09"). No type locality has been officially described (pers. comm., Bultynck, 2005).

Hollard (1974) described the El Otfal Formation based upon a section at Jbel El Otfal, located south along the same range as Jbel bou Lachral. The formation encompasses dm1.1 – dm1.4 (dm = Middle Devonian stratum/strata used by the Subcommission on Devonian Stratigraphy), within the Eifelian.

The Taboumakhloûf Formation was also defined by Hollard (1974), and is named after the Taboumakhloûf section on the dip slope of Issoumour located at approximately N 30° 02' 0.8" and W 05° 00' 36.0". Hollard (1974) defined it as dm2 (therefore, from dm2.1 – dm2.3), within the Givetian, though the type locality is located near bou Dib.

The final formation within the Ma'der to be discussed is the Bou Dib Formation named after the town of bou Dib, located at the following coordinates: N 31° 03' 44" and W 04° 52' 26". The Bou Dib Formation was defined by Hollard (1974) as dm3, encompassing dm3.1 – dm3.3, of the Givetian, and is located at bou Dib.

Within the Tafilalt region, only the Amerboh Group is relevant to this thesis, for the Merzouga '*Proetus* horizon' (Figure 3-10) correlates with the Tazoulaït and Timrhanrhart Formations (Bultynck and Walliser, 2000). The Amerboh Group has had not been officially described but was named by Henri Hollard, after the Amerbouh River (pers. comm., Bultynck, 2005) (coordinates are approximately N 31° 23' and W 04° 13'), and it is upper Emsian in age (Bultynck and Walliser, 2000; Aitken et al., 2002).

Systematics of southern Moroccan trilobites within the Order Proetida

Despite the fact that much research has been undertaken to classify trilobites from Devonian localities worldwide, proetids from the southern region of Morocco have not been extensively studied. Alberti (1969; 1970) published on Moroccan proetids, focusing on the northwestern region of Morocco and Hamar Laghdad near Erfoud in the southeast. His work was largely based on disarticulated specimens for the assignment of species.

Hamar Laghdad is a region from which we also collected specimens, though we found that the localities in the Dra Valley, Ma'der and Tafilalt regions of southern Morocco produced the best and most complete specimens, many of which are beautifully articulated. Our specimens have not, however, demonstrated enough synapomorphies to correlate them as equivalent species to Alberti's (1969; 1970). This inconsistency was possibly explained by the fact that a trough was developing from Marrakech to the northeast to Oujda during the Devonian, referred to as the 'Marrakech-Oujda Basin' (Pique and Michard, 1989), which may have created a dispersal barrier between the species of the south and northwest of Morocco.

Richter and Richter (1943; 1956) also published some work on Moroccan proetids, though their material is also quite disarticulated and/or fragmented. Even given the incomplete state of Richter and Richter's, and Alberti's specimens, their research has been useful for comparison and provided a foundation on which to build.

Methodology

Correlation of Horizons and Localities

Fieldwork began in 1995, when Dr. B.D.E. Chatterton and Kevin Brett traveled to Morocco to assess localities and collect specimens. Since that time, five more excursions have been made to collect specimens and log the strata. Kevin Brett collected the majority of the stratigraphic information over the course of three field seasons. To obtain a clear and precise understanding of every horizon at all localities would require a thesis unto itself. Thus, every attempt has been made to identify the age for each horizon by studying all field notes, identifying ammonoids, trilobites, ostracodes, and conodonts, and extensively searching existing publications.

Collection and Preparation of Specimens:

The trilobites used to establish the systematics of the Order Proetida were collected on various research trips, as gifts from local fossil collectors, and by purchasing from local fossil sellers. Some of the purchased specimens were already prepared, while the rest were mechanically prepared by K. Brett, B.D.E. Chatterton, A. Lindoe (professional preparator for B.D.E. Chatterton) or myself. Acid digestion of rock obtained from various horizons was also undertaken to retrieve microfauna and disarticulated trilobites.

Different mechanical preparation techniques were used depending upon the type and amount of matrix encasing the trilobite. The most basic of all techniques involved the use of a needle and a microscope to remove matrix without destroying minute details. This technique is exceptional if the matrix is soft and can be quickly removed. It can be an arduous task if this is the primary technique used, as is often the case when preparation is performed by Moroccan fossil collectors who lack sophisticated tools. The collectors that use this technique will initially remove matrix with a hammer and nail, and then pop the remaining matrix off with a sharp nail or a finer and more precise tool. The more sophisticated mechanical technique involved the use of a 'MicroJack' (either size 5 or 3, dependent upon the detail work required) either by Moroccan dealers, A. Lindoe, or myself. For fine cleaning of the specimen, air abrasive equipment ('Swam-Blaster™') was used.

Acid digestion provided microfossils used for correlation and systematic work. Acid digestion technique involves placing fist-sized rock in a bucket of either 10% hydrochloric acid or 10% acetic acid (for the most complete faunal suite (St. Clair, 1935)). Jeppsson et al. (1985), Jeppsson (1987), and Jeppsson and Feldholm (1987) cover the process of acetic acid digestion thoroughly; therefore the technique will not be rephrased. Upon the completion of the acid digestion, the residue was sieved using 5 different sieve mesh sizes (10, 30, 40, 80, and 200), and then dried. The larger residues were picked under a microscope for fragmented or complete trilobite sclerites, ostracodes, conodonts, and any other faunal material that might prove to be chronologically important and/or environmentally informative.

The finer residues were separated into two groups dependent upon specific gravity (that of 2.825-2.830) through the use heavy liquid extraction. The technique makes use of sodium polytungstate, which separates out conodonts from the lighter fractions due to the fact that conodonts possess a specific gravity greater than the sodium polytungstate (Merrill, 1987; Stone, 1987). The conodonts were titrated out, dried, imaged using the scanning electron microscope and identified. The lighter fractions could be analyzed for ostracodes, trilobite fragments and other faunal groups, and any presumed to be useful were also imaged and identified.

Format

This thesis adheres to paper/published format. The systematics of two major genera of trilobites, *Timsaloproetus* (Chapter 2 – has been sent out for review) and *Gerastos* (Chapter 3) shall be addressed and subsequently published upon where appropriate. The editorial format shall be in the style of the Journal of Paleontology; therefore, the locality and repository information shall be provided or referred to within each distinct chapter.

Literature Cited

AITKEN, S. A., C. J. COLLOM, C. M. HENDERSON, AND P. A. JOHNSTON. 2002. Stratigraphy, paleoecology, and origin of Lower Devonian (Emsian) carbonate mud buildups, Hamar Laghdad, eastern Anti-Atlas, Morocco, Africa. Bulletin of Canadian Petroleum Geology, 50(2):217-243.

ALBERTI, G. K. B. 1964. Neue Trilobiten aus dem marokkanischen und deutschen Unter- und Mitteldevon. Senckenbergiana lethaea, 45(1-4):115-133.

ALBERTI, G. K. B. 1966. Über einige neue Trilobiten aus dem Silurium und Devon, besonders von Marokko. Senkenbergiana Lethaea, 47:111-121.

ALBERTI, G. K. B. 1967a. Neue obersilurische sowie unter- und mitteldevonische Trilobiten aus Marokko, Deutschland und einigen anderen europäischen Gebieten. 1. Senckenbergiana lethaea, 48(5):463-479.

ALBERTI, G. K. B. 1967b. Neue obersilurische sowie unter- und mitteldevonische Trilobiten aus Marokko, Duetschland und einigen anderen europäischen Gebieten. 2. Senckenbergiana lethaea, 48(6):481-509.

ALBERTI, G. K. B. 1969. Trilobiten des jüngeren Siluriums sowie des Unter- und Mitteldevons. I. Abhandlungen der Senckenbergischen Naturforschenden Gesellschaft, 520:1-692.

ALBERTI, G. K. B. 1970. Trilobiten des jüngeren Siluriums sowie des Unter- und Mitteldevons. II. Abhandlungen der Senckenbergischen Naturforschenden Gesellschaft, 525:1-233.

ALBERTI, G. K. B. 1975. Zur paläozoogeographischen Verbreitung von *Warburgella rugulosa* (ALTH 1874) (Trilobitae, Devon-Basis). Mitteilungen aus dem Geologisch-Palaeontologischen Institut der Universitaet Hamburg, 44:1-10.

ALBERTI, G. K. B. 1980. Neue Daten zur Grenze Unter-/Mittel-Devon, vornehmlich aufgrund der Tentaculiten und Trilobiten im Tafilalt (SE-Marokko). Neues Jahrbuch fuer Geologie und Palaeontologie. Monatshefte, 39:581-594.

ALBERTI, G. K. B. 1981a. Beziehungen zwischen "herzynischen" Trilobiten-Faunen aus NW-Marokko und Deutschland (Unter- und Mittel-Devon). Natur und Museum, 111(11):362-369.

ALBERTI, G. K. B. 1981b. Scutelluidae (Trilobita) aus dem Unter-Devon des Hamar Laghdad (Tafilalt, SE-Marokko) und das Alter der "mud-mounds" (Ober-Zlichovium bis tiefstes Dalejum). Senkenbergiana Lethaea, 62:193-204.

ALBERTI, G. K. B. 1981c. Trilobiten des jüngeren Siluriums sowie des Unter-und Mittel-Devons III: Mit Beiträgen zur Devon-Biostratigraphie (insbesondere nach Nowakiidae) in N-Afrika, Sardinien, Oberfranken und im Harz. Senkenbergiana Lethaea, 62:1-75.

ALBERTI, G. K. B. 1982a. Der Hamar-Laghdad (Tafilalt, SE-Marokko), eine bedeutende Fundstätte devonischer Trilobiten. Natur und Museum, 112(6):172-182.

ALBERTI, G. K. B. 1982b. Zur Frage einer Emersion der noerdlichen NW-Sahara am Ende des Lochkoviums (Unter-Devon). Newsletters on Stratigraphy, 11(1):8-16.

ALBERTI, G. K. B. 1988. Stratigraphische Untergliederung einiger Lochkovium/Pragium-Grenzprofile (Unter-Devon) in NW-Marokko, Oberfranken und Victoria (SE-Australien) auf Grund von Dacryoconariden und Conodonten. Senckenbergiana lethaea, 68:479-493.

ALBERTI, H. 1975a. Neue Trilobiten (Waribole) aus dem Ober-Devon IV-V (Nord-Afrika und Mittel-Europa); Beitrag 4, Nebst Revision einger Typus-Spezies der Proetidae Salter 1864, aus dem Ober-Devon II-V. Neues Jahrbuch für Geologie und Palaeontologie. Abhandlungen, 150(2):207-226.
ALBERTI, H. 1975b. Neue Trilobiten (*Waribole*) aus dem Ober-Devon IV-VI (Nord-Afrika und Mittel-Europa) -- Beitrag 3. Neues Jahrbuch für Geologie und Palaeontologie. Abhandlungen, 149(2):180-210.
BECKER, G., N. LAZREQ, AND K. WEDDIGE. 2003. Ostracods of Thuringian provenance in the Lower Devonian of Eurasia and North Africa with special reference to the Emsian of Morocco. Courier Forschungsinstitut Senckenburg, 242:39-49.
BECKER, T. R., U. JANSEN, G. PLODOWSKI, E. SCHINDLER, S. Z. ABZOUSSALAM, AND K. WEDDIGE. 2004. Devonian litho- and biostratigraphy of the Dra Valley area -- an overview. Devonian Neritic-Pelagic Correlation and Events in the Dra Valley (Western Anti-Atlas, Morocco). Documents de l'Institut Scientifique(19):3-18.
BELKA, Z., B. KAUFMANN, AND P. BULTYNCK. 1997. Conodont-based quantitative biostratigraphy for the Eifelian of the eastern Anti-Atlas, Morocco. Geological Society of America Bulletin, 109(6):643-651.
BULTYNCK, P. 1985. Lower Devonian (Emsian) -- Middle Devonian (Eifelian and lowermost Givetian) conodont successions from the Ma'der and the Tafilalt, southern Morocco. Courier Forschunginstitut Senckenberg, 75:261-286.
BULTYNCK, P. 1989. Conodonts from a potential Eifelian-Givetian Global Boundary Stratotype at Jbel Ou Driss, southern Ma'der, Morocco. Bulletin de l'institut Royal des sciences naturelles de Belgique, Sciences de la Terre, 59:95-03.
BULTYNCK, P., AND H. HOLLARD. 1980. Distribution comparée de Conodontes et Goniatites dévoniens de plaines du Dra, de Ma'der et du Tafilalt (Maroc). Leuven University Press, 1, 73 p.
BULTYNCK, P., AND L. JACOBS. 1981. Conodontes et sédimentologie des couches de passage du Givetien au Frasnien dans le Nord du Tafilalt et dans le Ma'der (Maroc Présaharien). Bulletin de l'institut Royal des sciences naturelles de Belgique, Sciences de la Terre, 53(2):1-23, pl.10, fig.23.
BULTYNCK, P., AND O. H. WALLISER. 2000. Devonian Boundaries in the Moroccan Anti-Atlas. Courier Forschungsinstitut Senckenburg, 225:211-226.
CAMPBELL, K. S. W., R. E. BARWICK, B. D. E. CHATTERTON, AND T. R. SMITHSON. 2002. A new Middle Devonian dipnoan from Morocco: structure and histology of the dental plates. Records of the Western Australian Museum, 21:39-61.
CHARPENTIER, R. R. 1984. Conodonts through time and space, p. 11-32. *In* D. L. Clark (ed.), Conodont Biofacies and Provincialism. Special Paper 196. The Geological Society of America, Inc., Boulder.
CHLUPÁC, I. 1983. Trilobite assemblages in the Devonian of the Barrandian area and their relations to palaeoenvironments. Geologica et Palaeontologica, 17:45-73.
CHLUPÁC, I., R. FEIST, AND P. MORZADEC. 2000. Trilobites and standard Devonian stage boundaries. Courier Forschungsinstitut Senckenburg, 220:87-98.
DINELEY, D. L. 1984. Aspects of a Stratigraphic System: The Devonian. MacMillan Publishers Ltd., London, 223 p.
FEIST, R., AND B. ORTH. 2000. Trilobites de la limite Eifélien/Givétien de la région stratotypique (Tafilalt, Maider, Maroc), p. 78-91. *In* A. Tahiri and A. El Hassani

(eds.), Proceedings of the Subcommission on Devonian Stratigraphy (SDS) -- IGCP 421 Morocco Meeting. Volume 20. Travaux de L'Institut Scientifique Série Géologie & Géographie Physique, Rabat, Morocco.

FETAH, S. E. M., M. BENSAÏD, AND M. DAHMANI. 1986. Carte Géologique de Maroc: Tafilalt - Taouz. Editions du Service Géologique de Maroc, Notes et Mémoires No. 244. Royaume du Maroc. Ministère de l'Énergie et des Mines. Direction de la Géologie, Rabat.

FETAH, S. E. M., M. BENSAÏD, AND M. DAHMANI. 1988. Carte Géologique de Maroc: Todrha-Ma'der (Anti-Atlas oriental, zones axiale et périphérique Nord et Sud). Editions du Service Géologique du Maroc, Notes et Mémoires No. 243. Royaume du Maroc. Ministére de l'Énergie et des Mines, Rabat.

FORTEY, R. A., AND R. M. OWEN. 1975. Proetida -- a new order of trilobites. Fossils and Strata, 4:227-239.

HECKEL, P. H., AND B. J. WITZKE. 1979. Devonian world palaeogeography determined from distribution of carbonates and related lithic palaeoclimatic indicators, p. 99-123. *In* M. R. House, C. T. Scrutton, and M. G. Bassett (eds.), The Devonian System: A Palaeontological Association International Symposium. Special Papers in Palaeontology No. 23. The Palaeontological Association, London.

HOLLARD, H. 1967. Le Dévonien de Maroc et du Sahara Nord-Occidental, p. 203-244. *In* D. H. Oswald (ed.), International Symposium on the Devonian System. Volume 1. Alberta Society of Petroleum Geologists, Calgary, Alberta.

HOLLARD, H. 1974. Recherches sur la stratigraphie des Formations du Dévonien Moyen, de l'Emsien Supérieur au Fransien, dans le Sud du Tafilalt et dans le Ma'der (Anti-Atlas oriental). Notes Service Géologique du Maroc, 36(264):7-68.

HOLLARD, H. 1978. Corrélations entre niveaux á brachiopodes et á goniatites au voisinage de la limite Dévonien inférieur -- Dévonien moyen dans les plaines du Dra (Maroc présaharien). Newsletter of Stratigraphy, 7(1):8-25.

JAÏDI, S. E. M., A. BENCHEQROUN, M. DIOURI, AND Y. ENNADIFI. 1970. Carte géologique de l'Anti-Atlas Central et de la Zone Synclinale de Ouarzazate. Feuilles Ouarzazate, Alougoum et Telouet Sud. Editions du Service Géologique du Maroc, Notes et Mémoires No. 138. Royaume du Maroc. Direction des Mines et de la Géologie, Rabat.

JAÏDI, S. E. M., M. DOUÏEB, M. DIOURI, M. SAÂDI, AND Y. ENNADIFI. 1971. Carte géologique des Plaines du Dra au sud de l'Anti-Atlas Central: Agadir Tissinnt - Oued Zemoul. Éditions de Service Géologique de Maroc, Notes et Mémoires No. 219. Royaume du Maroc. Ministère du Commerce, de l'Industrie, des Mines et de la Marine Marchande: Direction des Mines et de la Géologie division de la Géologie, Rabat.

JANSEN, U., G. BECKER, G. PLODOWSKI, E. SCHINDLER, O. VOGEL, AND K. WEDDIGE. 2004. The Emsian to Eifelian near Foum Zguid (NE Dra Valley, Morocco. Devonian Neritic-Pelagic Correlation and Events in the Dra Valley (Western Anti-Atlas, Morocco). Documents de l'Institut Scientifique(19):19-28.

JEPPSSON, L. 1987. Some thoughts about future improvements in conodont extraction methods, p. 45-51. *In* R. L. Austin (ed.), Conodonts: Investigative techniques and applications. Ellis Horwood Limited, Chichester.

JEPPSSON, L., AND D. FREDHOLM. 1987. Temperature dependence of limestone dissolution in conodont extraction, p. 39-42. *In* R. L. Austin (ed.), Conodonts: Investigative techniques and applications. Ellis Horwood Limited, Chichester.

JEPPSSON, L., D. FREDHOLM, AND B. MATTIASSON. 1985. Acetic Acid and phosphatic fossils -- A warning. Journal of Paleontology, 59(4):952-956.

JOHNSON, J. G., AND A. J. BOUCOT. 1973. Devonian Brachiopods, p. 89-96. *In* A. Hallam (ed.), Atlas of Palaeobiogeography. Elsevier Scientific Publishing Company, Amsterdam.

MERRILL, J. 1987. Cryogenic density separation of conodonts, p. 63-64. *In* R.L. Austin (ed.), Conodonts: Investigative techniques and applications. Ellis Horwood Limited, Chichester.

MORZADEC, P. 2001. Asteropyginae trilobites from the Devonian of the Anti-Atlas (Morocco). Palaeontographica Abt. A, 262:53-85.

MULLER, K. J., AND M. BENSAID. 1969. Devonian conodonts from Morocco, p. 523-534. *In* R. Said, J. P. Beckmann, M. A. Ghorab, S. El Ansary, C. Viotti, and M. T. Kerdany (eds.), Proceedings of the Third African Micropaleontological Colloquium (Cairo, March 4-10, 1968). The National Information and Documentation Centre, Cairo.

PHILIP, G. 1991. Political: Africa, Philip's World Atlas. Reed International Books Limited, London.

PIQUE, A., J.-J. CORNEE, J. MULLER, AND J. ROUSSEL. 1991. The Moroccan Hercynides, p. 229-263. *In* R. D. Dallmeyer and J. P. Lécorché (eds.), The West African orogens and Circum-Atlantic correlatives. Springer-Verlag, New York.

PIQUE, A., AND A. MICHARD. 1989. Moroccan Hercynides: A synopsis. The Paleozoic sedimentary and tectonic evolution at the northern margin of West Africa. American Journal of Science, 289:286-330.

PLODOWSKI, G., G. BECKER, R. BROCKE, U. JANSEN, N. LAZREQ, E. SCHINDLER, G. SCHRAUT, O. H. WALLISER, K. WEDDIGE, AND W. ZIEGLER. 1999. The section at Jebel Issimour (NW Maïder, Early to Early Middle Devonian) First results with respect to lithology and biostratigraphy. Notes Service Géologique du Maroc, 399:43-48.

RICHTER, R., AND E. RICHTER. 1943. Studiem im Palaeozoikum der Mittelmeer-Laender; 4a, Trilobiten aus dem Devon von Marokko, mit einem Anhand über Arten des Rheinlands. Senckenbergiana, 26(1-3):116-199.

RICHTER, R., AND E. RICHTER. 1956. Annular-Teilung bei Trilobiten am Beispiel besonders von *Proetus (Pr.) cuvieri* und *prox*. Senckenbergiana Lethaea, 37(3-4):343-381.

SCHRAUT, G. 2000. Trilobiten aus dem Unter-Devon des südöstlichen Anti-Atlas, Süd-Marokko. Senkenbergiana Lethaea, 79(2):361-433.

SCHRAUT, G., AND R. FEIST. 2004. The Devonian Styginid trilobite *Paralejurus*, with new data from Spain and Morocco. Journal of Paleontology, 78(4):709-722.

SCOTESE, C. R. 2001. Paleogeographic Atlas, PALEOMAP Progress Report 90-0497. Department of Geology, University of Texas at Arlington, Arlington, Texas, 45 p.

SCOTESE, C. R. 2002. PALEOMAP Project: Climate History. http://www.scotese.com/climate.htm.

ŠNAJDR, M. 1980. Bohemian Silurian and Devonian Proetidae (Trilobita). Vydal Ústrední ústav geologick'y, Praha, 324 p.

ST. CLAIR, D. W. 1935. The use of Acetic Acid to obtain insoluble residues. Journal of Sedimentary Petrology, 5(3):146-149.

STONE, J. 1987. Review of investigative techniques used in the study of conodonts, p. 17-34. *In* R. L. Austin (ed.), Conodonts: Investigative techniques and applications. Ellis Horwood Limited, Chichester.

TÖNEBÖHN, R. 1991. Bildungsbedingungen epikontinentaler Cephalopodenkalke (Devon, SE-Marokko). Göttinger Arbeiten zur Geologie und Paläontologie, 47:1-131.

CHAPTER 2: SYSTEMATIC PALAEONTOLOGY I

TIMSALOPROETUS NEW GENUS (PROETIDA, TRILOBITA), AND INCLUDED SPECIES FROM LOWER AND MIDDLE DEVONIAN STRATA OF SOUTHERN MOROCCO[1]

INTRODUCTION

Morocco has proven to be a palaeontological Mecca for scholars studying Devonian trilobites. The large number of complete specimens available for purchase on the open market demonstrates the wealth of research material available from this region. Based upon recently discovered specimens, this paper proposes a new genus, *Timsaloproetus*, for a species originally described from Germany (Alberti, 1971) and two new species, *Timsaloproetus elguerrouji* and *Timsaloproetus dibbanus*, from Morocco. Alberti (1971) described a new species from the Dill Syncline in Germany, as *Cornuproetus (Sculptoproetus) haasi*, possibly from the early Middle Devonian, which is almost identical to articulated specimens from near bou Dib (BD5), southeastern Morocco and the uppermost trilobite-bearing horizon at Zguilma (ZGEE3). We designate this species as the type species for a new genus *Timsaloproetus*. Disarticulated segments, including several pygidia, cranidia, free cheeks, hypostomes, thoracic segments, and several complete specimens from Zguilma, southern Morocco, belong to the two new species that we are assigning to *Timsaloproetus*. This work describes known Moroccan representatives of a genus of small proetid trilobites that may be useful for

[1] A version of this chapter, under the same title, with the authorship of S. Gibb and B.D.E. Chatterton has been submitted to Journal of Paleontology on 8th of February 2005.

biostratigraphy, correlating different sections within Morocco, and between Europe and Morocco.

STRATIGRAPHY AND AGE RELATIONSHIPS

Locality near bou Dib.— Specimens of *Timsaloproetus haasi* (Alberti, 1971) have been found near the village of bou Dib, south of the village of Tazoulaït in southeastern Morocco (Figure 2-1.2). The coordinates for the locality (BD5) that the specimens were retrieved from are N 31° 05' 10.3" and W 4° 53' 45.7". Stratigraphically, the bed is within the El Otfal Formation (Bultynck and Hollard, 1980; Hollard, 1967; Hollard, 1974; Morzadec, 2001), of the Lower Eifelian (Hollard, 1967; Hollard, 1974; Morzadec, 2001). The bed is mined for trilobites, and is referred to locally as the '*Harpes/Thysanopeltis* horizon'. Lithologically, it is limestone (semi-nodular dark grey wackestone to calcareous mudstone), interbedded with calcareous shale. The part of the section that is mined for trilobites at this locality is composed of three beds of limestone (10 cm thick or slightly less) that are rubbly wackestone to calcareous mudstone, and it is overlain by interbedded light grey crumbly calcareous shale and wackestone (Figure 2-2.2).

Basse (1997) described *Timsaloproetus haasi* (his *Sculptoproetus*) occurring with *Thysanopeltis speciosa* in the Kellerwald region of Germany, and he stated that it is probably early or middle Eifelian in age, conforming with the probable age of the '*Harpes/Thysanopeltis* horizon' near bou Dib. Schraut (2000) proposed that during this time, Germany, France, the Czech Republic and Morocco, among other regions, were interconnected on a massive shallow continental shelf, as can be observed in

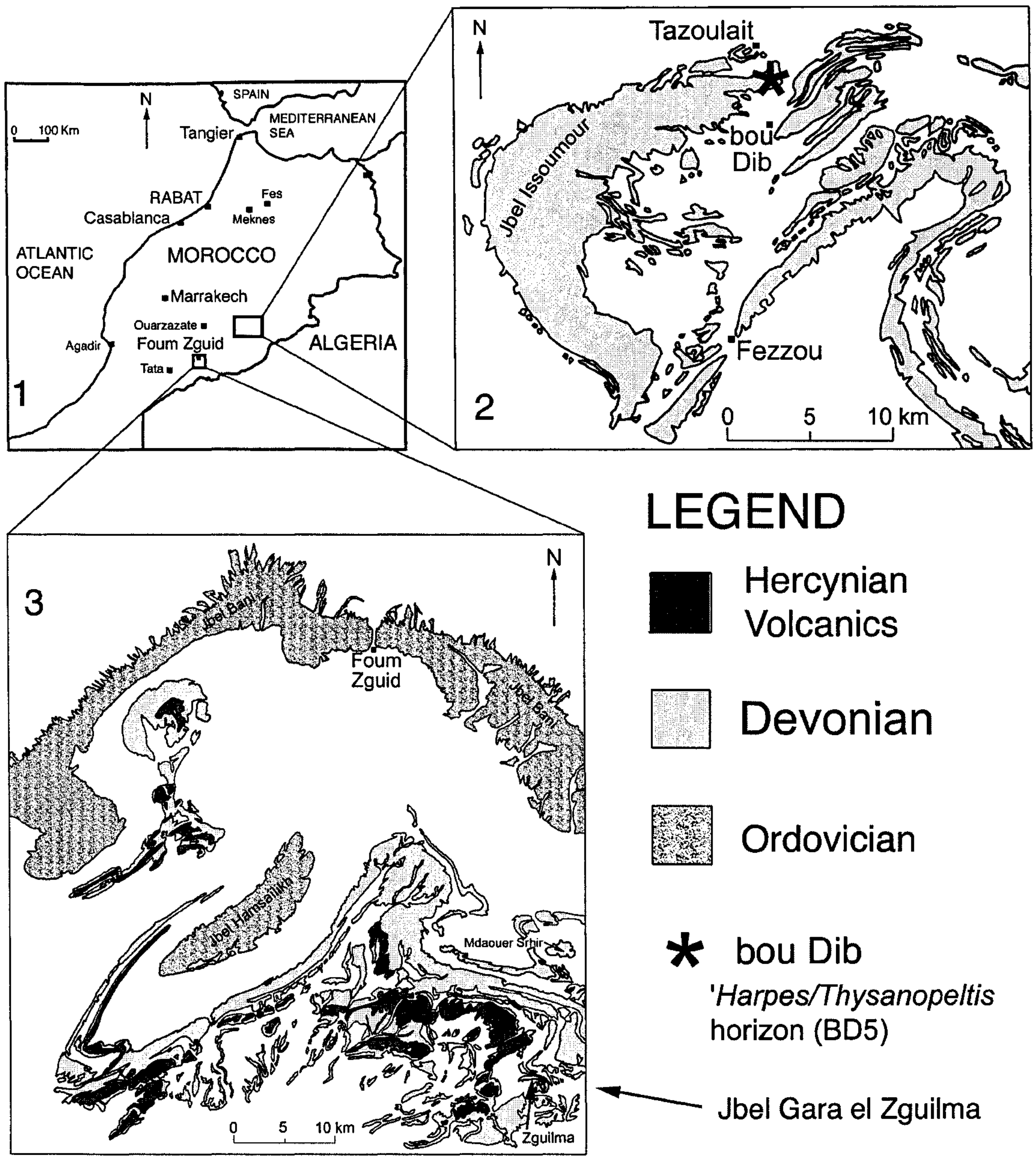

FIGURE 2-1--Locality map. *1*, general locality map including northeastern Morocco. *2*, detailed map of the northern part of the Ma'der region, including the location of the section between bou Dib and Tazoulaït (modified from Fetah et al, 1988). *3*, detailed map showing the geology of Foum Zguid, and including location of Jbel Gara el Zguilma (modified from Jaïdi et al, 1970; Jaïdi et al., 1971).

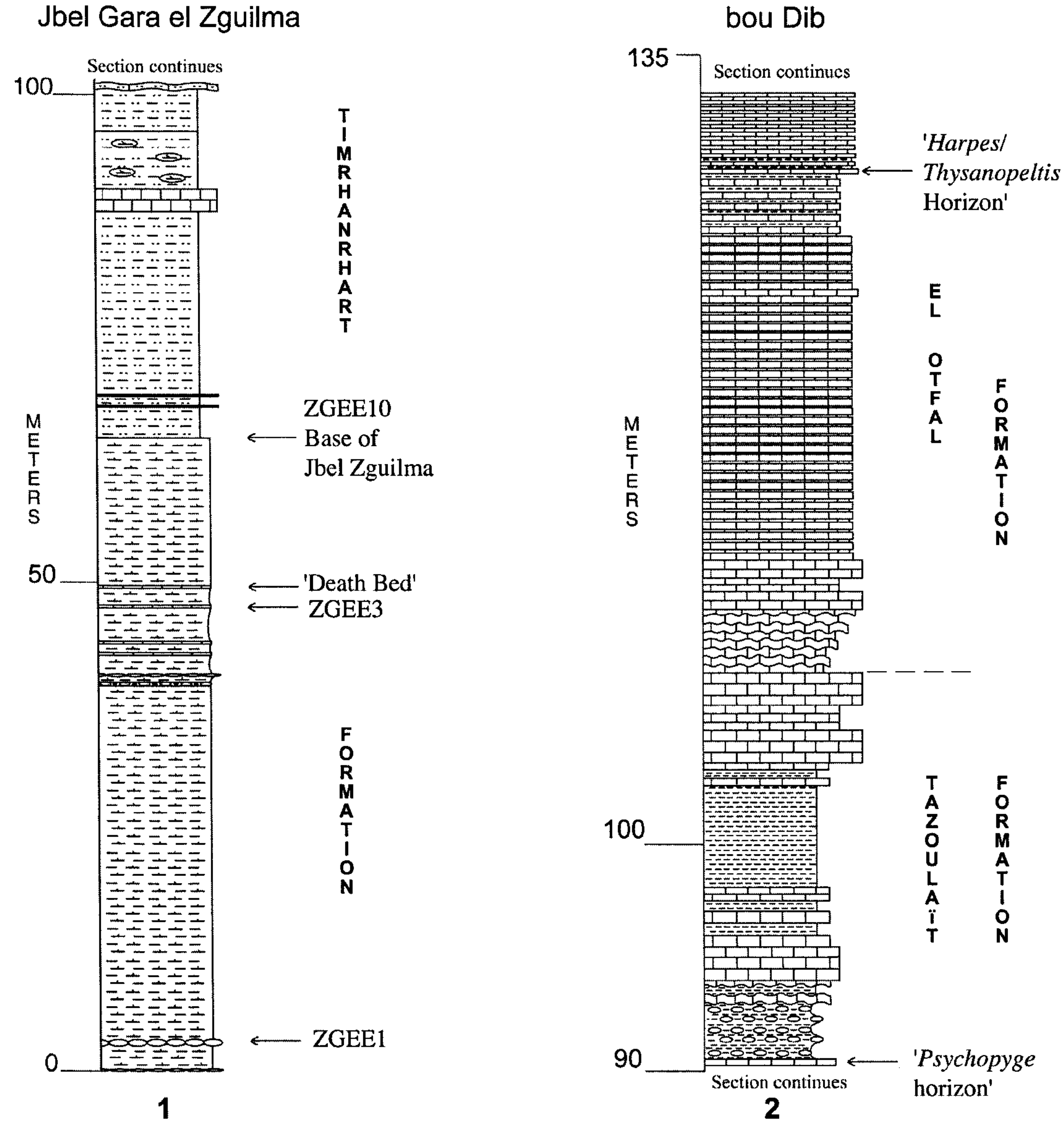

FIGURE 2-2--Stratigraphic columns for parts of the two sections from which specimens of *Timsaloproetus* were obtained for this work. *1*, lower part of the section at Jbel Gara el Zguilma (*Timsaloproetus dibbanus* new species occurs at ZGEE1; *Timsaloproetus haasi* (Alberti, 1971) and *Tismaloproetus elguerrouji* new species both occur at ZGEE3). *2*, part of the section between Tazoulaït and El Otfal Formations (*T. haasi* occurs in the '*Harpes/Thysanopeltis* horizon').

palaeogeographic maps produced by Scotese (2001). Schraut (2000) further posited that there were no barriers that would hinder movement of species along this shelf (Alberti, 1969; Šnajdr, 1980 Chlupác et al., 2000; Schraut and Feist, 2004).

The bou Dib region is part of what was referred to by Belka et al. (1997) as the Ma'der Basin, with the Ma'der Platform to the west. The Ma'der Basin merged with the Tafilalt Basin to the east, with the Tafilalt Platform encompassing the north, northeast and eastern region of the Ma'der Basin.

Section at Zguilma.— This section occurs on the northeast side of Jbel Gara el Zguilma, in the Dra Valley region, which is located on the northern flank of the Tindouf Basin (Bultynck and Walliser, 2000). The location of the Zguilma section is south of Foum Zguid, at the approximate coordinates of N 29° 42' 35.2" and W 06° 42' 10.2" for the lower bed (ZGEE1), while the coordinates for the upper horizon (ZGEE3) are N 29° 42' 18.5" and W 06° 42' 11.5" (Figure 2-1.2). The trilobites were collected from the Timrhanrhart Formation (Hollard, 1978; Bultynck and Hollard, 1980; Bultynck and Walliser, 2000; Morzadec, 2001; El Hassani, 2004). This rock unit is composed of calcareous shale interbedded with limestone or calcareous mudstone that is either nodular or layered, in this section (Fig. 2-2.1). The locality has been considered to be late Emsian to Eifelian in age (Hollard, 1967;1978; Bultynck and Hollard, 1980; Bultynck and Walliser, 2000; Becker et al., 2004; Jansen et al., 2004). Though the three new species to be discussed are all from the same section, they come from two different horizons. *Timsaloproetus dibbanus* is from the ZGEE1 bed, and *T. elguerrouji* and *T. haasi* occur in the ZGEE3 horizon. These horizons are stratigraphically 54.5 meters apart (Figure 2-2.1). The horizons are either nodular (ZGEE1) or layered (ZGEE3) argillaceous calcareous mudstone (note that Chatterton et al. are discussing the age and taphonomy of these beds in detail elsewhere in a work in progress). In summary, based on goniatites and trilobites, ZGEE1 is upper Emsian and ZGEE3 is Eifelian. This matches the ages of other sections through the Timrhanrhart Formation nearby where conodonts have also been found (Bultynck and Hollard, 1980; Becker et al., 2004; Jansen et al., 2004).

We have included silicified specimens of *Timsaloproetus haasi* (Alberti, 1971), obtained from the Timrhanrhart Formation near the base of a section near Zguilma, in this work. Rare silicified specimens of *Timsaloproetus elguerrouji* new species were obtained from the same level (NZ10). We called this section 'near Zguilma', and samples from it are labeled with the acronym NZ. From the trilobites and other fossils occurring in the 'near Zguilma' section, the lithologies present, and its stratigraphic position relative to other rock units, we have concluded that the trilobite-bearing beds may be correlated with horizon ZGEE3 of the Zguilma section, and that the base of the "near Zguilma" section is younger than the base of the section at Zguilma. The GPS coordinates for a point near the middle of the 'near Zguilma' section are: N 29° 45' 04.7"; W 06° 42' 20.2".

SYSTEMATIC PALEONTOLOGY

Most of the morphological terms used here are defined in the glossary of the revised trilobite Treatise on Invertebrate Paleontology (Whittington & Kelly, 1997). Some terms, more specific to proetid trilobites, are taken from Owens (1973), in particular, some measurements of the cephalon and pygidium (Figure 2-3). The names for the overall shape of the glabella ($A_1 + A_4$) and pygidium follow Šnajdr (1980).

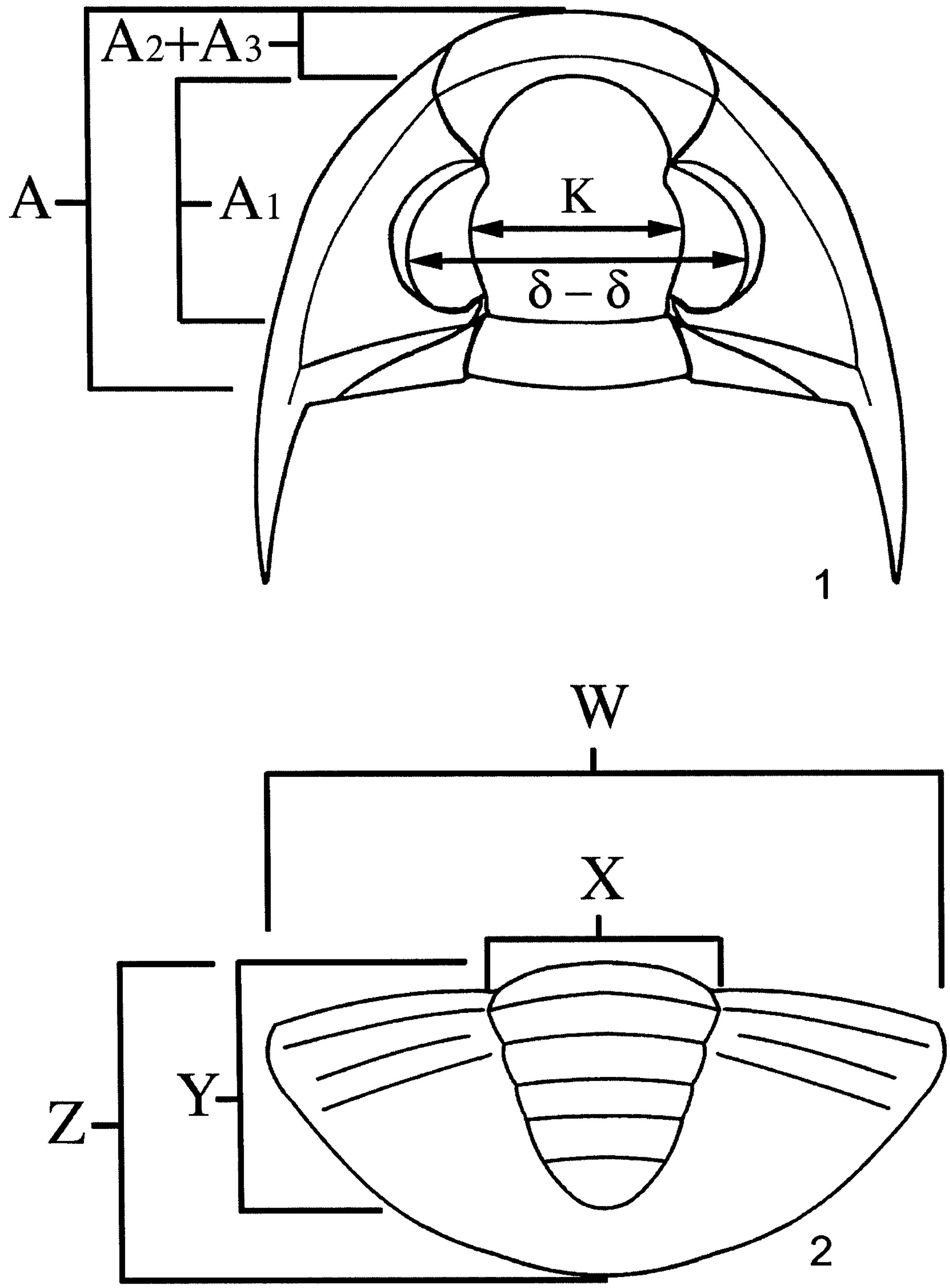

FIGURE 2-3--Diagrams showing some of the measurements of cephalon and pygidium used in descriptions of *Timsaloproetus* (modified from Owens, 1973). *1*, Labels for cephalon. *2*, Labels for pygidium.

Order PROETIDA Fortey and Owens, 1975

Family CORNUPROETINAE R. and E. Richter, 1956

Genus TIMSALOPROETUS new genus

Type species.— *Sculptoproetus haasi* G. ALBERTI, 1971, p. 373-374, pl. 1, figs. 1-3, from strata of Eifelian age in Germany.

Other included species.— *Timsaloproetus elguerrouji* new species and *Timsaloproetus dibbanus* new species.

Diagnosis.— Entire exoskeleton is sculpted with fine subparallel terrace ridges. In some species, terrace ridges are associated with defined pustules. Anterior border slopes downward forward, and is oriented at angle of 20°-30° to horizontal (in lateral profile, assuming palpebral lobe is horizontal). Preglabellar field is short to absent medially (sag.), and weakly convex. Anterior border furrow is shallow, little more than change in angle between anterior border and preglabellar field. Glabella is pear- to violin-shaped. Width across occipital ring (tr.) is equivalent to maximum width of glabella farther forward. Palpebral lobes are set just in front of S0.

Thorax is comprised of nine segments.

Pygidium has comparatively long axis composed of articulating half ring, four rings and terminal piece. Postaxial lobe is present immediately behind axis. Up to four pleural furrows are discernible, though last two are poorly defined, and only anteriormost pleural furrow is distinct. Pygidial border is weak.

Etymology.— *Timsâl* is Romanized Arabic for sculpture, acknowledging similarity/relationship to *Sculptoproetus*.

Occurrence.— Lower Middle Devonian of the Rheini Slate Mountains, Germany (Alberti, 1971; Alberti, 1983; Basse, 1997), lower Middle Devonian (Eifelian) at bou Dib, southern Morocco and upper Lower Devonian (Emsian) and lower Middle Devonian (Eifelian) at and near Jbel Gara el Zguilma, southwestern Morocco.

Discussion.— Erben (1951) proposed *Cornuproetus (Sculptoproetus)*, based upon the type species *Proetus sculptus* Barrande, 1846, though his diagnosis was less than complete. Alberti (1969) expanded upon Erben's (1951) work, but Šnajdr (1980) provided the most comprehensive diagnosis for *Sculptoproetus* to date. It is from Šnajdr's (1980) diagnosis, and the features of the type species of *Sculptoproetus,* that we conclude that *Sculptoproetus haasi* Alberti, 1971 and the Moroccan specimens described herein should be assigned to a new genus, *Timsaloproetus*. Devonian Proetidae have been split fairly finely at the generic level. Our recognition of *Timsaloproetus* as a distinct genus fits within this tradition. Eventually, a phylogenetic analysis needs to be completed for a large number of cornuproetine species in order to determine just how many genera should be recognized. Such an analysis is beyond the scope of the present work.

There are a number of differences between *Sculptoproetus* and *Timsaloproetus*. The preglabellar field in *Sculptoproetus* is marginally convex to nearly flat and has a very distinct anterior border furrow, while the anterior border is moderately convex (Šnajdr, 1980). *Timsaloproetus*, on the other hand, has a convex preglabellar field in lateral view and a weak (shallow) anterior border furrow that is only differentiated medially by a change in slope and the slight convexity of the anterior border. The preglabellar field of *Sculptoproetus* is shorter (sag., exsag.) than that of *Timsaloproetus*. The lateral portion of the preglabellar field (anteriormost portion of fixed cheek) forms more of an equilateral triangle (exsag.) in *Timsaloproetus* than in *Sculptoproetus,* which portrays more of an elongate triangle that is narrower (tr.) than that of *Timsaloproetus*. The angle between β, γ and the exsagittal line is greater (exsag.) in *Timsaloproetus*; and the angles between γ to δ to ε also differ from those of *Sculptoproetus*. The glabellar shape of the type species of *Sculptoproetus*, *S. sculptus* (Barrande, 1846), is ovoid (Šnajdr, 1980), while *Timsaloproetus* demonstrates a pear-shaped or violin-shaped glabella (Šnajdr, 1980). The occipital ring of *Sculptoproetus* is wider than the glabella (tr.) farther forward, while in *Timsaloproetus* the maximum width (tr.) of the glabella (K) in front of S0 is equivalent to the width (tr.) of the occipital ring.

The pygidial axis of *Sculptoproetus* was described as short by Šnajdr (1980), whereas *Timsaloproetus* has a longer axis that comprises 0.71 to 0.77 of the pygidial length (Z, sag.). *Timsaloproetus* does not demonstrate a moderately vaulted profile for the pygidial region as Šnajdr (1980) described for *Sculptoproetus*, but is more flattened with only a slight convexity. The pleural furrows were described for *Cornuproetus (Sculptoproetus)* by Alberti (1969) as consisting of 2+1, but it can be observed on *Timsaloproetus* that the pleural furrow number can be as high as 3+1. This number appears to increase with an increase in size; therefore previously assigned small, disarticulated pygidia that have a 2+1 pattern should be reexamined for synapomorphies consistent with *Timsaloproetus*. This is not always a reliable character, as the more posterior furrows on the pleural lobes are very shallow, and only discernible on well-preserved specimens.

TIMSALOPROETUS HAASI (Alberti, 1971)

Figures 2-4.1-2-4.11, 2-5.1-2-5.10, 2-6.1-2-6.14, 2-9.3, 2-9.5-2-9.8, 2-9.10. 2-9.13

1971 *Cornuproetus (Sculptoproetus) haasi* G. ALBERTI, 1971, p. 373-374, pl. 1, figs. 1-3.

1983 *Sculptoproetus haasi* G. ALBERTI, 1971: Alberti, p. 26, pl. 5, fig. 47.

?1994 *Sculptoproetus haasi* G. ALBERTI, 1971: Basse, pl. 1, fig. 9.

?1997 *Sculptoproetus haasi* G. ALBERTI, 1971: Basse, p. 93, pl. 5, fig. 17.

Diagnosis.— Facial suture flares distinctly forward from γ to β. Palpebral lobe is wide and long. Distinct vertical drop, but only slight lateral displacement, occurs in facial suture from ε to ξ. Anterior margin of cranidium is weakly convex forward medially. Anterior pleural band on thoracic segments drapes over posterior band; and anterior pleural band is longer (exsag.) than posterior pleural band on thoracic segments. Axial rings on pygidium have a slight *m*-shape, therefore are convex backward at midline. Sculpture consists of fine terrace lines, without any tubercles or pustules.

Description.— Overall exoskeleton is only moderately inflated, except for axis of thorax and pygidium. Cephalon has overall shape of semicircle (almost precisely if occipital ring is excluded), with genal spines extending posteriorly. Cephalon length (A, sag.) in relation to entire exoskeleton length is 0.36. Maximum width of cephalon is located at genal angle or across genal spines, and ratio of cephalon length (sag.) to width (tr.) is 0.55. Cephalon is ornamented with fine terrace ridges that sometimes anastomose. Anterior and lateral margins have 3-4 ridges and grooves. Most dorsal marginal ridge is asymmetrical, but recurring ridges are symmetrical. Anterior border has appearance of segment of circle, with shallow anterior border furrow, and is marginally convex and down turned. Terrace lines on anterior border sweep anteromedially from lateral edges, but medial terrace lines are near transverse. Anterior border length comprises 0.10 of length of cephalon (A, sag.). Preglabellar field and anterior border (A_3+A_2, sag.) comprise 0.18 of cephalon length (A, sag.). Preglabellar field is short medially (0.08 of cephalon length, sag.), and it flares laterally to form rotated equilateral triangle. Axial and preglabellar furrows are incised distinctly. Glabella (A_1) forms flared pear or nostril shape, with slight pinching of sides of glabella at γ-γ, and with straight (tr.) posterior margin. Glabellar length (A_1, sag.) to width (K, tr.) ratio is 1.06, and glabellar length (A_1, sag.) to cephalon length (A, sag.) is 0.63. Terrace lines on glabella follow general shape of glabella, though posterior terrace lines are more tightly convex forward medially. Glabella (A_1) is slightly convex (sag. and tr.). Glabellar furrows are not defined, but glabella inflates slightly in region of L1, though lobe is not clearly defined. Palpebral lobes have kidney-shaped appearance, with lobes sloping inward; and they lobes have weak terrace lines that anastomose. Ratio of maximum width of glabella to δ–δ is 0.64 (tr.), and ratio of δ to δ (tr.) to cephalon length (A, sag.) is 0.93. Occipital ring (A_4) gently arches posterodorsally in lateral profile, and posterior margin drops off vertically. Viewed dorsally, occipital furrow (S0) is deep and transverse. Occipital ring (A_4) length comprises 0.17 length of cephalon (sag.); occipital ring width (tr.) to cephalon width (tr.) ratio is 0.33; and occipital ring width (tr.) in relation to δ to δ (tr.) is 0.64, equivalent to width of glabella (tr.) at K. Terrace ridges on occipital ring arch forward around median node or pustule. Posterior border is short, comprising 0.12 (exsag.) of cephalon length (sag.), with almost transverse terrace ridges. Posterior border furrow is deeply incised, and joins lateral border furrow at approximately 63°. Posterior and lateral border furrows merge, and extend as shallow furrow backward on genal spine. This furrow disappears approximately midway along spine. Facial suture diverges posterolaterally from α towards β; it converges posteromedially from β to γ; it diverges posterolaterally from γ to δ; it converges posteromedially from δ to ε (not accounting for curvature around palpebral lobe); ε to ξ displays weak sutural ridge abaxial to suture; suture diverges from ε to ξ posterolaterally; and suture diverges posterolaterally from ξ to ω (not accounting for slight convex forward curvature that peaks midway between ξ and ω). Eye is kidney-shaped, with ratio of maximum length (exsag.) in relation to glabella length (A_1, sag.) of 0.59 and to cephalon length (sag.) of 0.37. Distinct eye socle and shallow eye socle furrow are present. Genal field width (from eye socle furrow to lateral border furrow, adjacent to δ) in relation to δ–δ is 0.17. Genal field is covered with fine terrace lines that are oriented almost parallel to posterior border furrow. Lateral border furrow is moderately incised. Lateral border is sculpted with fine terrace lines. Upon genal spine, terrace lines converge within amalgamation of posterior and lateral border furrow in shallow U-shape and become indistinct posteriorly. Width across genal spines in relation to maximum cephalon width (tr.) is near equal (0.99); genal spine length (exsag.) from midpoint on occipital ring to end of spine in relation to cephalon length (sag.) has ratio of 0.74; and genal spine length (exsag.) in relation to thoracic length (sag.) is 0.61.

Hypostome described here was obtained from silicified material in 'near Zguilma' section that contains *Timsaloproetus haasi,* as far most common proetid. Hypostome is shield shaped. Length of hypostome is 1.48 times width preserved. Posterolateral corners have distinct, short, rounded and posteriorly directed marginal spines. Anterior margin is distinctly convex forward, and is downturned (ventrally), particularly medially. Outline of hypostome is only slightly pinched inward at antennal notches. Width across rounded shoulders is almost equal to that across anterior wings (although these may not be complete). Posterolateral margins, behind shoulders, are slightly convergent backward, and slightly concave outward. Posterior margin, between marginal spines, is slightly convex backward. Lateral and posterior border furrows are continuous and moderately impressed. Anterior border furrow is shallow. Middle body is poorly differentiated by very shallow middle furrows into short, smooth, slightly inflated, crescent shaped posterior lobe, and much longer, shield shaped anterior lobe. Maculae are weakly discernible. Anterior portion of anterior lobe is pinched into a moderately, ventrally elevated rhynchos that is most pronounced near front, just behind anterior border furrow. Sculpture is of prominent terrace lines that converge forward to top of rhynchos on anterior half of anterior lobe of middle body, some short terrace lines that run roughly exsagittally adjacent to and in region of anterior border furrow, and some terrace lines that are most prominent on lateral border opposite antennal notch. These latter terrace lines spread out across ventral portions of anterior wings, and disappear or become inconspicuous at shoulder and farther back. Posterolateral and posterior borders are almost smooth.

Thorax has 9 segments, and length (sag.) in relation to entire exoskeleton length (sag.) is 0.44, while the maximum thoracic width is attained across first thoracic segment. Length (sag.) to width (tr.) ratio for thorax is 0.80. Axial region is inflated, and tapers by 33%, from anterior to posterior, to 67.4% of anterior width (tr.). Individual axial rings of thoracic segments, in lateral profile, have dorsally convex forward slope and near vertical posterior margins, and so whole thoracic axis appears imbricated. Prosopon on axial rings of thorax consists of fine terrace lines that arch forward medially, and terrace lines that parallel this pattern laterally. Axial furrows are firmly incised. Pleural regions of thoracic segments curve ventrally at fulcrum, and terminate distally with anterior part of segment rounded and posterior part pointed. Pleural furrows are shallow and become moderately incised distally. Pleural furrow disappears distally at articulating facet. Facet displays terrace lines that point abaxially. Anterior pleural band is shorter (exsag.) than posterior band, and terrace lines on anterior band are oriented at 45° (to exsag.), while posterior pleural band has terrace lines that are almost transverse along its posterior margin, but farther forward are oriented obliquely and parallel anterior pleural band prosopon.

Pygidial overall shape is that of segment of circle, though shape of axis is more rounded, and similar to axis defined by Šnajdr (1980) as parabolic. Pygidial length (Z, sag.) is 0.20 of entire length (sag.) of exoskeleton, and pygidial width (W, tr.) in relation to cephalon width (tr.) is 0.64 – hence pygidium is micropygous. Pygidial width is 2.16 times length (Z, sag.). Axial region width (X, tr.) is 0.31 of maximum pygidial width (W), and pygidial axial length (Y, sag.) is 0.77 of maximum pygidial length (Z). Axial width (X, tr.) decreases from anteriormost segment to posteriormost segment by 27.5%. Axis has inflated profile viewed laterally. In axis, there are four axial rings and terminal piece; first axial ring is transverse, while remaining three rings demonstrate more pronounced posterior protuberance on posterior margin. Terminal piece is rounded backward; and small postaxial lobe is present. Prosopon on pygidial axial rings is similar to that of thoracic axial rings, with medial anterior arching terrace lines. Axial furrows are firmly incised. Pleural region of pygidium is textured with fine terrace lines that are generally transverse to roughly parallel to posterior margin of pygidium. Pleural regions display extinguishing imbricate pleural rib pattern. Pleural and interpleural furrows are distinctly shallower towards back of pygidium. First pleuron is defined by moderately deep pleural furrow, accentuating anterior pleural band. Pleural and interpleural furrows disappear along weak pygidial border. Medial portion of pygidial pleural region is slightly convex (tr. and exsag.) and pygidium flattens progressively abaxially to pygidial border.

Type material.— Holotype, Mbg. 2076-2077 (complete specimen). Plesiotypes: UA13256, UA 13265 - UA13269, UA13272 - UA13275, UA 13269, UA13282 – UA13291.

Occurrence.— Lower Middle Devonian of the Rheini Slate Mountains, Germany (Alberti, 1971; Alberti, 1983; Basse, 1997); lowermost Middle Devonian, '*Harpes/Thysanopeltis* horizon' (=BD5), El Otfal Formation near bou Dib, southern Morocco; and Eifelian, Timrhanrhart Formation, horizon ZGEE3, '*Thysanopeltis/Leonaspis* horizon', Jbel Gara el Zguilma, and NZ3.5-NZ10, 'near Zguilma' section, near Foum Zguid, southern Morocco.

Discussion.— The Moroccan specimens that we assign to *T. haasi* from bou Dib, Zguilma and 'near Zguilma' are described above in detail because we have several well-preserved specimens available for study. The fact that the German type of this species and Moroccan specimens are of approximately the same size, with similar ratios with regard to exoskeleton measurements, supports our inclusion of the Moroccan material in this species, originally described from the Middle Devonian of Germany (Table 2-1).

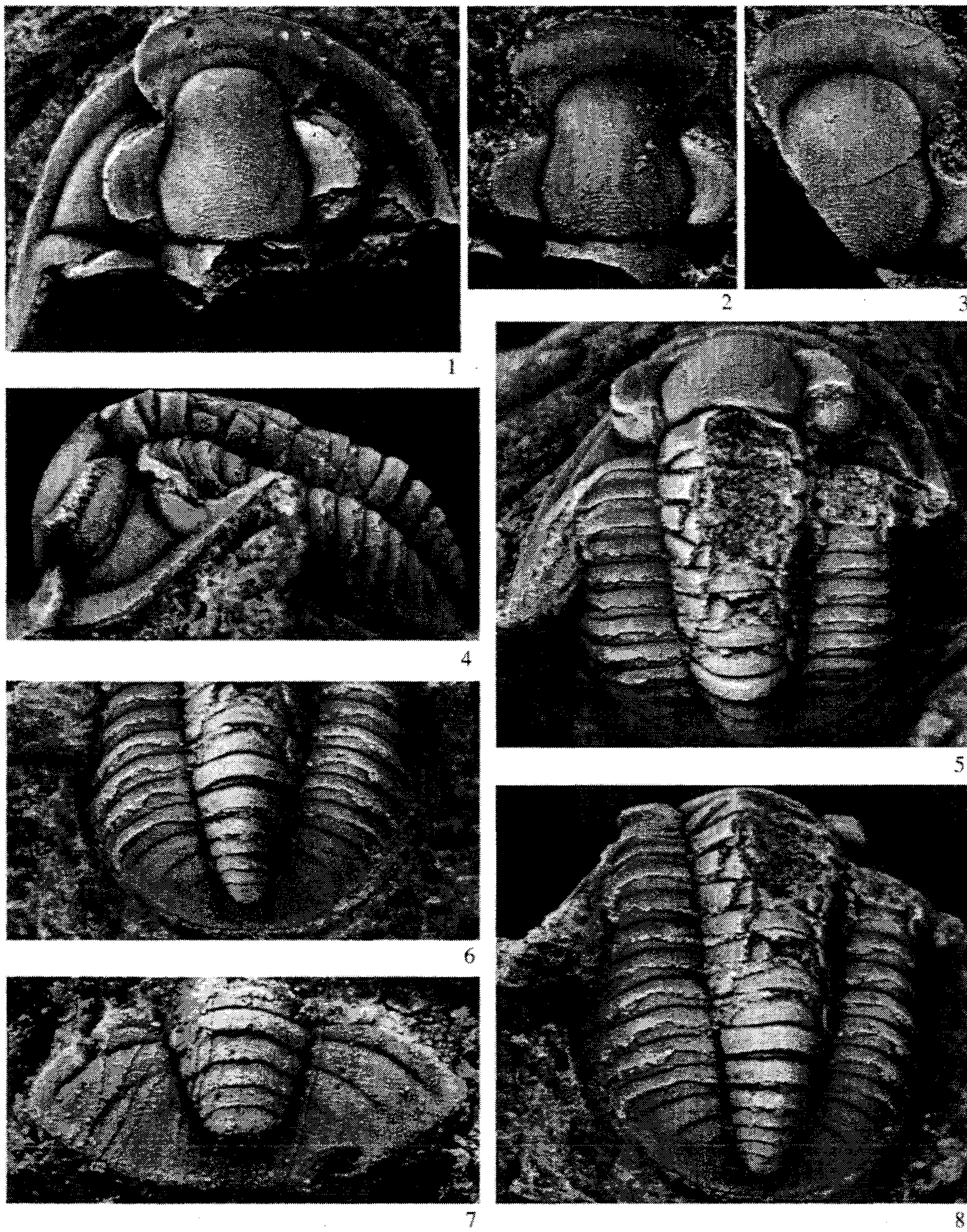

FIGURE 2-4—*1-8*, *Timsaloproetus haasi* (Alberti, 1971). All specimens are from bou Dib '*Harpes/Thysanopeltis* horizon' (BD5), El Otfal Formation, lower Eifelian, Ma'der Basin, southern Morocco. *1, 4-6, 8*, almost complete exoskeleton UA13272. *1*, dorsal view of cephalon X16.9; *4*, lateral view X13.9; *5*, dorsal view X15.6; *6*, dorsal view of posterior of thorax and pygidium X15.7; *8*, dorsal view minus cephalon X15.4. *2*, dorsal view of almost complete cranidium UA13275 X11.8; *3*, dorsal view of fragmented cranidium UA13274 X11.2; *7*, dorsal view of pygidium UA13273 X21.1.

FIGURE 2-5—*1-2, 4-6, 8, 9*, *Timsaloproetus haasi* (Alberti, 1971); '*Harpes/Thysanopeltis* horizon', El Otfal Formation, lower Eifelian, from bou Dib, Ma'der, southern Morrocco. Almost complete articulated individual UA13256. *1*, dorsal view X7.2; *2*, dorsal view X7.2; *4*, lateral view X6.5; *5*, dorsal view of crandium X18.6; *6*, oblique dorsolateral view X6.9; *8*, dorsal view of pygidium X21.3; *9*, dorsal view of cranidium X16.3. *3, 7, 10*, ZGEE3 horizon, Timrhanrhart Formation, lower Eifelian, Zguilma, southern Morocco. Damaged articulated exoskeleton UA13269. *3*, dorsolateral oblique view of cehalon X10.3; *7*, dorsal view X5.7; *10*, dorsal view of partial pygidium X11.7.

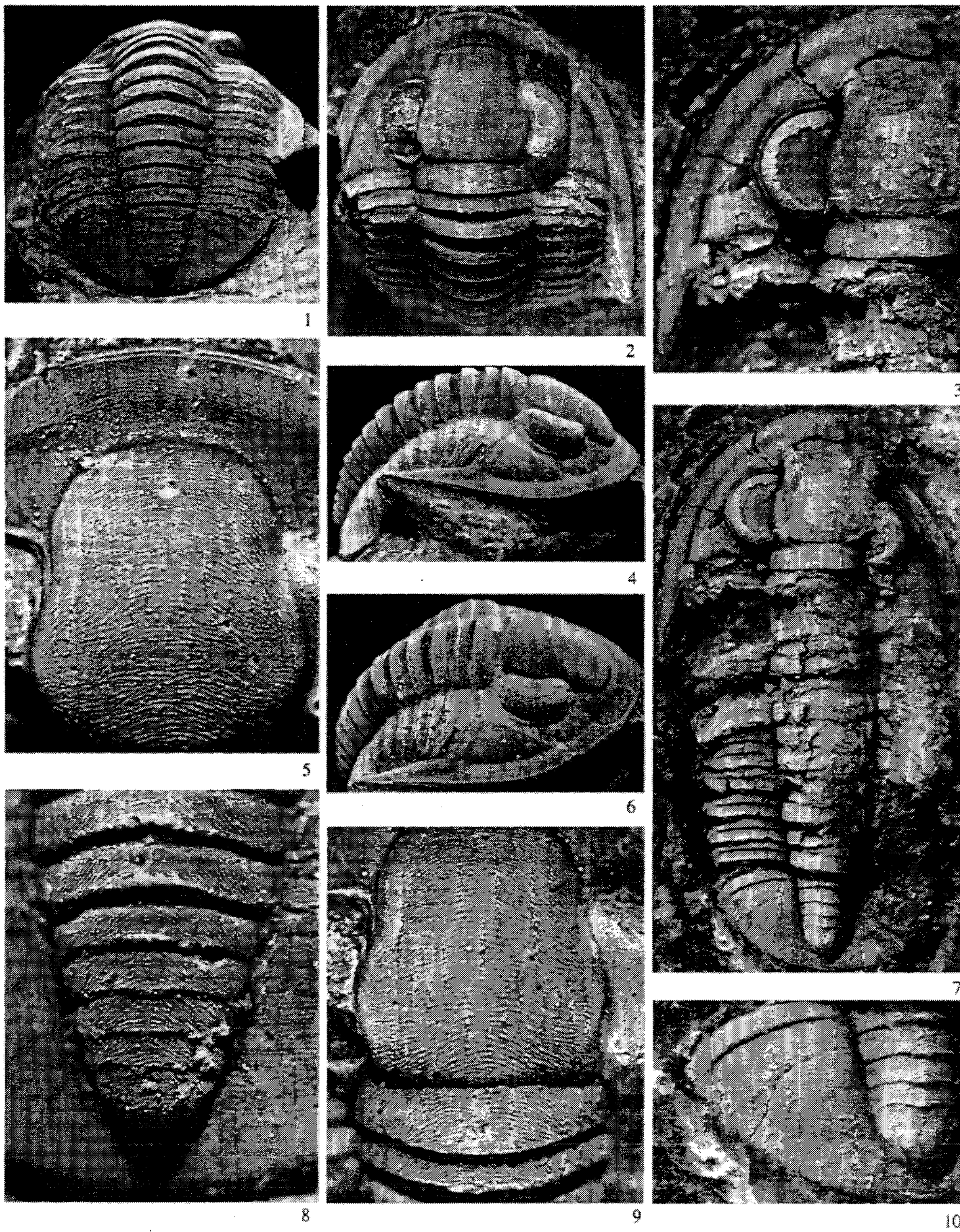
1
2
3
4
5
6
7
8
9
10

FIGURE *2-6*—*1-14, Timsaloproetus haasi* (Alberti, 1971), NZ10 horizon ('near Zguilma' section), Timrhanrhart Formation, lower Eifelian, near Foum Zguid, southern Morocco. *1, 3, 6*, cranidium UA13282. *1*, lateral view X15.4; *3*, dorsal view X22.2; *6*, anterior view X16.5. *2*, hypostome UA13283, ventral view X45.9; *4*, right free cheek UA13284, dorsal view, X25.4; *5*, right free cheek UA13285, dorsal view, X19.8; *7*, fragmented thoracic segment UA13286, ventral view X25.1; *8*, left free cheek UA13287, ventral view X23.1; *9, 11, 14,* pygidium UA 13288; *9,* lateral view X12.5; *11,* posterior view X16.6; *14*, dorsal view X16.8; *10,* fragmented hypostome UA13289, ventral view X30.5. *12,* fragmented thoracic segment UA13290, dorsal view X26.7; *13*, fragmented pygidium UA13291, dorsal view X18.3.

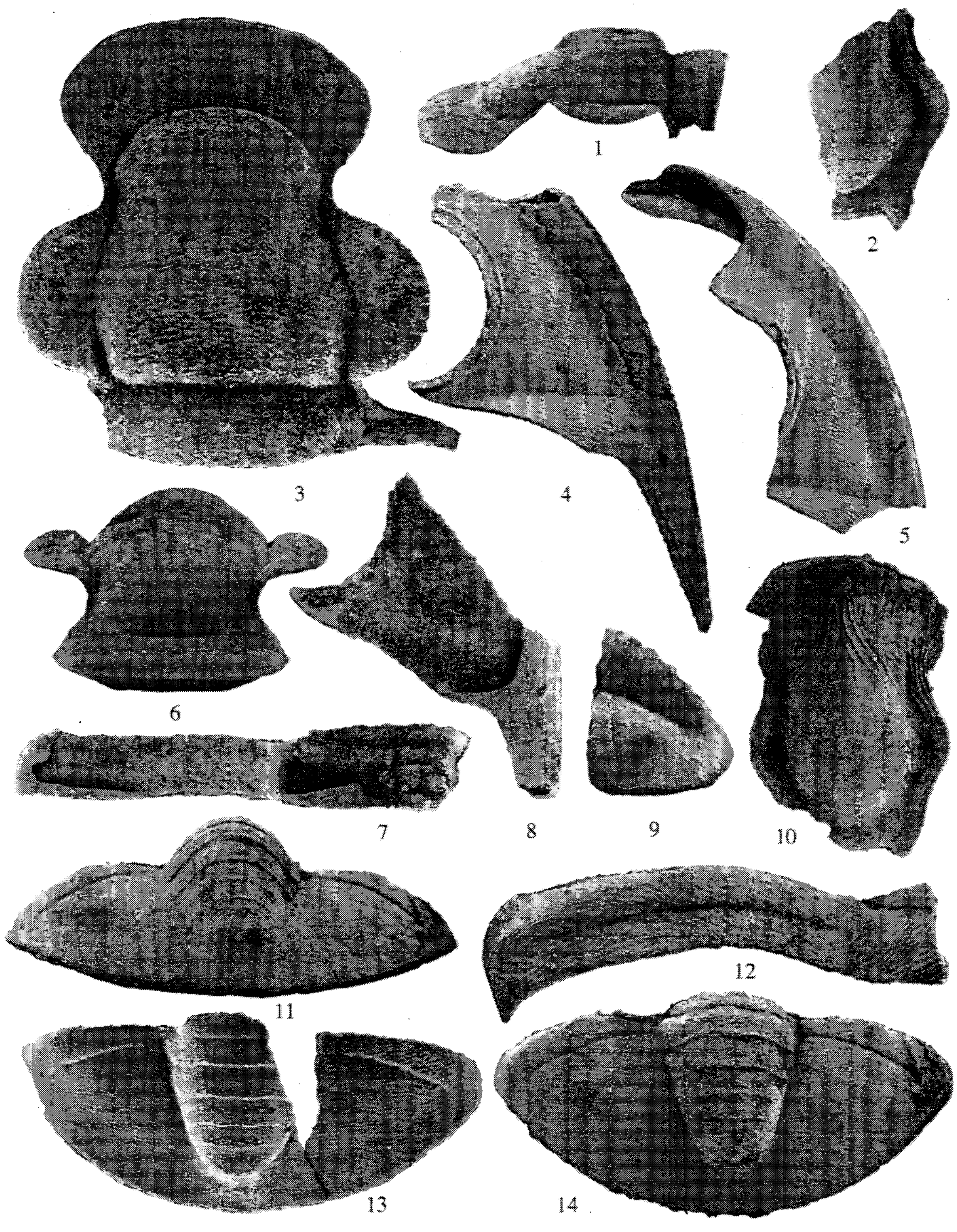
1
2
3
4
5
6
7
8
9
10
11
12
13
14

	German specimen	Moroccan specimen
Exoskeleton length (sag.)	9.8 mm	13.45 mm
Cranidium length (sag.)	4.0 mm	4.87 mm
Glabella length (sag.)	2.5 mm	3.07 mm
Eye length (exsag.)	1.7 mm	1.82 mm
Pygidium length (sag.)	2.2 mm	2.63 mm
Pygidium width (tr.)	4.9 mm	5.67 mm
Glabella (A_1) to Cranidium (sag.)	0.625	0.63
Pygidial length (sag.) to pygidial width (tr.)	0.449	0.464
Pygidial length to entire exoskeleton (sag.)	0.22	0.20

Table 2-1: Morphologic marker measurements and ratios in a comparison of *Timsaloproetus haasi* (Alberti, 1971) of Germany and that of Morocco (Moroccan specimen is from the bou Dib locality, UA13256).

Alberti (1971) observed that a number of the character states of his species, in particular the preglabellar field and anterior border, are different from those of the type species of *C. (Sculptoproetus)*. He also stated "the flat front seam (+ side seam)... like the entire front field [demonstrates] a clear inclination forward". He acknowledged that "the seam furrow [anterior border furrow] becomes visible thereby only as narrow shade after MgO dusting" (translated from Alberti, 1971).

Alberti (1971) contrasted a limited number of species with *T. haasi*, such as *C. (S.) sculptus sculptus* and *C. (S.) sculptus posterior*.

For comparison of *T. haasi* with *Timsaloproetus dibbanus* new species and *Timsaloproetus elguerrouji* new species, see below under the discussions of those species.

TIMSALOPROETUS DIBBANUS new species

Figures 2-7.1-2-7.12

Diagnosis.— Sculpture of fine subparallel terrace lines. Anterior border furrow is weakly convex forward, and curves more distinctly posterolaterally. Preglabellar field is short (sag.) and lateral portions are slightly pinched to give appearance of acute right angle triangle with hypotenuse curved along axial/preglabellar furrows. Anterior portions of facial suture are only weakly divergent forward from γ to β. Palpebral lobes are short and posteriorly oriented upon glabella (from near S0 to S2). Anterior margin of cranidium is distinctly convex forward medially. Pygidium has weak border and postaxial lobe. Axial rings on pygidium have slight elongate *m*-shape (tr.). Terminal piece of pygidial axis is subtransverse medially.

Description.— Cranidium is ornamented with fine anastomosing terrace ridges arched forward medially. Anterior margin has discrete ridges, and is distinctly convex forward. Anterior border is quarter moon shaped, weakly convex dorsally, and slopes forwards. Preglabellar furrow is shallow, but is slightly deeper laterally than medially. Terrace ridges on anterior border are curved into swirling pattern. Anterior border comprises 0.21 length of cranidium (A, sag.). Preglabellar field and anterior border (A_2+A_3, sag.) comprise 0.23 of length of cranidium (A). Preglabellar field is short medially (0.02 of cranidium length, A, sag.) and it flares laterally. Axial and preglabellar furrows are firmly incised. Glabella forms blunt, rounded bell shape, with length (sag.)/width (tr.) of 1.0/0.99, with slight pinching of sides of glabella adjacent to γ-γ. Anterior lobe of glabella is only slightly convex dorsally in lateral profile. L1 is weakly inflated. Slight disruptions or weakening of sculpture laterally are interpreted as S1 and S2. Length of glabella (A_1, sag.) is 0.62 of length of cranidium (A, sag.), and width across K (tr.) is 0.69 of width of δ-δ (tr.). Palpebral lobes are almost horizontal close to facial suture, but fixigena slopes steeply into axial furrows opposite eyes. Occipital ring length (A_4) comprises 0.15 length (sag.) of cranidium (A), and its width (tr.) is 0.69 of distance from δ–δ, exhibiting equivalent width (tr.) to that of glabella at K. Terrace ridges on occipital ring arch forward, around and under median pustule. Terrace ridges terminate along posterior margin of L0, creating finely pustulated/knobbed edge. Lateral (subsidiary) occipital lobes are partly delineated anteriorly by lateral occipital furrows of moderate depth that incise anterior half of occipital ring. Small median pustule, on occipital ring (L0), is posteriorly pointed, and situated at 0.66 length (sag.) of occipital ring (A_4) from occipital furrow (S0). Posterior border is short (exsag.), comprising 0.08 of cranidium length (A, sag.), and sculpted by terrace ridges running almost transversely. Facial sutures diverge from α to β, and then converge slightly posteromedially from β to γ. Palpebral lobes are distinctly convex laterally. Sutures pinch inward at ε, and then plunge ventrally between ε + ξ. Final segments of facial sutures, from ε + ξ to ω, are divergent posterolaterally.

Free cheeks, hypostome and thorax are unknown.

Pygidium is sculpted with fine terrace ridges that are generally aligned with shape of pygidium distally, but are transverse medially on pleurae, and convex forward on axis. Axial region is moderately inflated, and its length (Y) is 0.78 of pygidial length (Z, sag.). Width (X, tr.) of axis is 0.38 width of pygidium (W), and axis width tapers backward so posterior ring is approximately 0.64 of width of first (anterior) ring. Maximum pygidial width (W, tr.) is 2.41 times maximum pygidial length (Z, sag.). Axial furrows are deep. Axial region is composed of four rings and terminal piece. Terminal piece is dorsally arched (tr.) with low, traverse postaxial lobe. Anterior articulating half ring is 0.11 (sag.) of length of Y (sag.) and 0.83 of width (tr.) of X. Posterior margins of axial rings have shape of elongated, sigmoidal *m*'s that are more pronounced towards back of axis. Terrace lines on axial region are arched forward on each ring, in opposite direction to sagittal-backward directed aspect of *m*-shaped posterior margin of each ring. Distal part of anterior margin (beyond fulcrum) angles at 22° to transverse direction anteromedially from lateral corner of pygidium. First pleuron is accentuated by moderately deep pleural furrow. First interpleural furrow is shallow and much less defined, exhibiting an extinguishing imbricate pattern on pygidium. Second pleural furrow is at least as shallow, and second interpleural furrow is barely distinguishable. All pygidial furrows terminate laterally at barely distinguishable pygidial border. Pygidial border is longest (exsag.) adjacent to axis. Posterior border furrow is shallow. Posterior margin is slightly flattened.

Etymology.— *Dibbân* is Romanized Arabic for "fly": the Berbers refer to proetids as flies, "for they are as common as flies".

Types.— Holotype: cranidium UA13257; and three paratype pygidia: UA13258, UA13259, and UA13281.

Occurrence.— Upper Emsian, Timrhanrhart Formation of Jbel Zguilma, south of Foum Zguid in southern Morocco, in the ZGEE1 horizon (Figure 2-2.1).

Discussion.— *Sculptoproetus maghrebus* ALBERTI, 1967b, occurs in strata of similar age in southeastern Morocco. There are, however, a number of character states that differentiate *T. dibbanus* from *S. maghrebus*. Some character states that differentiate *S. maghrebus* from *T. dibbanus* include, in the former species, a different profile of the anterior border (much more dorsally convex), a longer preglabellar field, the facial suture shape and more defined glabellar furrows. Unfortunately only the cranidium has been described for *S. maghrebus;* therefore, further comparisons cannot be made.

Timsaloproetus dibbanus differs from the type species, *T. haasi,* in the following character states: the front of the cranidium is not as expanded forward (does not flare forward as much between γ and β); the eyes are smaller, with the back of the palpebral lobes slightly farther forward; the front of the cranidium is more tightly convex forward; and the furrows on the pleural lobes of the pygidium are shallower and less conspicuous. In other respects, these two species are very similar, and *T. dibbanus* could well be the ancestor of *T. haasi.*

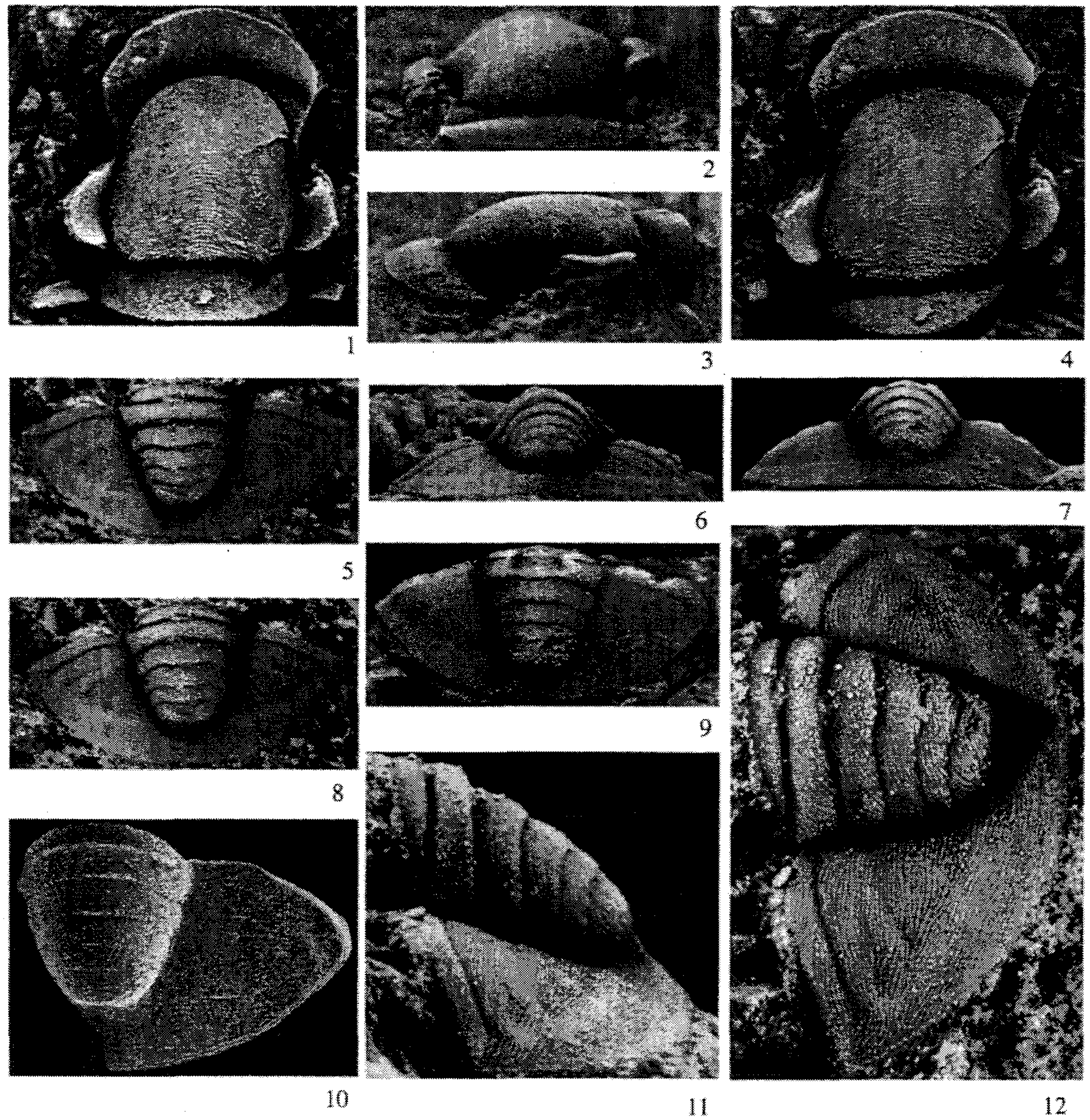

FIGURE 2-7—*1-12*, *Timsaloproetus dibbanus* new genus and species. ZGEE1 horizon, Timrhanrhart Formation, upper Emsian, from Zguilma, southern Morocco. *1-4*, cranidium UA13257: *1*, dorsal view X11.1; *2*, anterior view X10; *3*, lateral oblique view X10.5; *4*, dorsal view X11.2. *5-6, 8, 11-12*, pygidium UA13258: *5*, dorsal view X10.6; *6*, posterior view X10.1; *8*, dorsal view X10.3; *11*, lateral view X25.2; *12*, dorsolateral oblique view X21.5. *7, 9*, pygidium UA13259: *7*, posterior view X10.7; *9*, dorsal view X10.9. *10*, incomplete pygidium UA13281, dorsal view X22.8.

For comparisons between *T. dibbanus* and *Timsaloproetus elguerrouji* new species, found higher in the same section, see below under the discussion of the latter species.

TIMSALOPROETUS ELGUERROUJI new species

Figures 2-8.1–2-8.7, 2-9.1–2-9.2, 2-9.4, 2-9.9, 2-9.11-2-9.12

Diagnosis.— Center of anterior border has transverse ovoid pattern of swirling terrace lines. Palpebral lobes are fringed with short ridges breaking up into pustules. Glabellar furrows S1, S2 and S3 are distinct. Glabella is ornamented by both terrace lines and small, posterodorsally directed tubercles that are also found clustered around median node on occipital ring; fine pustules are scattered sparsely on posterior half of genal field and posterior border. Anterior margin of cranidium is moderately convex forward medially. Thoracic and pygidial axial rings have elongate (sag.) median tubercle or ridge. Thoracic axial rings and posterior pleural bands also possess row of pustules along posterior margin (smaller on pleurae). Pygidial border is weakly expressed.

Description.— Exoskeleton is slightly dorsoventrally compressed in pleural regions, but axial regions of thorax and pygidium are moderately inflated. Generalized cephalon shape is semicircle with posterolateral corners drawn out into genal spines that are directed slightly posterolaterally. Length of cephalon (A, sag.) in relation to entire exoskeleton length is 0.39. Maximum width of cephalon (tr.) cannot be ascertained due to absence of posterior (distal) regions of genal spines in specimens available. Cephalon ornament consists of fine terrace ridges that anastomose, and are associated with scattered small tubercles. Tubercles are asymmetrical, pointed, and project dorsally and backward. Anterior and lateral margins exhibit 2 ridges and intermediate groove along most of edge. Anterior and lateral borders are curved, and of equal width/length (radial). Anterior border and preglabellar field (A_2+A_3) comprise 0.14 to 0.16 of cephalon length (A, sag.). Terrace ridges on anterior border appear to swirl around transverse ellipse; fine ridges on lateral part of anterior border and on lateral border run roughly perpendicular to margin. Anterior and lateral borders are ventrally inclined (slope outward) at a moderate angle. Border furrows, both anterior and lateral, are moderately impressed posterolaterally, but shallower anteromedially so anterior border furrow is very shallow in front of glabella. Extremely short preglabellar field (sag.) flares laterally into a triangular shape on anterior aspect of fixed cheek. Glabella is violin-shaped. Glabellar length (A_1, sag.) is similar to width (K, tr.); and glabellar length (A_1) to cranidium length (A) ratio is 0.64. Prosopon on frontal lobe of glabella (A_1) is composed of terrace lines that mimic shape of front of glabella, tightening into forward arching lines posteromedially. Some terrace lines are interrupted by tubercles congregated within medial region of frontal lobe of glabella (A_1). Tubercles are absent or sparse laterally (a few scattered on proximal part of L1), and diminish to smaller pustules more sparsely distributed on anterior region of A_1. Most prominent tubercles, within posteromedian region of A_1, are asymmetrical, sloping backward. Intermittent pustules, located farther forward, are more vertically inclined. S1 is clearly incised posteriorly, and it flares and shallows anteriorly. It is oriented aterally, at approximately 27° to exsagittal line, and disappears close to S0 and firmly impressed axial furrows. Gently incised S2 runs inward and slightly backward, at angle of 32° to transverse line, from slightly behind γ. S3 is as clearly incised as S2, and oriented 17° anteromedially from transverse, distally ending adjacent to γ. S3 terminates laterally some distance from axial furrows, and is short, and does not extend anywhere near median part of glabella. L1 is elongate, slightly bulbous, oriented posteromedially to anterolaterally, and merges with L2 laterally. L2 is also elongate though more transverse and more posteromedially recurved. L3 is only discernible through being bounded by S2 and S3. Palpebral lobes are kidney-shaped, with medial portion sloping inward, and with sculpture of terrace lines mimicking generalized shape of back of palpebral lobe. Palpebral lobe is fringed with radial ridges breaking up into pustules. Glabellar width (K, tr.) to δ-δ ratio is 0.71, and cranidial length (A, sag.) to δ-δ (tr.) ratio is 0.89. Occipital furrow (S0) is deep and transverse. Occipital ring is strongly vaulted dorsally. Lateral (subsidiary) occipital furrows are shallow, short, and extend backward and inward from S0 to form apostrophe shape on left side (of trilobite) and mirror image on right side. Terrace lines on occipital ring are arched forward. Median node is situated at midlength of occipital ring, and it is surrounded by concentration of fine pustules. Lateral, subsidiary occipital lobes are not defined by independent swelling. Axial furrows are deeply incised. Posterior margin of occipital ring is sculpted with continuous row of pustules, projecting posterodorsally. Similar pustules occur on back of posterior border. Posterior border is short (exsag.), comprising 0.10 of total cephalon length (A, sag.). Posterior border terrace lines are subtransverse, though slightly posteriorly curved distally, simulating shape of border. Posterior border furrow is deeply incised, and merges with lateral border furrow of similar depth at genal angle.

Facial sutures diverge from α to β; from β to γ they converge; from γ to δ they diverge; from δ to ε they converge; from ε to ξ they diverge slightly, though drop steeply ventrally to ξ; and from ξ to ω they diverge strongly. Eye is kidney-shaped, with maximum length (exsag.) in relation to glabellar length (A_1) (sag.) of 0.48, and to cephalon length (A) (sag.) of 0.30. Lenses are clearly visible on eye and display diagonal packing pattern when viewed laterally. Eye socle is prominent and narrow. Width of genal field (from eye socle to lateral border furrow, adjacent to δ) in relation to δ-δ is 0.22. Eye socle is surrounded by two distinct furrows. Two lobes (crescent or "eyelid" shaped) occur on proximal part of genal field, adjacent to anterior and posterior regions (1/3) of socle. These lobes are weakly inflated and are smooth or have sculpture suppressed so terrace lines are similar to but much lower than those of rest of genal field. Sculpture on genal field is of anastomosing terrace lines running outward and backward, but becoming more transverse distally. Area adjacent to posterior corner of genal field has few distinct but minute pustules. Lateral border furrow is moderately incised. Lateral and posterior furrows merge then extend as distinctly shallower furrow onto outer surface of genal spine, disappearing distally some distance along spine. Lateral border sculpture is of terrace lines perpendicular to lateral border furrow, continuous with distal ends of terrace lines on genal field. Genal spines continue transverse terrace line pattern virtually uninterrupted from posterior border and posterior aspect of lateral border. Genal spine is slightly shorter than gena farther forward.

Hypostome is unknown.

Thorax consists of nine segments. Thorax length (sag.) in relation to entire exoskeletal length (sag.) is 0.40. Thorax overall profile is of arched axial region, deep axial furrows, near horizontal pleural regions out to fulcrum, and then ventrolateral downturning of distal parts of segments. Terminal ends of thoracic segments are pointed backward, with rounded anterior margin. Axis tapers in width slightly backward, so ninth axial ring is 35-40% of width of first axial ring. Axial region profile, in lateral view, displays each ring as convex anterodorsally, rising to posterior edge, with imbricate pattern apparent for whole thorax. Axial region is sculpted with terrace lines that arch forward across sagittally elongated median tubercle and ridge. Tip of median tubercle/ridge is posterodorsally directed. Posterior margins of segments have row of tubercles. Pleural furrows are moderately incised. Anterior pleural band is short (exsag.), with terrace lines oriented at roughly 45° to adjacent axial furrow, in anterodistal direction. Articulating facet forms transversely elongate triangle lacking in ornamentation. Terminal section of anterior pleural band is posteriorly pointed, with approximately 2-3 terrace lines skirting edge of segment. Posterior pleural band is longer than anterior pleural band (exsag.). Ornamentation on posterior pleural band is of slightly forward arched terrace lines.

Pygidial shape is segment of circle, with posterior margin faintly flattened. Pygidial length (Z, sag.) in relation to entire length of exoskeleton is 0.18-0.20, and pygidial width (tr.) in relation to δ–δ width ratio is 1.25. Cephalon width (tr.) in relation to pygidial width (tr.) could not be provided due to loss of distal parts of genal spines. Pygidium is micropygous. Pygidial width (tr.) is from 2.16 to 2.25 of pygidial length (sag.). Axis is composed of articulating half ring, four axial rings and terminal piece. Terminal piece is rounded in front of small postaxial lobe. Axial region width (X, tr.) of pygidium to maximum pygidial width (W, tr.) ratio is 0.32, and axial length (Y, sag.) to pygidial length (Z, sag.) is 0.71 to 0.82. Fourth axial ring is 26-37% narrower (tr.) than first axial ring. Axis, viewed laterally, has inflated profile. Each axial ring has elongate median tubercle and forward arching terrace lines (similar to those on thoracic axial rings). Axial furrows are acutely incised. Pygidial pleural region is sculpted with subtransversely aligned terrace lines. 3+1 pleural furrows decrease in depth backward: first pleural furrow is well defined, accentuating anterior pleural band; first interpleural furrow is lightly incised; second pleural furrow is slightly incised; second and third interpleural furrows are faint; third pleural furrow is lightly incised; and fourth pleural furrow is almost indiscernible. Both pleural and interpleural furrows terminate laterally within weakly defined pygidial border. Medial portion of pygidial pleural region is marginally convex (tr. and exsag.) and pleuron progressively flattens abaxially within pygidial border.

Etymology.— Named for Hicham El Guerrouj, great Moroccan distance runner.

Type.— Holotype: complete specimen UA13262; Paratypes: complete specimen UA13260, cranidium UA13261 and right free cheek UA13263.

Occurrence.— Timrhanrhart Formation of Jbel Zguilma, south of Foum Zguid in southern Morocco, in the ZGEE3 horizon, of Eifelian in age (Figure 2-2.1).

Discussion.— The obvious tubercles scattered on the cephalon, the defined glabellar furrows and the median tubercles/ridges on the occipital ring and the thoracic and pygidial axial rings clearly differentiate *T. elguerrouji* from both *T. haasi* and *T. dibbanus*. The palpebral lobes of *T. elguerrouji,* both in size and sculpture, differ from those of *T. haasi*. The anterior portions of the facial suture in *T. elguerrouji* are more flared forward than those of *T. dibbanus* and less flared forward than those of *T. haasi*. The anterior margin of the cranidium is more curved than that of *T. haasi* and less curved

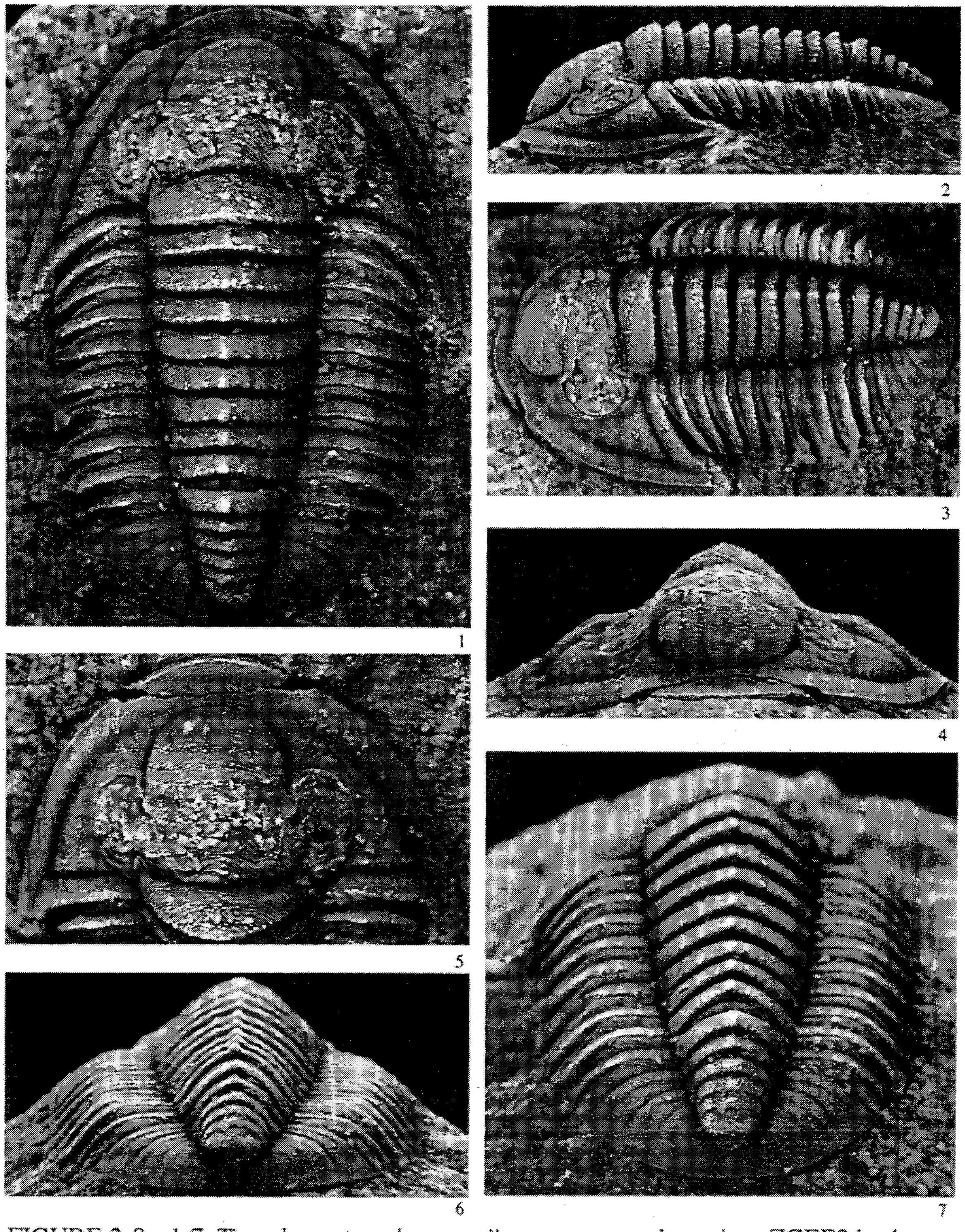

FIGURE 2-8—*1-7*, *Timsaloproetus elguerrouji* new genus and species. ZGEE3 horizon, Timrhanrhart Formation, upper Emsian, from Zguilma, southern Morocco. Almost complete articulated individual, holotype, UA13262. *1*, dorsal view X8.6; *2*, lateral view X8.1; *3*, dorsolateral oblique view X6.9; *4*, anterior view X10.4; *5*, dorsal view X11.4; *6*, posterior view X11.2; *7*, posterodorsal view X11.1.

FIGURE *2-9*—All specimens are from ZGEE3 horizon, Timrhanrhart Formation, lower Eifelian, Zguilma, southern Morocco. *1-2, 4*, *Timsaloproetus elguerrouji* new genus and species. *1*, left free cheek UA13263, dorsal view X15.5. *2, 4*, cranidium UA13261: *2*, dorsal view X9.6; *4*, lateral view X9.9. *9, 11-12*, incomplete exoskeleton UA13260: *9*, anterolateral oblique view, X5.3; *11*, dorsal view, X7.5; *12*, dorsal view, X7.2. *5-13*, *Timsaloproetus haasi* (Alberti, 1971). *3, 7*, cranidium UA13265. *3*, dorsal view X15.4; *7*, lateral view X14.5. *5-6*, cranidium UA13267: *5*, lateral view X11.7; *6,* dorsal view X11.2. *8, 10*, pygidium UA13268: *8*, posterior view X14.7; *10*, dorsal view X15.3. *13,* pygidium UA13266, dorsal view X9.4.

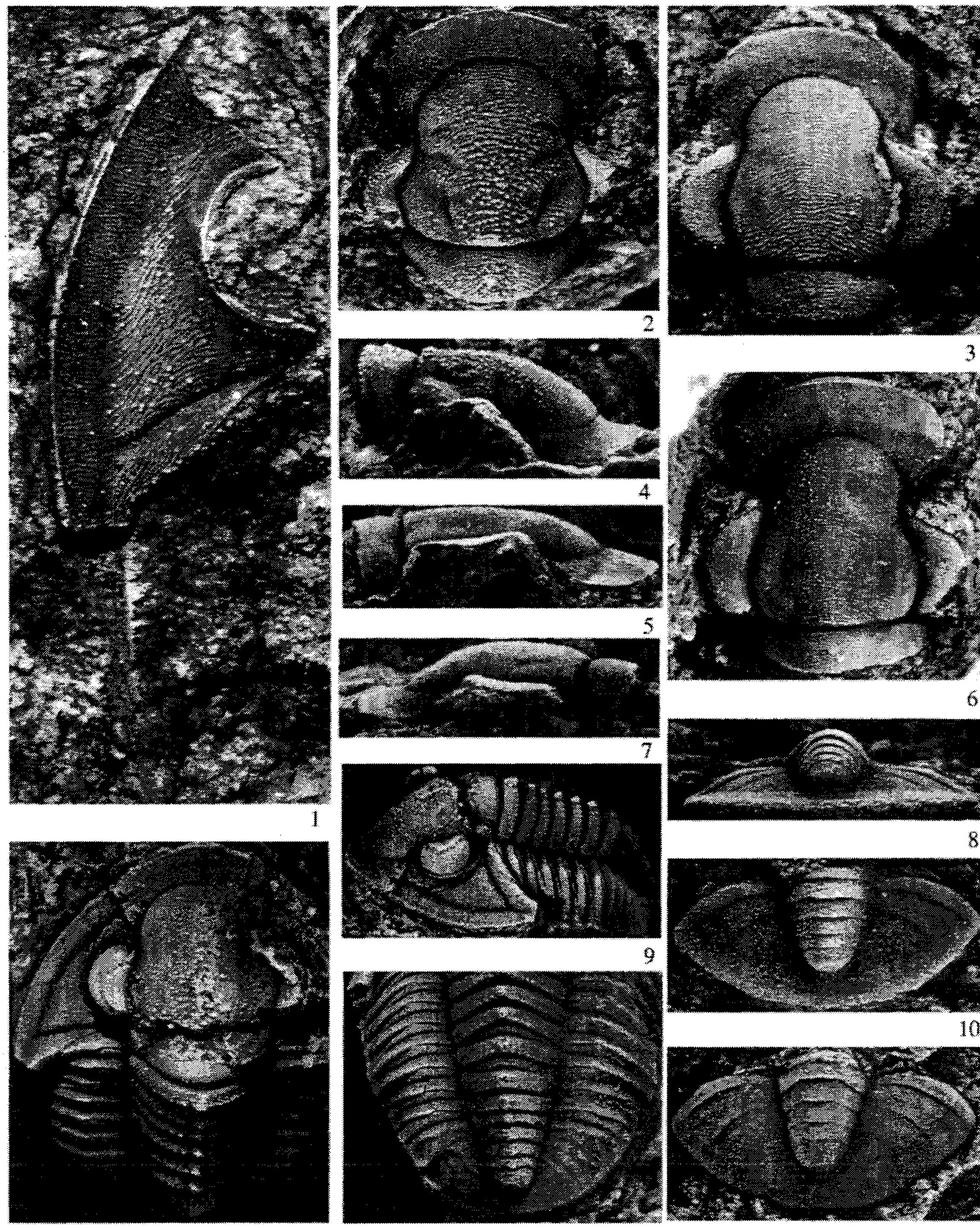
1
2
3
4
5
6
7
8
9
10
11
12
13

than that of *T. dibbanus*. The furrows on the pleural regions of the pygidium of *T. elguerrouji* are more distinctly impressed than those of *T. dibbanus*.

Haas (1968) erected a new subspecies, *Cornuproetus (Cornuproetus) chouberti acrodactylium* that shows some synapomorphies with *T. elguerrouji*, such as glabellar furrows, S1, S2, and S3, depicted in a sketch (Haas, 1968, abb. 7, p. 80) though these are not as visible on the photographic images provided in the same publication. Both species share similar ornamentation, the fine terrace lines with scatterings of pustules on the cranidium, and continued terrace lines over the entire exoskeleton. Though these two species share a number of character states we concluded that they are not the same species for the following reasons: in lateral view, the cranidium of *C. (C.) chouberti acrodactylium* demonstrates that the preglabellar field is concave and not exceedingly short, while *T. elguerrouji* has a short, marginally convex preglabellar field; the palpebral lobes are narrower and less ornamented in *C. (C.) chouberti acrodactylium*; and there is a lack of median tubercles on the axial regions, at least on the pygidium, since the thorax was not figured, while *T. elguerrouji* possesses tubercles/ridges on each axial ring.

Timsaloproetus elguerrouji can be differentiated from *Cornuproetus (Lepidoproetus) regulus* Haas, 1968. While both species display pustules/tubercles upon the glabella, occipital ring and genal field, the degree to which these pustules project is different. Also *C. (L.) regulus* has even more pustules upon the exoskeleton than does *T. elguerrouji*, and they are scattered on the lateral border, the preglabellar field and the pleural and axial regions of the pygidium. *C. (L.) regulus* does have eyes that extend beyond the narrow palpebral lobes, though a 'bald patch' adjacent to the eye socle furrow only appears near the back of the eye and is not present near the front of the eye. *C. (L.)*

regulus appears to lack distinct median tubercles on the pygidial axial rings (thorax is not known).

Cornuproetus (Sculptoproetus) maghrebus Alberti, 1967b shares a number of synamorphies with *Timsaloproetus elguerrouji*, but once again the differences outweigh the similarities. Alberti (1967b, 1969) figured only cranidia of *C. (S.) maghrebus*; also Alberti (1969) assigned several different cranidia to his species, some of which show a considerable range of form for *C. (S.) maghrebus* (more than we think is reasonable for a species). The holotype, figured in Alberti (1969), displays a similar sloping anterior border to *T. elguerrouji*, but every other figured specimen has the anterior border distinctly convex. Obviously the holotype is the primary specimen to consider. It lacks the pustules that are present on the glabella of some of the other cranidia assigned to *C. (S.) maghrebus* (the latter being a synapomorphy with *T. elguerrouji*). Also, due to the incomplete nature of his specimens, it is not possible to ascertain whether Alberti's (1967b; 1969) *C. (S.) maghrebus* has a median node on the occipital ring, and therefore this character state is in question. On the whole, the lack of information provided by Alberti (1967b; 1969) for *C. (S.) maghrebus* makes that species difficult to relate to other forms, and this will be the case until more topotypes are collected.

Another form that should be considered is *Cornuproetus (Sculptoproetus) sculptus antiquus* Alberti, 1967a. Alberti (1967a; 1969) illustrated cranidia and a pygidium (Alberti, 1969) for this subspecies from which one can conclude that this taxon is not conspecific with our new taxon. The holotype of *C. (S.) sculptus antiquus* has prominent glabellar furrows (S0, S1, S2, and S3), as does *T. elguerrouji*, though the other cranidia figured (Alberti, 1967a; 1969) do not display these features as prominently, if at all. Both the preglabellar field and the anterior border are dissimilar to those of *T. elguerrouji*, as the preglabellar field is longer and the anterior border is more convex, accentuating the depth of the anterior border furrow (Alberti, 1967a; 1969). One of the cranidia figured in Alberti (1969, plate 13, figure 3) has some pustules on the posterior region of the glabella, a small scattering upon the medial occipital ring and a slight fringe along the posterior aspect of the occipital lobe, but none of the other cranidia (Alberti, 1967a; 1969) demonstrate these traits. The pygidium figured in Alberti (1969) portrays a similar overall shape and pleural furrow number of 3+1 to *T. elguerrouji*, though the dimensions between *C. (S.) sculptus antiquus* and *T. elguerrouji* are quite different. The percent taper of the pygidial axis in *C. (S.) sculptus antiquus* is 48.34% (i.e. fourth pygidial axial ring is 48.34% smaller than first pygidial axial ring) while *T. elguerrouji* has a taper of 26-37%; the axial length (Y, sag.) to pygidial length (Z, sag.) of *C. (S.) sculptus antiquus* does fall within the range demonstrated by *T. elguerrouji* (0.71 to 0.82), with a ratio of 0.80; the axial width (X, tr.) to pygidial width (W, tr.) of *C. (S.) sculptus antiquus* is 0.39 while that of *T. elguerrouji* differs with a range from 0.31 to 0.32; and finally the pygidial length (Z, sag.) to pygidial width (W, tr.) for *C. (S.) sculptus antiquus* is 0.56 while that of *T. elguerrouji* ranges from 0.44 to 0.52. Thus, these ratios suggest the two taxa are different. It should also be noted that *C. (S.) sculptus antiquus* is Pragian "from 10 km NE of Jbel Issoumour (Maider, SE Morocco)" (translated from Alberti, 1967a), while *T. elguerrouji* is probably early Eifelian.

ACKNOWLEDGEMENTS

Special thanks must be given to Hammi Ait Hssain. His extraordinary knowledge of the Moroccan localities and the trilobites themselves has proven invaluable. The assistance of the Moroccan Geological Survey has been greatly appreciated. Kevin Brett provided some of the stratigraphic measurements. Allan Lindoe prepared most of the specimens that we illustrate. We thank Jim Bohun, Kevin Brett, Allan Lindoe, Ryan McKellar, and Hammi Ait Hssain for assistance in the field. We thank the Berber miners for cooking for us in the field (desert bread, brochettes, tajine, etc.). A Natural Sciences and Engineering Research Council of Canada operating grant to B.D.E. Chatterton funded this research.

REFERENCES

ALBERTI, G. K. B. 1964. Neue Trilobiten aus dem marokkanischen und deutschen Unter- und Mitteldevon. Senckenbergiana lethaea, 45(1-4):115-133.

ALBERTI, G. K. B. 1967a. Neue obersilurische sowie unter- und mitteldevonische Trilobiten aus Marokko, Deutschland und einigen anderen europäischen Gebieten. 2. Senckenbergiana lethaea, 48(6):481-509.

ALBERTI, G. K. B. 1967b. Neue obersilurische sowie unter- und mitteldevonische Trilobiten aus Marokko, Deutschland und einigen anderen europäischen Gebieten. 1. Senckenbergiana lethaea, 48(5):463-479.

ALBERTI, G. K. B. 1969. Trilobiten des jüngeren Siluriums sowie des Unter- und Mitteldevons. I. Abhandlungen der Senckenbergischen Naturforschenden Gesellschaft, 520:1-692.

ALBERTI, G. K. B. 1971. *Cornuproetus* (*Sculptoproetus*) *haasi* n. sp. (Trilobiten, Proetidae) aus dem Devon des Rheinischen Schiefergebirges. Senckenbergiana Lethaea, 52(4):371-375.

ALBERTI, G. K. B. 1983. Trilobiten des jüngeren Siluriums sowie des Unter- und Mittel-Devon. IV. Senckenbergiana Lethaea, 64(1):1-87.

BARRANDE, J. 1846. Notice préliminaire sur le systême Silurien et les Trilobites de Bohême. Hirschfeld, Leipzig, 97p.

BASSE, M. 1994. Kellerwald Trilobiten: Arten und Verbreitung. Fossilien, 6:334-339.

BASSE, M. 1997. Trilobiten aus Mittlerem Devon des Rhenohercynikums: II. Proetida (2), Ptychopariida, Phacopida (1). Palaeontographica Abteilung A, 246(3-6):53-142.

BECKER, T. R., U. JANSEN, G. PLODOWSKI, E. SCHINDLER, S. Z. ABOUSSALAM, and K. WEDDIGE. 2004. Devonian litho- and biostratigraphy of the Dra Valley area – an overview. In A. El Hassani (ed.). Devonian neritic-pelagic correlation and events in the Dra Valley (western Anti-Atlas, Morocco). Subcommission on Devonian Stratigraphy. International Meeting on Stratigraphy, Rabat, March 1-10, 2004. Documents de l'Institut Scientifique, 19:3-18.

BELKA, Z., B. KAUFMANN, AND P. BULTYNCK. 1997. Conodont-based quantitative biostratigraphy for the Eifelian of the eastern Anti-Atlas, Morocco. Geological Society of America Bulletin, 109(6):643-651.

BULTYNCK, P., AND H. HOLLARD. 1980. Distribution comparée de Conodontes et Goniatites dévoniens de plaines du Dra, de Ma'der et du Tafilalt (Maroc). Leuven University Press, 1, 73 p.

BULTYNCK, P., AND O. H. WALLISER. 2000. Devonian Boundaries in the Moroccan Anti-Atlas. Courier Forschungsinstitut Senckenburg, 225:211-226.

CHLUPÁC, I., R. FEIST, AND P. MORZADEC. 2000. Trilobites and standard Devonian stage boundaries. Courier Forschungsinstitut Senckenberg, 220:87-98.

ERBEN, H. K. 1951. Beitrag zur Gliederung der Gattung *Proetus* Stein., 1831 (Trilobitae). Neues Jahrbuch für Geologie und Palaeontologie. Abhandlungen, 94(1):5-48.

EL HASSANI, A. (ed.). 2004. Devonian neritic-pelagic correlation and events in the Dra Valley (western Anti-Atlas, Morocco). Subcommission on Devonian Stratigraphy. International Meeting on Stratigraphy, Rabat, March 1-10, 2004. Documents de l'Institut Scientifique, 19:1-100.

FETAH, S. E. M., M. BENSAÏD, and M. DAHMANI. 1988. Carte Géologique de Maroc: Todhra-Ma'der (Anti-Atlas oriental, zones axiale at périphérique Nord du Sud). Éditions de Service Géologique de Maroc, Notes et Mémoires No. 243. Royaume du Maroc. Ministère de l'Energie et des Mines, Rabat.

FORTEY, R. A., AND R. M. OWENS, 1975. Proetida – a new order of trilobites. Fossils and Strata, 4:227-239.

HAAS, W. 1968. Trilobiten aus dem Silur und Devon von Bithynien (NW-Türkei). Palaeontographica Abt. A, 130(1-6):60-207.

HOLLARD, H. 1967. Le Dévonien de Maroc et du Sahara Nord-Occidental, p. 203-244. *In* D. H Oswald (ed.), International Symposium on the Devonian System. Calgary, 1967. Volume I. Alberta Association of Petroleum Geologists, Calgary, Alberta, 1055 p.

HOLLARD, H. 1974. Recherches sur la stratigraphie des Formations du Dévonien Moyen, de l'Emsien Supérieur au Fransien, dans le Sud du Tafilalt et dans le

Ma'der (Anti-Atlas oriental). Notes du Service Géologique de Maroc, 36(264):7-68.

HOLLARD, H. 1978. Corrélations entre niveaux á brachiopodes et á goniatites au voisinage de la limite Dévonien inférieur -- Dévonien moyen dans les plaines du Dra (Maroc présaharien). Newsletter of Stratigraphy, 7(1):8-25.

JAÏDI, S. E. M., A. BENCHEQROUN, M. DIOURI, AND Y. ENNADIFI. 1970. Carte géologique de l'Anti-Atlas Central et de la Zone Synclinale de Ouarzazate. Feuilles Ouarzazate, Alougoum et Telouet Sud. Editions du Service Géologique du Maroc, Notes et Mémoires No. 138. Royaume du Maroc. Direction des Mines et de la Géologie, Rabat.

JAÏDI, S. E. M., M. DOUÏEB, M. DIOURI, M. SAÂDI. and Y. ENNADIFI. 1971. Carte géologique des Plaines du Dra au sud de l'Anti-Atlas Central: Agadir Tissinnt – Oued Zemoul. Éditions de Service Géologique de Maroc, Notes et Mémoires No. 219. Royaume du Maroc. Ministère du Commerce, de l'Industrie, des Mines et de la Marine Marchande: Directions des Mines et de la Géologie division de Géologie, Rabat.

JANSEN, U., G. BECKER, G. PLODOWSKI, E. SCHINDLER, O. VOGEL, and K. WEDDIGE. 2004. The Emsian to Eifelian near Foum Zguid (NE Dra Valley, Morocco). In A. El Hassani (ed.). Devonian neritic-pelagic correlation and events in the Dra Valley (western Anti-Atlas, Morocco). Subcommission on Devonian Stratigraphy. International Meeting on Stratigraphy, Rabat, March 1-10, 2004. Documents de l'Institut Scientifique, 19:19-28.

LÜTKE, F. 1977. Neue Proetidae (Trilobita) aus dem herzynischen Unter-Devon des Harzes. Senckenbergiana Lethaea, 58(1-3):99-111.

MORZADEC, P. R. 2001. Asteropyginae trilobites from the Devonian of the Anti-Atlas (Morocco). Palaeontographica Abt. A, 262:53-85.

OWENS, R. M. 1973. British Ordovician and Silurian Proetidae (Trilobita). Palaeontographical Society Monographs:1-98, 15 pls.

PIQUE, A., AND A. MICHARD. 1989. Moroccan Hercynides: A synopsis. The Paleozoic sedimentary and tectonic evolution at the northern margin of West Africa. American Journal of Science, 289:286-330.

RICHTER, R. AND. E. RICHTER, 1956. Annular-Teilung bei Trilobiten am Beispiel besonders von *Proetus (Pr.) cuvieri* und *prox.* Senckenbergiana lethaea, 37:343-381.

SCHRAUT, G. 2000. Trilobiten aus dem Unter-Devon des südöstlichen Anti-Atlas, Süd-Marokko. Senkenbergiana Lethaea, 79(2):361-433.

SCHRAUT, G., AND R. FEIST. 2004. The Devonian Styginid trilobite *Paralejurus*, with new data from Spain and Morocco. Journal of Paleontology, 78(4):709-722.

SCOTESE, C. R. 2001. Paleogeographic Atlas, PALEOMAP Progress Report 90-0497. Department of Geology, University of Texas at Arlington, Arlington, Texas, 45 p.

ŠNAJDR, M. 1980. Bohemian Silurian and Devonian Proetidae (Trilobita). Vydal Ústrední ústav geologick´y, Praha, 324 p.

WHITTINGTON, H. B., AND S. R. A. KELLY. 1997. Morphological terms applied to Trilobita, p. 313-329. *In* R. L. Kaesler (ed.), Treatise on Invertebrate Paleontology, Part O, Arthropoda 1, Trilobita, Revised. Volume 1. The Geological Society of America, Inc. and The University of Kansas, Boulder, Colorado and Lawrence, Kansas.

CHAPTER 3: SYSTEMATIC PALAEONTOLOGY II

TRILOBITES FORMERLY KNOWN AS *PROETUS*: SOUTHERN MOROCCAN *GERASTOS* (C. TRILOBITA) FROM THE LOWER TO MIDDLE DEVONIAN[1]

INTRODUCTION

Proetid trilobites occur in many localities throughout the Lower and Middle Devonian of southern Morocco. Species of the proetid genus *Gerastos* are particularly common, and occur in a number of localities. In fact, the Berber miners who obtain most of the specimens refer to specimens of this genus as *izine* (flies), suggesting that they are particularly abundant. The eclectic nature of the scholarly work on the proetids, however, has also led some to refer to proetids as a "disorderly order of trilobites" (Bergström, 1977). The Moroccan localities from which the specimens were retrieved are presented from west to east, while the species are arranged stratigraphically from old to young, from the Timrhanrhart Formation (Emsian) to the Bou Dib Formation (Givetian). A phylogenetic analysis of various species of *Gerastos* is included after the locality descriptions. Finally, the Moroccan species are described and discussed in the section on systematic palaeontology, introducing a number of new species/subspecies of *Gerastos*. The new species/subspecies introduced are: *Gerastos tuberculatus marocensis, G. aintawilus, G. lisanrasus, G. ainrasifus, G. discombobulatus, G. cuvieri malisus, G. taqus, G. malisjildus, G. raribus, G. emmetus,* and *G. izius*.

[1] A version of this chapter, under the same title, with the authorship of S. Gibb and B.D.E. Chatterton will be submitted to the Journal of Paleontology, forthwith.

PREVIOUS WORK

The genus *Proetus* was first erected by Steininger in 1831, who assigned *Calymene concinna* Dalman, 1827, as the type species. Only a few years later Goldfuss in 1843 established the genus *Gerastos* to which all of the species described here are assigned. As is discussed in the section on systematic palaeontology, the classification of *Proetus* and *Gerastos* can be contentious. Owens (1973) defined differences between *Proetus* and *Gerastos*, and also completed a useful reference of the British Proetidae from the Ordovician and Silurian.

Fortey and Owens in 1975 created the Order Proetida, which had previously been classified in the Order Ptychopariida (Swinnerton, 1915). This has allowed a better understanding of the group, although not all workers were convinced that the new order is monophyletic and Bergström (1977) called the Order Proetida "a disorderly order of trilobites". Liebermann (1994) provided a phylogenetic analysis of the order. However, we have some problems with this work and consider a number of his characters difficult to code or of doubtful value and thus his conclusions to be questionable.

Adrain (1997) provided a very thorough account of the *Gerastos* from the Silurian of the Canadian Arctic, more specifically the Cape Phillips Formation (Wenlock-Ludlow). Several other researchers have also provided useful contributions about *Gerastos,* including: Lütke (1977; 1990), Maksimova (1978), Šnajdr (1980), Morzadec (1983), Kowalski (1990), Ellerman (1992), Basse (1996; 1998), and Schöne et al. (1998).

The *Gerastos* of Morocco have been specifically addressed by Richter and Richter (1943; 1956), Pillet (1972), Feist and Orth (2000), and most extensively by Alberti

(1964; 1966a; 1966b; 1967a; 1967b; 1969; 1970; 1980; 1981; 1982). Many of these publications are elaborated on in this paper.

STRATIGRAPHY AND AGE RELATIONSHIPS

The proetids are found throughout an extensive area of southern Morocco, both at a locality and horizon level (Figure 3-1). Hollard (1967; 1974; 1978; 1981) published a series of works on the geology of the Devonian strata of Morocco, and proposed a number of formation names. This work was expanded upon by other researchers, either individually or in conjunction with Hollard, (e.g. Muller and Bensaid, 1969; Bultynck and Hollard, 1980; Bultynck and Jacobs, 1981; Bensaid et al., 1985; Bultynck, 1985; 1987; 1989; Pique and Michard, 1989; Pique et al., 1991; Töneböhn, 1991; R. T. Becker and House, 1994; Plodowski et al., 1999; Bultynck and Walliser, 2000; Morzadec, 2001; G. Becker et al., 2003). These workers included useful biostratigraphic information on such groups as conodonts, ammonoids, ostracodes and trilobites.

LOCALITIES

These are organized geographically, approximately from west to east.

Zguilma locality

Zguilma is south of Foum Zguid, at approximately N 29° 42' 35.2" and W 06° 42' 10.2 (ZGEE1) adjacent to Jbel Gara el Zguilma (Figure 3-2). The locality is within the Dra Valley region, and situated on the northern flank of the Devonian Tindouf Basin (Bultynck and Walliser, 2000). The lithology of the interval that contains *Gerastos* in this section (ZGEE1 & ZGEE2) is composed of calcareous shale interbedded with a

FIGURE 3-1—*1-4*, Generalized locality map for Morocco depicting the three regions of study. *1*, Ma'der region Devonian outcrop map (modified from Fetah et al., 1988); *2*, Tafilalt region Devonian outcrop map (modified from Fetah et al., 1986); *3*, Map of Morocco and surrounding areas; *4*, Dra Valley region Devonian outcrop (modified from Jaïdi et al., 1970; Jaïdi et al., 1971).

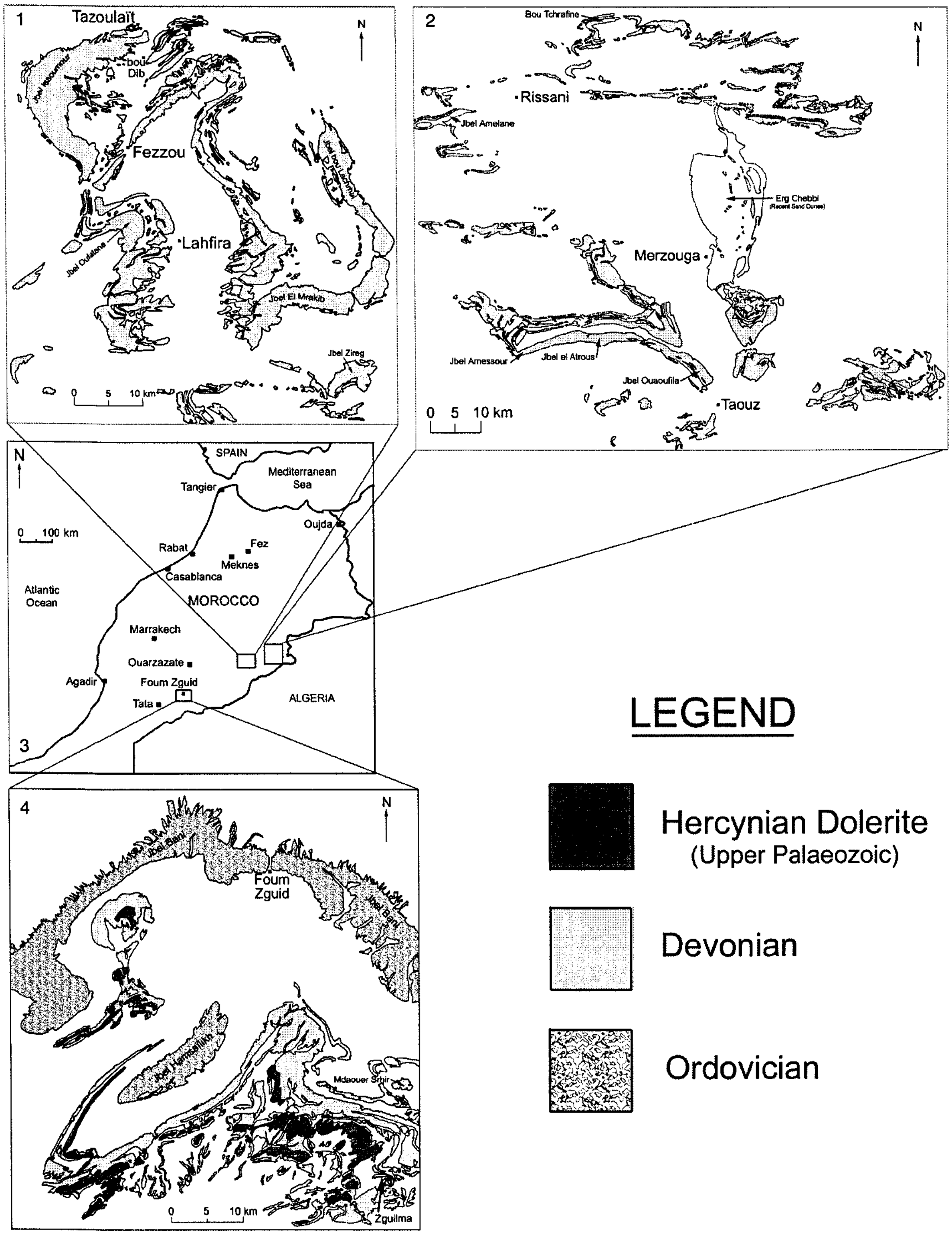
1
Tazoulaït
Dib
Fezzou
Lahfira
Jbel El Mrakib
Jbel Zireg
0 5 10 km
N
2
Bou Tchrafine
Rissani
Jbel Amelane
Erg Chebbi
Merzouga
Jbel Amessour
Jbel el Atrous
Jbel Ouaoufila
Taouz
0 5 10 km
N
3
N
SPAIN
Mediterranean Sea
Tangier
Oujda
0 100 km
Rabat
Fez
Meknes
Casablanca
Atlantic Ocean
MOROCCO
Marrakech
Ouarzazate
Agadir
Foum Zguid
Tata
ALGERIA
4
N
Foum Zguid
Mdaouer Srhir
0 5 10 km
Zguilma
LEGEND
Hercynian Dolerite
(Upper Palaeozoic)
Devonian
Ordovician

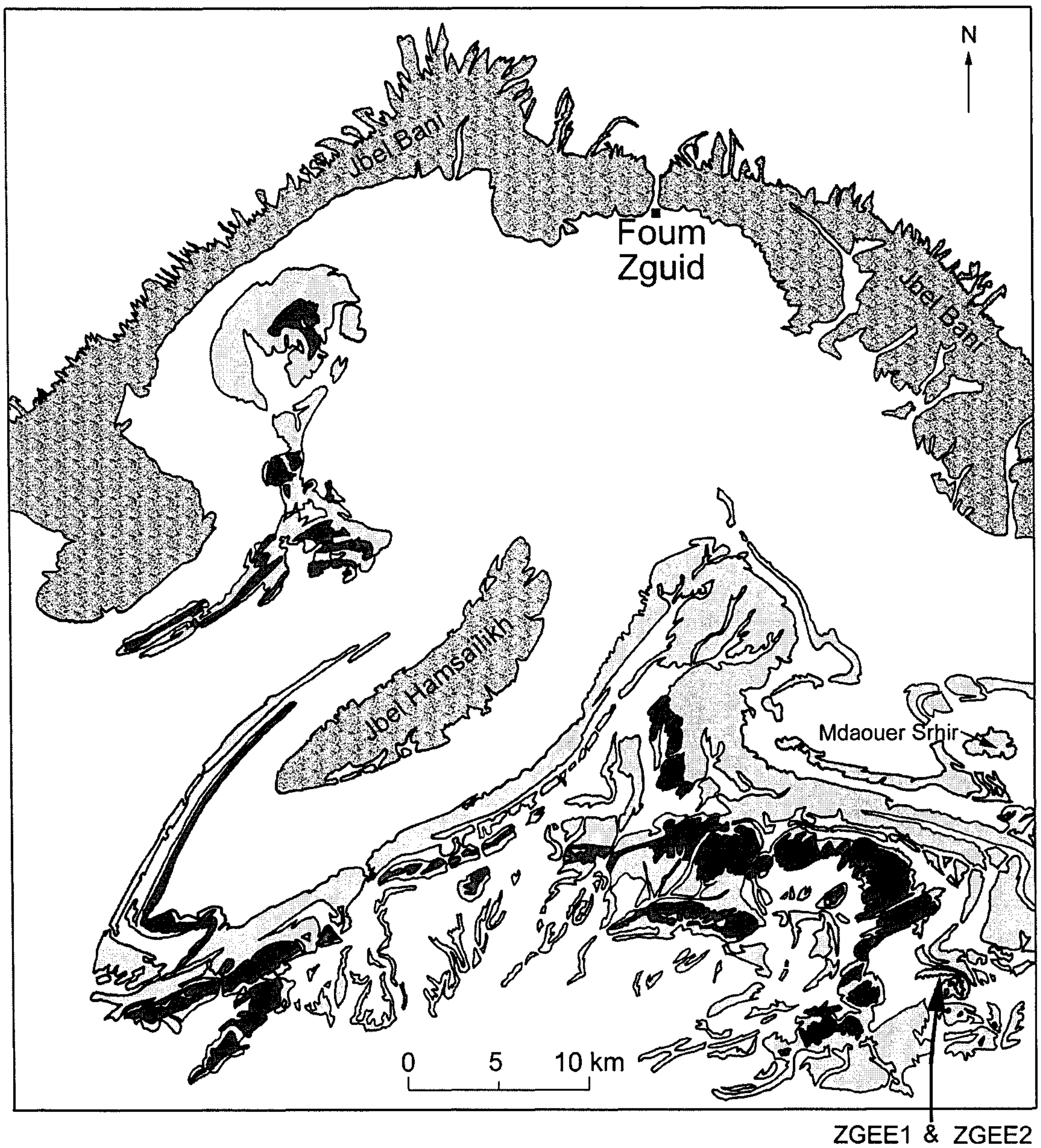

FIGURE 3-2--Dra Valley Devonian outcrop map (modified from Jaïda et al., 1970; Jaïda et al., 1971) depicting Zguilma locality site (ZGEE1 & ZGEE2) (See Figure 3-1 for legend).

nodular calcareous mudstone (Fig. 3-3) (Legend diagram for stratigraphic columns – Figure 3-4). The interval that contains *Gerastos* in this section (ZGEE1 & ZGEE2) is within the Timrhanrhart Formation (Hollard, 1978) and it is thus late Emsian to Eifelian in age (Hollard, 1967; 1978; Bultynck and Hollard, 1980; Bultynck and Walliser, 2000; T. R. Becker et al., 2004) (note that Chatterton et al. are discussing the age and taphonomy of these beds elsewhere in a work in progress). The two horizons from which *Gerastos* was obtained in this section (ZGEE1 and ZGEE2) are very close stratigraphically, and are located near the base of the section in beds considered to be of upper Emsian age (based on ammonoids and trilobites).

Issoumour localities

Issoumour is an extensive mountain (Jbel) range skirting the northwest of the Ma'der region to approximately a few kilometers south and west of Fezzou (Figure 3-5). The majority of our research was done on the steep western aspect of the range, though the opportunity was also available to work on the eastern side (dip slope) of the range. As a result, specimens were only collected from eastern dip slope where the '*Drotops megalomanicus* horizon' occurs. The east has been referred to as the Taboumakhloûf section. The stratigraphic column (Figure 3-6) is based upon stratigraphic information collected by Kevin Brett during fieldwork in 1998, from the upper section found at Taboumakhloûf (Campbell et al., 2002).

'Koneprusites (KPE high) horizon'

Situated on the east side of the Jbel Issoumour range (in the dip slope), the '*Koneprusites* horizon' is located at N 31° 0' 15.9" and W 04° 58' 39.3". The horizon is approximately

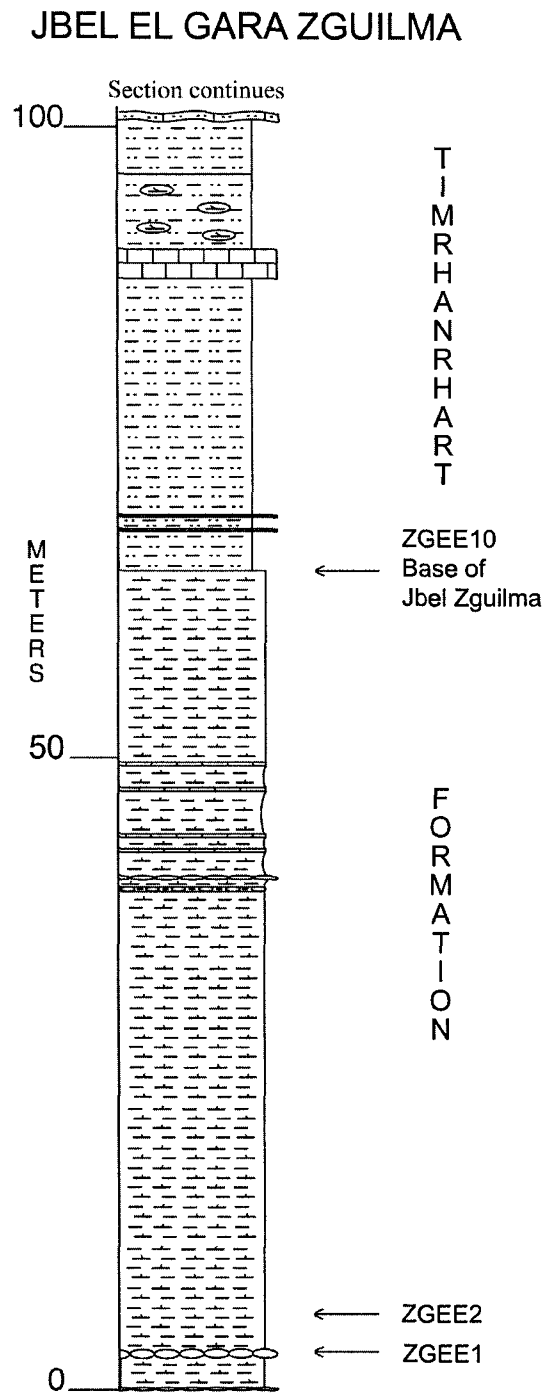

FIGURE 3-3--Zguilma (Jbel El Gara Zguilma) stratigraphic column of Timrhanrhart Formation, depicting the two *Gerastos*-bearing horizons of ZGEE1 & ZGEE2.

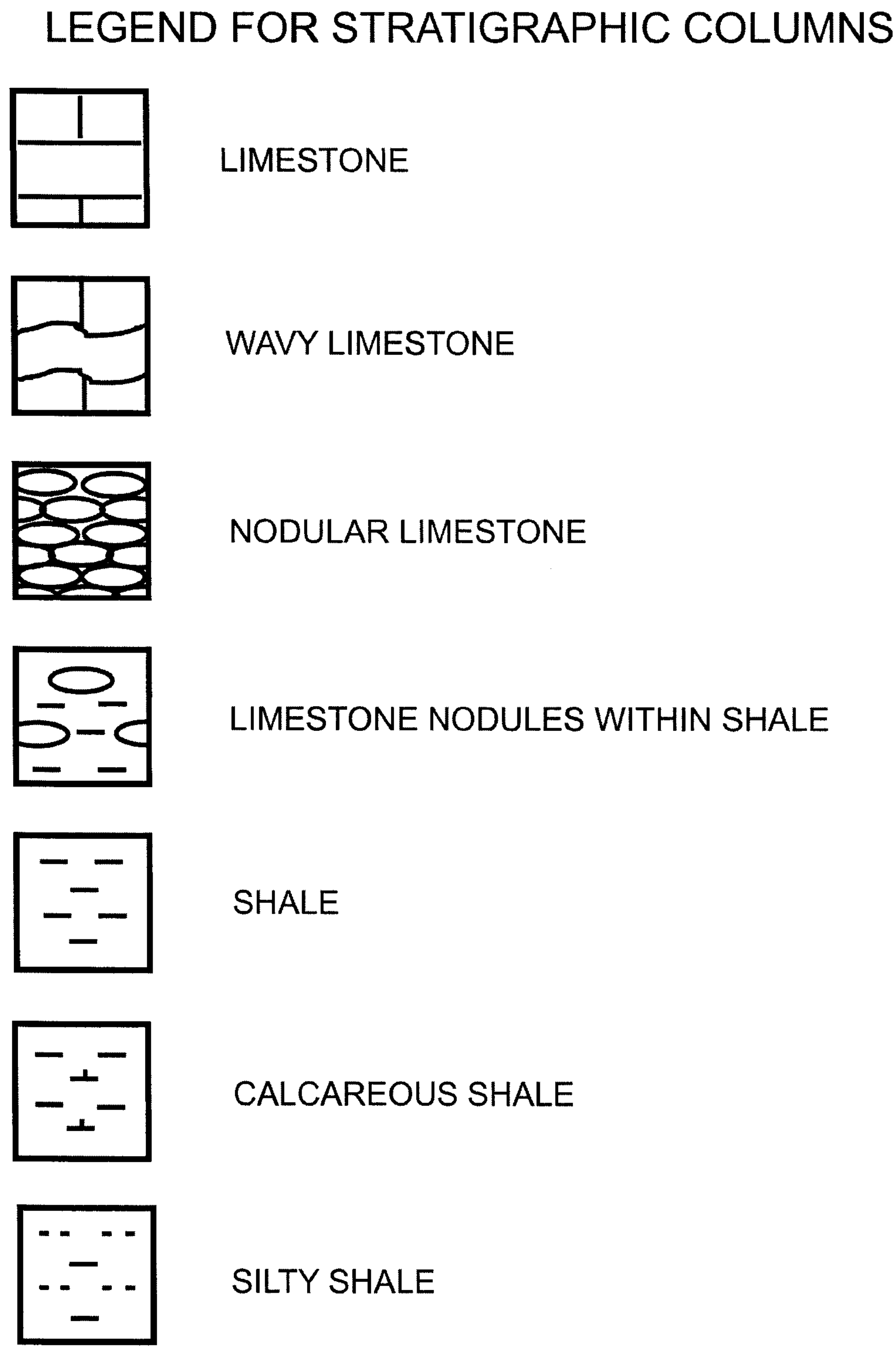

FIGURE 3-4 -- All encompassing legend for stratigraphic columns.

FIGURE 3-5—Ma'der region Devonian outcrop map depicting the following localities/horizons: Taharajat (Tt); '*Harpes/Thysanopeltis*' horizon at bou Dib (BD5); '*Cerataarges* horizon' at Zireg; '*Proetus* horizon' at Mrakib (MM1); '*Diademaproetus* horizon' at Oufatene; '*Thysanopeltis* horizon' at both Mrakib (MM2) and Zireg; '*Koneprusites* horizon' (KPE) on dip slope of Issoumour; '*Drotops megalomanicus* horizon' at both dip slope of Issoumour = Taboumakhloûf section and Mrakib (MDM); and '2cc horizon' at Mrakib (modified from Fetah et al., 1988).

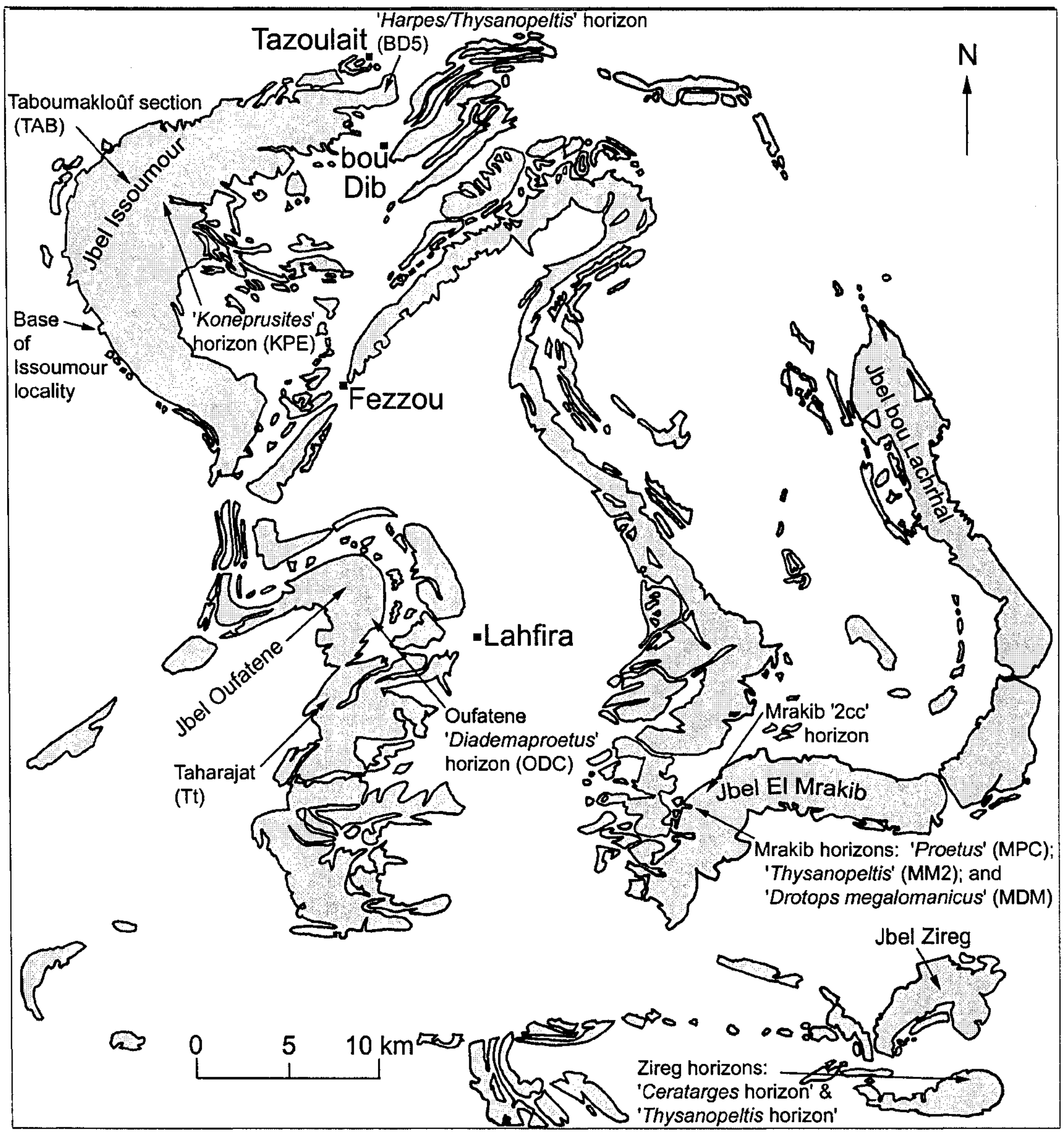
'Harpes/Thysanopeltis' horizon
Tazoulait
(BD5)
N
Taboumakloûf section
(TAB)
Jbel Issoumour
boû
Dib
'Koneprusites'
horizon (KPE)
Base
of
Issoumour
locality
Fezzou
Jbel bou Lachrhal
Lahfira
Jbel Oufatene
Oufatene
'Diademaproetus'
horizon (ODC)
Taharajat
(Tt)
Mrakib '2cc'
horizon
Jbel El Mrakib
Mrakib horizons: 'Proetus' (MPC);
'Thysanopeltis' (MM2); and
'Drotops megalomanicus' (MDM)
Jbel Zireg
0
5
10 km
Zireg horizons:
'Ceratarges horizon' &
'Thysanopeltis horizon'

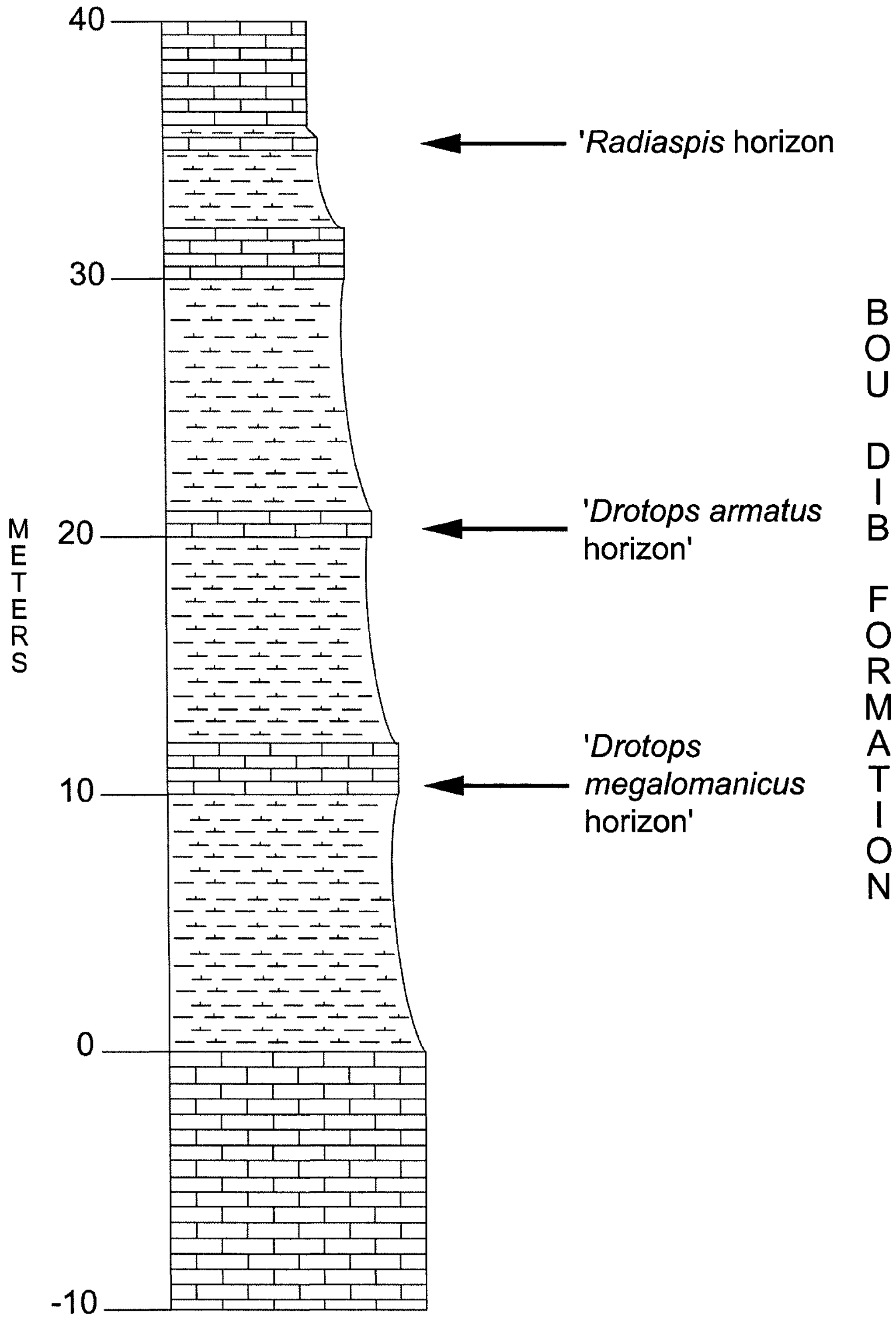

FIGURE 3-6--Taboumakhloûf section on the dip slope of Jbel Issoumour (modified from Campbell et al., 2002).

20-30 centimetres thick composed of a finely recrystallized limestone and is actually 2.2 metres stratigraphically above the GPS coordinates. It has been assumed that since there are two '*Drotops* beds' a short distance stratigraphically (~ 32 metres) above this horizon, that the section is within the Bou Dib Formation or the Taboumakhloûf Formation both of which are Givetian (Bultynck and Hollard, 1980; Bultynck, 1987; Bultynck and Walliser, 2000).

'*Drotops megalomanicus* horizon'

Campbell *et al.* (2002) published a stratigraphic analysis, based upon Hollard (1974), Bensaid et al. (1985), and Bultynck (1985) listing conodonts that they found in this horizon, suggesting it belongs to the Bou Dib Formation (Hollard, 1974); and the conodonts suggest "the lower *varcus* Subzone, of early to middle Givetian age" (Campbell et al., 2002). The '*Drotops megalomanicus* horizon' is composed of approximately 1.5 meters of limestone (Figure 3-6), and overlies and is overlain by calcareous shales. The GPS coordinates for this locality were provided by Kevin Brett, cited in Campbell et al. (2002) as N 30° 02' 00.8" and W 05° 00' 26.0".

Bou Dib locality (BD5)

Belka et al. (1997) established that the bou Dib locality was on the northwestern edge of the Ma'der Basin during the Eifelian and was a neritic setting abundant in fossils within limestones and mudstones. The specimen discussed herein was more specifically from the '*Thysanopeltis/Harpes* horizon', situated at N 31° 05' 16.6" W 04° 52' 32.2" within the El Otfal Formation (Hollard, 1974) of the Eifelian (Hollard, 1974; Morzadec, 2001). The horizon itself is a dark grey calcareous mudstone on a fresh surface or buff coloured on a weathered surface. The calcareous mudstone is semi-nodular with three distinct layers, one being 10 centimeters thick and the remaining two are slightly less than 10 centimeters, each interbedded by a fissile shale (Figure 3-7). Our collection of trilobites for this horizon supports an Eifelian age for this locality.

Oufatene localities

Jbel Oufatene appears to be on a limb of an anticline approaching the hinge (Fetah et al., 1988). Oufatene is to the west and northwest of the village of Lahfira (Figure 3-5), and exposes a thick sequence of strata here, though only one horizon is addressed.

'Diademaproetus horizon'

The '*Diademaproetus* horizon' at Oufatene is located to N 30° 50' 21.3" and W 04° 52' 58.7". The generalized composition of the bed is that of a light grey-green limestone on a fresh surface that weathers to an orange-grey. The interval itself, which is producing *Gerastos*, is approximately 2 metres thick. The '*Diademaproetus* horizon' is within the Taboumakhloûf Formation (Hollard, 1974), Eifelian, Middle Devonian. This assignment can be supported by the conodonts identified from this horizon: *Polygnathus augustipennatus, Paderodus* sp., and *Polygnathus augusticostatus*, among other conodonts which are not as useful for correlation purposes. Bultynck and Hollard (1980), Bultynck (1987) and Belka et al. (1997) provided approximate stratigraphic ranges for the aforementioned conodonts in this region, while the work of Bultynck and Hollard (1980), Bultynck (1985) and Bultynck and Walliser (2000) allows us to assign a formation name to the horizon. We note here that many of the formations named by

BOU DIB SECTION (BD5)

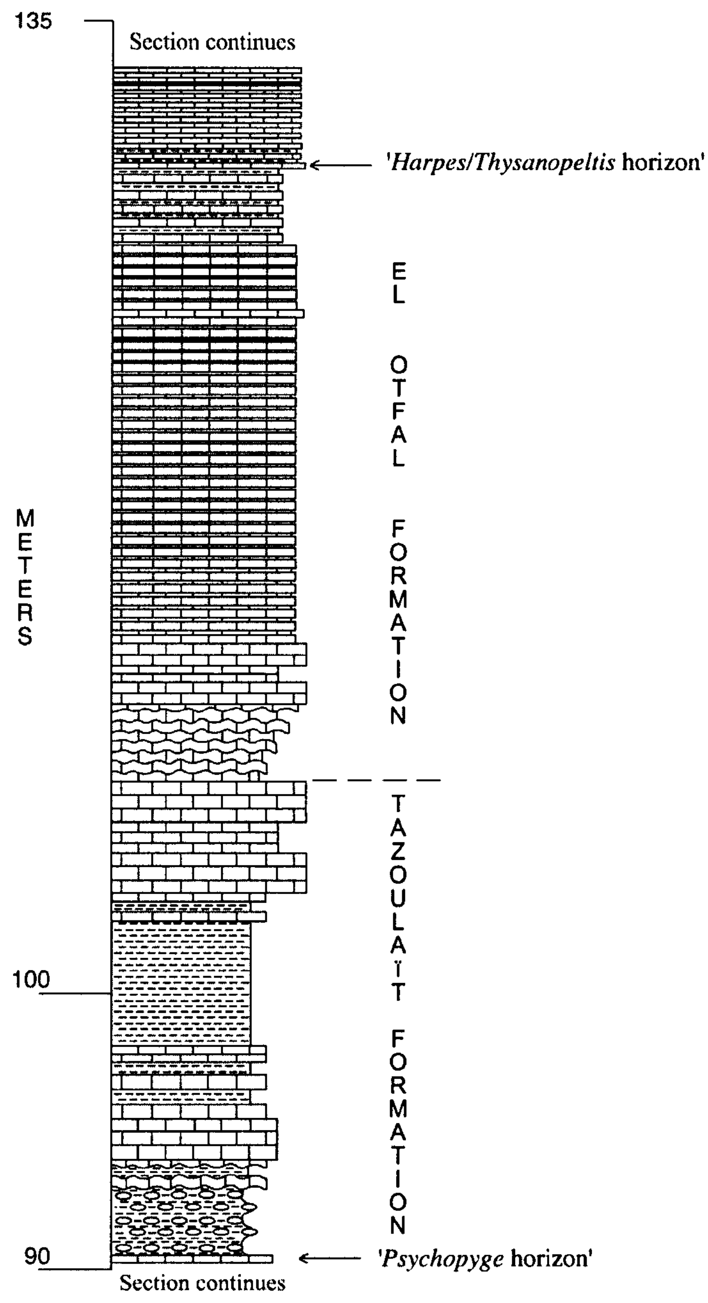

FIGURE 3-7--bou Dib stratigraphic column (based upon measurements by K. Brett), depicting the '*Harpes/Thysanopeltis* horizon' (BD5) producing *Gerastos aintawilus*.

Hollard have rather similar lithologies and so are difficult to identify in small stratigraphic intervals.

Taharajat

Taharajat is a locality composed of two horizons ('a *Metacanthina* horizon' situated approximately 3 metres stratigraphically above a '*Morocconites* horizon'), but thus far they have been equated as only one due to the limited stratigraphic distance between the horizons and the fact the *couche*-workers who sell specimens do not typically know which specific horizon they came from. This locality is close to Jbel Oufatene, and is within the Ma'der basin.

Thus far only one conodont, *Icriodus corniger*, has been identified. The stratigraphic range on this species (or subspecies *I. corniger corniger*) is broad: from upper Emsian to lower Eifelian (Bultynck, 1985; Plodowski et al., 1999; Bultynck and Walliser, 2000;). Based on the *Gerastos* subspecies (*G. tuberculatus marocensis*) found at this locality, we have been able to equate it with the lower section at Zguilma (ZGEE1) and the '*Proetus* horizon' at Merzouga, therefore within the upper Emsian. Several other trilobites are also shared with ZGEE1 including species of *Hollardops* and *Scabriscutellum*.

The bed that contains the specimens from this locality consists of micritic limestones (recrystallized wackestone) of medium grey grading into an orange grey colour on a fresh surface, that weather into a light grey.

Mrakib localities

Mrakib is an extensive section located in the southeastern part of the Ma'der region. During the Early Devonian shelf limestones were deposited in this area (Pique et al., 1991) and during the Middle Devonian a neritic facies were deposited (Belka et al., 1997). There is even a large hill in the region composed of Middle Devonian reef limestones called Aferdout. From Jbel Issoumour one must travel to the south and slightly east to reach the locality of Jbel El Mrakib (referred to herein as Mrakib). Thus far, horizons from which *Gerastos* have been obtained at Mrakib range from the Upper Emsian/Lower Eifelian (equivalent to '*Psychopyge* horizon') to the Givetian with the '2cc horizon', and is finally capped with a thick biostromal (in places biohermal) coral grainstone. The coral grainstone has only been tentatively dated via a single conodont, *Bellodella*, in which Bultynck (1987), from the Taboumakhloûf region, placed from the middle *ensensis* to the end of the middle *varcus* conodont zone thus confirming that the coral grainstone is within the Givetian.

'Proetus horizon'

The '*Proetus* horizon' is approximately 1.9 metres stratigraphically above a '*Ceratarges* bed'. The '*Proetus* horizon' consists of a recrystallized grey-green layered calcareous mudstone, with an average thickness of 10-20 centimeters, interbedded with less resistant platy shale, with a total thickness for the horizon of approximately 90 centimeters (Figure 3-8). The coordinates from which the specimens were collected are N 30° 44' 50.2" and W 04° 41' 25.3". From the lithologic and other fauna collected from this locality it has been established that it belongs to the Taboumakhloûf Formation

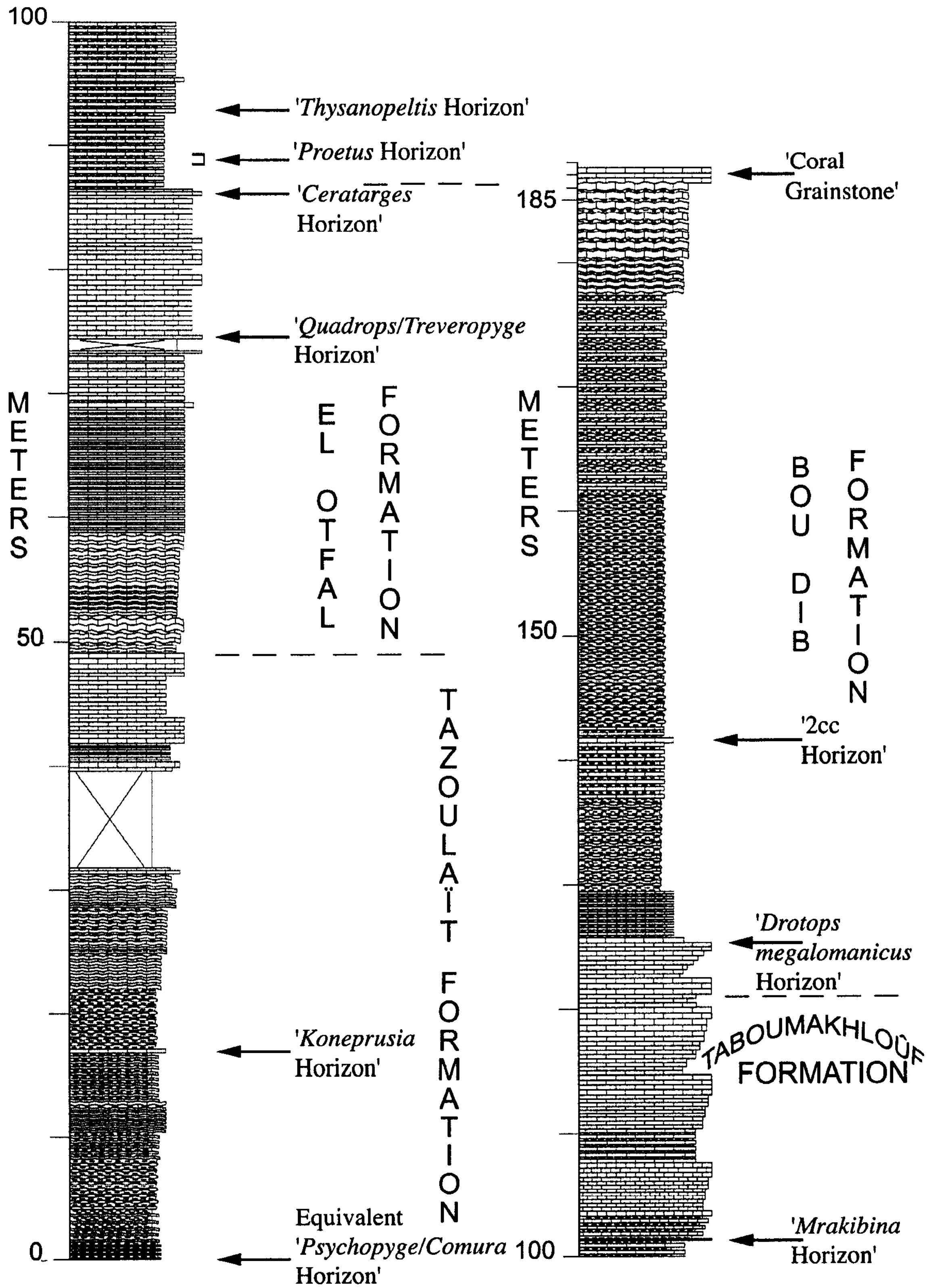

FIGURE 3-8--Mrakib stratigraphic column (based upon measurements by K. Brett).

(Hollard, 1974), Eifelian, Middle Devonian (Hollard, 1974; Bultynck and Hollard, 1980; Morzadec, 2001).

'Thysanopeltis horizon'

The '*Thysanopeltis* horizon' is located approximately 3 metres stratigraphically above the '*Proetus* horizon' (Figure 3-8). The bed is composed of a dark grey limestone with iron oxide crystals, weathering to an orangish light grey. The horizon is within the Taboumakhloûf Formation (Hollard, 1974), Eifelian, Middle Devonian.

'Drotops megalomanicus horizon'

The '*Drotops megalomanicus* horizon' at Mrakib is quite similar to the bed that bears *D. megalomanicus* on Jbel Issoumour. As established by Belka et al. (1997), both Issoumour and Mrakib were near the margins of the Ma'der Basin during the Eifelian and exhibit neritic facies, which are "represented by well-bedded fossiliferous mudstones and wackestones containing both pelagic and benthic fauna" (Belka et al., 1997). The thickness of the trilobite-bearing beds is approximately 2 meters and is composed of approximately thirteen wackestone beds usually 20-40 centimetres thick, each interbedded with thin beds of fissile shale (Figure 3-8). This particular locality is located at N 30° 44' 50.1" and W 04° 41' 44.8" (approximately 6 metre accuracy) with a dip of 8° and dip direction of 340°. Campbell et al. (2002) stated that the Issoumour horizon is that of the Bou Dib Formation (Hollard, 1974); since the facies and ages of the beds are similar in both regions, we have assigned this locality to the same formation.

'2cc horizon'

The '2cc horizon' is located at the following coordinates: N30° 45' 48.6" and W 04° 40' 42.7" (with ~5 metres accuracy). The trilobite-bearing bed is composed of a dark, silver grey to a weathered light grey to a whitish orange-grey colour of limestone (mudstone to wackestone), with a dip angle of 37° and dip direction of 314°. The '2cc horizon' is situated 14.9 metres stratigraphically above the '*Drotops megalomanicus* horizon' (Figure 3-8). It is included here in the Bou Dib Formation (Hollard, 1974; Bultynck and Walliser, 2000; Campbell et al., 2002), and is almost certainly of Givetian age.

Zireg locality

Zireg is located within the southeastern most part of the Ma'der region, within the Ma'der basin. It is separated from the Mrakib section/mountain range, to the northwest, by an anticline that exposes the Ordovician at Jbel El Mzioda (Fetah et al., 1988) (Figure 3-5).

'Ceratarges horizon'

The '*Ceratarges* horizon' is located at the following coordinates: N 30° 36' 41.6" and W 04° 32' 21.8". The horizon is approximately 28 centimetres thick and composed of a medium-light grey weathering to a slightly buff grey limestone (recrystallized mudstone to wackestone). The horizon is within the Taboumakhloûf Formation (Hollard, 1974), Eifelian, Middle Devonian.

'Thysanopeltis horizon'

The '*Thysanopeltis* couche' is approximately 27 metres stratigraphically above the '*Ceratarges* horizon'. It is composed of a medium-light grey slightly recrystallized mudstone, which is 15 centimetres thick. It is within the Taboumakhloûf Formation (Bultynck and Walliser, 2000), Eifelian, Middle Devonian.

Merzouga locality

The Merzouga locality is situated at N 31° 16' 28.5" and W 03° 53' 29.4" (approximately 7 metres of accuracy) upon the side of one of many small hills northeast of the *Erg Chebbi* (Figure 3-9). The horizon (MRZP = 'Merzouga Proetus *couche'*) consists of a weathered buff-green-grey calcareous mudstone, with a thickness of approximately 10-20 centimeters, overlain by and overlying calcareous fissile shale (Figure 3-10). Analysis of *Gerastos*, *Diademaproetus*, and phacopid specimens, leads to the conclusion that this horizon is similar in age to that of the lower Zguilma horizons (ZGEE1 & ZGEE2); therefore it is late Emsian, within the Amerboh Group (Bultynck and Walliser, 2000; Aitken et al., 2002) of the Tafilalt region, correlative with the Timrhanrhart Formation (Hollard, 1978) of the Dra Valley (Bultynck and Walliser, 2000).

PHYLOGENETIC ANALYSIS

Many species that are now assigned to *Gerastos* were originally assigned to *Proetus*. We consider *Gerastos* to be a distinctive genus that may be distinguished readily from *Proetus* (see below under Systematic Section).

Lieberman (1994) conducted cladistic analyses on the Subfamily Proetinae, and the genera *Crassiproetus*, *Basidechenella, Dechenella,* and *Monodechenella*. His fauna was not incorporated into this study due to a number of inconsistencies, and because they are from localities in Eastern North America. There seems to have been little, if any, effective dispersal between these regions during the Early and Middle Devonian.

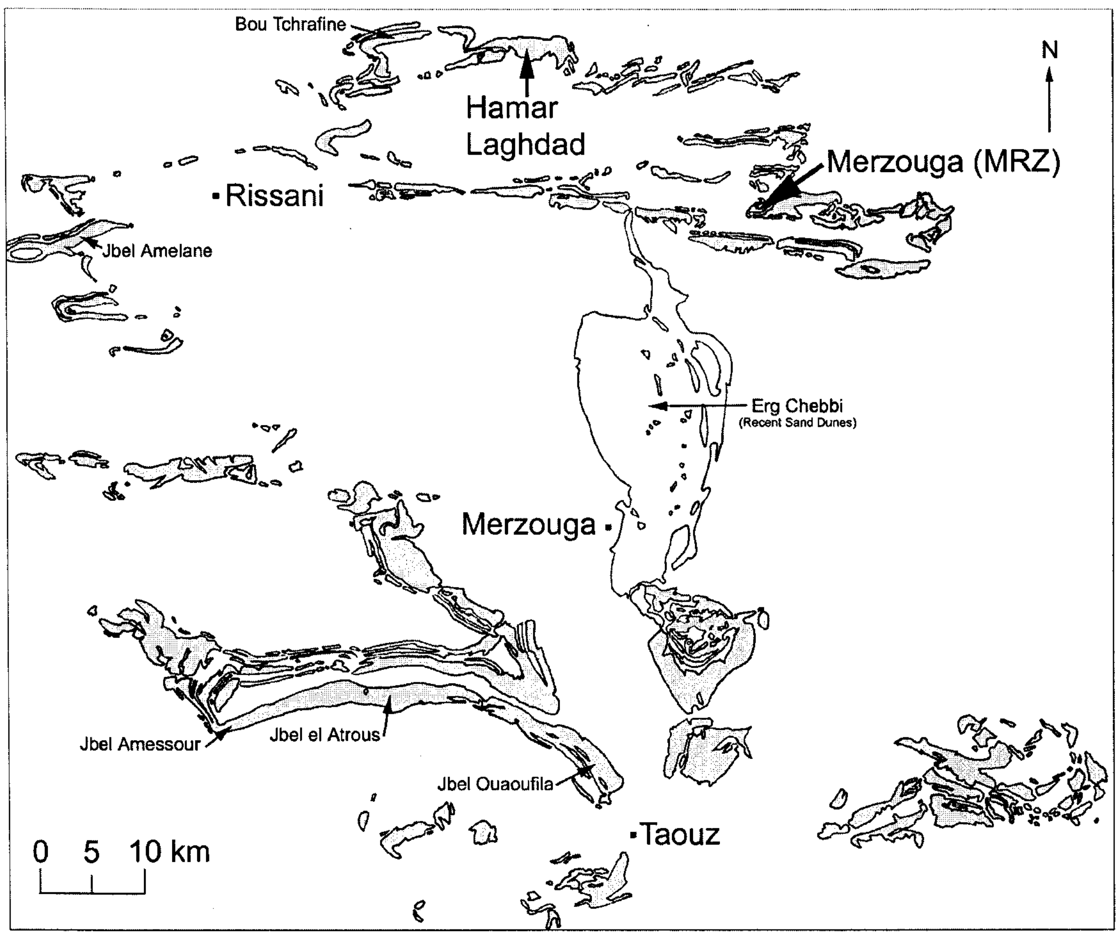

FIGURE 3-9--Tafilalt region Devonian outcrop map (modified from Fetah et al., 1986), depicting the Merzouga '*Proetus* horizon' as MRZ and also noting the Hamar Laghdad locality and the '*Erg Chebbi*' (recent sand dunes).

FIGURE 3-10—Merzouga stratigraphic column depicting the '*Proetus* horizon' (MRZ-P) (based on measurements by R. McKellar).

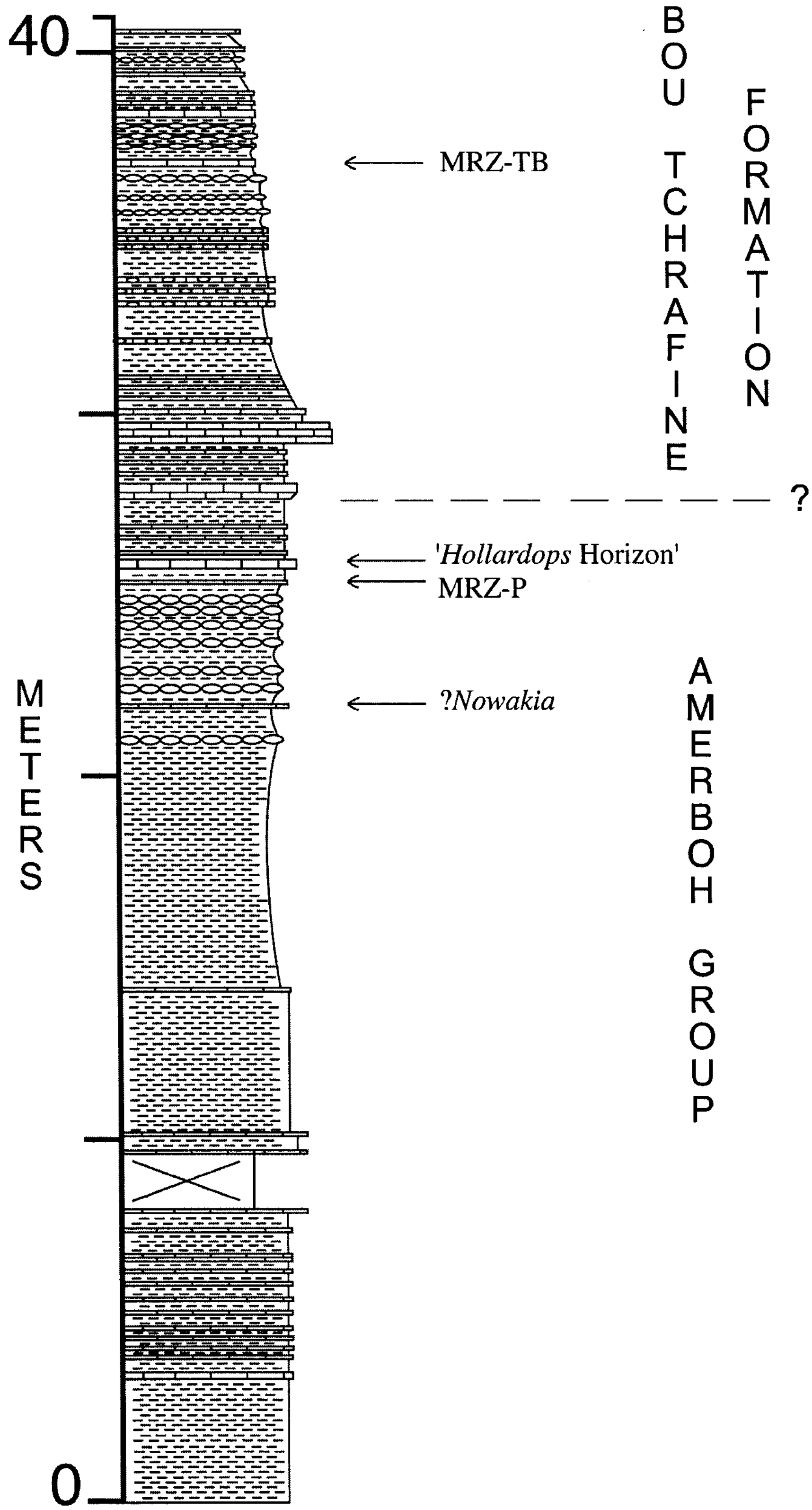

40
0
METERS
MRZ-TB
BOU TCHRAFINE FORMATION
?
'*Hollardops* Horizon'
MRZ-P
?*Nowakia*
AMERBOH GROUP

The cladistic analysis was conducted on 14 species/subspecies to determine the relationships among some *Gerastos* species from Morocco and Europe. From the phylogenetic analysis, it is concluded that *Gerastos* is monophyletic and can not be subdivided readily at this time into well supported subgroups.

TAXA USED IN THE ANALYSIS

Outgroup.— The outgroup taxa decided upon were *Gerastos mellishae* ADRAIN 1997 and *Gerastos milleri* ADRAIN 1997. These species were chosen because they are from the Silurian, near the base of the stratigraphic range of the genus; hence, one could assume they should be plesiomorphic in most of their character states relative to Devonian taxa. They are particularly well preserved, and have been described in great detail (Adrain, 1997) making coding of most character states possible. We note, however, that they originate from Arctic Canada of Laurentia, while the species under study within this paper are all younger and from Gondwana. *Proetus morinensis* PŘIBYL 1960 was to be included within the outgroup as a representation of another Silurian taxon, for as Schuh (2000) stated: "The outgroup need not be limited to a single taxon, and indeed, analyses are probably best conducted using multiple outgroups". The problem arose that *Proetus morinensis* nested within the ingroup (Appendix 1); therefore, a closer analysis of this species should be done to deduce an appropriate generic assignment for it.

Ingroup.— The ingroup consists of all the specimens assigned to *Gerastos* and referred to as '*Proetus*' by the Moroccan collectors at the beginning of the thesis. Initially, every specimen was coded and measured separately (Appendix 2) to eliminate any possible bias in the identification of species-level taxa. As one would suspect, specimens from individual beds nested together, along with those specimens from any other localities that contained the same species. Localities that have more than one species, however, showed specimens clustering on different parts of the tree. This initial phylogenetic analysis enabled us to group specimens into species with a higher level of confidence.

The measurements were done in hopes that ratios of measurements between different morphological landmarks could be used as character states. Unfortunately only one set of ratios demonstrated any clear subdivision into distinct character states, and that is the maximum width of the glabella (K, tr.) to δ-δ (tr.). When plotted on histograms, no other ratio revealed any significant clustering. The ranges of ratios of different species appeared to overlap in such a random fashion that it was not apparent where boundaries could be placed to discriminate informative character states. Almost all boundaries picked lead to several species coding multiple character states. Thus these measurements are only used in the descriptions of the species.

The species within the ingroup are: *Gerastos tuberculatus tuberculatus* (Barrande, 1846), *G. tuberculatus marocensis* new species, *G. aintawilus* new species, *G. lisanrasus* new species, *G. ainrasifus* new species, *G. discombobulatus* new species, *G. cuvieri malisus* new subspecies, *G. taqus* new species, *G. malisjildus* new species, *G. raribus* new species, *G. emmetus* new species, and *G. izius* new species. *Gerastos tuberculatus tuberculatus* (Barrande, 1846) was included within the ingroup to confirm that the specimens from Zguilma, Taharajat and Merzouga-*Proetus* horizon were nesting together and therefore closely similar, sister groups, to each other.

TAXA NOT INCLUDED IN ANALYSIS

As stated previously, *Proetus morinensis* PŘIBYL 1960 was not included in the final analysis due to the nesting of the species within the ingroup taxa. *P. morinensis* did not change the overall appearance of the cladogram, aside from nesting within the ingroup, both in two of the three trees from branch-and-bound analysis and 50% majority rule. *Longiproetus tenuimargo* (RICHTER, 1909) was also considered for the analysis, for a number of Moroccan *Gerastos* specimens displayed *Longiproetus* characteristics, and because *L. tenuimargo* is the type species for *Longiproetus*. When an analysis was done with both *L. tenuimargo* and *P. morinensis*, they nested within the ingroup, once again, both two of the three trees from branch-and-bound analysis and 50% majority consensus. When *L. tenuimargo* was used without *P. morinensis*, *L. tenuimargo* nested slightly higher within the ingroup; therefore, *P. morinensis* should be assessed to ascertain if it should not be within the genus *Gerastos* then suggesting that *Longiproetus* (Richter, 1909) is a junior synonym of *Gerastos* (Goldfuss, 1843). The assignment of *L. tenuimargo* will be addressed anon.

EXPLANATION OF CHARACTERS AND CHARACTER STATES

The characters used for the cladistic analysis are based upon a number of different resources (i.e. glabellar and pygidial shape (Šnajdr, 1980; p. 14, fig.1; p.23, fig.8)). Lieberman (1994) carried out a phylogenetic analysis on a number of proetid trilobites for the Devonian of North America. His characters and character states were reviewed, but only a few were found to be relevant or cladistically informative in the present analysis. The majority of characters, herein, were arrived at through examining characters used by various workers to diagnose and contrast species of *Gerastos* and *Proetus* (e.g. Richter and Richter, 1918; Alberti, 1969; 1970; Owens, 1973; Šnajdr, 1980; Adrain, 1997). A number of other characters were eliminated as not being cladistically informative (only synplesiomophies and/or autapomorphies). The data matrix is accessible in Appendix 3. *Gerastos mellishae* and *G. milleri*, from the Silurian of Laurentia, were used as an outgroup.

1. *Genal angle.*— The angle whereupon the posterior and lateral borders meet and either a genal spine extends posteriorly or not. (0) Rounded; (1) Pointed; (2) Square. Outgroups demonstrate both pointed (1) (*G. mellishae*) and rounded (0) (*G. milleri*).

2. *Glabellar shape.*— Based upon Šnajdr's (1980) descriptions of glabellar shape (p. 14). (0) Ovoid; (1) Tongue-shaped. Outgroup displays an ovoid glabella (0).

3. *Glabellar furrows.*— The number of distinct glabellar furrows upon the glabella anterior to S0. (0) S1 & S2; (1) S1, S2 & S3. Outgroup has only S1 and S2 (0).

4. *Glabellar sculpture.*— The ornamentation upon the glabella anterior to S0. (0) large, some pointed and/or amalgamated; (1) Small tubercles/pustules that progressively grade smaller anteriorly; (2) no ornamentation on anterior aspect of glabella. Outgroup displays trait 0.

5. *'Ocular platform'.*— The dorsally raised platform encircling the eye socle furrow upon the genal field. (0) Present; (1) Absent. Outgroup does not have an ocular platform (1).

6. *Lateral border furrow of cephalon.*— The depth of the furrow adaxial to the lateral border. (0) Shallow; (1) Moderately incised. The outgroup taxa *G. milleri* and *G. mellishae* both display a moderately incised furrow (1).

7. *Lateral occipital furrows.*— The paired furrows incising the lateral aspect upon the occipital ring. (0) Furrows are recurved laterally to create a *hooked* appearance; (1) Furrows marginally incise the occipital ring and lateral occipital lobes are distinguishable. The outgroup displays marginally paired lateral occipital furrows (1).

8. *Occipital ring sculpture.*— The nature of the sculpture upon the occipital ring. (0) Absent/Smooth; (1) Abundant and large pustules/tubercles; (2) Few pustules and/or tubercles that are randomly dispersed. Outgroup displays character state 1.

9. *Eye socle.*— The prominence of an eye socle or lack thereof. (0) Prominent; (1) Faint; (2) Constrained at the base with a slight indentation. A prominent eye socle (0) is observed on the outgroup.

10. *Pygidial border.*— The depth or lack of any depth that the pygidial border displays. (0) Deep; (1) Shallow; (2) Weak; (3) Absent. The outgroup displays two different traits: *G. milleri* has a deep border (0) while *G. mellishae* has a weak border (2).

11. *Pygidial axial ring sculpture.*— The degree of ornamentation upon the glabella: (0) Abundant and large pustules/tubercles; (1) Abundant granules; (2) Constrained/Limited ornamentation; (3) No ornamentation = smooth. The outgroup has abundant granules covered the pygidial rings (1).

12. *Number of pygidial axial rings.*— The number of rings on the axis of the pygidium plus the terminal piece: (0) Seven plus a terminal piece; (1) Eight plus a terminal piece. The outgroup displays both states: *G. milleri* = 0 and *G. mellishae* = 1.

13. *Convexity of glabella.*— In lateral profile, the degree of convexity of the glabella. (0) Inflated; (1) Low. Both *G. milleri* and *G. mellishae* are low (1).

14. *Convexity of pygidial axial region.*— In lateral profile, the convexity of the axial region of the pygidium. (0) Inflated; (1) Low. *G. milleri* and *G. mellishae* both have low convexity (1).

15. *Anterior border sculpture of cephalon.*— Ornamentation adorning the anterior border of the cephalon. (0) Smooth; (1) Fine granules; (2) Terrace ridges. The outgroup is the only species to display terrace ridges upon the anterior border (2).

16. *Lateral border sculpture of cephalon.*— Prosopon upon the lateral borders of the cephalon. (0) Smooth; (1) Fine granules; (2) Pitted; (3) Very limited, randomly dispersed ornamentation. *G. milleri* could not be ascertained and *G. mellishae* has pitted (2) lateral borders.

17. *Thoracic pleural region sculpture.*— The ornamentation of pustules upon the pleural region of the thoracic region. (0) Absent; (1) Present. Both species within the outgroup are adorned with a degree of sculpture upon the pleural regions of the thorax (1).

18. *Sculpture on lateral edge of palpebral lobes.*— Along the most lateral edge of the palpebral lobes, a *Gerastos* can either exhibit some prosopon, none or a variation involving some ornamentation. (0) Smooth, therefore lacking any ornamentation; (1) A fine, single row of pustules skirting the lobe; (2) Ornamentation only posterior to δ. The outgroup display a single row of fine pustules encircling the lateral aspect of the palpebral lobes (1).

19. *Postaxial lobe.*— The presence, however slight, or absence of a postaxial lobe off of the terminal piece. (0) Present; (1) Absent. The outgroup displays no postaxial lobe (1).

20. *Cephalic marginal pores.*— As used by Adrain (1997) in his diagnosis of *Gerastos*. "cephalic and pygidial borders with prominent subparallel terrace lines, between which occur single rows of small perforations". (0) Present; (1) Absent. Since the outgroup is from Adrain's (1997) publication, the outgroup does possess this trait (0).

21. *K/δ–δ ratio.*— A numerical landmark ratio of the maximum width (tr.) of the glabella anterior to S0 divided by the width (tr.) of δ–δ, based on averages arrived at from histographic analysis. (0) ~ 0.665; (1) ~ 0.715; (2) ~ 0.775. The outgroup fell within the character trait of ~ 0.775 (2).

CHARACTERS EXCLUDED FROM ANALYSIS

Hypostome. Although a number of hypostomes were retrieved from some beds, no characters based on hypostomes were included because hypostomes are not known for the majority of the species included in the analysis.

Morphometric ratio data: Each specimen was measured thoroughly and numerous ratios of measurements were calculated. These ratios were plotted as histograms. In most cases the ranges of ratios for different species overlapped to such an extent, and in such a random fashion, that it was impossible to determine reliable, useful boundaries between character states that would allow for coding the majority of species as a single state.

Number of marginal ridges upon cephalon and pygidium: Though this character is one that is discussed in almost all descriptions, preparation techniques or weathering had effaced the specimens to a degree that a precise number could not always be arrived at. Therefore, use of this character when specimens could be mis-coded was avoided. Some of the characters seriously considered, but then eliminated from the analysis, are listed below.

Height of eye in relation to maximum dorsal convexity of glabella: This is affected by deformation, and in published illustrations by the angle of photography. Thus it was felt that coding might prove unreliable for enough species to eliminate this character from the analysis.

Occipital median node: It was found that the presence or absence of an occipital median node was not an informative character due to the number of specimens displaying this morphological structure (symplesiomorphy for all of the species); therefore, it was eliminated from the data matrix.

Sculpture upon the librigenae: One would imagine that this would be informative, but only a few species showed any perceptible differences.

Shape of pygidial axial rings: Although a small proportion of specimens demonstrated 'straight' (transverse) axial rings, this character was found to be uninformative. The majority of specimens display, at least from the second and more posterior axial rings, an elongate *m*-shape. Thus, this character was eliminated.

Convexity of Anterior Border: While some specimens did demonstrate a flattened anterior border, others apparently belonging to the same species (from the same locality) did not portray this trait. With closer inspection of some of the purchased specimens, it appeared that the preparator may have had an undue influence on the character state and thus modified a few specimens.

RESULTS

A phylogenetic analysis was done using PAUP* 4.0b 10 (Swofford, 2002) and MacClade 4.06 (Maddison and Maddison, 2001). The characters were treated as unordered, of equal weight, and as parsimoniously-informative. Upon running a branch-and-bound search, only one tree was found (Figure 3-11). Since the 'Branch-and-Bound" algorithm guarantees finding all of the shortest trees, there was no need to utilize some of the methods available to eliminate alternate trees. The length of the tree is 64, consistency index is 0.53, retention index 0.59 and the rescaled consistency index is 0.32.

The tree does not group species based on their stratigraphic positions, but seems to demonstrate mosaic evolution. If one observes the changes upon the tree (Figure 3-12), it can be seen that there are a number of reversals. 'Dollo's Rule' stated "the principle that evolution is irreversible to the extent that once complex structures or functions are lost, they cannot be restored exactly to their prior condition" (Mayr and Ashlock, 1991). Taking this into account, and disregarding 'Dollo's Rule', this tree is likely a true indication of the evolutionary process for the analyzed specimens. Reversals will not produce the 'exact' structure and/or function, but it can be close enough not to be differentiated when coding character states on trilobites.

SYSTEMATIC PALEONTOLOGY

The morphological landmarks and regions found upon the cephalon and pygidium are terms used by Owens (1973) (Figure 3-13). The glabellar shape ($A_1 + A_4$) and pygidial outline are based upon Šnajdr (1980; p. 14, fig. 11; p. 23, fig. 8) though the glabellar shape does not conform to Šnajdr's (1980) generalized genera assignment. All other terminology complies with Whittington & Kelly (1997).

PHYLOGENETIC TREE

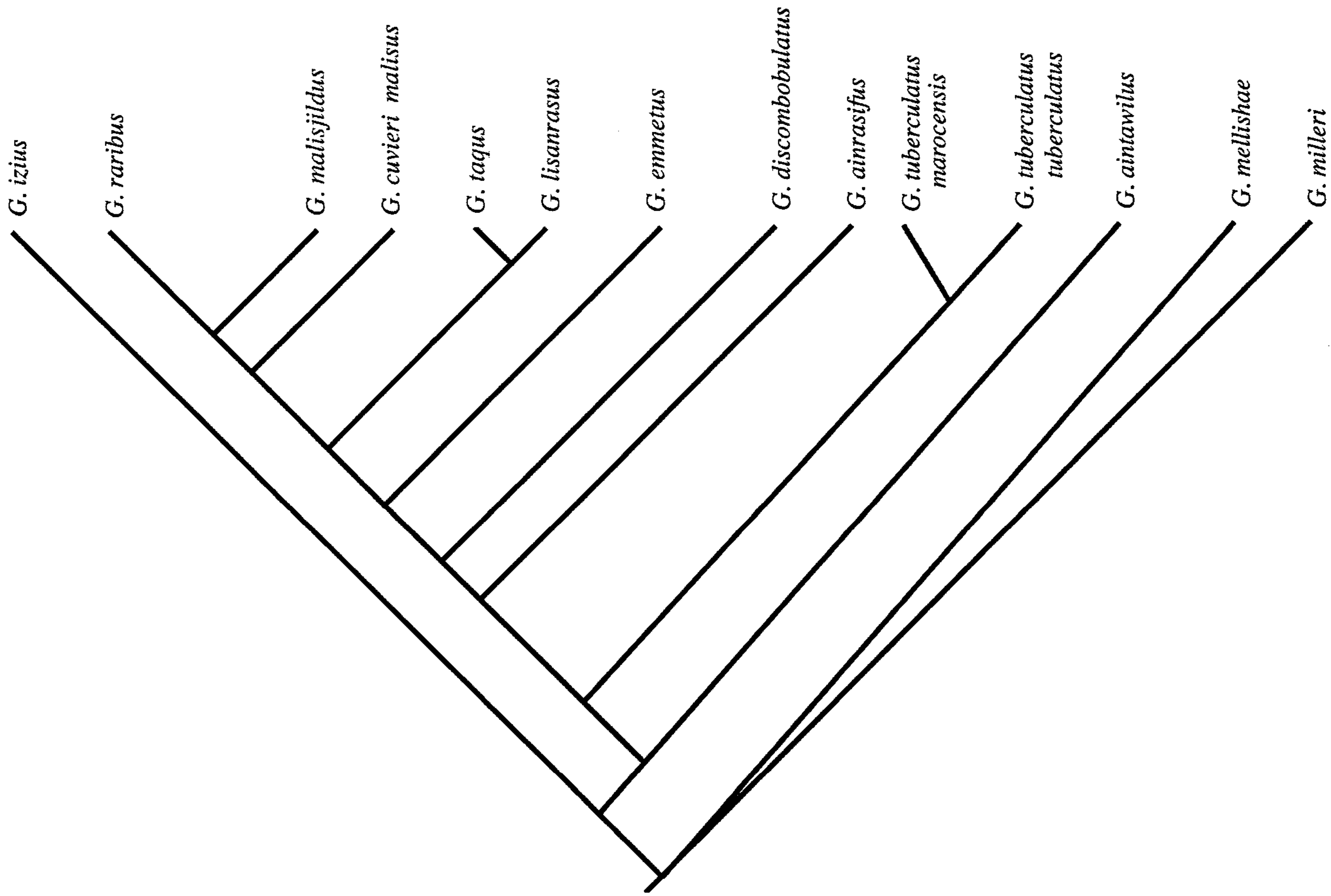

FIGURE 3-11--Phylogenetic tree derived using MacClade 4.06 (Maddison and Maddison, 2001) and PAUP* 4.0 Beta 10 (Swofford, 2002).

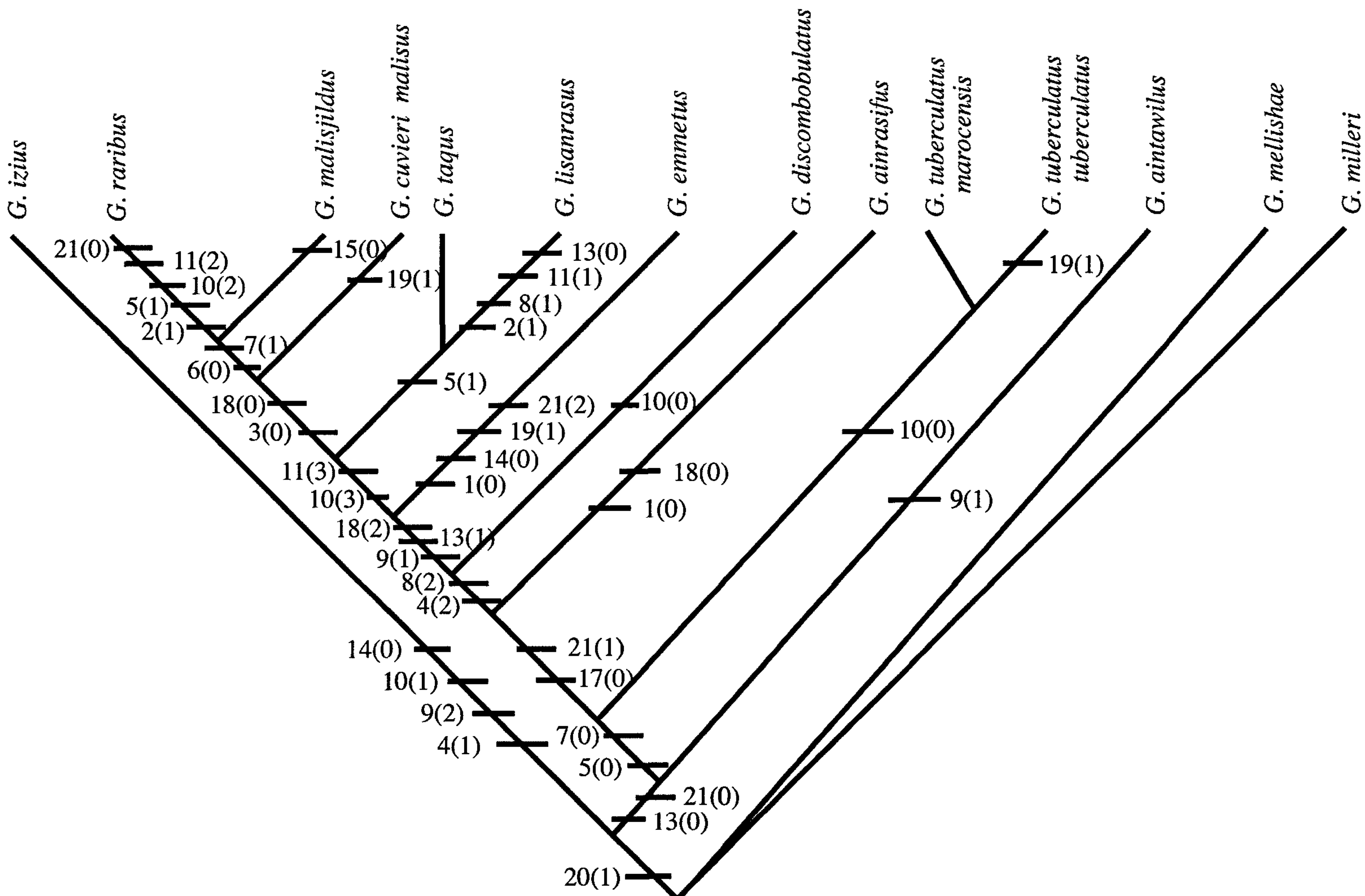

FIGURE 3-12 – Distribution of character states on the phylogenetic tree generated by PAUP* 4.0 Beta 10 (Swofford, 2002) and MacClade 4.06 (Maddison and Maddison, 2001).

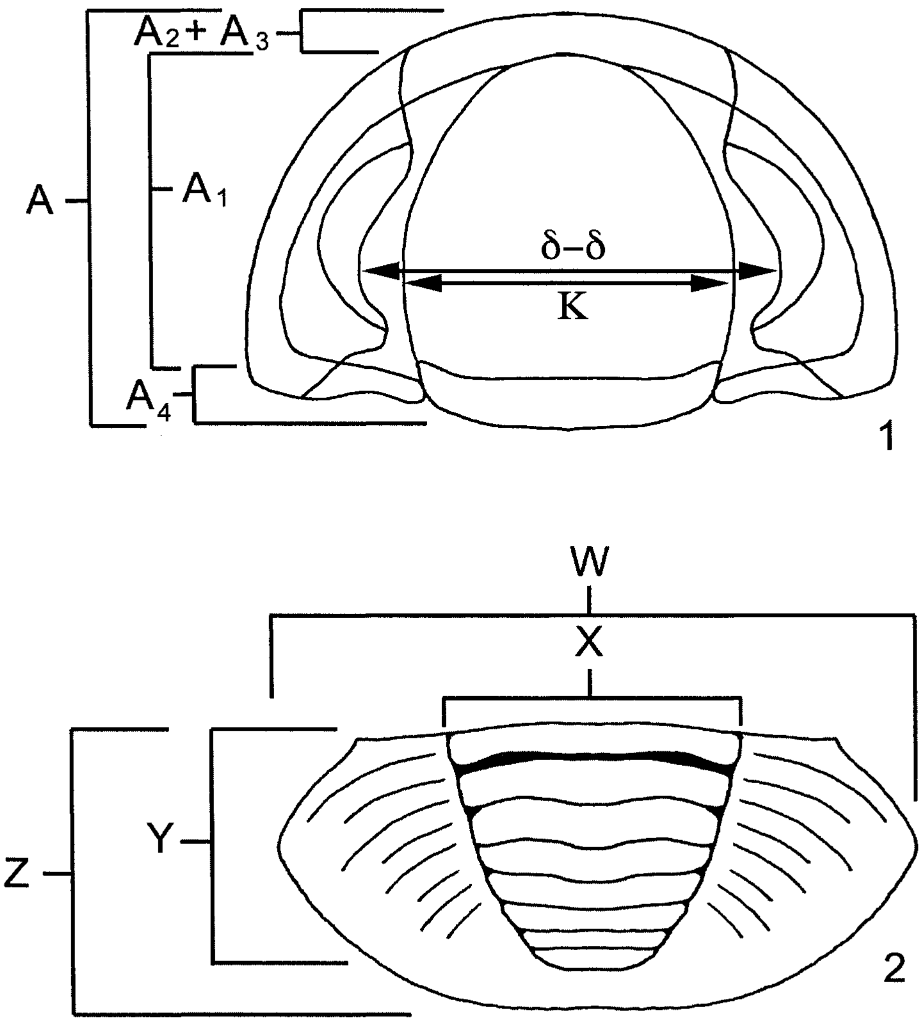

FIGURE 3-13 -- Generalized *Gerastos* cephalon (1) and pygidium (2) (based upon Owens, 1973).

Order Proetida Fortey and Owens, 1975

Family Proetidae Salter, 1864

Genus GERASTOS Goldfuss, 1843

1958 *Proetus (Longiproetus)* CAVET & PILLET, 1958, p. 23-24.

1980 *Gerastos (Longiproetus)* CAVET & PILLET, 1958: Šnajdr, p. 62.

1990 *Longiproetus* CAVET & PILLET, 1958: Lütke, p. 30-31, text-fig. 8.

?1994 *Longiproetus* CAVET & PILLET, 1958: Lieberman, p. 27.

1996 *Longiproetus* CAVET & PILLET, 1958: Basse, p. 151.

Type species.— *Proetus cuvieri* Steininger, 1831, from the Ahrdorf Formation, Gees, Eifelian, of Germany.

Included species from Morocco.— *Gerastos tuberculatus marocensis* new subspecies, *Gerastos aintawilus* new species, *Gerastos lisanrasus* new species, *Gerastos ainrasifus* new species, *Gerastos discombobulatus* new species, *Gerastos cuvieri malisus* new subspecies, *Gerastos taqus* new species, *Gerastos malisjildus* new species, *Gerastos raribus* new species, *Gerastos emmetus* new species, and *Gerastos izius* new species.

Remarks.— Owens (1973, p. 9) illustrated the type species of *Gerastos, Longiproetus* and *Coniproetus*. He provided a list of characteristics that may be used to distinguish *Proetus cuvieri*, the type species of *Gerastos*, from *Proetus concinnus*, the type species of *Proetus*:

> (a) ε and ξ widely separated, ε a wide angle (c. 160 °); (b) lateral margin of glabella abaxially convex; (c) glabella as long as wide; (d) distinct eye platform; (e) no genal spine; (f) indistinct lateral occipital lobes; (g) no incurving terrace lines on margin of pygidium; and (h) band of parallel terrace lines around pygidial margin (Owens, 1973).

The characteristics of *Gerastos* fit some of the Moroccan species, though it is thought that the character state of possessing a "distinct eye platform" (Owens, 1973) is not always a distinctive enough morphological feature to assist in defining the difference between *Proetus* and *Gerastos*. As well, not all *Gerastos* lack a genal spine. These may have been perfect character states to differentiate between the type species for both *Proetus* and *Gerastos*, but they do not necessarily carry beyond *Proetus cuvieri* and the *Proetus concinnus* group.

Another idea introduced by Owens (1973) was the incorporation of *Longiproetus* within *Gerastos*, for which he provided a diagnosis:

> Glabella as wide (trans.), or wider than long, lateral margins abaxially convex; lateral glabellar furrows not incised; eye platform commonly present; ε and ξ widely separated, ε a wide angle (*c.* 160°); no preglabellar field; long genal spine on some species, but commonly short or absent; lateral occipital lobes indistinct or absent; pygidial border typically absent; band of parallel terrace lines around pygidial margin; sculpture granular, or exoskeleton smooth (Owens, 1973).

Though *Longiproetus* had been reinstated by Šnajdr (1980), the phylogenetic analysis herein shows this to be incorrect, and that Owens (1973) was right to incorporate it within *Gerastos*. Before outlining the phylogenetic analysis that led to the reinstatement of *Longiproetus*, it should be noted that when the type species, *Proetus tenuimargo* Richter, 1909, was coded and run through PAUP* 4.0 Beta 10 (Swofford, 2002) along with the species analyzed in this work, it was located amongst the ingroup of *Gerastos* species, suggesting that it is a *Gerastos*.

Šnajdr (1980) provided a diagnosis for *Longiproetus*, though many of the character states are shared with *Gerastos* and therefore cannot be used as defining states for *Longiproetus*. Indeed, when the character states written by Šnajdr (1980) were included in the phylogenetic analysis using PAUP* 4.0 Beta 10 (Swofford, 2002) and MacClade 4.06 (Maddison and Maddison, 2001), *Longiproetus* still was placed among

Gerastos species in the cladogram. Work completed after Šnajdr (1980) continued to maintain *Longiproetus*, this only compounded the problems within the genus. Morzadec (1983) tentatively assigned *Proetus (Gerastos)* sp. aff. *tenuimargo* and *P. (G.)* cf. *tenuimargo*, though he felt that this assignment was possibly ill-founded as they did not share enough character traits with *Longiproetus* to sustain this assignment. Basse (1996) further confused matters when he stated that Morzadec's (1983) species should be classified within *Longiproetus*. The phylogenetic analysis of *Gerastos*, however, supports Morzadec (1983) in assigning his specimens to *Gerastos*, but not to the species that he identified. Morzadec's (1983) specimens should be re-examined to identify them correctly, though given the fragmented and disarticulated condition of the specimens, an accurate taxonomic assignment may never be concluded. Lütke (1990) continued the mistaken use of *Longiproetus*, even though a number of his character states are also visible within *Gerastos*. He refined the definition of *Longiproetus*, and stated that only the type species should be included within the genus. It should be noted that the type species was used for the phylogenetic analysis in this study, and as stated previously, it fell within *Gerastos*. Therefore, even with the differing rostral plate and anterior cephalic border, it is thought that this is not enough to classify *Longiproetus* into another genus. The traits manifested by Lütke (1990) can be explained by the Darwin principle ("The more useful a character is in adapting an organism to a specific habitat or niche, the less valuable it is in classification (Darwin 1859:414)" (Mayr and Ashlock, 1991)) and hence have little relevance to the diagnosis of *Longiproetus*. Lieberman (1994) continued to use *Longiproetus*, though he had stated within his discussion that *Longiproetus* "may be a taxonomic grab bag as presently constructed… [and] that several of the taxa that have been assigned to *Longiproetus* in the past should instead be placed in other genera, such as *Coniproetus* and *Proetus*" (Lieberman, 1994). Given all of these facts, *Longiproetus* should no longer be recognized as a genus.

Adrain (1997) provided a diagnosis for *Gerastos* that is based upon a Middle Devonian species from Germany, but did so after including a number of Wenlock species from the Canadian Arctic in the genus. One of the characteristics that he included in his diagnosis for the genus is the presence of a "single rows of small perforations" between prominent subparallel terrace lines on the cephalic and pygidial margins (Adrain, 1997). These perforations are clear on the silicified Silurian specimens that he illustrated (and also on closely related undescribed silicified species of similar age from the Mackenzie Mountains, northwestern Canada; in possession of B. D. E. C., work in progress). They are not, however, apparent on any of the Devonian species we would assign to *Gerastos* from Morocco or Europe. This is even true for a silicified holaspid free cheeks found in the base of the section at Zguilma, and so cannot be ascribed to differences of preservation between silicified and calcareous specimens of this genus. Thus, this characteristic appears to be a synapomorphy for a clade of Laurentian Silurian species, and not to be a defining feature of all species of *Gerastos*. Whether or not this synapomorphy of the Silurian group is adequate to regard them as forming a different genus-level taxon (a sister group to *Gerastos sensu stricto*) is open to debate.

GERASTOS TUBERCULATUS (Barrande, 1846)

GERASTOS TUBERCULATUS MAROCENSIS new subspecies

Figures 3-14.1 – 3-14.12; 3-15.1 – 3-15.10; 3-16.1 – 3-16.13; and 3-17.1 – 3-17.6

Diagnosis.— Sculpture on glabella consists of pointed tubercles, much coarser than elsewhere on exoskeleton, and tubercles sometimes are composite (composed of > 1 tubercle); distinct tuberculose ridge ('*ocular platform*') is present on genal field; genal spines are short, but distinct and pointed; hypostomal rhynchos is only moderately inflated; hypostomal shoulder and posterolateral corners are subangular; and border furrow on pygidium is shallow.

Description.— Exoskeleton is inflated. Cephalon length (A, sag.) is about 0.3 (0.26-0.34) length of exoskeleton (sag.). Cranidial width (tr.) of β-β is 0.69-0.73 to width (tr.) of ∂ - ∂; width (tr.) across palpebral lobes (∂ - ∂) is roughly 1.08 -1.35 times length of cephalon (A, sag.). Anterior portions of facial suture run forward from palpebral lobes roughly sub-parallel, then weakly converge, diverge (to β) and then converge forward (to α), in gentle sinuous path. Posterior portions of facial suture initially concave laterally (at ξ), then curve outward to trend almost subtransversely before curving to cross posterior border posterolaterally (at ω). Axial furrows are deep and narrow, deflected outward around ovoid glabella. Glabellar maximal width (K, tr.) is close to maximum (0.92-1.2) length of glabella (A_1, sag.) in front of S0 (A_4). S0 is deep, short and subtransverse. Glabella distinctly overhangs anterior border/preglabellar furrow anteriorly, when viewed dorsally. L0 (occipital ring = A_4) is similar in width (tr.) to glabella (A_1) across back of L1 (WL0/WL1 = 0.96-1.06). Lateral occipital lobes are defined by furrows that are distinct anteriorly, but disappear posterolaterally approximately half way down L0. S0 is slightly deflected anterolaterally distally in front of occipital lobes. S1 forms shallow curved furrow that is convex anteromedially, and runs posteriorly and slightly abaxially to join or almost join axial furrows near midlength of palpebral lobe. S1 is mainly distinct from glabella through lack of sculpture. Shallow to almost obscure S2 is shorter than but subparallel with S1, and runs towards axial furrows near front of palpebral lobe. S3 is weak and subcircular, located anterior to midpoint of S2. Glabellar lobes lack any distinct independent inflation. Preglabellar furrow is deep, and confluent with anterior border furrow in front of median third of glabella. Glabellar sculpture consists of fine to coarse, slightly distally pointed tubercles, with finer tubercles concentrated on margins of glabella. Some larger tubercles appear to be coalescing or dividing (budding). Tubercles on L0 are smaller, and consequently more sparsely distributed than on glabella (A_1). Median occipital tubercle or node is small and usually defined, but cannot be discriminated readily on some specimens. Anterior border is furrow firmly impressed, with front of fixed cheek slightly overhanging border furrow. Anterior region of fixed cheeks has scattered fine tubercles or granules. Palpebral lobe is smooth except for dense fine tubercles or coarse granules (1 – 2 deep) round rim of palpebral lobe. Very shallow sub-crescent furrow runs sub-parallel with margin of palpebral lobe near midlength of lobe. Posterior border furrow is firmly impressed and subtransverse, with little or no signs of interruption by sutural ridge; becomes shorter (exsag.) and slightly shallower distally at genal angle. Posterior portion of fixed cheeks and posterior border are smooth. Posterior border is moderately inflated, turns slightly backward and becomes longer (exsag.) distally beyond the fulcrum. Anterior border is slightly convex dorsally and approximate equal in length (sag.) to L0 ($A_{2+3}/A:A_4/A$ = 0.04-0.19:0.14-0.21). Anterior border has sculpture of scattered granules, with two to three fine, sharp ridges and grooves running around anterior and lateral margins of cephalon.

Free cheeks are slightly flared abaxially, therefore widest point (tr.) of cephalon is across genal spines. Lateral border furrows are moderately incised anteriorly, but shallow slightly near genal angle where they abut posterior border furrows at approximately 70° to 90°. Genal spines are short (roughly length of posterior border) and pointed. Shallow but distinct furrow runs around base of eye, below distinct blunt crescent socle present under visual surface (slightly less inflated near anterior of eye). Genal field is sculpted with fine tubercles; width of genal field is at its narrowest point beneath socle, adjacent to δ; overhangs lateral border slightly anteriorly; has low to distinct tuberculose ridge running sub-parallel with eye = ocular platform. Lateral border is comparatively convex dorsally and sculpted with fine, sparsely scattered granules dorsally, with stronger sculpture of fine ridges and grooves along margins. Visual surface is higher than genal field. Ventral surface of doublure of free cheeks has numerous asymmetrical terrace lines (steep sides outward).

Rostral plate is subtriangular, with sculpture of terrace lines that matches sculpture of doublure of free cheeks. Connective sutures converge back at angle of about 110°. Width of rostral plate (tr.) is approximately 0.22 width of cephalon (tr.).

Hypostome is typical proetid-shield-shaped, with long, dorsolaterally flaring anterior wings. Width (tr.) across anterior wings is 0.28 width of cephalon (tr.). Firmly impressed anterior border furrow, slightly shallower and broader lateral border furrows, and still shallower and broader posterior border furrow bound middle body. Rhynchos is moderately prominent anteriorly but not strongly pinched laterally. Middle portion of middle body is sculpted by anastomosing terrace lines, accentuating rhynchos. Posterior lobe is weakly separated from anterior lobe laterally by shallow, broad middle furrows that almost disappears medially. Middle furrows are weakly concave adaxially. Shoulder is small, rounded, and located posterior to midlength of hypostome, and extends outward only to width (tr.) of hypostome immediately behind base of anterior wings. Lateral and posterior borders have series of three to four terrace ridges separated by grooves. These ridges extend anteriorly onto proximal portions of anterior wings, and additional terrace ridges are present on distal regions of anterior wings. Posterolateral corners of margin are slightly protuberant but not spinose.

Thorax has 10 segments. Axis tapers slightly, almost uniformly, in width (tr.) posteriorly (posteriormost of axis 0.71-0.83 width (tr.) of anteriormost of axis). Axis is approximately 0.43 width (tr.) of thorax. Axial rings are short, with length (sag.) about 0.15 of width (tr.). Preannulus is present on all segments, but longer (sag.) on anterior segments than on posterior segments (still present as interannular lobe behind first axial ring of pygidium). Inner region of pleura runs transversely to fulcrum, and then distal portion of segment is turned ventrally and laterally. Pleural furrows are short (exsag.) and deep, and extinguish distally on upper part of distinct articulating facets that occupy two-thirds length (exsag.) of segments. Distal ends of segments are rounded anteriorly, and subangular to pointed posteriorly. Anterior pleural bands are slightly shorter (exsag.) than slightly more elevated posterior pleural bands. Sculpture of fine tubercles is present on axial rings. Pleural ribs are smooth, or with few minute tubercles on posterior pleural bands. Anterior and posterior edges of axial rings are steep. Articulating half rings are short (sag.), steep posteriorly, and bounded from interannular lobe by firmly impressed furrow.

Pygidium is in form of segment of a circle, and is micropygous. Axis is comparatively wide: maximum width (tr.) of axis (X) is about 0.43 (0.34 – 0.48) maximum width (tr.) of pygidium (W). Axis has seven rings and terminal piece. Posteriormost axial ring of pygidium is 42 – 61% width (tr.) of anteriormost of pygidial axial ring. Axis is slightly inflated, and axial furrows are firmly impressed. Pleural furrows slightly deeper than interpleural furrows. Both sets of furrows curve posteriorly and expire distally in broad border region. At least six pairs of anterior and posterior bands are present on each pleural lobe, therefore forming 5+1 furrow pattern. Border furrow is shallow or of moderate depth, and more distinct posteromedially than anterolaterally. Axial rings are subtransverse anteriorly and posteriorly, but broadly *m*-shaped sagitally. Row of distinct furrows occurs in anterior two-thirds of axial ring close to axial furrows, behind first axial ring (slightly farther from axial furrows on more anterior segments). Each of these furrows is oriented slightly anterolateral to posteromedial, relative to exsagittal line. Finer tubercles occur on pleural ribs proximal to border region. Small number (1-2) of fine terrace ridges is present along margin of pygidium.

Etymology.— This subspecies is named for its geographic location in Morocco (versus *Gerastos tuberculatus tuberculatus* (Barrande, 1846), which occurs in Bohemia, in the Czech Republic).

Types.— Holotype, complete specimen UA13276. Paratypes, complete specimens UA13277-13280, 13464-13465.

Occurrence.— Zguilma specimens from near base of section (ZGEE1), Timrhanrhart Formation, upper Emsian on north to northeast flank of Jbel Zguilma, south of Foum

FIGURE 3-14—*1-12*, *Gerastos tuberculatus marocensis* new subspecies from ZGEE1 & ZGEE2, Timrhanrhart Formation, Jbel Zguilma, Dra Valley, southern Morocco. *1, 3-4, 7, 9* (UA13277) (complete specimen). *1*, anterodorsal view X3.4; *3*, lateral view X2.7; *4*, lateral view X3.2; *7*, dorsal view X3.6; *9*, posterolateral view X3.5. *2, 5, 8, 11-12* (UA13278) (complete specimen). *2*, anterior view X4.0; *5*, dorsal view X3.9; *8*, dorsal view X3.9; *11*, dorsal view X5.1; *12*, lateral view X4.2. *6, 10* (UA13279) (complete specimen). *6*, anterodorsal view X4.1; *10*, dorsal view X4.0.

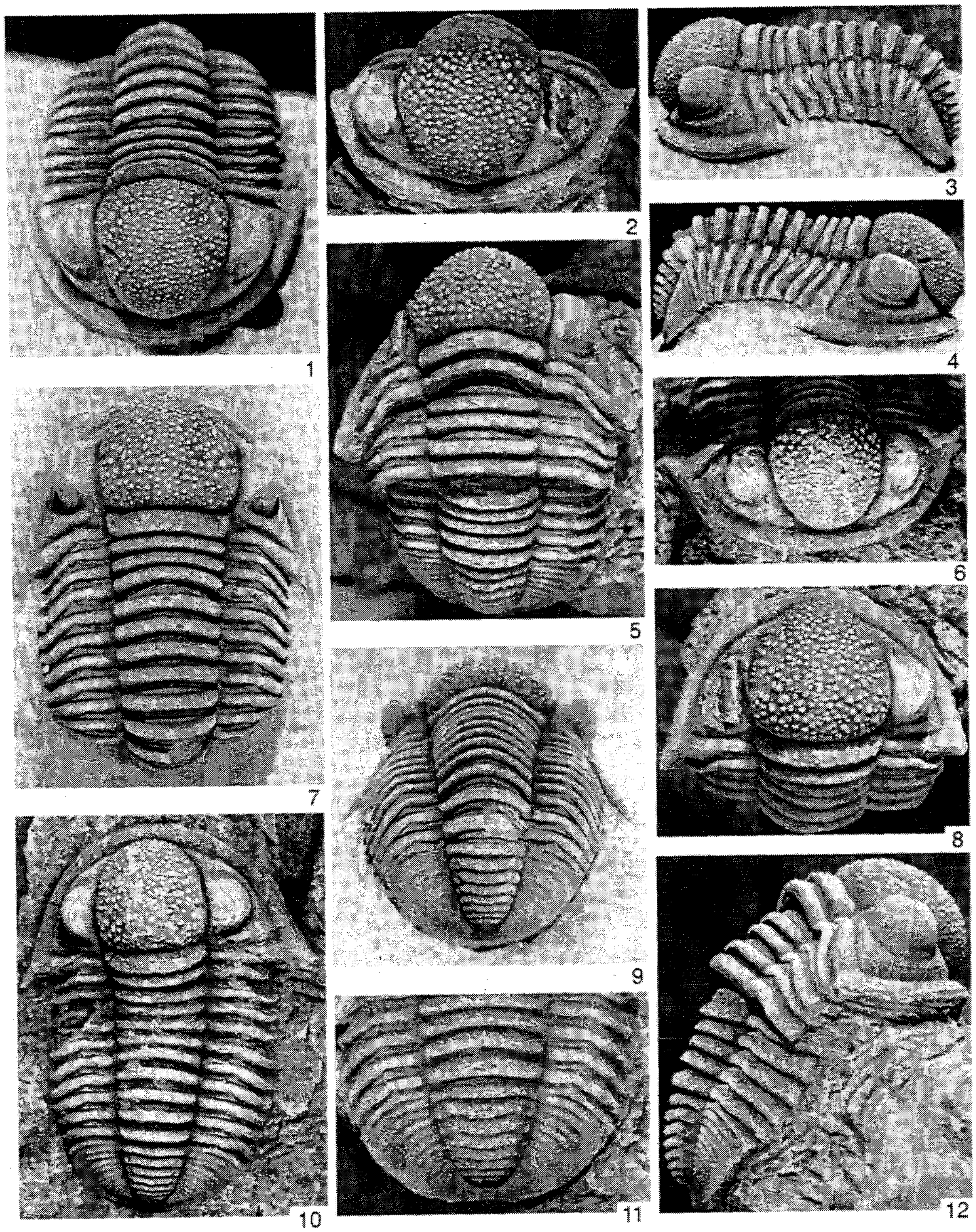
1
2
3
4
5
6
7
8
9
10
11
12

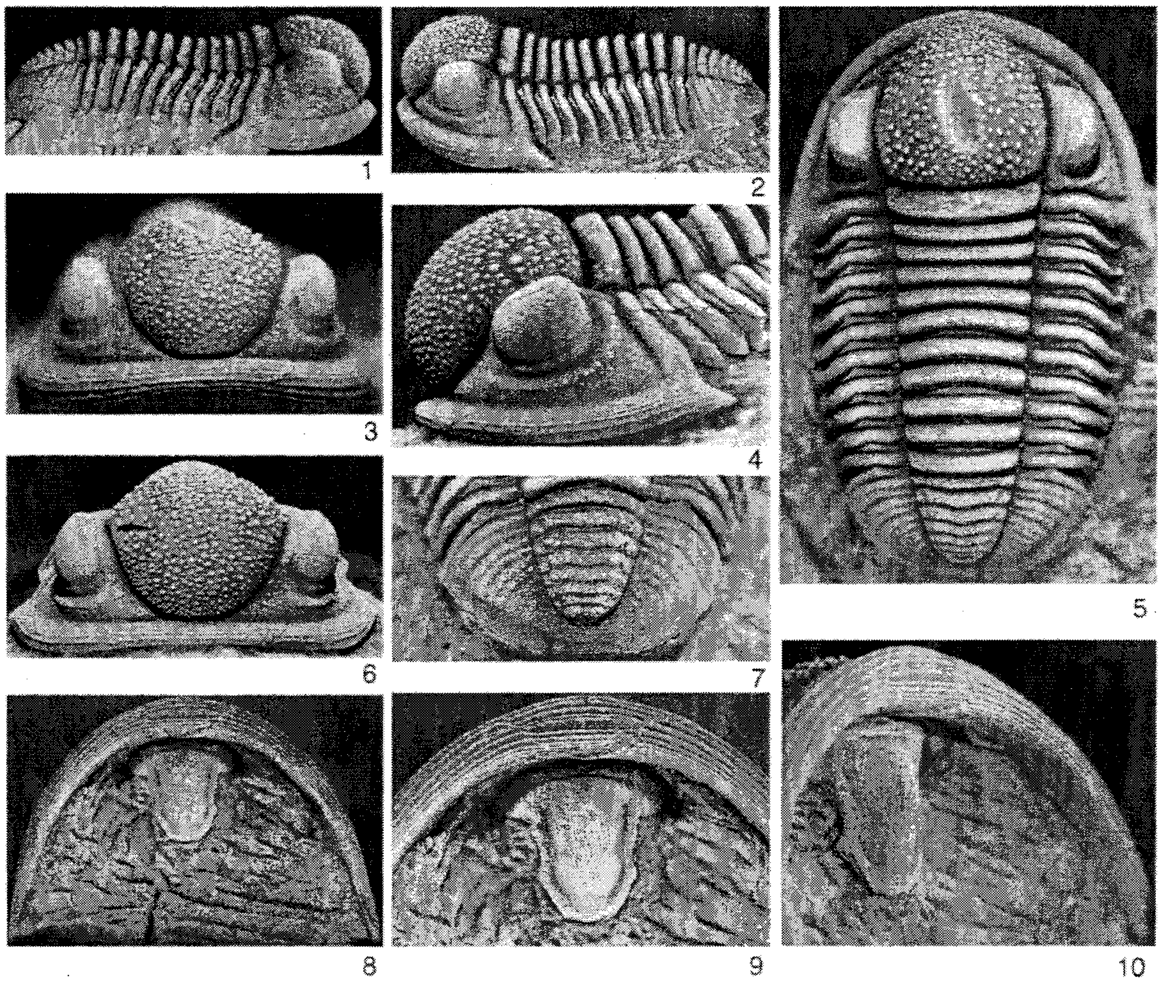

FIGURE 3-15—*1-6, Gerastos tuberculatus marocensis* new subspecies from ZGEE1 & ZGEE2, Timrhanrhart Formation, Jbel Zguilma, Dra Valley, southern Morocco. *1-3, 5, 7-10* (UA13276) (complete specimen). *1*, lateral view X2.1; *2*, lateral view X2.1; *3*, anterior view X3.4; *5*, dorsal view X3.4; *7*, dorsal view X4.1; *8*, ventral view hypostome X3.5; *9*, ventral view of hypostome X5.4; *10*, oblique lateral view X5.9. *4, 6* (UA13277) (complete specimen). *4*, oblique lateral view X4.9; *6*, anterior view X3.4.

FIGURE 3-16—*1-13, Gerastos tuberculatus marocensis* new subspecies from Taharajat, Tazoulaït Formation, Ma'der region, southern Morocco. *1-5* (UA13464) (complete specimen). *1*, anterior view X3.0; *2*, posterodorsal view X3.2; *3*, lateral view X2.1; *4*, lateral view X2.1; *5*, dorsal view X3.1. *6-9* (UA13465) (complete specimen). *6*, lateral view X2.1; *7*, posterior view X3.0; *8*, dorsal view X2.9; *9*, anterior view X2.8. *10-13*, (UA13466) (complete specimen). *10*, anterior view X3.7; *11*, lateral view X3.4; *12*, dorsal view X3.6; *13*, posterodorsal view X3.6.

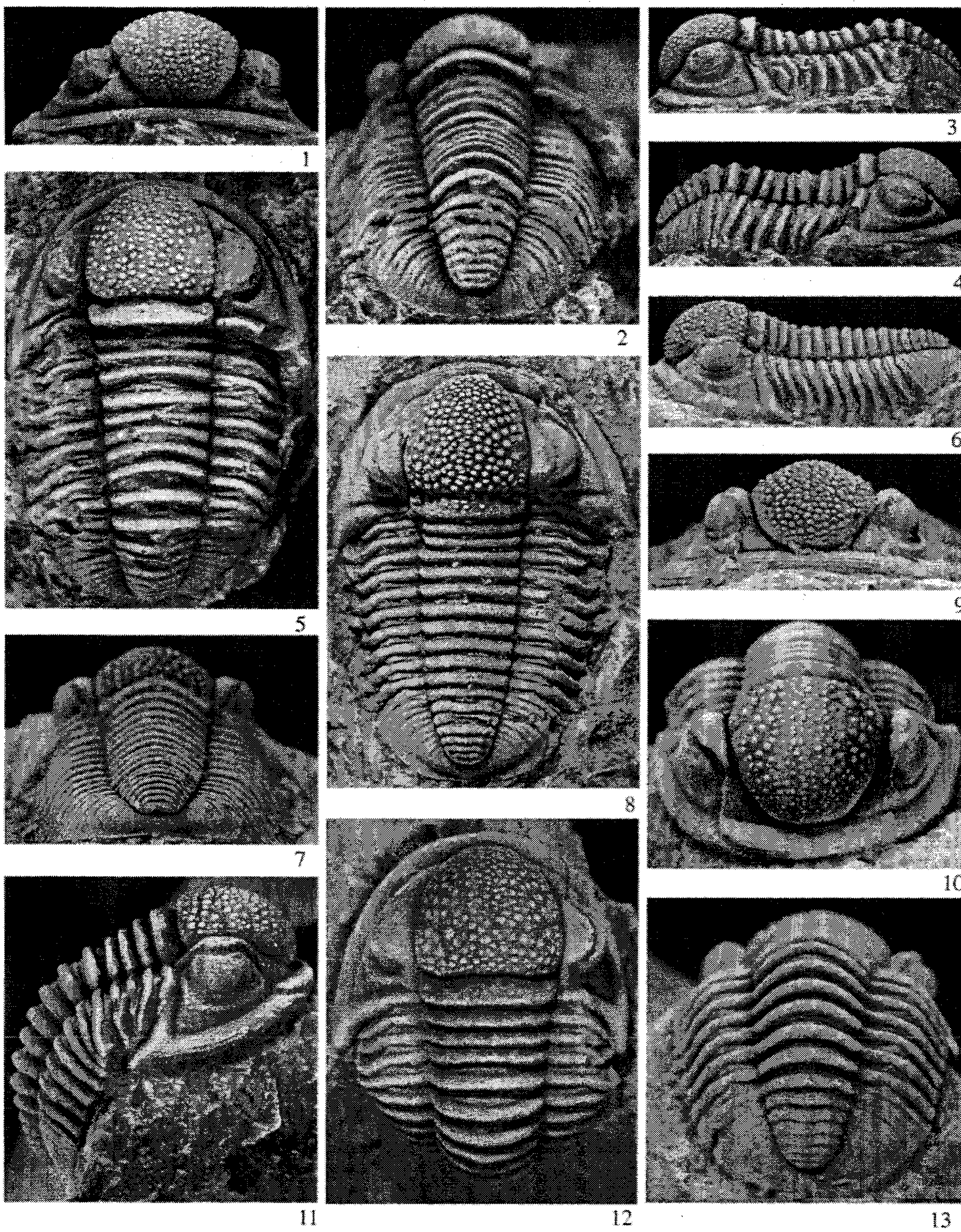
1
2
3
4
5
6
7
8
9
10
11
12
13

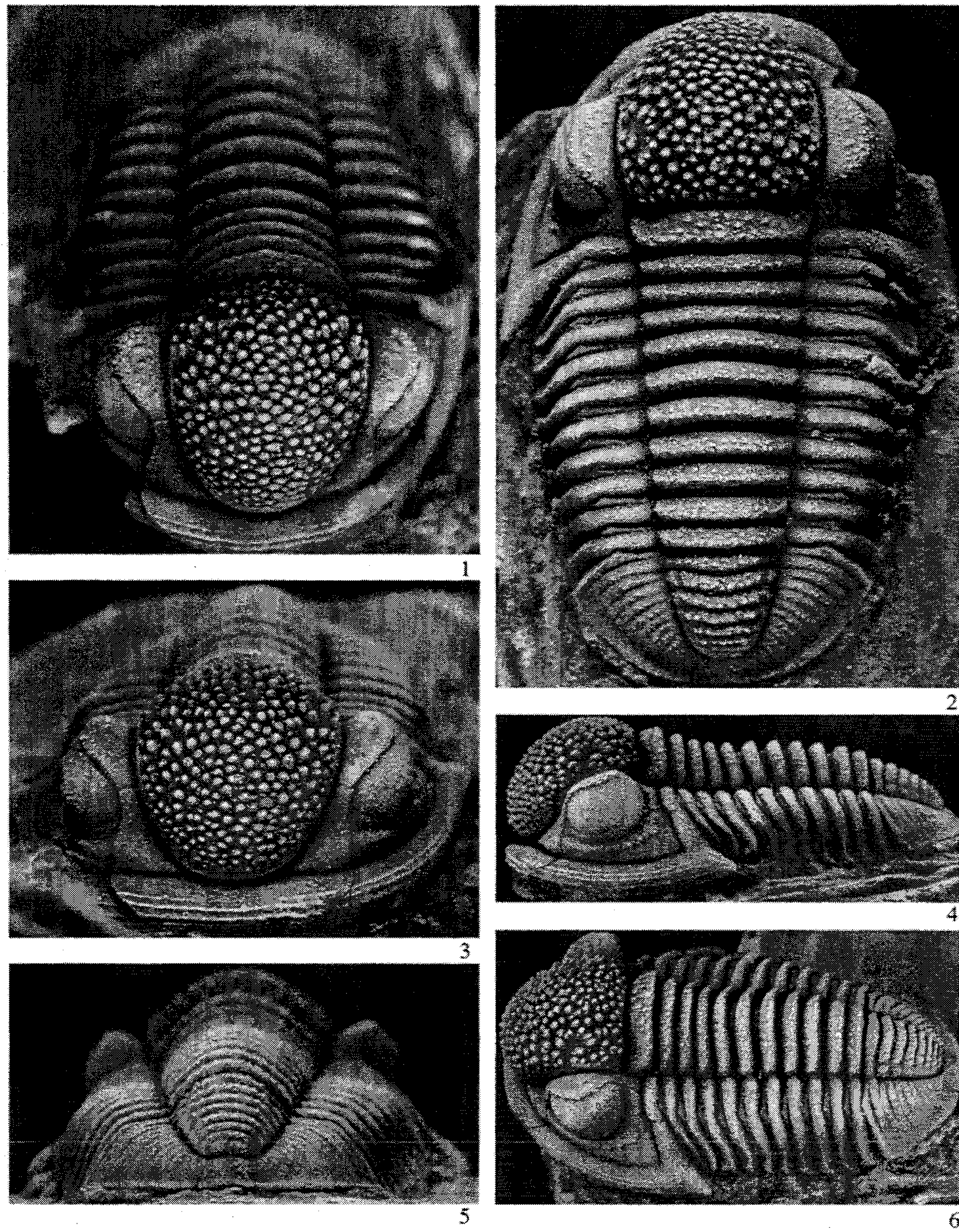

FIGURE 3-17—*1-6*, *Gerastos tuberculatus marocensis* new subspecies from the '*Proetus* horizon', Amerboh Group, Merzouga, Tafilalt region, southern Morocco. *1-6* (UA13280) (complete specimen). *1*, anterodorsal view X9.6; *2*, dorsal view X9.6; *3*, anterior view X9.9; *4*, lateral view X6.4; *5*, posterior view X9.5; *6*, anterolateral view X5.6.

Zguid, southern Morocco; Merzouga specimen from the upper Emsian, Amerboh Group (Bultynck and Walliser, 2000) [equivalent formation in the Tafilalt to the Timrhanrhart Formation of the Dra], eastern Morocco; and Taharajat specimens from the *Morocconites/Hollardops/Scabriscutellum* horizon of the Tazoulaït Formation, upper Emsian (Bultynck and Walliser, 2000) [equivalent to both Timrhanrhart Formation and Amerboh Group], Taharajat, Oufatene, Ma'der, southeastern Morocco.

Discussion.— *Gerastos tuberculatus marocensis* and *Gerastos tuberculatus tuberculatus* (Barrande, 1846; see Šnajdr 1980, p. 48-49; pl. 2, figs. 9-21), from strata of similar age in the Dalejan (upper Emsian) Suchomasty Limestone of Bohemia share a number of characteristics, including: tuberculose ridge on the genal field, short but distinct genal spines, and tuberculose sculpture on glabella. Differences between these species include details of the morphology of the hypostome. *Gerastos tuberculatus tuberculatus* has more ornamentation in the form of terrace lines upon the middle body, a foreshortened posterior border, and lacks the small, rounded shoulders observed in *Gerastos tuberculatus marocensis*. A specimen assigned to *G. tuberculatus* illustrated by Alberti (1969, pl. 1, figs. 7a, 7b) has a granulose sculpture on the lateral border of the free cheek and more divergent anterior branches to the facial suture than *G. tuberculatus marocensis*; therefore, one might conclude that Alberti (1969) does not have the correct species name for the figured images. Other Bohemian proetids illustrated by Šnajdr (1980) are not as similar. Therefore, due to the morphological differences and the palaeogeographic separation of Morocco and Bohemia in the Emsian, it was concluded that the Zguilma specimens should be included in an allopatric subspecies. These two subspecies existed at the same time in two different regions, where the amount of genetic interchange was insufficient for them to form a single range of characteristics.

Heckel & Witzke (1979) presented a generalized palaeogeographic representation of the Middle Devonian, while Charpentier (1984) confirmed Heckel & Witzke's (1979) conclusions based upon conodont faunal distribution during the Early Devonian. Heckel & Witzke (1979) depicted a warm subtropical current circulating from Bohemia in a counterclockwise direction to North Africa and back up into the southern European region and marginally east, therefore possibly accounting for the same species occurring in both Morocco and Bohemia. This also explains the widespread distribution of the Moroccan subspecies in southern Morocco.

A number of specimens have been identified as *G. granulosus* by various workers (e.g. Kielan, 1954; Alberti, 1970; Schrank, 1972; Kowalski, 1990), though it is thought that this is the incorrect species assignment for these specimens. It is believed that *G. granulosus* has often been a grab-bag for any extremely pustulated *Gerastos*. The character states that differentiate *G. tuberculatus marocensis* from *G. granulosus* are that *G. granulosus* possesses the following traits while *G. tuberculatus marocensis* does not: limited pustulation upon the glabella (A_1) (not as extensive to that of *G. tuberculatus marocensis)*, with the tubercles loosely packed; the genal field is more ornamented than that of *G. tuberculatus marocensis*; genal spines are not pointed, they are more subangular to rounded, nor do they extend much beyond the transverse field of the cephalon; and the pygidial border is less pronounced, though the pygidial pleural and interpleural furrows are more defined.

It should also be noted that *G. granulosus* has been affiliated to a number of younger specimens (Eifelian), by Alberti (1970) from the Ma'der region, and one from the Late Emsian, that shall be discussed further with younger species in this work.

Alberti (1969) described two species that we would assign to *Gerastos* from Morocco. Both of these are based only on cranidia, making detailed comparisons with other species difficult. *Gerastos akrechanus* (Alberti, 1969) from northwestern Morocco, differs from *G. tuberculatus marocensis* in that the glabella sculpture has fewer coarse tubercles, the occipital lobes are wider (tr.), the anterior border is slightly shorter, and the dorsal surface of the glabella is less evenly convex dorsally when viewed in profile. *Gerastos prox umerbianus* (Alberti, 1969) from near Marrakech is not as similar, having distinctly coarser tubercles in the glabellar sculpture, a more convex forward anterior margin, and anteriorly divergent anterior portions to the facial sutures. The fact that these taxa, both *G. akrechanus* and *G. prox umerbianus*, demonstrate morphological differences from *Gerastos tuberculatus marocensis* could in part be accounted for by regional provinciality and the "deep and turbiditic Marrakech-Oujda basin" (Pique and Michard, 1989) that separated northern Morocco from southern Morocco. The Marrakech-Oujda basin was forming during the Early Devonian (Pique and Michard, 1989), and therefore possibly creating a dispersal barrier between *Gerastos* before the Late Emsian specimens of Zguilma. Though it might appear that this is a contradiction to the research of Heckel and Witzke (1979) and Charpentier (1984), if one considers the current to run from northeast to southwest along the Marrakech-Oujda basin into the Dra Valley region, this is still a strong argument. This can also be supported by Pique *et al.* (1991) when they figured the Early Devonian of Morocco and along the trend of Oujda-Marrakech there was deposition of a pelagic and turbiditic environment, hence assisting in the Marrakech-Oujda basin (Heckel and Witzke, 1979; Charpentier, 1984; Pique and Michard, 1989). One must also consider that migration is going to occur along a shallow shelf (Schraut, 2000; Scotese, 2001) rather than across a deep basin.

GERASTOS AINTAWILUS new species

Figures 3-18.1 – 3-18.4, 3-18.6 – 3-18.7

Diagnosis.— Granulated sculpture occurs on whole exoskeleton, prominent on glabella and axial region of thorax and pygidium, and reduced to granular size on remainder of exoskeleton. Pointed genal angle merges into small, pointed genal spine. Glabellar furrows S1, S2 and S3 present. S3 is elliptical, instead of the traditional semicircular shape. Glabella (A_1), in lateral view, is inflated. Pygidial border is shallow.

Description.— Exoskeleton is inflated. Cephalon length (A, sag.) is approximately 0.37 length of exoskeleton (sag.). Cephalon is bordered by number of terrace lines (maximum of 6 on lateral aspects). δ-δ (tr.) is 1.04 times length of cephalon (A) (sag.). Anterior portions of facial sutures, from δ to γ, convergence of approximately 64°, γ to β are near exsagittal and from β to α converge at approximately 76°. Posterior portions of facial sutures from δ converge in slightly tighter curve than that of δ to γ, γ diverges marginally to ξ just above posterior border furrow, and ξ diverges subtransversely and then hooks back to ω. Axial furrows and preglabellar furrow are deep, outlining ovoid glabella. Maximum length (sag.) of glabella (A_1) is 0.76 to maximum length (sag.) of cephalon. Glabellar sculpture is similar to Strømer's (1980) descriptions of sculpture, with some fused smooth composite tubercles (amalgamating tubercles) and ordinary smooth tubercles more posterior on A_1 grading into granule-type smooth tubercles without a "thin vertical canal" (Strømer, 1980) more anteriorly. Maximum width of glabella (K, tr.) is equivalent to maximum length (sag) of A_1. S0 is deep, short and transverse. Widths (tr.) of L0 and posterior edge of A_1 are equivalent. L0 (A_4, sag.) is approximately 0.11 in relation to length of cephalon (A, sag.). Lateral occipital furrows are short and incise moderately anterior half of occipital ring distinct though weak lateral occipital lobes. S1, S2 and S3 are shallow, only distinct through lack of ornamentation. S1 originates at axial furrow, adjacent to δ and curves adaxially to position above occipital lateral furrows, though S1 ends approximately midway between δ and ε. S2 mimics shape of, and parallels S1, and originates midway between γ and δ. S2 is narrower than S1, lacking extension adaxially into glabella. S3 is adjacent to γ and occurs approximately at midlength (tr.) of S2. S3 has convex shape, resembling an eyebrow. Glabellar lobes lack independent inflation. Anterior tip of glabella overhangs approximately 20% of anterior border when viewed dorsally and appears quite bulbous, in lateral profile. Preglabellar field is absent. Occipital ring has sculpture of tubercles marginally smaller than those on back of A_1. Median node of occipital ring is small, though distinct, located at back of L0. Anterior aspect of fixed cheeks marginally overhang moderately incised anterior border furrow. Fine granulations adorn anterior fixed cheeks. Single row of pustules skirts abaxial edge of palpebral lobes, anteriorly originating adjacent to S2 and posteriorly disappearing at back of lobe. Remainder of palpebral lobe lacks ornamentation. Posterior portions of fixed cheeks are smooth. Posterior border furrow is moderately incised, shallowing adaxially beyond sutural ridge. Posterior border is moderately convex, and becomes longer (exsag.) abaxially. Anterior border (A_2+A_3) is noticeably convex, and is approximately 0.12 length (sag.) of cephalon (A, sag.). Sculpture on anterior border is of fine granules.

Free cheeks flare abaxially, therefore widest point (tr.) on cephalon is at tips of genal spines. Genal spines are short, and flex laterally to sharp posterior tip. Lateral border is covered with fine granules and is moderately convex, lessening posteriorly. Lateral border furrow is moderately incised anteriorly and becomes slightly shallower posteriorly where it merges with posterior border furrow. Genal field is entirely ornamented with fine granules. Eye socle furrow is more incised posteriorly than anteriorly. Eye socle is weak. Length (exsag.) of eye to length of glabella (A_1, sag.) is approximately 0.54.

Hypostome is unknown.

Thorax is composed of ten segments. Length of thorax (sag.) is 0.41 length (sag.) of exoskeleton. Axial region (tr.) of thorax tapers from first to tenth segment by 25%. Axial region comprises approximately 0.39 width (tr.) of thorax. Anterior edge of axial ring slopes posterodorsally from shallow intra-annular furrow and posterior edge is steep, creating an imbricate pattern of axial rings. Ornamentation is of abundant tubercles on axial rings. Anterior pleural bands of pleural region of thorax appear stunted laterally, only extending just beyond fulcrum and extinguishing at articulating facet. Therefore posterior pleural band is considerably longer (exsag.) than anterior band (exsag.). Pleural furrows are deeply incised and extinguish at facet. Posterior pleural band displays a transverse profile to fulcrum and then curves ventrally and finally hooks anteriorly at distal end. Prosopon on pleural regions is limited to few pustules on dorsal apex of posterior pleural band, and articulating facet is smooth.

Pygidium resembles segment of circle, and is micropygous. Pygidium is 1.6 times wider (W, tr.) than it is long (Z, sag.). Axial region, viewed laterally, lacks prominent convexity, and is incised by deep axial furrows. Axis is comprised of seven rings and terminal piece that has weak postaxial lobe. Axial rings have elongate *m*-shape, and are incised with marginal pits situated distally on rings. Axial region (Y, sag.) comprises 0.73 pygidial length (Z, sag.) and maximum width of axis (X, tr.) is 0.39 of W (tr.). Axial rings taper from first to seventh ring by 38.5%. Prosopon upon axial rings is tuberculated and abundant. Interpleural furrows are slightly more incised than pleural furrows. Pleural furrows display a 3+1 pattern, with anterior pleural bands and posterior pleural bands equivalent in length. Pleural regions have very limited sculpture represented by fine granules. Pygidial border is present but weak and ornamented with fine granules.

Etymology.— Due to the extended nature (sag.) of the eyes, the species is termed 'eye long' in Romanized Arabic: eye = *ain* and long = *tawîl.*

Type.— Holotype, complete specimen UA13454. Paratype, pygidium UA13455.

Occurrence.— '*Harpes*/*Thysanopeltis* horizon' (BD5), El Otfal Formation, Eifelian, lowermost Middle Devonian, bou Dib, Ma'der region, southern Morocco.

Discussion.— Though *Gerastos aintawilus* shares a number of character states with *Gerastos tuberculatus marocensis*, there are a number of morphological features that may be used to differentiate the two species. *G. aintawilus* is basal to *G. tuberculatus marcocensis* in the phylogenetic analysis performed herein therefore demonstrating that they are closely related. *G. aintawilus* displays the following features, while *G. tuberculatus marocensis* does not: sculpture upon glabella, anterior to L0 is pustulated

FIGURE 3-18—*1-4, 6-7, Gerastos aintawilus* new species from the '*Harpes/Thysanopeltis* horizon' (BD5), El Otfal Formation, bou Dib, Ma'der region, southern Morocco. *1-4, 6-7* (UA13454) (complete specimen). *1*, oblique anterolateral view X4.5; *2*, lateral view X4.1; *3*, dorsal view X10.2; *4*, dorsal view X10.7; *6*, oblique anterolateral view X3.6; *7*, dorsal view X10.2. *5*, *Gerastos izius* new species form the '2cc horizon', Bou Dib Formation, Mrakib, Ma'der region, southern Morocco (UA13455) (pygidium), dorsal view X13.5.

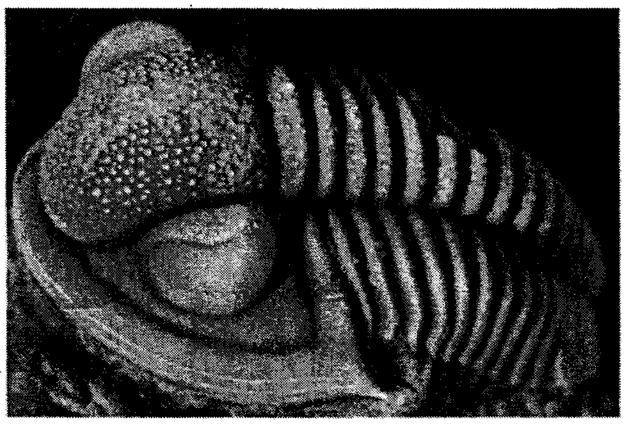

1

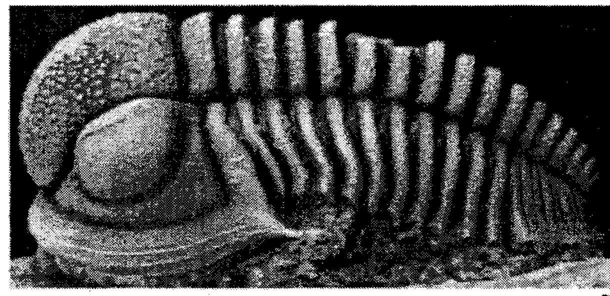

2

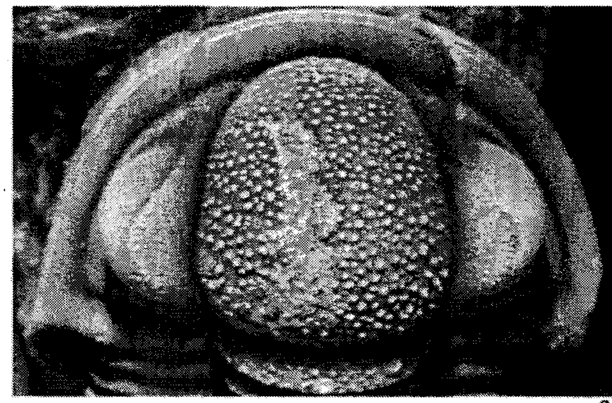

3

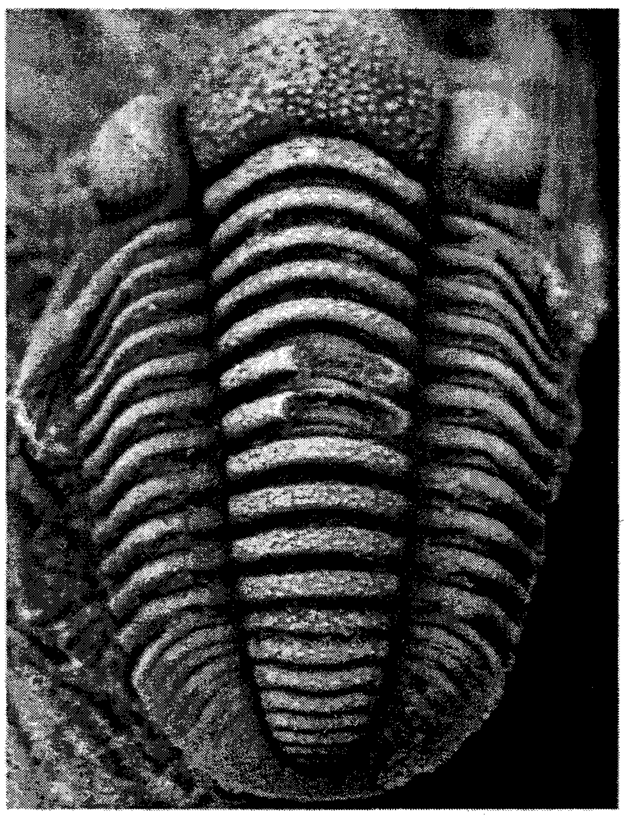

4

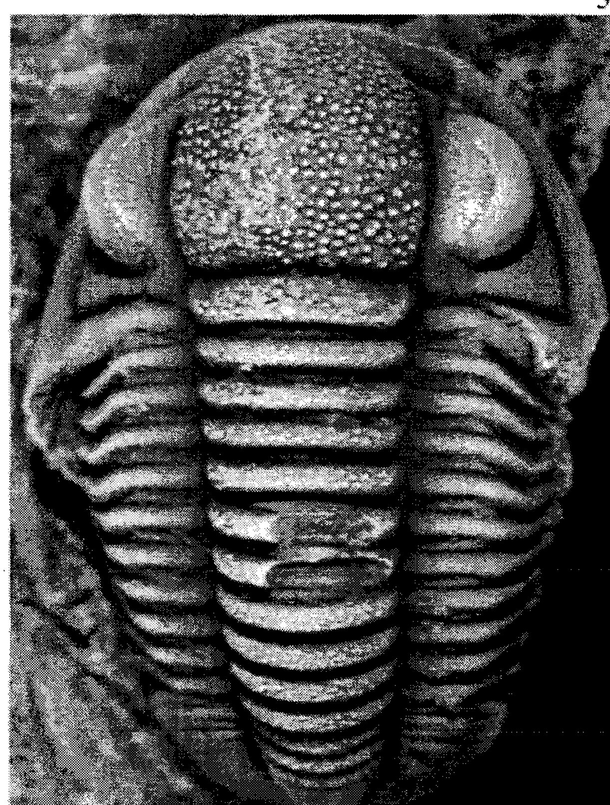

7

5

6

and displays amalgamated posterior tubercles, but the anterior sculpture is not as pronounced as that of *G. tuberculatus marocensis*; the facial sutures from γ–β–α do not diverge as strongly at β, therefore *G. aintawilus* displays a more convergent forward suture compared to *G. tuberculatus marocensis*; the ocular platform is absent or very reduced, though it does have some small pustules encompassing the eye socle furrow, but they do not produce a platform of any significance; the eye socle is quite faint and gives the appearance of a constricting furrow above the socle along with a marginal socle; the occipital ring only has marginally incising lateral occipital furrows, thus not producing the pronounced 'hooked' lateral occipital lobes that occur in *G. tuberculatus marocensis*; there are fewer pleural and interpleural furrows, with *G. aintawilus* exhibiting a 3+1 pattern and *G. tuberculatus marocensis* a 5+1 pattern; finally, the pygidial border is present, but weak in *G. aintawilus*, while it is distinct in *G. tuberculatus marocensis*.

All of the morphological features that differentiated *G. granulosus* from *G. tuberculatus marocensis* apply equally to *G. aintawilus*, except that *G. granulosus* and *G. aintawilus* both display a less pronounced pygidial border.

GERASTOS LISANRASUS new species

Figures 3-19.1 – 3-19.6

Diagnosis.— Distinct tongue-shaped glabella; fine granules cover almost entire exoskeleton, though are absent on front of glabella; anterior border is flattened; genal spines are pointed; and pygidium has 'rounded pentagon' shape and lacks distinct border.

Description.— Exoskeleton is inflated. Length of cephalon (A, sag.) is approximately 0.36 of length of exoskeleton (sag.). Six terrace ridges encircle cephalon, with one only skirting front of cephalon, marginally extending laterally across facial sutures upon anterior and lateral border. δ–δ width (tr.) is 0.9 times length of cephalon (A, sag.). Facial sutures converge from δ forward to γ in gentle curve, γ to β diverges slightly, and β to α converges almost transversely. Posterior facial sutures from δ converge tightly behind ε, diverge slightly from ε to ξ, and then diverge abaxially for short distance before curving tightly posterolaterally to ω. Axial furrows and anterior border furrow are deeply incised around tongue-shaped glabella. Length of glabella (A_1, sag.) is 0.75 length of cephalon (A, sag.). Length of glabella (A_1, sag.) is approximately 1.1 times width (K, tr.). S0 is short, deep, transverse laterally but curves forward at point in front of lateral occipital furrows. Sculpture upon glabella, anterior to S0, is composed of fused smooth composite tubercles (Strømer, 1980), that rapidly decrease in size and abundance to become smooth granule type tubercles (without central canal) (Strømer, 1980) anterior to S2 and further decrease in size and number, grading into smooth anteriormost glabella, approximately adjacent to midpoint between γ–β. S1, S2 and S3 are weakly defined, only distinguishable due to lack of ornamentation. S1 is more prominent and longer than either S2 or S3; and it originates at axial furrow marginally anterior to position (tr.) of δ, travels posteromedially to approximately a position opposite (tr.) δ, and cuts posteriorly to position opposite (tr.) ε, that is in front of lateral occipital furrows. S2 is shorter and essentially parallels S1, and terminates approximately quarter distance from midline of glabella. S3 is positioned approximately opposite (tr.) γ and anterior to position where S1 turns backward. S3 has shape similar to centrally pointed eyebrow. Glabellar lobes lack independent convexity. Anterior tip of glabella overhangs approximately half of anterior border, viewed in lateral profile and has pointed bulbous appearance similar to tip of tongue. Width (tr.) of back of glabella anterior to S0 is equivalent to width (tr.) of occipital ring. Occipital ring (A_4) length (sag.) comprises 0.15 length (sag.) of cephalon (A). Lateral occipital furrows are short and posterolaterally curved to give a 'hooked' appearance. Ornamentation upon occipital ring is comprised of abundant granules, with posteriorly placed small, median occipital node and marginally larger granules along abaxial flank of lateral occipital furrows. Preglabellar field is absent. Anterior border (A_2+A_3) length (sag.) comprises 0.08 of cephalon (A) length (sag.); is flattened in lateral profile; and is ornamented with fine granules. Fronts of fixed cheeks are adorned with fine granules. Palpebral lobes essentially lack ornamentation, except for posterior to δ, fine single row of pustules or ridge-like lines skirt lateral edge and disappear adjacent to ε. Width of K (tr.) comprises 0.75 of δ–δ width (tr.); and δ–δ (tr.) is 0.63 maximum width (tr.) of cephalon (across genal spines) therefore K (tr.) is 0.47 maximal width (tr.) of cephalon. Posterior portions of fixed cheeks lack any ornamentation. Posterior border furrow is moderately incised, and shallows medial to sutural ridge. Posterior border is convex, short adaxially and becomes marginally longer abaxially.

Free cheeks have oval contour shape laterally. Genal spines are short, extend back to second thoracic posterior pleural band, and are pointed. Lateral border is defined by a moderately incised lateral border furrow that shallows posteriorly where it merges at right angles with posterior border furrow. Lateral border is only marginally convex and ornamented with fine granules. Right and left genal fields adjacent to δ comprise 0.15 width (tr.) of maximum width (tr.) of cephalon. Genal field is ornamented with fine granules. Ocular platform is absent. Eye socle furrow is encircled by small pustules, accentuating furrow, and furrow is moderately incised. Eye socle is faint. Length of eye (exsag.) is 0.41 length (sag.) of A_1.

Hypostome is unknown.

Thorax is comprised of ten segments. Thoracic length (sag.) is 0.42 length (sag.) of exoskeleton. Thoracic axial region (tr.) tapers from first to tenth segment by 24%, and comprises, on average, approximately 0.41 width (tr.) of thorax. Axial rings have imbricate appearance in lateral profile: anterior aspect slopes down forward, and posterior edge is steep. On 8^{th}, 9^{th} and 10^{th} axial rings, preannulus and articulating half ring are visible providing evidence that intra-annular furrow is shallow and articulating furrow is deeply incised. Prosopon of axial rings consists of abundant fine granules. Pleural region resembles that of *Gerastos cuvieri*-type thorax segment of Lütke (1980). Pleural regions of thorax are ornamented by minute granules on convex edge of posterior pleural band. Articulating facets are smooth. Pleural furrows are deeply incised and shallow at fulcrum to almost immediately terminate. Anterior pleural bands are considerably shorter than posterior pleural bands.

Pygidium has shape of a rounded pentagon, and is marginally micropygous (pygidium width (W, tr.) is 0.73 width of cephalon (tr.)). Pygidium length (Z, sag.) is 0.22 length (sag.) of exoskeleton. Pygidial width (W. tr.) is 1.68 times pygidial length (Z, sag.). Lateral profile of pygidial axial region lacks prominent convexity. Axial region is outlined by deep axial furrows. There are seven axial rings plus terminal piece. Anteriormost axial ring is transverse but more posterior rings are slightly *m*-shaped, and terminal piece is blunt in front of visible postaxial lobe. Pygidial axial length (Y, sag.) is 0.78 of pygidial length (Z, sag.). Pygidial axial ring sculpture is of abundant granules and weakly incised marginal pits. From 1st to 7th axial ring there is 40% taper. Pygidial pleural region presents 5+1 furrow pattern, with pleural furrows deeper than interpleural furrows, and anterior pleural bands and posterior pleural bands being equivalent in length (exsag.). Pleural region has scattered fine granules, that become more densely packed along lateral and especially posterior margins of pygidium. Pygidial border is absent.

Etymology.— Due to the tongue-shaped configuration of the glabella, the species epithet of *lisanrasus* was decided upon, for in Romanized Arabic: tongue = *lisân* and *râs* = head.

Type.— Holotype, complete specimen UA13461.

Occurrence.— '*Ceratarges* horizon', El Otfal Formation, Eifelian, lower Middle Devonian, Zireg, Ma'der region, southern Morocco.

Discussion.— Obviously dissimilar to both *G. tuberculatus marocensis* and *G. aintawilus*, *G. lisanrasus* possesses the following distinctive character states: flattened to slightly convex anterior and lateral cephalic borders; tongue-shaped glabella; no pustules on front of glabella, and comparatively small pustules upon rest of glabella; fine row of ornamentation upon palpebral lobes is restricted to posterolateral margin; free cheeks are adorned with large pustules encircling eye socle furrow and smaller pustules and granules on remainder of genal field; thoracic pleural regions lack ornamentation; shape of pygidium is a rounded pentagon; pygidial axis is composed of straight transverse rings near front and marginally elongated *m*-shaped rings

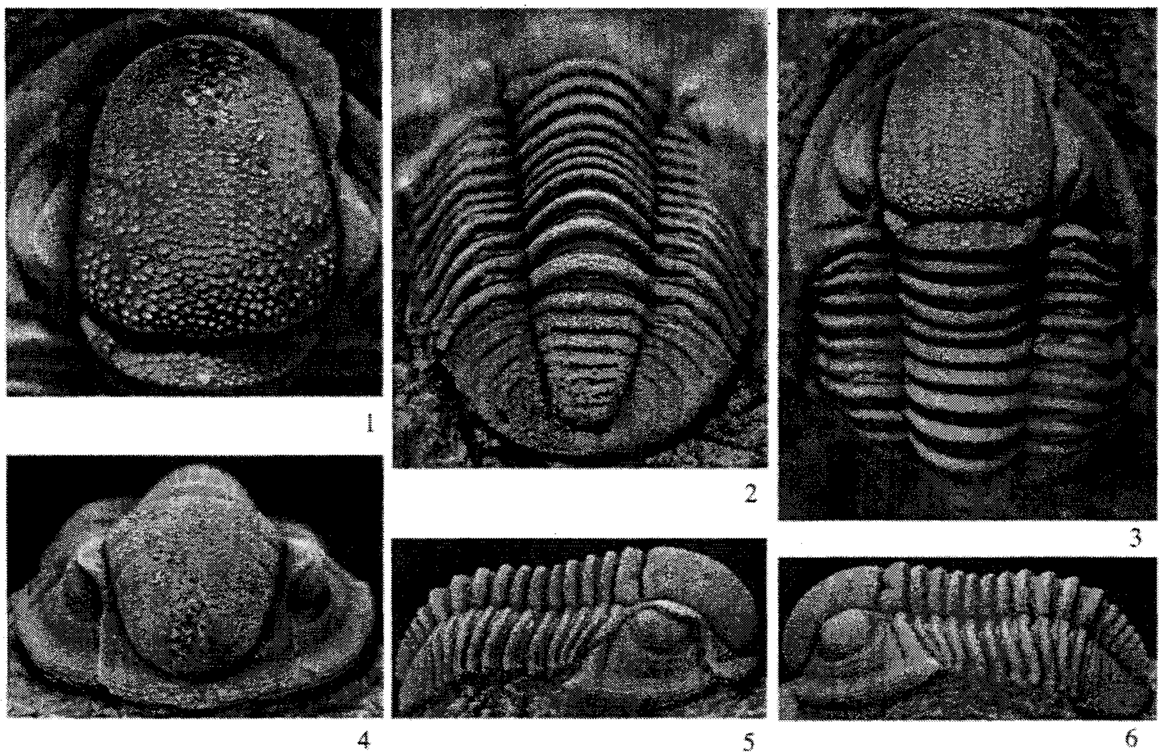

FIGURE 3-19—*1-6*, *Gerastos lisanrasus* new species from the '*Cerataraes* horizon', El Otfal Formation, Zireg, southern Morocco (UA13461) (complete specimen). *1*, dorsal view X6.2; *2*, posterodorsal view X4.5; *3*, dorsal view X4.1; *4*, anterior view X4.2; *5*, lateral view X2.8; *6*, lateral view X2.8.

towards back, with weak paired marginal pits; and pygidial axial ornamentation is of abundant granules. Along with the aforementioned differences, *G. tuberculatus marocensis* and *G. lisanrasus* also differ in that *G. lisanrasus* displays: no ocular platform, a faint eye socle, and no pygidial border. *G. aintawilus* is different from *G. lisanrasus* in other traits as well, for the latter exhibits hooked lateral occipital furrows and no pygidial border. *G. lisanrasus* shall be compared and/or contrasted with remaining new species in appropriate species discussions.

Basse (1996) figured *G. suborbitatus* (Holzapfel, 1895) on plate 7, figures 1-6, and at first glance, *G. suborbitatus* and *G. lisanrasus* appear quite similar. With closer analysis of both species, one can conclude that there are a number of differences between the two species. *G. suborbitatus* has convex anterior and lateral borders, a blunt anterior tip to the glabella, much larger pustules upon the genal field, a square or only slightly pointed glabellar angle, elongate *m*-shaped pygidial axial rings, and a shallow pygidial border.

Richter and Richter (1918) first introduced *Proetus (Eoproetus) cultrijugatus* from the "'*Cultrijugatus* Layer', Lauch Formation, Lower Eifelian, Gees, Eifel Mountains" (translated from Lütke, 1990). *Proetus (Eoproetus) cultrijugatus* (Richter and Richter, 1918), it is difficult to conclude from the sketches produced if these are the same species. This species was later transferred into the new subgenus of *Proetus (Longiproetus)* of Cavet and Pillet (1958). As discussed earlier, it has been confirmed through the cladistic analysis that *Longiproetus* is a synonym of *Gerastos*, and Owens (1973) was correct to eliminate it and place the species into *Gerastos*. But the last identification of this species had it placed within *Gerastos (Devonoproetus) cultrijugatus* by Lütke (1990). Through close analysis of his figures, it has been concluded that *Gerastos lisanrasus* is not equivalent and *Devonoproetus cultrijugatus* and should be placed within *Gerastos*. These two species can be differentiated, but as will be demonstrated in our analysis of *G. discombobulatus*, very little separates them. *G. cultrijugatus* has the following traits that *G. lisanrasus* lacks: an anterior border that is relatively convex in lateral profile; coarser ornamentation upon the glabella, anterior to S0, which does not reduce in size as rapidly anteriorly; presence of an ocular platform which is encircled with prominent tubercles; longer genal spines; overall ornamentation of tubercles rather than small granules; a pygidium with more an elliptical shape; and all the pygidial axial rings are of an elongate *m*-shape.

GERASTOS AINRASIFUS new species

Figures 3-20.1 – 3-20.12

Diagnosis.— Cephalon and pygidium are pustulated but thorax has suppressed or no ornamentation; ocular platform is defined with pustules accentuating distal edges; genal angle is rounded to subangular; and facial sutures converge slightly forward in front of eyes.

Description.— Exoskeleton is inflated. Cephalon (A) length (sag.) is 0.3 to 0.39 length of complete exoskeleton (sag.). Cephalon is surrounded by several terrace lines on anterior and lateral borders (at least five, possibly more). Width (tr.) of δ-δ in relation to maximum length of cephalon (A, sag.) is 1.0-1.2 times. Anterior facial sutures from δ converge with a gentle curvature to γ; γ to β is continuance of convergence, therefore β does not flare laterally; β to α is small convergence, and distance between two morphological landmarks. Posterior facial sutures, from δ converge to ε, with tighter curvature that than that of δ to γ; converge slightly from ε to ξ and the distance is short; and from sutures ξ diverges marginally to posterior border furrow, turns subtransversely within furrow to point just behind δ, and then turns posterolaterally to ω. Preglabellar and axial furrows are deeply incised around ovoid glabella. Glabella is convex in lateral profile. Glabella (A_1) has maximum length (sag.) of 0.71 – 0.83, with extreme outlier of 0.88, in relation to maximum length (sag.) of cephalon (A). Maximum width (K, tr.) of glabella (in front of S0) to length (sag.) of A_1 of 0.92-1.08, with two outliers of 0.81 and 1.15. A_1 portrays fused smooth composite tubercles (Strømer, 1980) posteriorly that reduce in size and dispersion anteriorly to become smooth tubercles of granular nature, lacking central canal (Strømer, 1980). S0 is short, deep and transverse. S1, S2 and S3 are shallow, only defined by lack of sculpture. S1 is opposite δ, originating at axial furrow and immediately begins adaxial-posterior curvature shape; S2 is opposite front of eye, and mimics S1, and is parallel to S1 though does not have final posterior curvature; S3 is situated opposite to anteriormost edge of eye socle furrow, and has shape of narrow line slightly posteriorly oriented and more adaxially. Glabellar lobes are not inflated. Width (tr.) of posterior edge of A_1 to width (tr.) of L0 is 0.93 to 1.03; k (tr.) to L0 (tr.) is 0.82-0.97; and L0 (A_4) length (sag.) to A (sag.) is 0.11-0.21. Lateral occipital furrows are moderately incised, and are directed from anterior to posterior in a hooked direction abaxially. Prosopon of occipital ring is continuous, and abundantly pustulated. Median node is located on back of L0, on circular base with small, defined tubercle. Anteriormost portion of glabella slightly overhangs anterior border. Preglabellar field is absent. Anterior border (A_2+A_3) length (sag.) comprises 0.04-0.10 length (sag.) of cephalon (A). Anterior border is ornamented with fine granules. Anterior portion of fixed cheeks is also ornamented, but granules on fixed cheeks are larger than those on anterior border. Palpebral lobes are smooth, as also are posterior portions of fixed cheeks. Maximum width (tr.) of A_1 (K) to maximum width (tr.) of palpebral lobes (δ-δ) has range of 0.70-0.78, though majority of specimens range from 0.70-0.73. Posterior border furrow is deeply incised. Posterior border is moderately convex, and becomes longer closer to genal angle.

Free cheeks are uniformly curved, accentuating half circle shape to cephalon; widest landmark on cephalon is at edge of genal angle. Genal angle is rounded to subangular. Lateral border is ornamented with fine granules. Lateral border furrow is moderately incised. Genal fields (combined) (opposite to δ to lateral border furrow, tr.) compare to δ-δ with ratio of 0.26-0.34. Sculpture upon genal fields is of abundant pustules, accentuated by ocular platform rimmed with larger tubercles. Eye socle furrow is shallow. Eye socle is prominent. Length of eye (exsag.) to A_1 length (sag) is 0.34 to 0.53.

Hypostome is unknown.

Thorax has 10 segments. Overall shape of thorax: inflated axial region becomes less inflated posteriorly, pleural region is near horizontal proximally and at fulcrum sharply angles (near 90°) ventrally, with distal ends slightly curved anteriorly. Length (sag.) of thorax comprises 0.36-0.49 maximum length (sag.) of exoskeleton. Axial region (tr.) is approximately 0.42 width (tr.) of thorax. Axial region (tr.) tapers from first segment to tenth segment approximately by 13-16.9%. Axial region in lateral profile is imbricate. Ornamentation of axial rings ranges from few low scattered pustules to smooth. Preannulus is visible on first thoracic segment, with shallow inter-annular furrow and incised articulating furrow. Anterior pleural band is shorter (exsag.) than posterior pleural band. Anterior pleural band has triangular shape, with apex at fulcrum. Pleural furrow is deeply incised and disappears within proximal portion of facet. Pleural region lacks any sculpture.

Pygidial shape resembles segment of circle, and is micropygous. Pygidial width (W, tr.) is 1.47 to 1.76 times length (Z, sag.). Pygidium has seven axial rings plus blunt terminal piece with minor postaxial lobe. Axial region is shallow when viewed laterally. Axial rings are ornamented with abundant tubercles and have elongate *m*-shape. Each axial ring is adorned by pair of marginal pits. Axial region (X, tr.) is 0.38-0.44 width of W (tr.); Y (sag.) is 0.76-0.86 of Z (sag.); and tapers from first ring to seventh by 40.6-52.9%. Pleural furrows display 6+1 pattern, with interpleural furrows more incised and pleural furrows shallow, and anterior and posterior pleural bands equivalent in length (exsag.). Pygidial border is shallow, and ornamented with fine granulations and posterior margin is wrapped with three terrace ridges. Within pleural region, sculpture becomes more pustulated.

Etymology.— The name was composed to reflect the prominent *ocular platform* on this species: in Romanized Arabic *ain* = eye and *raSîf* = platform.

Type.— Holotype, complete exoskeleton UA13459. Paratype, complete exoskeleton UA13460.

Occurrence.— '*Proetus* horizon', Taboumakhloûf Formation, Eifelian, Middle Devonian, Jbel el Mrakib, Ma'der region, southern Morocco.

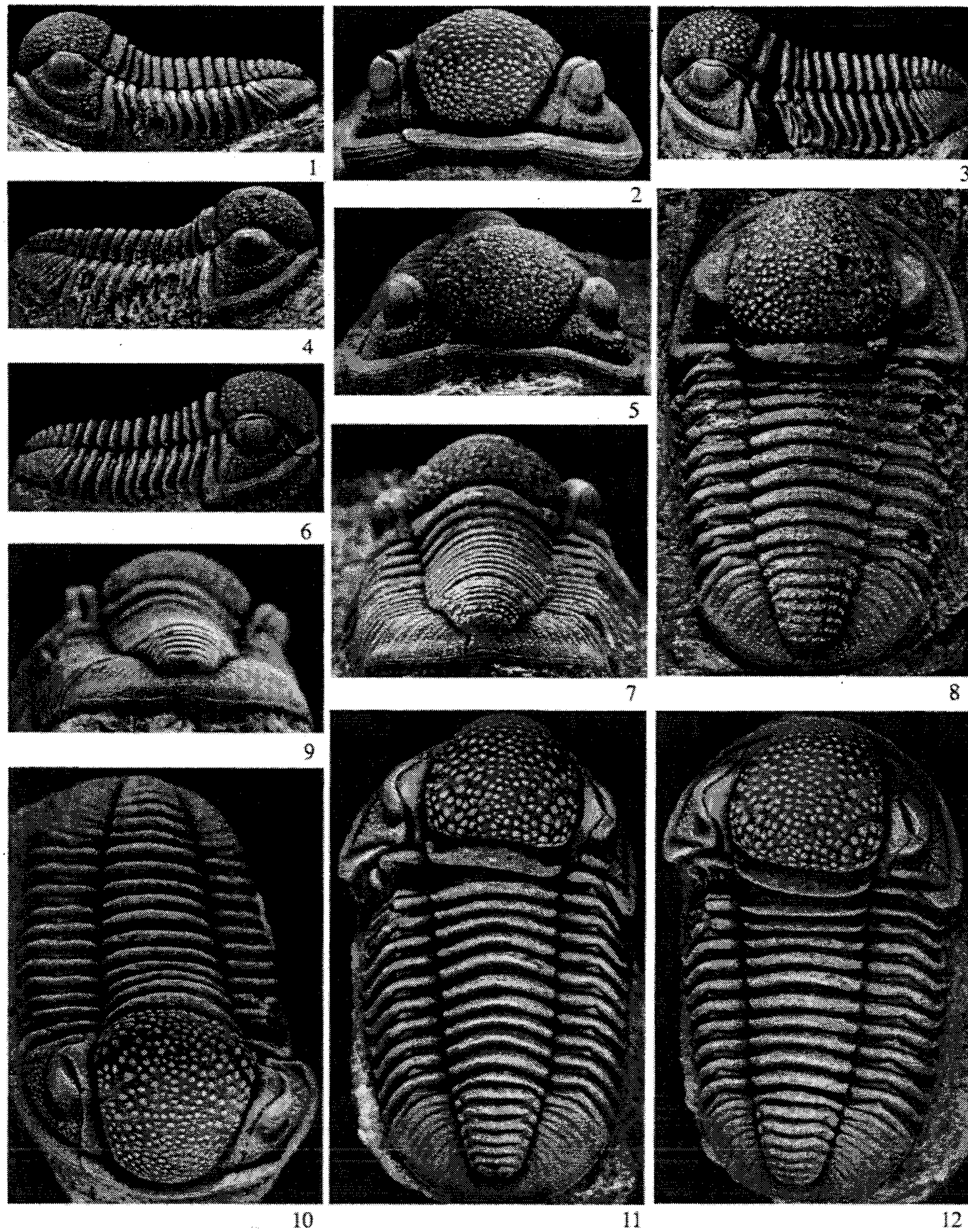

FIGURE 3-20—*1-12, Gerastos ainrasifus* new species from the '*Proetus* horizon', Taboumakhloûf Formation, Mrakib, Ma'der region, southern Morocco. *2, 3, 6, 9, 10-12* (UA13459) (complete specimen). *2*, anterior view X2.7; *3*, lateral view X1.7; *6*, lateral view X1.7; *9*, posterior view X3.1; *10*, oblique anterodorsal view X2.8; *11*, dorsal view X2.7; *12*, dorsal view X2.7. *1, 4, 5, 7, 8* (UA13460) (complete specimen). *1*, lateral view X1.7; *4*, lateral view X1.7; *5*, anterior view X2.6; *7*, posterior view X2.7; *8*, dorsal view X2.6.

Discussion.— At first analysis, *Gerastos ainrasifus* appeared to be *Gerastos prox* (Richter and Richter, 1956) due to the possible proximity stratigraphically to material discussed by Lieberman (1994) (though vague, since he only indicated Morocco with a stratigraphic range of Emsian or Eifelian) and the approximate equivalent stratigraphic range (Eifelian) of Richter and Richter's (1956) material. Although there are similarities, it is posited that Lieberman (1994) misidentified his specimens as *G. prox*. Alberti (1969) erected a new subspecies *Proetus (Proetus) prox umerbianus* thus moving the types of *P. (P.) prox* to *P. (P.) prox prox* Richter and Richter, 1956. Through close observation of Alberti's (1969) material for what is now *Gerastos prox umerbianus*, it is evident that Alberti's (1969) material of *G. umerbianus* is sufficiently different from *G. prox* that it should be accorded species rather than subspecies level. Although Alberti (1969) had poor disarticulated material, the glabellar shape of *G. umerbianus* is not as tapered forward as that of *G. prox*, and the ornamentation on *G. umerbianus* is much larger and more pointed than that of *G. prox,* and it diminishes to either much smaller or nonexistent ornamentation anteriorly. Therefore, Alberti's (1969) subspecies should now be recognized as *G. umberianus* and no longer be directly associated with *G. prox*.

It should also be noted that *G. ainrasifus* is not synonymous with *G. prox*, despite displaying a number of synapomorphies, for the following reasons: the ornamentation on the glabella of *G. ainrasifus* is much more pronounced, demonstrating a 'fused smooth composite' pattern, and then progressing anteriorly with smaller 'smooth ordinary tubercles' and 'granular smooth tubercles' (lacking the central canal) (Størmer, 1980); *G. prox* has 'smooth ordinary to granular tubercles' (Størmer, 1980) ornamentation posteriorly and the anterior aspect is much more reduced to granulations or lacking in any ornamentation; the ocular platform on *G. prox* is much more pronounced than that of *G. ainrasifus* for *G. prox* has a singe defined distal row of tubercles encompassing the platform, while *G. ainrasifus* displays a number of tubercles and pustules encircling the platform; the genal field distal to the ocular platform appears to have more ornamentation in the form of pustules on *G. ainrasifus* than on *G. prox*; on most of the material figured by Richter and Richter (1956) the genal field appears lacking of prosopon, or with few pustules; and glabellar furrows of *G. prox* are not as prominent upon the figured holotype or other material used by Richter and Richter (1956), as that of *G. ainrasifus*, though this is not a reliable character state, since it may vary intraspecifically.

The glabellar furrow prominence is not a reliable character state due to the ecdysis process; if the trilobite does not contract the attached muscles during the tanning process (secretion of exoskeleton), the furrows are not going to display as prominently. Another character trait is the mathematical morphological landmark ratio of $K/\delta\text{-}\delta$: *G. prox* falls outside of the range of *G. ainrasifus*, but since *G. prox* is demonstrating $\delta\text{-}\delta$ becoming smaller in relation to *k*, it is a significant trait. The ratio for the holotype of *G. prox* is 0.79 while the majority of specimens of *G. ainrasifus* range from 0.70-0.73 (with outliers of 0.77 and 0.78). Richter and Richter (1956) do not have a thorax for the holotype; therefore, this cannot be compared or contrasted to *G. ainrasifus*. The pygidium displays similar ornamentation between the two species, but the pygidial border upon *G. prox* is much more pronounced, hence deeper than that of *G. ainrasifus*. *G. ainrasifus* does display a pygidial border but it has a more convex shape with the interpleural and pleural furrows disappearing at the proximal edge of the pygidial border, thus displaying a shallower pygidial border than that of *G. prox*.

G. ainrasifus is defined as a different species to *G. tuberculatus marocensis* because it possesses the following traits not observed in *G. tuberculatus marocensis*: palpebral lobes lack ornamentation; genal angle is rounded to subangular; thoracic axial ornamentation of few pustules to a smooth state; no ornamentation upon thoracic pleural region; and weak pygidial border. Very little differentiates *G. ainrasifus* from *G. tuberculatus marocensis*, hence the *G. tuberculatus* clade being the basal species to *G. ainrasifus* on the phylogenetic tree (Figure 3-11).

G. aintawilus from bou Dib differs from *G. ainrasifus* due to the following character state differences displayed by *G. ainrasifus*: palpebral lobe lacks prosopon; prominent eye socle; presence of ocular platform; rounded to subangular genal angle; hooked lateral occipital furrows; axial thoracic rings have few to no pustules; and the absence of thoracic pleural ornamentation.

Finally, *G. ainrasifus* differs from *G. lisanrasus* because *G. ainrasifus* portrays the following: glabellar shape is ovoid; large pustules occur upon the glabella, anterior to S0; ocular platform is present; eye socle is prominent; palpebral lobes are smooth; genal field is entirely covered with granules; genal angle is rounded to subangular; thoracic axial region has few to no pustules; shape of pygidium is a segment of a circle; pygidial rings form elongate *m*-shape; pygidial axial rings are adorned with large, abundant pustules and strong paired marginal pits; and pygidial border is weak.

GERASTOS DISCOMBOBULATUS new species

Figures 3-21.1 – 3-21.13

Diagnosis.— Anterior and lateral borders are flattened; glabella is tongue-shaped; glabella is convex in lateral profile; pustules are absent front of glabella; single row of pustules occurs on lateral margins of palpebral lobes; ocular platform is present; pygidial axial rings are straight anteriorly but demonstrate posterior flexure on more posterior axial rings; and pygidial border is shallow.

Description.— Exoskeleton is dorsoventrally flattened, except for glabella and thoracic axis. Cephalon portrays shape of half-oval, with back anteriorly arched. Cephalon is ornamented on lateral and anterior margins by up to six terrace lines. Length of cephalon (A, sag.) is 0.36-0.44 length of exoskeleton (sag.), and width of cephalon (across genal spines, tr.) is 0.53-0.68 length of cephalon (sag.). Glabella has tongue-shaped appearance deeply incised by axial and anterior border furrows. Length of glabella (A_1, sag.) is 0.69-0.77 length of cephalon (sag.), and is 0.91-1.02 width of glabella (K, tr.). S0 is deeply incised and generally straight (tr.), though with slight distal forward, turn. Ornamentation of glabella (anterior to S0) is composed of smooth ordinary tubercles, with some fused smooth tubercles (Størmer, 1980) posteriorly, that regress to granules anteriorly to complete absence of any ornamentation on front of glabella. S1, S2 and S3 are shallow, and differentiated due to lack of ornamentation. S1 and S2 originate at axial furrows, while S1 is opposite to δ, with straight medial trend until in front of lateral occipital furrow where it angles approximately 45° in posteromedial direction. S2 is opposite to γ and runs posteromedially at 25° to transverse direction for quarter width (tr.) of glabella. S3 is subcircular, located marginally in front of (exsag.) S2 and behind (exsag.)

intersection of axial furrow with anterior border furrow. Glabellar lobes (anterior to S0) are not prominent due to lack of inflation. Front of glabella is semi-pointed, bulbous, and marginally overhangs anterior border in lateral profile. Width (tr.) of glabella (anterior to S0) is 0.94-1.06 width (tr.) of occipital ring (A_4). Length of occipital ring (sag.) is 0.12-0.17 cephalon length (sag.). Lateral occipital furrows are curved posterolaterally, providing hooked appearance. Occipital ring is ornamented with few, interspersed pustules and small, defined, posteriorly placed median node. Anterior border (A_2+A_3) length (sag.) is 0.04-0.1 length of cephalon (sag.). Anterior border has little or no convexity in lateral profile, and is adorned with fine granules. Preglabellar field is absent. Front of fixed cheeks ornamented with small pustules. Palpebral lobes (δ–δ) (tr.) are 0.59-0.70 width of cephalon (tr.). Width of glabella (tr.) is 0.7-0.77 width of δ–δ (tr.). Palpebral lobes are smooth, except for single fine row of granules running along margin. Back of fixed cheeks displays no ornamentation. Posterior border furrow is moderately incised, though shallow at sutural ridge, and merges with lateral border furrow at approximately 60° (extr.). Posterior border is short adaxially, slightly longer abaxially, and lacks ornamentation.

Free cheeks are defined medially by facial suture with following profile: α diverges back with shallow angle to β; suture lacks much curvature at β, and then marginally converges to γ; behind γ suture diverges along gentle curvature to δ; from δ to ε suture displays convergent curvature; from ε to ξ suture descends backward; behind suture ξ diverges posteriorly with gentle slope until posterior border furrow, whereupon it curves sharply back to ω. Lateral border furrow is moderately incised, accentuating lateral border, displaying little to no convexity; and is ornamented with fine granules.

Genal spines range from short and pointed to slightly longer and pointed. Genal fields (right and left) [from eye socle furrow, adjacent to δ distally to lateral border furrow] (tr.) are 0.10-0.16 width of cephalon (tr.). Prosopon of genal fields consists of fine granules. Ocular platform is present. Shallow eye socle furrow occurs below prominent eye socle. Length of eye (exsag.) is 0.42-0.58 length of A_1 (sag.).

Hypostome is unknown.

Thorax is composed of ten segments. Length of thorax (sag.) is 0.33-0.39 length of entire exoskeleton (sag.). Axial region of thorax tapers from first to tenth ring by 18-25% (tr.). Width of axial region (tr.) is on average 0.41 of thorax width (tr.). Axial rings have rounded anterior edge, and posterior edge is steep. Ornamentation of axial rings is composed of sparse pustules. Intra-annular furrow is shallow, preannulus displays little convexity and concentric shape; articulating furrow is deeply incised; and articulating half ring is convex. Pleural regions display Lütke's (1980) *Gerastos cuvieri*-type segment style. Pleural furrow is deeply incised and shallows to terminate on articulating facet. Anterior pleural band is shorter than posterior pleural band, and neither display ornamentation.

Pygidium is shape of segment of circle, and is encompassed by visible terrace ridges on posterior and lateral margins. Pygidium is micropygous; pygidial width (W, tr.) is 0.62-0.71 of cephalon width (tr.). Length of pygidium (sag.) is 0.23-0.25 entire length of exoskeleton (sag.). Pygidial width (tr.) is 1.68-1.93 times pygidial length (Z, sag.). Axial region is shallow in lateral profile, and composed of seven axial rings plus posteriorly blunt terminal piece, with postaxial lobe extending farther posteriorly. Axial region width (X, tr.) is 0.38-0.39 of pygidial width (tr.), and from first to seventh ring demonstrates a taper of 40-50% (tr.). Axial length (Y, sag.) is 0.73-0.87 pygidial length (sag.). Axial rings portray straight profile, though more posterior rings tend to develop some posterior flexure to stimulate modified elongate *m*-shape. Ornamentation of axial rings consists of abundant large pustules, with paired marginal pits. Pygidial pleural region presents 4+1 furrow pattern, where pleural furrows are deeper than interpleural furrows. Anterior pleural bands and posterior pleural bands are equivalent in length (exsag.), and neither displays ornamentation. Shallow pygidial border is adorned with fine granules.

Etymology.— Due to the frustration that this horizon and species caused me with regard to the decision to split the species, *discombobulate* seemed like an appropriate term for this species.

Type.— Holotype, complete exoskeleton, UA13467. Paratypes, complete exoskeletons, UA13469-13470 and cephalon with three thoracic segments, UA13468.

Occurrence.— '*Proetus* horizon', Taboumakhloûf Formation, Eifelian, lower Middle Devonian, Jbel el Mrakib, Ma'der region, southern Morocco.

Discussion.— As was stated in the discussion of *G. lisanrasus*, *G. discombobulatus* is a species that helps confirm that *Longiproetus* is a synonym of *Gerastos*, as suggested by Owens (1973). Lütke (1990) reclassified Richter and Richter's (1918) species, originally identified as *Proetus (Eoproetus) cultrijugatus*, which clearly displays a number of character traits similar to those of *G. discombobulatus*. Lütke (1990) stated that *Gerastos (Devonoproetus) cultrijugatus* is different from the:

> Typical subgenus *G. (Gerastos)* by a protruding anterior cephalic border with librigenal spines and by an only incipient eye platform. The pygidium has a narrower axis and distinctly splitted [sic] and scalloped pleural ribs (A1 type), which nearly reach the posterior margin.

FIGURE 3-21—*1-13*, *Gerastos discombobulatus* new species from the '*Proetus* horizon', Taboumakhloûf Formation, Mrakib, Ma'der region, southern Morocco. *1, 4, 8, 11* (UA13467) (complete specimen). *1*, lateral view X3.8; *4*, anterior view X4.3; *8*, posterodorsal view X6.5; *11*, dorsal view X5.6. *3, 10, 13* (UA13470) (complete specimen). *3*, anterior view X3.8; *10*, dorsal view X5.2; *13*, dorsal view X4.1. *2, 5, 7, 9, 12* (UA13469) (complete specimen). *2*, lateral view X2.0; *5*, oblique dorsolateral view X1.7; *7*, dorsal view X4.4; *9*, posterior view X3.2; *12*, dorsal view X3.0. *6* (UA13468) (cephalon and three thoracic segments), lateral view X6.2.

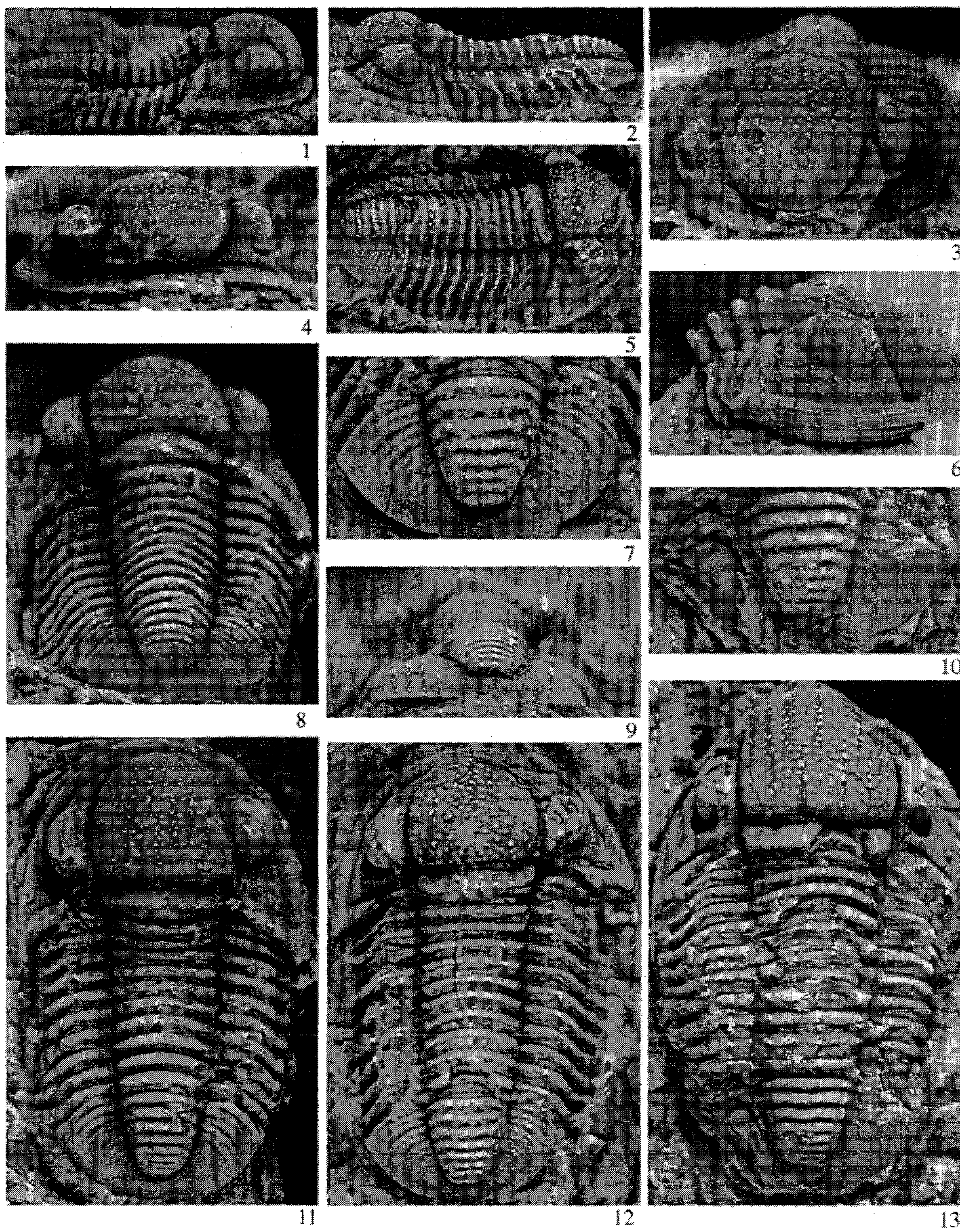
1
2
3
4
5
6
7
8
9
10
11
12
13

It is those traits, shared with *G. discombobulatus,* that place it firmly within the *'Gerastos'* phylogenetic tree (Figure 3-5). Therefore, *Devonoproetus cultrijugatus* (Richter & Richter, 1918) shall now be classified as *Gerastos cultrijugatus*. There are only a few differences between the two species, and the palaeogeographic distance between the two species (Gees, Eifel Mountains, and Mrakib, Ma'der Region, southern Morocco), suggests that *G. discombobulatus* could actually be regarded as a subspecies of *G. cultrijugatus*. *G. cultrijugatus* displays the following states that are clearly different from *G. discombobulatus*: anterior border is convex in lateral profile; occipital ring is more ornamented; and pygidial axial rings, from first to seventh ring, display an elongate *m*-shape. *Gerastos tuberculatus* is shown in the phylogenetic analysis (Figures 3-11 & 3-12) to be the sister species to the sister species (*G. ainrasifus*) of *G. discombobulatus*.

Gerastos tuberculatus marocensis differs from *G. discombobulatus*, as the latter possesses the following traits: anterior and lateral borders are flattened; glabellar shape is tongue-shaped; limited to no ornamentation is present on the anteriormost aspect of the glabella; occipital ring displays few pustules; thoracic pleural sculpture is absent, and thoracic axial ornamentation is constrained to a few pustules; and the anterior pygidial axial rings are straight, and transverse and more posterior rings display some posterior flexure giving them an open *m*-shape.

Gerastos discombobulatus displays the following traits that provide evidence of the difference between it and *G. aintawilus*: anterior and lateral borders that lack any convexity; tongue-shaped glabella; absence of prosopon on anterior aspect of glabella; prominent eye socle; presence of ocular platform; hooked occipital furrows; few pustules upon occipital ring; lack of sculpture upon thoracic pleural region and few pustules upon axial region; straight anterior pygidial axial rings to very elongate *m*-shaped posterior rings; and shallow pygidial border.

It is not surprising that the '*Proetus* horizon' from Mrakib would be producing at least two different species: *G. ainrasifus* and *G. discombobulatus*. Of course, one must realize that the local trilobite miners titled this horizon before they knew that they were actually collecting species currently classified as *Gerastos*. *G. ainrasifus* is shown in the phylogenetic analysis to be the basal species to *G. discombobulatus*. *G. discombobulatus* exhibits the following traits not seen in *G. ainrasifus*: anterior and lateral borders lack any dorsal convexity; tongue-shaped glabella; limited ornamentation on front of glabella; single row of fine granules along margin of palpebral lobes; pointed genal angle, with genal spines extending posteriorly; occipital ring ornamented with few pustules; thoracic axial region adorned with limited pustules; pygidial axial rings that are straight anteriorly and become more a *m*-shaped posteriorly; and a shallow pygidial border.

GERASTOS CUVIERI MALISUS new subspecies

Figures 3-22.1 – 3-22.12 and 3-23.1 – 3-23.6

Diagnosis. Genal angle is square. There are upwards of 8 imbricate terrace lines surrounding cephalon. Glabellar (A_1) prosopon pustules are low and sparse on back of glabella, while front of glabella is almost smooth. Only S1 and S2 are found upon A_1. Ocular platform is present and it is surrounded by distinct ring of larger pustules. Prosopon diminishes to smaller pustules both laterally and anteriorly. Hypostome has enlarged ventrally protruding keel on front of middle body. Thoracic axial prosopon consists of small, low pustules in limited numbers, while pleural region is smooth. Shape of pygidial axial rings is elongated *m*-shape. Pygidium lacks distinct border.

Description. Exoskeleton is inflated. Cephalon length (A, sag.) is 0.32 – 0.39 maximum length (sag.) of exoskeleton. Shape of cephalon is semi-circular, with near square genal angle. Cephalon is ornamented on lateral and anterior borders with approximately 7-8 short terrace; at least two terrace ridges originate on dorsal surface of anterior and lateral borders. Anterior border is inflated, ornamented with fine granules and obscured marginally by glabella when viewed dorsally. Preglabellar field is absent. Anterior border furrow and axial furrows are deeply incised, accentuating ovoid glabella. Glabellar sculpture consists of low, reduced tubercles, especially forward; more posterior and lateral regions display low, reduced pustules. Shallow glabellar furrows of S1 and S2 differentiated due to lack of ornamentation. Both S1 and S2 are moderately incised at axial furrow origin, but both immediately become shallow. S1 originates opposite to δ traverses adaxially and then curves at near 90° posteriorly to create faint L1, though L1 is not inflated. S2 initiates approximately adaxial to γ and curves inward slightly behind transversely. Glabella is arched along sagittal line, and in transverse direction. Length (sag.) of A_1 occupies 0.73 – 0.79 of total cephalon length (A, sag.) and length (A_1, sag.) to width (K, tr.) ratio is 0.92 - 1.08. S0 is deeply incised and lateral occipital furrows are slightly recurved or 'hooked'. Occipital ring length (A_4, sag.) is 0.13 – 0.17 length of cephalon (A, sag.), and its width is approximately equal in width (tr.) to width of back of glabella anterior to S0 (tr.). Occipital ring lacks prosopon, and has a small, barely defined, posteriorly placed median node. Front of fixed cheek is ornamented with granules. Palpebral lobes are short (exsag.), near horizontal, and lack prosopon. Ratios for K (tr.) to δ-δ (tr.) are 0.70 - 0.77, and δ-δ width (tr.) to length (sag.) ratios of A are 1.00 – 1.09.

Facial sutures portray following shape: anterior part facial sutures from δ forward converge with gentle curvature to γ; from γ to β sutures diverge at acute angle; from β sutures converge sharply to α; β does not extend laterally beyond palpebral lobe. Facial sutures from δ posteriorly: from δ sutures diverge to ε with tight curvature; from ε sutures descend posteriorly to ξ, located within posterior border furrow; from ξ sutures turn posterolaterally to ω. Eye is kidney-shaped, and ratio of length of eye (exsag.) to glabellar length (A_1, sag.) ranges from 0.44 to 0.52. Weak eye socle has shallow eye socle furrow that appears deeper due to accentuation by pustulated ocular platform that runs from opposite midpoint between β and γ to approximately opposite ξ, surrounding smooth, shallow eye socle furrow. Remainder of genal region is ornamented with pustules. Lateral border furrow is moderately incised and convex; lateral border has prosopon of fine granules. Posterior border is convex, smooth and adaxial edge is short, blunt and posteriorly downturned medially adjacent to fulcrum and flares abaxially to merge with lateral border at near right angle, hence creating a square genal angle.

Rostral plate, as with rest of doublure, is smooth, though bounded anteriorly by terrace ridges from anterior and lateral borders, and two distinct terrace lines on most posterior aspect of doublure (though the posterior terrace lines do not appear to pass through rostral plate). Anteroventral margin (tr.) of rostral plate has a ratio of 0.30 in relation to δ-δ (tr.). Rostral plate tapers backward at approximately 45° to exsagittal line, therefore having appearance of an equilateral triangle flanked by connective sutures.

Hypostome is shape of proetid shield. Entire hypostome is surrounded by convex terrace ridged borders. Posterior and lateral border furrows are moderately incised. Maximum hypostome length (HL, sag.) is 0.79 of maximum width of hypostome (HW_1). Length of hypostome (HL, sag.) is 0.55 length of A_1 (sag.). Anterior border is transverse, with marginal curvature laterally, in front of anterior wings that are laterally flared and lack ornamentation. Anterior lobe of middle body possesses distinct keel that is pinched ventrally, simulating a ridge. Keel is accentuated by 3-4 terrace ridges that surround and profile shape of keel. Keel terminates at shallow middle furrows that highlight maculae that occur at anterolateral ends of posterior lobe. Maculae are flanked posteriorly by two distinct posteriorly convex terrace ridges that traverse posterior lobe, resembling facial smile. HW_3 (tr.) extends laterally beyond HW_2 (tr.) only marginally, essentially equivalent in width (0.98). Posterior border/margin is rounded.

Thorax is composed of ten segments. Length of thorax (sag.) is 0.37-0.47 length (sag.) of exoskeleton. Width of axial region (tr.), from first to tenth ring, tapers approximately 20-25%, and is approximately 50% of thorax width (tr.). Lenticular preannulus is visible in some segments, bounded posteriorly by shallow intra-annular furrow and anteriorly by moderately incised articulating furrow. Both preannulus and articulating half ring are slightly convex. Ornamentation upon axial region is constrained to few granules or low pustules. Thoracic segments exhibit *Gerastos cuvieri*-type pattern (Lütke, 1980). Pleural region lacks ornamentation. Anterior pleural band is shorter than posterior pleural band. Pleural furrows are deep, and terminate within articulating facet.

Pygidium has shape of segment of circle and is marginally micropygous. Pygidium length (Z, sag.) is 0.21-0.24 length (sag.) of exoskeleton. Width (tr.) of pygidium (W) is 1.61-1.74 (with outlier of 1.30) of length (sag.) of pygidium (Z). Pygidial axial length (Y, sag.) is 0.77-0.81 length (sag.) of pygidium (Z). First to seventh axial rings display a taper of approximately 37-42%. Axial region lacks prominent convexity in lateral profile. Axial region is composed of seven rings plus terminal piece, and is bounded by deep axial furrows. Axial rings display broad *m*-shape with no ornamentation and distal marginal paired apodeme pits. Pygidial pleural region is ornamented with fine granules that become denser distally. Furrow pattern is 4+1, with pleural furrows more deeply incised than interpleural furrows, also anterior pleural band and posterior pleural band are essentially equivalent in length (exsag.). Pygidial border is absent.

Etymology.— Due to the overall appearance of the subspecies, the Romanized Arabic for smooth was decided upon: *mâlis* = smooth.

Types.— Holotype, complete exoskeleton with hypostome UA13456. Paratypes, complete exoskeletons UA13457-UA13458.

Occurrence.— '*Diademaproetus* horizon', Taboumakhloûf Formation, Eifelian, Middle Devonian, Oufatene, Ma'der region, southern Morocco.

Discussion.— Due to the numerous similarities of the specimens from the Oufatene '*Diademaproetus*' horizon to *Gerastos cuvieri* (Steininger, 1831), it was decided that the Moroccan specimens should be identified as a new subspecies *Gerastos cuvieri malisus*. There are minor differences between *G. cuvieri cuvieri* and *G. cuvieri malisus*. Because *G. cuvieri cuvieri* is from the Gesser Horizon, Ahrdorf Layers, Gees, Gerolstein, while *G. cuvieri malisus* is from Morocco, a subspecies (geographic) was erected. It should be noted that both occur during the Middle Devonian, more specifically the Eifelian;

FIGURE 3-22—*1-12*, *Gerastos cuvieri malisus* new subspecies from the '*Diademaproetus* horizon', Taboumakhloûf Formation, Oufatene, Ma'der region, southern Morocco. *1-9* (UA13456) (complete specimen with hypostome). *1*, dorsal view X3.2; *2*, anterior view X3.3; *3*, oblique anterolateral view X2.8; *4*, lateral view X2.7; *5*, oblique anterolateral view X3.9; *6*, anterior view X3.2; *7*, ventral view X5.6; *8*, oblique ventrolateral view X5.7; *9*, dorsal view X3.2. *10-12* (UA13458) (complete minus free cheeks). *10*, anterodorsal view X3.8; *11*, dorsal view X3.7; *12* dorsal view X3.8.

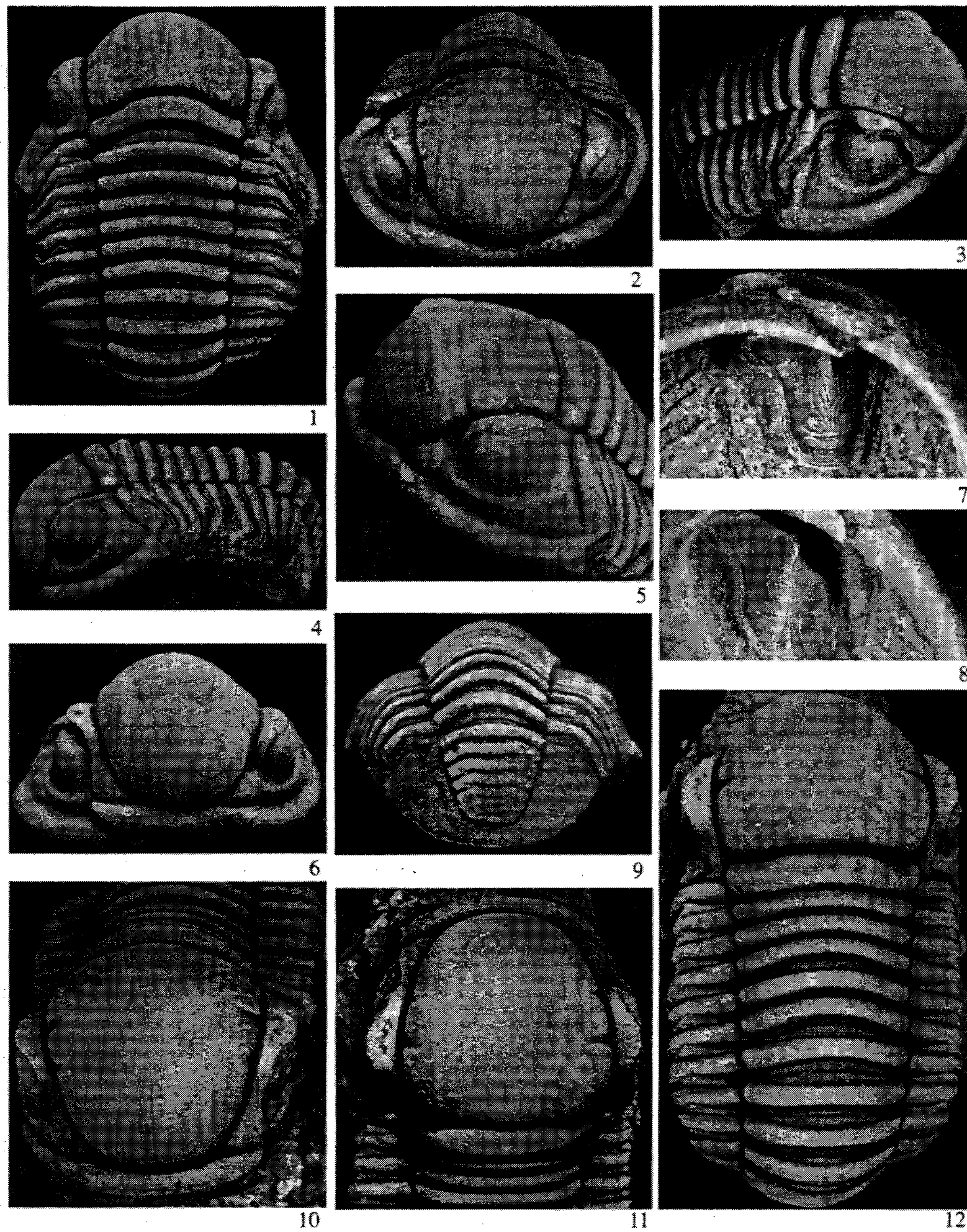
1
2
3
4
5
6
7
8
9
10
11
12

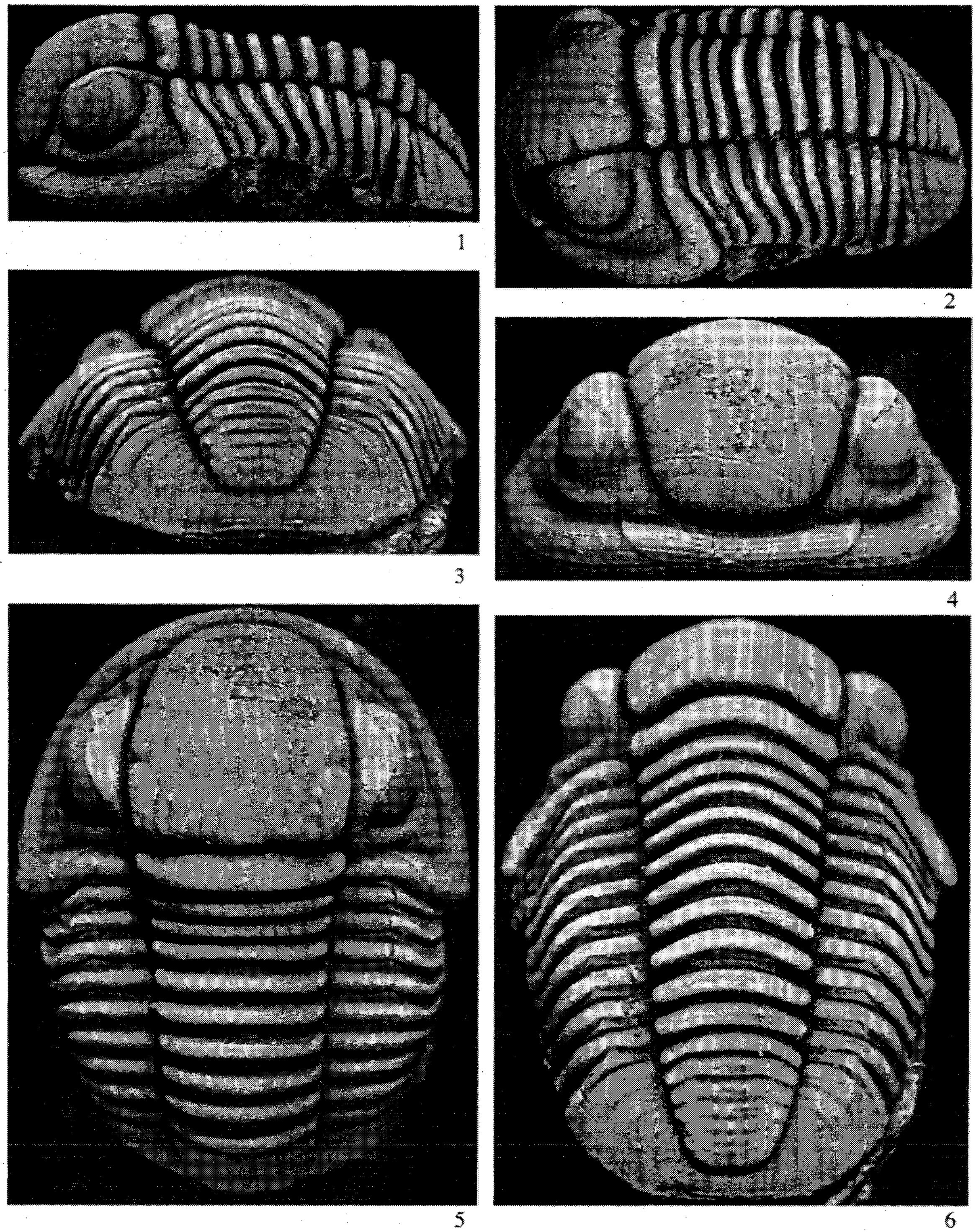

FIGURE 3-23—*1-6*, *Gerastos cuvieri malisus* new subspecies from the '*Diademaproetus* horizon', Taboumakhloûf Formation, Oufatene, Ma'der region, southern Morocco (UA13457) (complete specimen). *1*, lateral view X5.1; *2*, oblique anterolateral view X4.2; *3*, posterior view X7.1; *4*, anterior view X6.9; *5*, dorsal view X6.9; *6*, dorsal view X7.0.

therefore, the warm subtropical counterclockwise current circulating over North Africa and into southern Europe (Heckel and Witzke, 1979), could account for similarities between these taxa. Some genetic exchange was probably occurring but not enough to subsume the two geographic races.

The differences between the two subspecies are not easy to distinguish, but those that do exist are: *G. cuvieri cuvieri* has a slightly more blunt front to the glabella, while *G. cuvieri malisus* has a slightly more rounded front to the glabella and in the latter form the glabella marginally overhangs the anterior border. This anomaly can be observed in Richter and Richter (1956) who provided excellent images of *G. cuvieri cuvieri.* Kowalski (1990) provided two images (fig. 9 and 10) of the holotype, where the abovementioned feature can be clearly observed. The facial suture depicted in Richter and Richter (1956) appears to have a less laterally extended β than the specimens from Morocco. One last difference between the two subspecies is the form of the hypostome. *G. cuvieri cuvieri* has a more highly ornamented middle body, with numerous terrace ridges surrounding the central keel (as depicted in Richter and Richter, 1956; pl. 5, fig. 31), while *G. cuvieri malisus* has only three pairs of ridges surrounding the keel. Aside from these few differences, these two subspecies are remarkably similar.

Lütke (1990) provided exceptional illustrations of rostral plates and anterior cephalic borders for *G. cuvieri cuvieri*, that are very similar to those of the Moroccan specimens.

Due to the fact that *G. cuvieri malisus* lacks definitive ornamentation upon the glabella anterior to S0, it is virtually impossible to confuse it with *G. tuberculatus marocensis, G. aintawilus, G. lisanrasus, G. ainrasifus* or *G. discombobulatus*.

GERASTOS TAQUS

Figures 3-24.1 – 3-24.6

Diagnosis.— Cephalon is semi-circular; genal angle is pointed; posteromedial part of glabella anterior to S0 exhibits smeared tubercles in triangular region; anteriormost part of glabella sparse, with fine tubercles; ocular platform is absent; only first 4 pygidial axial rings display *m*-shape, remaining rings are straight (tr.); and pygidial border is very shallow to absent.

Description.— Exoskeleton is relatively inflated. Cephalon is semi-circular in dorsal view, encompassed on lateral and anterior margins by five terrace ridges. Maximum width (tr.) of cephalon is across posteriormost part of genal angle. Length of cephalon (A, sag.) in relation to entire exoskeleton (sag.) is 0.39, and length of cephalon (sag.) is 0.65 of maximum width of cephalon (tr.). Deeply incised axial and anterior border furrows accentuate ovoid glabellar shape. Length of glabella (A_1, sag.) is 0.76 of length of cephalon (sag.), and nearly equivalent (0.99) to width of glabella (K, tr.). Width of glabella (tr.) is 0.5 maximum width of cephalon (tr.). S0 is deep, short, and exhibits elongate *w*-shape (midpoint and distal ends are anteriorly directed). Prosopon of glabella anterior to S0 has tubercles smeared anteriorly in shape of triangle on posteromedial portion; remaining tubercles on back glabella are smooth, ordinary tubercles (Størmer, 1980) grading anteriorly opposite γ into smooth granule tubercles (without a central canal) (Størmer, 1980), finally becoming fine granules or completely lacking in ornamentation. S1, S2 and S3 are weakly defined, and largely discernible due to lack of ornamentation: S1 originates at axial furrow adjacent to δ, extends inward just behind transversely ε; S2 originates at axial furrow opposite γ and traverses subtransversely for quarter width (tr.) of glabella; S3 is circular in shape, scarcely discernible and located in front of lateral occipital furrows (exsag.), in front of S2 (exsag.). L1 is slightly inflated, L2 and L3 are not. Bulbous front of glabella overhangs anterior border furrow as well as most of anterior border in lateral profile; and it is blunt in anterior view (medially transverse). Posterior width of glabella (tr., anterior to S0) is same as width of occipital ring (L0, tr.). Length of occipital ring (A_4, sag.) is 0.15 of length of cephalon (sag.). Lateral occipital furrows originate at S0 and trend with hooked profile posterolaterally. Occipital ring displays few pustules, scattered randomly upon lobe. Lateral occipital lobes are adorned with limited, but more densely distributed and larger pustules; and small, defined medial node is placed on posterior edge of L0. Preglabellar field is absent. Anterior border (A_2+A_3) length (sag.) is 0.09 length of cephalon (sag.). Anterior border is convex and covered with fine granules. Pustules adorn front of fixed cheeks and prosopon upon palpebral lobes is unknown. Width of glabella (K) (tr.) is 0.72 width of δ–δ (tr.), while δ–δ width (tr.) is 0.7 width of cephalon (tr.). Posterior border furrow is deeply incised adaxially originating opposite midlength (exsag.) of occipital ring, and furrow shallows upon merging with lateral border furrow at approximately 70°. Posterior border is convex in lateral profile, is shallow adaxially, and is longer nearing genal angle.

Free cheeks are characterized by facial suture pattern as follows: from α to β sutures display tight diverging curvature; from β sutures gently converge with little medial trend to γ; from γ sutures diverge with gentle curvature to δ; from δ to ε sutures converge on tighter curvature than from γ to δ; from ε to ξ sutures run backward with little divergence; and from ξ sutures reside within posterior border furrow, diverging at approximately 45° angle from exsagittal line with distal end of facial suture curving back to ω. Lateral border is only slightly convex, with minute granules as ornamentation, and is accentuated by moderately incised lateral border furrow. Lateral border and posterior border merge and extend back slightly into short pointed genal spine. Prosopon of free cheeks is composed of fine granules to pustules. Genal field's width (tr.) (from eye socle furrow adjacent to δ to lateral border furrow) is 0.19 of cephalon width (tr.). Ocular platform is absent. Eye socle furrow is shallow and eye socle is faint. Length of eye (exsag.) is 0.47 length of A_1 (sag.) and 0.36 length of cephalon (sag.).

Hypostome is unknown.

Thorax is composed of ten segments. Thoracic length (sag.) is 0.42 length (sag.) of entire exoskeleton. Axial region of thorax tapers (tr.) from first to tenth ring by 18%, averages 0.43 of thorax width (tr.), and is delineated by deep axial furrows. Axial rings lack any ornamentation. Deeply incised pleural furrows shallow and terminate at articulating facet upon *Gerastos cuvieri*-type thoracic segments described by Lütke (1980). Anterior pleural band is shorter than posterior pleural band, and is pointed at fulcrum. Pleural region of thoracic segments also lacks ornamentation.

Pygidium is shaped like segment of circle, and is micropygous (pygidial width (tr.) is 0.73 of cephalon width (tr.)). Pygidial lateral and posterior margins edged with 3.5 terrace ridges, with 0.5 terrace ridge only extending along posterodorsal aspect. Length of pygidium (Z, sag.) is 0.26 of length (sag.) of entire exoskeleton; and pygidial width (W, tr.) is 1.68 times length (sag.) of pygidium. Axial region is composed of seven axial rings and blunt terminal piece in front of weak postaxial lobe. Axial width (X, tr.) is 0.42 width of pygidium; axial length (Y, sag.) is 0.84 of pygidial length (sag.). First axial ring to seventh axial ring displays 39% taper (tr.). First four axial rings are shaped like elongate *m*-shape, while remaining three rings are more transverse. Axial rings are smooth, with shallow paired marginal pits. Pleural region of pygidium presents 5+1 pleural furrow pattern, with pleural furrows deeper than interpleural furrows, though both are shallow. Pleural region prosopon consists of fine granules that are densest on posterior region, especially behind axis.

Etymology.— This specimen is nondescript leaving me at a loss for an appropriate name. Therefore I chose the Arabic for 'suffer', which reflects the difficulty in naming this specimen. Romanized Arabic: *Tâq* = suffer.

Type.— Holotype: UA13292 (complete specimen).

Occurrence.— '*Thysanopeltis* horizon', Taboumakhloûf Formation, Eifelian, lower Middle Devonian, Jbel el Mrakib, Ma'der region, southern Morocco.

Discussion.— Only a single species, *Gerastos granulosus* (Goldfuss, 1843) demonstrated close similarity to *Gerastos taqus*. There are only vague similarities between the two, however, although Alberti (1970) figured two specimens that he thought have an affinity to *G. granulosus* from both Mrakib and Oufatene, despite their different ages. Kowalski (1990) refigured *G. granulosus*, but unfortunately the specimen appears to be highly polished with the result that some morphological traits are obscured, and he only figured it in lateral view. Aside from these problems, a number of character states differentiate these two species. *G. taqus* possesses the following traits not observed upon *G. granulosus*: genal angle is pointed with small 'spines' extending posteriorly (square genal angle in *G. granulosus*); ocular platform is absent; eye socle is faint (prominent in contrasting species); and first four pygidial axial rings from elongate

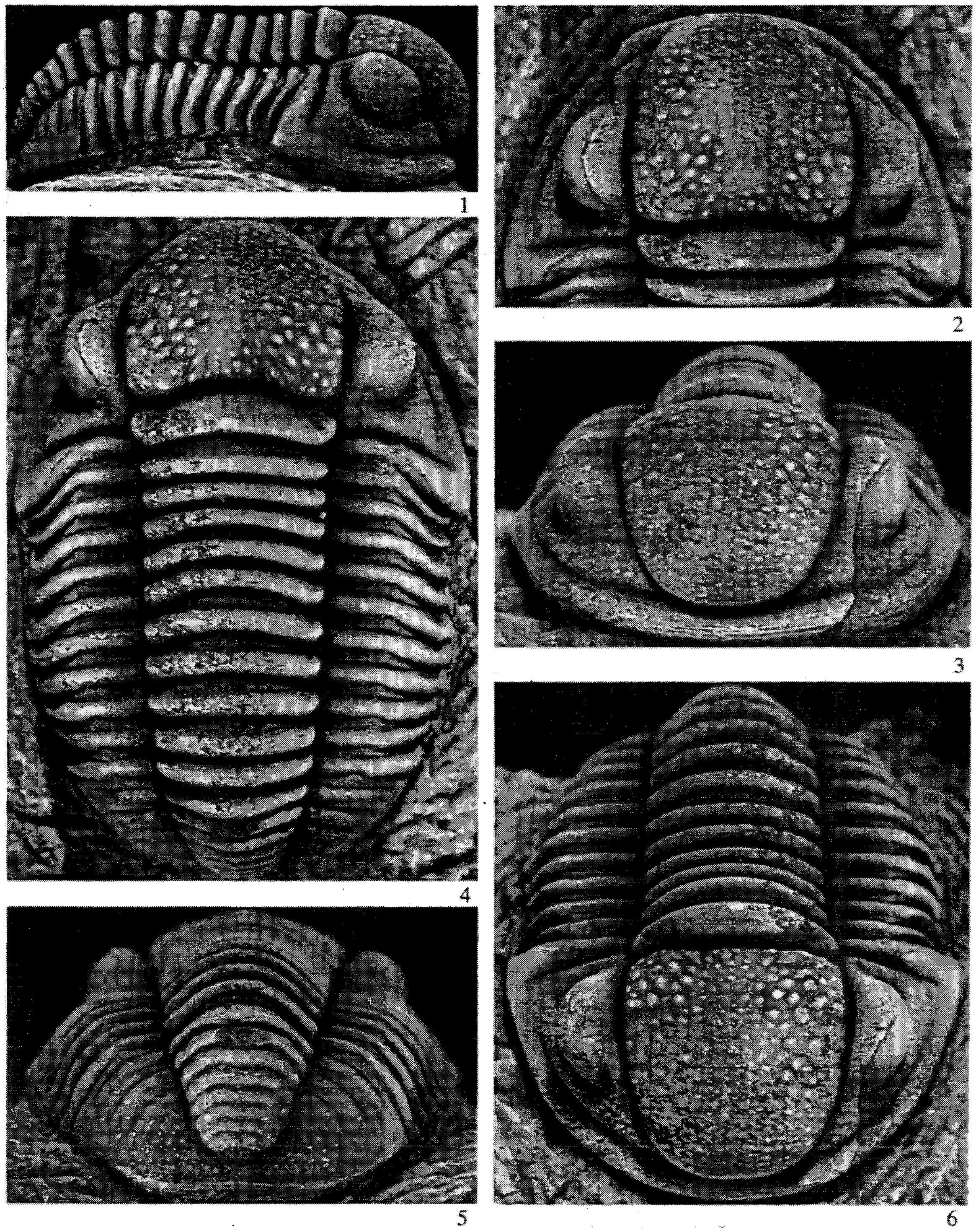

FIGURE 3-24—*1-6*, *Gerastos taqus* new species from the '*Thysanopeltis* horizon', Taboumakhloûf Formation, Mrakib, Ma'der region, southern Morocco (UA13292) (complete specimen). *1*, lateral view X4.2; *2*, dorsal view X5.7; *3*, anterior view X5.7; *4*, dorsal view X5.6; *5*, posterior view X5.9; *6*, anterodorsal view X5.7.

m-shapes, and the remaining axial rings are straight, while *G. granulosus* exhibits straight axial rings.

Gerastos taqus is also contrasted here to *G. lisanrasus* because of its sister group relationship on the phylogenetic tree (Figure 3-11) and stratigraphic propinquity; and is contrasted with *G. cuvieri malisus*, *G. ainrasifus* and *G. discombobulatus* due to its occurrence in strata of similar age in the same section. Observing differences to its sister species *G. lisanrasus*, *G. taqus* demonstrates the following contrasting character states: low convexity of cephalon; convex anterior and lateral borders; ovoid glabellar shape; free cheek prosopon of fine pustules to granules; constrained ornamentation upon the occipital lobe; lack of any ornamentation upon axial region of thorax and pygidium; pygidium shaped like a segment of a circle; pygidial axial rings 1-4 are elongate *m*-shaped and remaining rings are straight; and pygidium has sculpture of granules that are densest near the back.

Gerastos cuvieri malisus can be immediately differentiated from *G. taqus* due to the lack of ornamentation found upon *G. cuvieri malisus*. Other character traits that *G. taqus* portrays that are not observed in *G. cuvieri malisus* are: exhibiting distinct S1, S2 and S3; presence of pointed genal angle; absence of ocular platform; presence of fine pustules to granules upon the genal field; first four axial rings forming elongated *m*-shapes and remaining axial rings being straight with weakly incised paired marginal pits upon pygidial axial rings; presence of postaxial lobe; and posteriorly concentrated prosopon of granules upon pygidium.

From the strata below the '*Thysanopeltis* horizon' (3 metres stratigraphically) to the '*Proetus* horizon' at Jbel Mrakib, two species of *Gerastos* are found. The first discussed is *G. ainrasifus*. Traits exhibited by *G. taqus* that are not observed in *G. ainrasifus* include: convexity of cephalon is low; front of glabella is limited or lacking in ornamentation; genal field shows fine pustules to granules; eye socle is faint; genal angle is pointed; occipital ring displays constrained prosopon; thoracic and pygidial axial prosopon is smooth; pygidial axial rings form elongated *m*-shapes from 1st - 4th ring and remaining rings are straight, all with shallow paired marginal pits; no pygidial border is present; and posteriorly concentrated granules ornament pygidium.

The final species to compare is *G. discombobulatus* from the '*Proetus* horizon' three metres below the '*Thysanopeltis* horizon' of *G. taqus* at Jbel Mrakib. *G. taqus* exhibits the following contrasting states: shallow convexity of cephalon in lateral profile; ovoid glabellar shape; genal field adorned with fine pustules to granules; absence of ocular platform; faint eye socle; lack of ornamentation upon axial region of thorax and pygidium; axial rings of pygidium are elongate *m*-shaped in first four rings, and straight in remaining three, with shallow paired marginal pits; pygidial border is absent; and posteriorly concentrated granules occur upon pygidium.

GERASTOS MALISJILDUS new species

Figures 3-25.1 – 3-25.6

Diagnosis.— Exoskeleton is flattened dorsoventrally; isolated terrace ridge runs round anterior and lateral borders of cephalon; ornamentation upon glabella is limited and dispersed (anterior to S0) which disappears forward; genal field is pitted; thorax and pygidium lack ornamentation; and pygidial border is absent.

Description.— Exoskeleton is relatively flattened dorsoventrally, with slight convexity in axial region, though low. Cephalon rimmed, on lateral and anterior margins, by two terrace ridges. Maximum cephalon width is across tips of 'genal spines'. Cephalon length (A, sag.) is 0.35 of length (sag.) of entire exoskeleton, and cephalon length (sag.) is 0.67 of maximum cephalon width (tr.). Anterior border furrow and axial furrows deeply incise ovoid glabella. Glabellar length (A_1, sag.) is 0.75 of length of cephalon (sag.), is 0.50 maximum width of cephalon (tr.), and is 1.02 times width of glabella (K, tr.). S0 is short, deeply incised, and has elongated *w*-shape, viewed dorsally. Prosopon of glabella (anterior to S0) is composed of small pustules that become smaller anteriorly, opposite to γ on glabella, to become granules eventually. S1 and S2 are weakly defined and shallow, due to lack of ornamentation. S1 originates at axial furrow, opposite to midpoint between δ–γ, and extends transversely and turns posteromedially at approximately 55° from transverse, in front of lateral occipital furrows. S2 begins at axial furrow, slightly behind γ, mimics shape of S1, although overall shape is not as sharp, and length is shorter (tr. and exsag.). L1 and L2 are discernible, but display little independent convexity. Anterior tip of glabella marginally overhangs anterior border furrow, with very limited convexity and is blunt along its anterior edge. Posterior width (tr.) of glabella is 0.96 (anterior to S0), therefore essentially equivalent to width (tr.) of occipital ring. Occipital ring (L0) length (A_4, sag.) is 0.16 length (sag.) of cephalon, and width (tr.) of L0 is 0.45 width (tr.) of cephalon. Lateral occipital furrows only slightly incise front of occipital ring, thus lateral occipital lobes are discernible but poorly defined. Ornamentation on occipital ring is absent, therefore smooth except for posteriorly placed, small, defined median node. Preglabellar field is absent. Anterior border length (A_2+A_3) (sag.) is 0.1 length (sag.) of cephalon. Anterior border is slightly convex and smooth texture except for terrace line much removed from others dorsally that skirts midway between ventral margin and border furrows. Front of fixed cheeks displays extraordinarily fine granules and fine pits. Palpebral lobes (δ–δ) width (tr.) is 0.68 width of cephalon, and width of glabella (tr.) is 0.73 width of δ–δ (tr.). Palpebral lobes lack any ornamentation and lobes near horizontal viewed in anterior profile. Posterior border furrow originates opposite midlength of occipital ring, is deep proximally but shallows at genal angle, where meets lateral border furrow at approximately 80°. Posterior border is convex dorsally adaxially but convexity decreases abaxially; medially border is short (exsag.), and increases in length (exsag.) laterally.

Free cheeks differentiated from cranidium by facial sutures that exhibit following pattern: sutures diverge moderately from α to β; they then converge only a little from β to γ; in γ sutures run almost straight and are divergent from γ to close of δ; they are tightly convex laterally close to δ and moderately convex outward as they come in from δ to ε; sutures are concave laterally at ε; and then diverge backward at about 45° from ε to ω. Lateral border is ornamented by very limited granules, and is accentuated by shallow lateral border furrow. Lateral border has slight convexity anteriorly, which grades to become less convex more posteriorly, and extends into short, pointed genal spine. Width (tr.) of right and left genal fields (from eye socle furrow, opposite to δ, to lateral border furrow) is 0.09 width of cephalon (tr.). Genal fields are finely pitted. Ocular platform is present. Eye socle furrow is shallow and eye socle is faint. Length of eye (exsag.) is 0.52 length of A_1 (sag.), and is 0.39 length of cephalon (sag.).

Hypostome is unknown.

Thorax is composed of ten segments. Length of thorax (sag.) is 0.47 length of entire exoskeleton (sag.). Width (tr.) of thoracic axial region comprises approximately 0.45 of thorax width (tr.); and width tapers from first to tenth axial ring by 25% (tr.). Axial rings are tightly convex dorsally in lateral view. Axial rings lack ornamentation. On 1^{st} to 5^{th} thoracic segments, shallow intra-annular furrow, lenticular preannulus (almost equivalent in length to axial ring), moderately incised articulating furrow and slightly convex, posterior part of articulating half ring are visible (preannulus may be present further back but can not be seen on specimen available. Pleural regions give appearance of *Gerastos cuvieri*-type of thoracic segment of Lütke (1980), though difficult to discern. Pleural furrows are deeply incised adaxially and shallow abaxially, close to articulating facet, though difficult to determine distally due to enrollment of only available specimen. Anterior pleural band is shorter than posterior pleural band, and neither display any ornamentation.

Pygidium is shape of compressed (sag. and exsag.) segment of circle, and is micropygous; width of pygidium (W, tr.) is 0.64 width of cephalon (tr.). Pygidial length (Z, sag.) is 0.17 length of entire exoskeleton (sag.). Pygidial width (tr.) is 1.91 times length of pygidium (sag.). Axial region is composed of seven rings plus terminal piece; first four rings exhibit elongate *m*-shapes, while remaining three rings become progressively straighter, and rings from first to seventh gradually become shorter. Axial rings display no ornamentation and weak paired marginal pits. Axial width (X, tr.) is 0.43 pygidial width (tr.); axial length (Y, sag.) is 0.82 pygidial length (sag.); and axial region from first to seventh ring tapers by 31%. Pygidial pleural region lacks ornamentation; furrow pattern is 3+1, with interpleural furrows shallower than pleural furrows that shallow to terminate along lateral margin due to absence of pygidial border. Interpleural and pleural furrows are essentially equivalent in length (exsag.).

Etymology.— Due to the smooth nature of the thorax and pygidium, this name is apropos; in Romanized Arabic: smooth = *mâlis*; skin = *jild.*

Type.— Holotype: UA13293 (complete specimen).*Occurrence.*— '*Thysanopeltis* horizon, Taboumakhloûf Formation, Eifelian, Jbel Zireg, Ma'der, southern Morocco.

Discussion.— This species is sister species to *Gerastos raribus* (see below under *G. raribus* for contrast between these species). Here *G. malisjildus* is only contrasted with the next most basal species in the phylogenetic analysis, *G. cuvieri malisus*, and those occurring in close proximity stratigraphically and geographically: *G. taqus, G. cuvieri malisus,* and *G. lisanrasus.*

Before proceeding with contrasting the various species, it should be noted that *G. malisjildus* has a unique distinguishing trait (distinctive autapomorphy) of an isolated terrace line upon the dorsolateral edge of the anterior and lateral borders/margins (this will not be listed below).

The closest basal species upon the phylogenetic tree (Figure 3-11) is *Gerastos cuvieri malisus*, which differs from *G. malisjildus* because the latter possesses the following contrasting character states: cephalic anterior border is smooth; front of fixed cheeks is ornamented with extraordinarily fine granules and fine pits; genal field is pitted; lateral border furrows are shallow; lateral borders are adorned with limited granules; genal angle is pointed; lateral occipital furrows are marginally incised; pygidial shape is of a compressed segment of a circle; pygidial axial rings 1-3 form elongate *m*-shapes and remaining four rings are straight and become considerably shorter

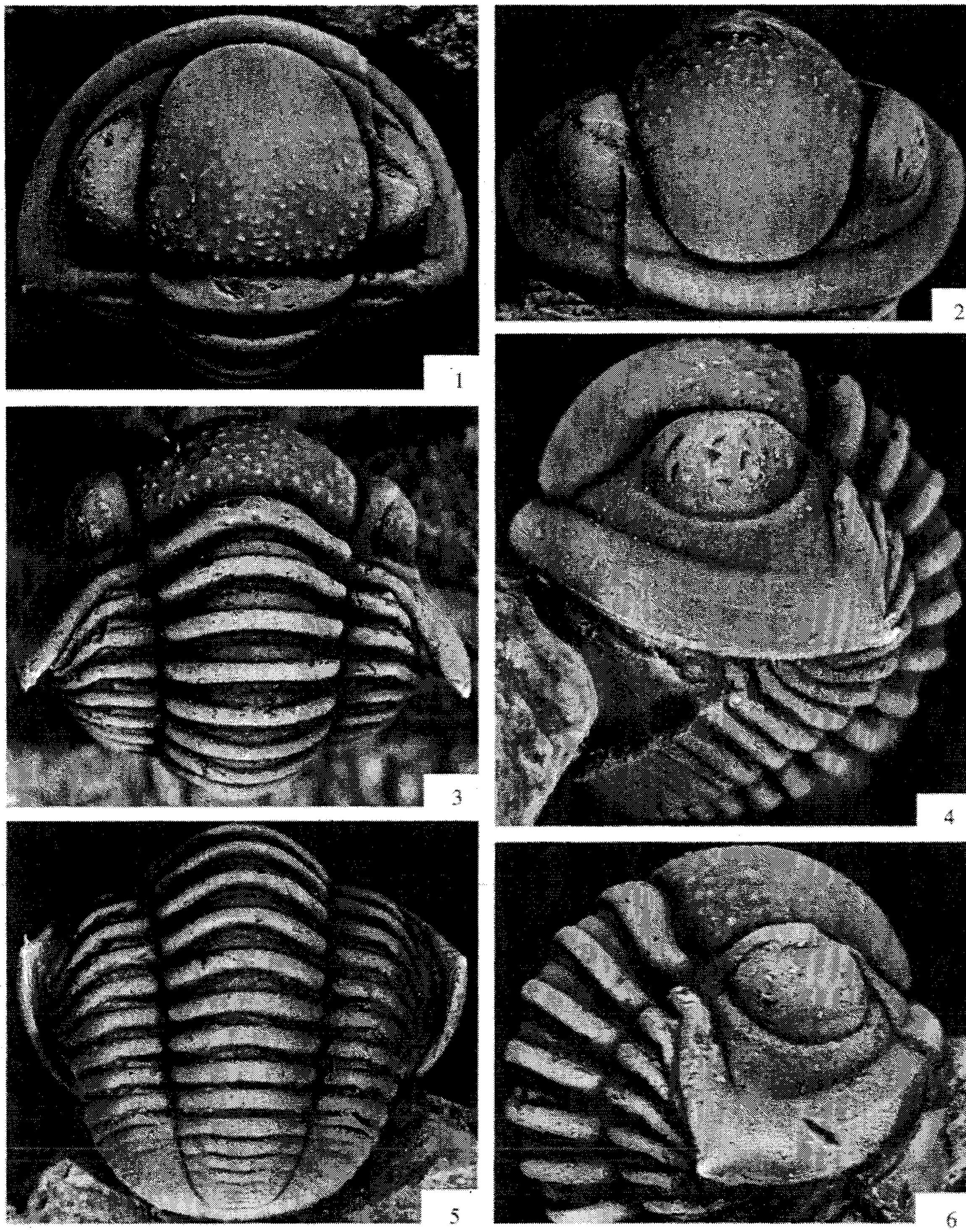

FIGURE 3-25—*1-6, Gerastos malisjildus* new species from the '*Thysanopeltis* horizon', Taboumakhloûf Formation, Zireg, Ma'der region, southern Morocco (UA13293) (complete specimen). *1*, dorsal view X8.4; *2*, anterior view X8.6; *3*, dorsal view X8.0; *4*, lateral view X10.2; *5*, dorsal view X8.0; *6*, oblique lateral view X9.4.

posteriorly; pygidial axial rings have weak paired marginal pits; and pleural regions of pygidium lack any ornamentation.

Gerastos taqus is from a bed that is approximately stratigraphically equivalent, at least in name, to the '*Thysanopeltis* horizon' at Mrakib. *G. malisjildus* has the following traits that are not exhibited by *G. taqus*: anterior border lacks ornamentation; front of fixed cheeks are adorned with extraordinarily fine granules and pits; only S1 and S2 are present; lateral border furrows are shallow; genal field is pitted; ocular platform is present; lateral occipital furrows are only marginally incised and occipital lobe lacks any ornamentation; pygidium has a dorsal profile of a compressed segment of a circle; pygidial axial rings from 1-3 are *m*-shaped and remaining rings are straight; postaxial lobe is absent; and pleural regions of pygidium lack any ornamentation.

Gerastos lisanrasus is older stratigraphically, but is from the same locality, the '*Ceratarges* horizon' that is separated by only 27 metres stratigraphically for the '*Thysanopeltis* layer' of *G. malisjildus*. *G. malisjildus* possesses the following character states not exhibited in *G. lisanrasus*: cephalon lacks dorsal convexity; anterior and lateral borders are convex; anterior border is lacking in any ornamentation; front of fixed cheeks adorned with extraordinarily small granules and fine pits; glabellar shape is ovoid; the glabella only has furrows S1 and S2 anterior to S0; lateral borders have very limited granules; lateral border furrows are shallow; genal field is pitted; ocular platform is present; palpebral lobes are smooth; marginally incised lateral occipital furrows slightly indent a smooth occipital ring; axial region of thorax and pygidium lack ornamentation; pygidium is the shape of a segment of a circle; first three axial rings of pygidium have elongate *m*-shapes and more posterior rings are foreshortened (sag.) and straight (tr.); and the pygidial border is absent, and there is no ornamentation present upon the pleural region of the pygidium.

GERASTOS RARIBUS new species

Figures 3-26.1 – 3-26.6 and 3-27.1 – 3-27.4

Diagnosis.— Exoskeleton has limited ornamentation; prosopon limited on glabella, to widely dispersed tubercles upon the posterior two-thirds of glabella anterior to S0; glabella is tongue-shaped; ocular platform is absent; pygidium has hexagonal shape; and pygidial axial region is narrow compared to pleural region.

Description.— Exoskeleton is only moderately inflated. Cephalon, in dorsal view, forms half-circle, with four terrace line encircling lateral and anterior margins. Length of cephalon (A, sag.) is 0.35 length (sag.) of exoskeleton. Cephalon width (tr.) is 1.86 times cephalon length (sag.). Anterior border furrow and axial furrows are deep, outlining tongue-shaped glabella. Glabella of limited convexity in lateral profile. Glabellar length (A_1, sag.) is 0.74-0.79 length (sag.) of cephalon (A); glabellar length (A_1, sag.) is 1.1-1.2 of glabellar width (K, tr.). S0 is short, deep and forms elongate *w*-shape, with distal ends directed anterolaterally in front of lateral occipital lobes. Glabella, anterior to S0, is ornamented with sparse smooth ordinary tubercles (Størmer, 1980) restricted to back two-thirds of glabella, with no ornamentation anterior of region opposite γ. Posteriorly tubercles are denser and become more infrequent and dispersed anteriorly. Glabellar furrows observed on anterior glabella are S1 and S2, both indiscrete and only visible due to lack of ornamentation and, slight indentation of glabella. S1 originates at axial furrow, opposite δ and continues on narrow posteromedial path curving slightly backward adaxially. S2 originates at axial furrow opposite γ, is narrow and angles in 'straight' posteromedial direction. Glabellar lobes (L1 and L2) are indistinct due to lack of inflation. Anterior tip of glabella is rounded and bulbous, similar to tip of tongue. Width of back of glabella (anterior to S0) is equivalent to width of occipital ring (0.98-1.01). Length of occipital ring (A_4, sag.) is 0.15 length (sag.) of cephalon. Lateral occipital furrows are shallow but complete, running from S0 in posterolateral curve to axial furrows, helping to circumscribe slight lateral occipital lobes. Prosopon of occipital ring is of scattered small pustules and posteriorly placed small, distinct median node. Preglabellar field is absent or very short medially. Anterior border (A_2+A_3) length (sag.) comprises 0.16 of cephalic length (A, sag.), vaguely convex in lateral profile, and ornamented with fine granules. Front of fixed cheeks is adorned with fine granules. Palpebral lobes lack any ornamentation. Width of glabella (K, tr.) is 0.64-0.68 width of δ–δ (tr.) and δ–δ (tr.) is 0.53 of maximum cephalon width (tr.). No ornamentation adorns back of fixed cheeks. Posterior border furrow is moderately incised, accentuating posterior border that is slightly convex.

Free cheeks are defined by facial sutures with following pattern: facial sutures anterior to δ converge along gentle sinuous path to γ and diverge again slightly to β; β is situated just anterior to anterior/lateral border furrows; and sutures converge from β to α in curve that tightens until near anterior margin. Posterior portion of facial sutures from posterolateral point on palpebral lobe to crossing of posterior border furrow curves in half circle adaxially, encompassing morphological landmarks of ε and ξ; sutures diverge farther from posterior border furrow crossing with slight hooked path to ω. Lateral margin of free cheeks has gentle curved shape, and terminates at square genal angle.

Lateral border is accentuated by lateral border furrow of moderate depth that joins posterior border furrow at near right angle. Lateral border is slightly convex, in lateral profile, and lacks ornamentation. Genal field (from eye socle furrow adjacent to δ to lateral border furrow, tr.) comprise 0.28 of cephalon width (tr.), and are ornamented with few pustules. Ocular platform is absent. Eye is encompassed by faint socle and shallow eye socle furrow. Eye length (exsag.) is 0.52 length (sag.) of A_1.

Hypostome is unknown.

Thorax is composed of ten segments. Length of thorax (sag.) is 0.38 length (sag.) of exoskeleton. Axial region of thorax (tr.) tapers from first to tenth segment by 17-20%, and comprises approximately 0.30-0.35 of thoracic width (tr.). In lateral profile, axial rings have imbricate pattern with front of ring sloping forward and convex and back of ring subvertical. Axial rings with few small granules on first three rings, gradually increasing in number more posteriorly to tenth ring that has abundant granules. Axial ring has shallow intra-annular furrow. Preannulus is lenticular in shape with moderately incised articulating furrow; articulating half ring is slightly convex. Pleural region of thoracic segments resembles *G. cuvieri*-type described by Lütke (1980). Anterior pleural band is shorter than posterior pleural band, though they are almost equivalent in length (exsag.) at fulcrum. Pleural furrow is deeply incised and terminates at articulating facet. Pleural regions of thorax display no ornamentation.

Pygidial shape is hexagonal, and pygidium is micropygous (pygidial width (W, tr.) is 0.75 to cephalon width (tr.)). Length of pygidium (Z, sag.) is 0.27 length of exoskeleton (sag.); pygidial width (W, tr.) is 1.70-1.93 times pygidial length (Z, sag.). Axial region displays low convexity in lateral profile. Axial region is comprised of 8 rings plus terminal piece in front of weak postaxial lobe. Pygidial axial width (X, tr.) is 0.29 pygidial width (W, tr.), and axial length (Y, sag.) is 0.78 pygidial length (Z, sag.). Axial region tapers from first to eighth ring by 35-40%. Shape of each axial ring on pygidium is elongated *m*-shape, with constrained ornamentation of fine granules, and paired marginal pits on distal ends of rings. Pleural region of pygidium presents 3+1 furrow pattern, with interpleural furrows shallow and pleural furrows slightly deeper. Anterior and posterior pleural bands on pygidium are equivalent in length (exsag.). Fine granules constrained to posterior region of weak pygidial border.

Etymology.— This species displays some character states that appear to be pleisomorphic, despite occurring in a stratigraphically younger species, which is quite atypical. Hence the name: in Romanized Arabic is *Rarîb* = strange.

Occurrence.— '*Koneprusites* horizon' (upper horizon), Bou Dib Formation, Givetian, Middle Devonian, east side of Issoumour, Ma'der region, southern Morocco.

Types.— Holotype, complete exoskeleton UA13462. Paratype, complete exoskeleton minus free cheeks, UA13463.

Discussion.— On the phylogenetic tree (Figure 3-11), *Gerastos raribus* is shown as sister species to *G. malisjildus* with *G. cuvieri malisus* sister to that clade. *G. raribus* exhibits a number of character states that separate it readily from the other two species: tongue-shaped glabella; ornamentation upon glabella that does not continue anteriorly; glabellar furrows of S1, S2 and S3 upon glabella anterior to S0; smooth lateral border; very limited prosopon upon genal field; absence of ocular

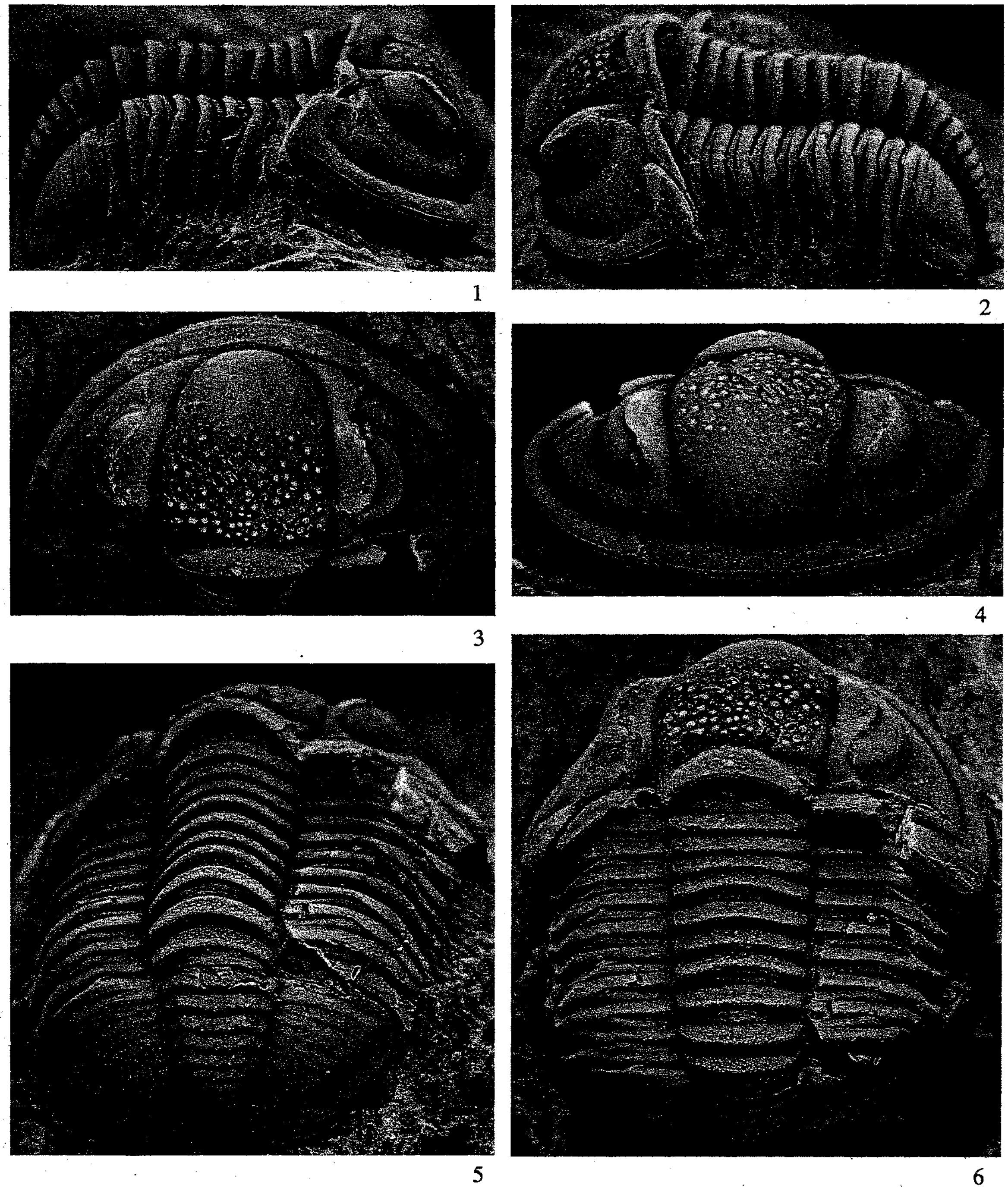

FIGURE 3-26—*1-6, Gerastos raribus* new species from the '*Koneprusites* horizon', Bou Dib Formation, Taboumakhloûf section of Issoumour, Ma'der region, southern Morocco (UA13462) (complete specimen). *1*, lateral view X4.9; *2*, lateral view X5.6; *3*, dorsal view X6.4; *4*, anterior view X6.3; *5*, oblique posterodorsal view X6.1; *6*, dorsal view X6.1.

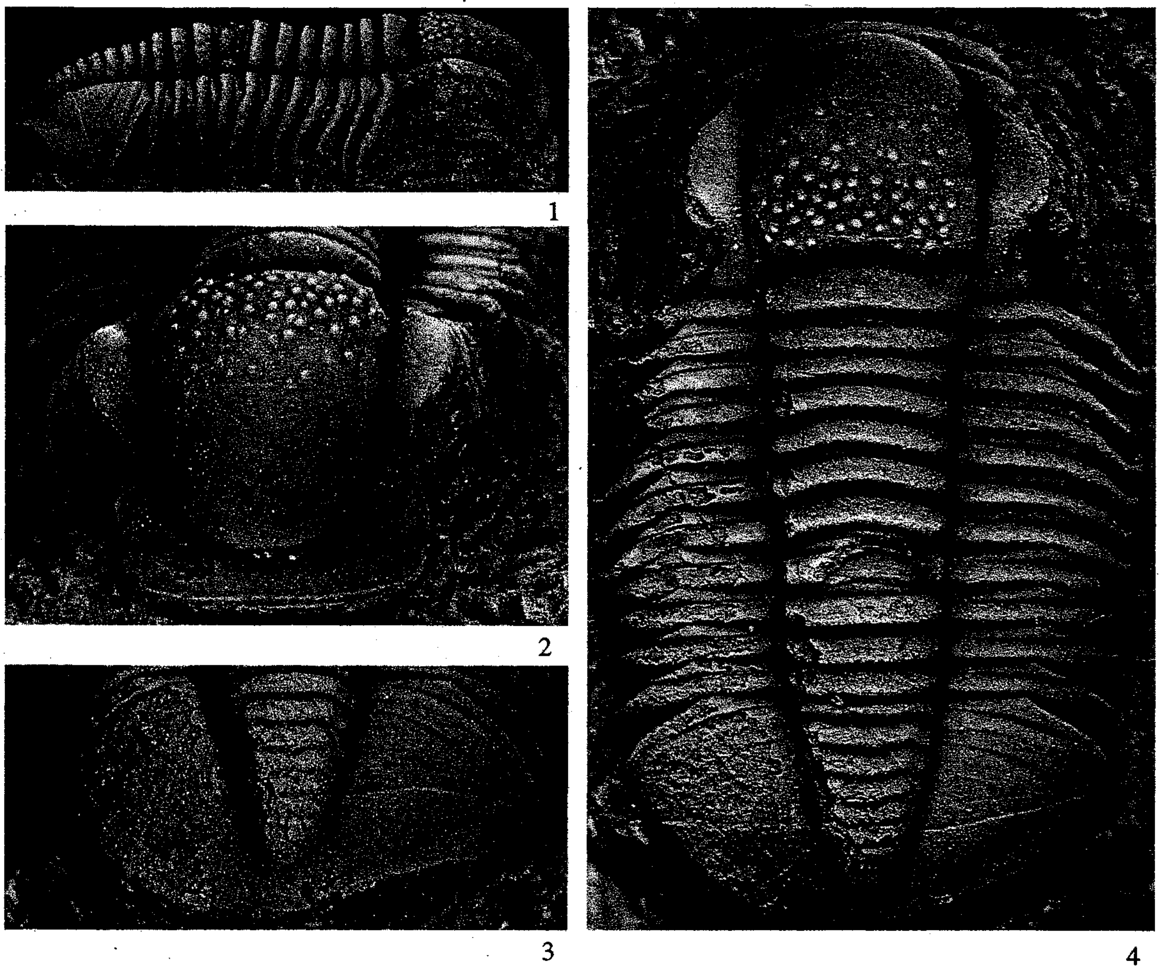

FIGURE 3-27—*1-4, Gerastos raribus* new species from the *'Koneprusites* horizon', Bou Dib Formation, Taboumakhloûf section of Issoumour, Ma'der region, southern Morocco (UA13463) (complete specimen minus free cheeks). *1,* lateral view X3.8; *2,* anterior view X7.3; *3,* dorsal view X7.1; *4,* dorsal view X6.2.

platform; axial region of thorax lacking ornamentation anteriorly and grading into an increasing number of granules farther back; hexagonal pygidium; seven pygidial axial rings plus a terminal piece with the presence of a postaxial lobe; constrained ornamentation upon pygidial axial rings; and a pygidial border that is weak.

Gerastos malisjildus is specifically different from *G. raribus* in that *G. malisjildus* possesses the following traits: anterior border of cephalon is adorned with fine granules as is the lateral border; front of fixed cheeks is sculpted by fine granules; genal angle is square; pygidial axial rings exhibit elongated *m*-shapes; marginal pits upon the pygidial axial rings are incised and paired; and pygidial border is composed of fine granules.

Gerastos cuvieri malisus, the sister group to the clade of *G. malisjildus* and *G. raribus*, has deeper lateral border furrows and lacks the marginally incised lateral occipital furrows that are exhibited in *G. raribus*.

GERASTOS EMMETUS new species

Figures 3-28.1 – 3-28.7 and 3-29.1 – 3-29.5

1970 *Proetus (Proetus)* sp. B. aff. *granulosus* (Goldfuss, 1843): Alberti, p. 36; pl. 3, figs. 1-2.

Diagnosis.— Cephalon forms half circle; glabellar ornamentation anterior to S0 is pointed, amalgamated, though not closely packed posteriorly, and disappears forward; genal field has row of tubercles accentuating ocular platform; thoracic axial rings increase in amount of ornamentation in form of pustules, from front to back; thoracic pleural region displays limited pustules on midsection of posterior pleural band; pygidial axial rings are adorned with limited number of tubercles; and pygidial pleural furrow pattern is 5+1.

Description.— Exoskeleton is inflated, though axial regions are low in glabella, thorax and pygidium in lateral profile. Cephalon has shape of half circle, flanked on lateral margin by five terrace ridges and anterior margin by six terrace ridges. Cephalic length (A, sag.) is 0.35 length (sag.) of entire exoskeleton, and cephalon length (A, sag.) is 0.65 maximum width of cephalon (tr., at genal angle). Axial furrows and anterior border furrow are deep around ovoid glabella. Glabellar length (A_1, sag.) is 0.82 of cephalon length (A, sag.), glabellar width (K, tr.) is 0.49 maximum cephalic width (tr.), and length of glabella (A_1, sag) is 1.1 times glabella width (K, tr.). S0 is deep, short and displays open *w*-shape that reflects shape of back of glabella in front of S0. Glabellar ornamentation anterior to S0 is composed of pointed tubercles oriented dorsoposteriorly; some tubercles are partly fused, hence have budding appearance, and tubercles are widely dispersed towards back. Tubercles thin in numbers and size opposite γ, thus more anterior ornamentation appears as smooth ordinary tubercles to granules (lacking central canal) described by Størmer (1980). Ornamentation is absent adjacent to anterior edge of eye. S1, S2 and S3 are weak but discernible upon glabella: S1 originates at axial furrow opposite (tr.) δ, hooks posteriorly and terminates opposite (tr.) ε and anterior (exsag.) to lateral occipital furrows. S2 is much weaker, originating at axial furrow and midway (exsag.) between δ and γ (tr.) with similar hooked shape to S1. Though barely discernible, S3 is circular and located almost immediately in front of S2 (exsag.) at 0.25 distance (tr.) from axial furrow. Glabellar lobes on glabella anterior to S0 are absent due to shallow nature of S1, S2 and S3. Anterior tip of glabella is rounded and only marginally overhangs anterior border when viewed in lateral profile. Posterior width (tr.) of glabella (anterior to S0) is equivalent to width (tr.) of occipital ring (A_4), length (sag.)

of occipital ring (A_4) is 0.15 of cephalon (A) length (sag.), and width (tr.) of occipital ring (A_4) is 0.47 of cephalic width (tr.). Sculpture of occipital ring is of limited granules scattered randomly with small, defined, posteriorly-placed median node. Lateral occipital furrows are moderately incised at S0 but shallow rapidly with posterolateral orientation. Anterior border (A_2+A_3) length (sag.) is 0.15 of cephalon length (A, sag.), is adorned with fine granules, and is marginally convex in lateral profile. Preglabellar field is absent. Front of fixed cheeks is ornamented with small pustules. Palpebral lobes (δ–δ) width (tr.) is 0.71 of cephalon width (tr.) and K (tr.) is 0.69 of width (tr.) of δ–δ. Palpebral lobes essentially lacking in ornamentation except for fine ridges oriented perpendicular to length and situated on lateral edge from δ to ε. Posterior portion of fixed cheeks lacks ornamentation. Posterior border furrow is deeply incised. Posterior border is moderately convex in lateral profile, and is shorter adaxially; becomes slightly longer abaxially and lacks any sculpture.

Free cheeks are defined by facial sutures with the following pattern from anterior to posterior: from α sutures diverge in curve to β; from β sutures run roughly exsagittaly in sigmoid curve to γ; from γ sutures diverge along to slightly curved path to δ; from δ sutures converge on tighter curve than from γ–δ to ε; from ε to ξ sutures run backward and downward; and from ξ sutures diverge almost transversely within posterior border furrow briefly, and then outward slightly behind transversely to ω. Genal angle is subrounded. Lateral border is ornamented with minute granules, is slightly convex, and is flanked medially by firmly incised lateral border furrow. Lateral border furrow and posterior border furrow join at approximately 90° angle. Right and left genal field widths (tr.) (opposite (tr.) δ and abaxially to lateral border furrow) comprise 0.12 of cephalon width (tr.). Genal fields display row of tubercles encircling ocular platform, hence ocular platform is present, though weak, with some variation but generally few granules on remainder of free cheek. Eye socle furrow is shallow and eye socle is faint. Length (exsag.) of eye is 0.5 glabellar (A_1) length (sag.) and 0.41 cephalon (A) length (sag.).

Hypostome is unknown.

Thorax has ten segments. Length of thorax (sag.) is 0.41 entire exoskeleton length (sag.). Axial region of thorax tapers (tr.) from first to tenth ring by 10%, and comprises 0.45 width (tr.) of thorax. Axial rings display imbricate pattern in profile with fronts angling posterodorsally to steeper posterior edge. Prosopon on axial rings is of fine pustules concentrated towards back. Pleural regions have *Gerastos cuvieri*-type thorax segment described by Lütke (1980). Pleural furrow is deeply incised, and becomes short and shallow upon proximal edge of articulating facet. Anterior pleural band is shorter than posterior pleural band. Distal end of anterior pleural band terminates at articulating facet. Ornamentation upon pleural region appears to consist of few (often three pustules) situated on fulcrum of posterior pleural band of some (often 4^{th} to 8^{th}) segments.

Pygidium is shaped like segment of circle, and is slightly micropygous (pygidial width (W, tr.) is 0.72 of cephalic width (tr.).); encompassed on posterior and lateral margins by three terrace lines. Length of pygidium (Z, sag.) is 0.24 length (sag.) of entire exoskeleton. Width of pygidium (W, tr.) is 1.62 times length (sag.) of pygidium (Z). Axial region is delineated by deeply incised axial furrows, and composed of seven rings plus terminal piece. Axial rings have shape of broad *m,* and terminal piece is blunt (tr.). Axial rings display ornamentation of number of small pustules verging on tubercles, with paired marginal pits on distal region of rings. Axial length (Y, sag.) is 0.90 of pygidial length (Z, sag.) and axial width (X, tr.) is 0.45 of pygidial width (W, tr.). Axial region tapers from first to seventh ring by 45% (tr.). Pygidial pleural furrow pattern is 5+1 with pleural furrows deeper than interpleural furrows. Pygidial anterior pleural bands and posterior pleural bands are approximately equivalent in length (exsag.). Ornamentation on pygidial pleural region is composed of restricted minute granules on weak pygidial border becoming more abundant posterior to terminal piece.

Etymology.— Due to the posterior region of the glabella anterior to S0 exhibiting pointed tubercles and the front of the glabella being barren of ornamentation, 'extinguished' was decided upon using the Berber language of Ouargli (unfortunately not the dialect of the Berbers that we worked with, for the Ouargli dialect is from two northern oases of Algerian Sahara): ə*mm* ə*t* = extinguish.

Types.— Holotype, complete exoskeleton UA13471. Paratype, complete exoskeleton UA13472.

Occurrence.— '*Drotops megalomanicus* horizon', Bou Dib Formation, early to middle Givetian, Middle Devonian, east side of Jbel Issoumour, Ma'der region, southern Morocco (UA13471) and *Drotops megalomanicus* horizon' Bou Dib Formation, early to middle Givetian, Middle Devonian, Jbel El Mrakib, Ma'der region, southern Morocco (UA13472).

Discussion.— Alberti (1970, pl. 3, figs. 1-2) illustrated a specimen of this species as *Gerastos* sp. B aff. *granulosus*. Although the exact location where Alberti (1970) found this specimen is unknown, it is likely from the '*Drotops megalomanicus* horizon' of the

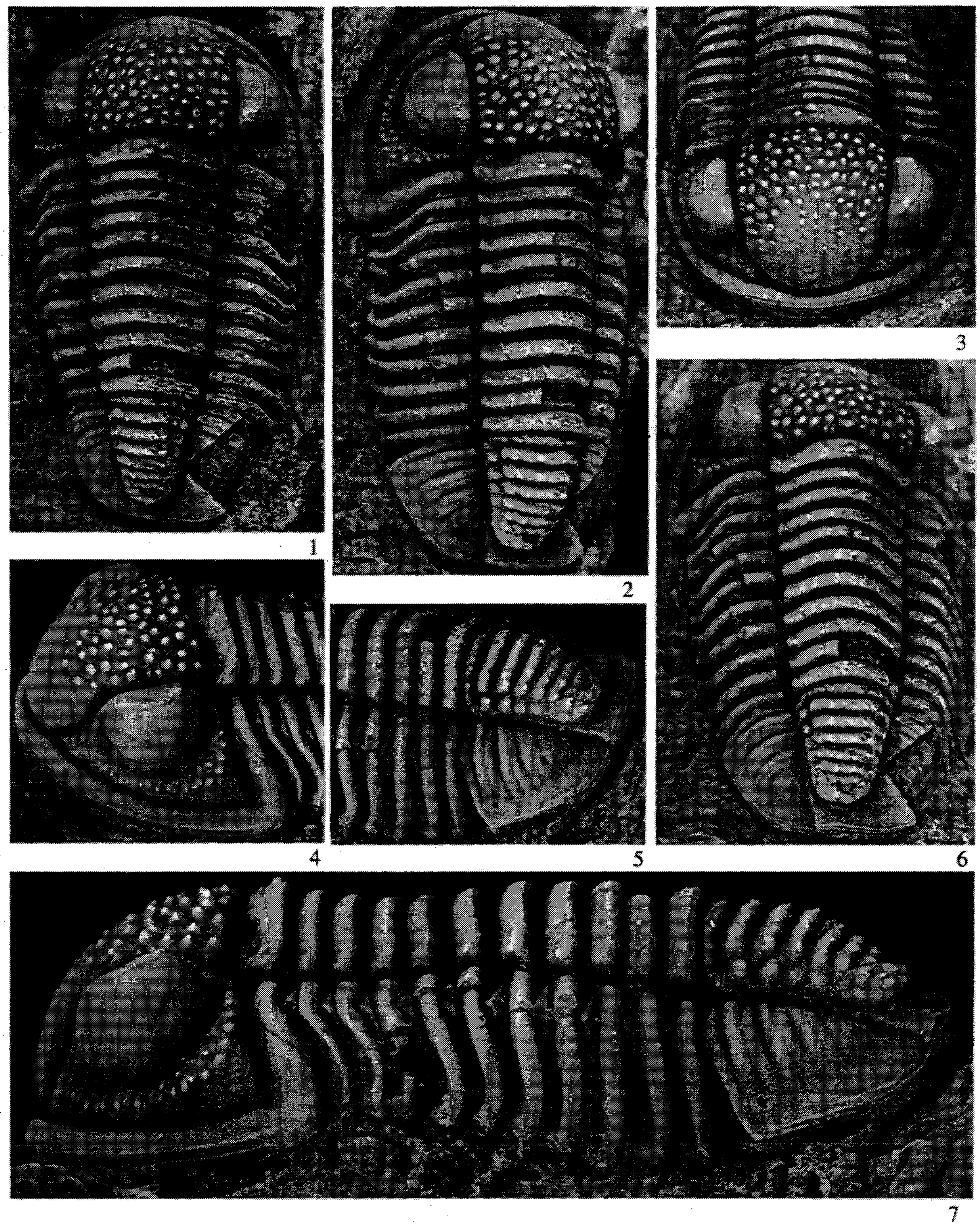

FIGURE 3-28—*1-7, Gerastos emmetus* new species from the '*Drotops megalomanicus* horizon, Bou Dib Formation, Taboumakhloûf section of Issoumour, Ma'der region, southern Morocco (UA13471) (complete specimen). *1*, dorsal view X4.0; *2*, dorsolateral view X4.5; *3*, anterodorsal view X4.5; *4*, oblique lateral view X5.6; *5*, oblique dorsolateral view X5.8; *6*, posterodorsal view X4.3; *7*, lateral view X7.5.

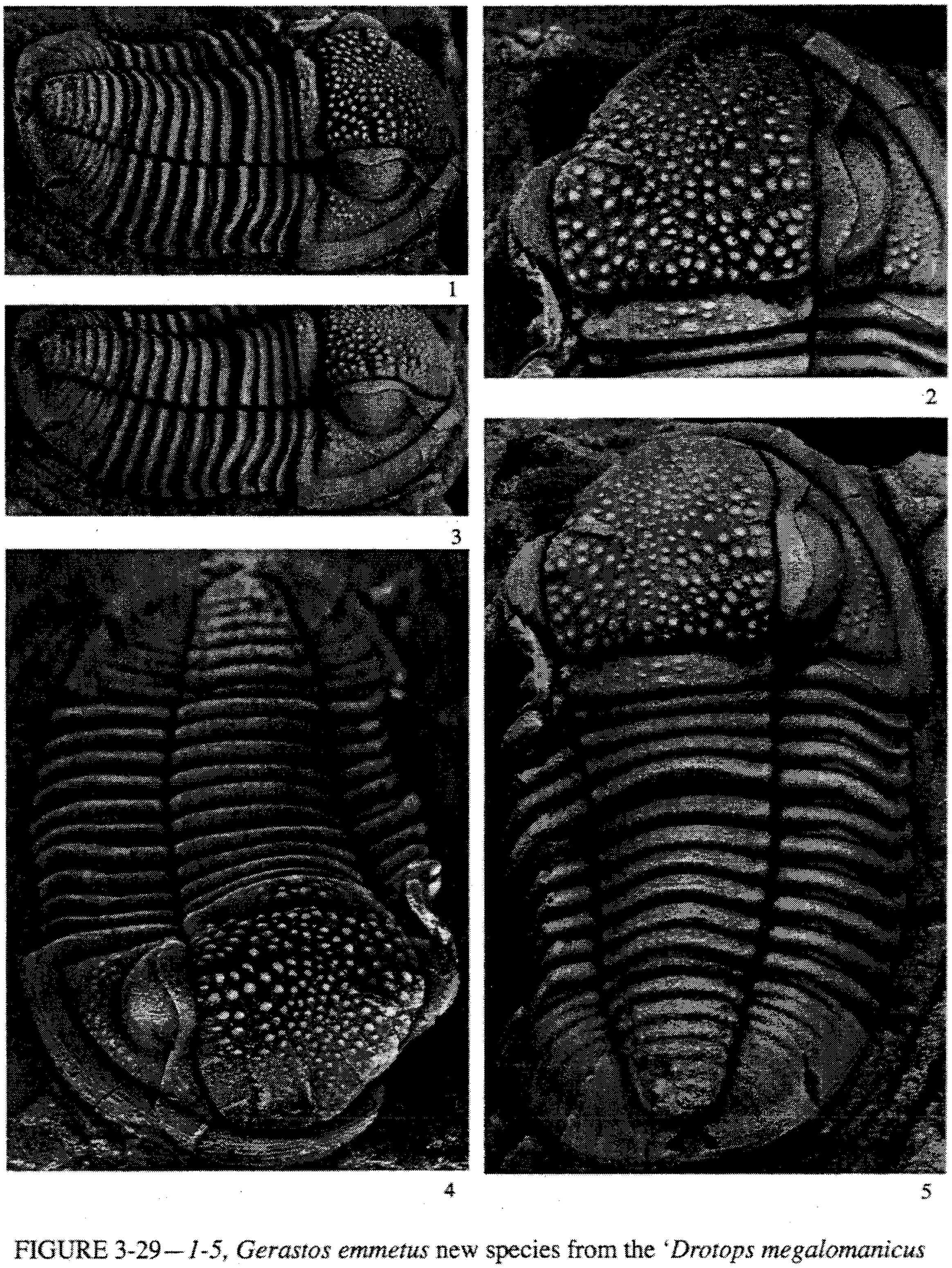

FIGURE 3-29—*1-5*, *Gerastos emmetus* new species from the '*Drotops megalomanicus* horizon, Bou Dib Formation, Mrakib, Ma'der region, southern Morocco (UA13472) (complete specimen). *1*, oblique dorsolateral view X3.5; *2*, dorsal view X6.8; *3*, oblique dorsolateral view X3.5; *4*, anterodorsal view X5.5; *5*, dorsal view X6.1.

early to middle Givetian (Campbell et al., 2002) where the specimen illustrated in Figure 3-29 was collected.

Gerastos emmetus is contrasted here with the three species that fell closest to it on the phylogenetic tree (Figure 3-11): *G. discombobulatus*, *G. lisanrasus* and *G. taqus*. It is also contrasted with the species that is most similar in age, *G. raribus*.

Gerastos emmetus differs from *G. discombobulatus* in the following differing traits: cephalon convexity is shallow; anterior and lateral borders are convex; glabellar shape is ovoid; genal field has definitive pustules surrounding ocular platform and limited randomly organized granules more laterally; eye socle is faint; palpebral lobes are adorned with posterolaterally placed ornamentation of ridges/pustules; genal angle is rounded; axial ornamentation of thorax is limited anteriorly, and there are more abundant granules posteriorly; pleural region of thorax displays few pustules; pygidial axial region displays an inflated convexity in lateral profile; pygidial axial rings are in the shape of very broad *m* in dorsal view; postaxial lobe is absent; and pygidial border is weak.

G. emmetus is the basal species to the branch containing the two species, *G. taqus* and *G. lisanrasus*. To avoid repetition, the differences between *G. emmetus* and both *G. taqus* and *G. lisanrasus* are outlined. These include: rounded genal angle; presence of an ocular platform; limited granules on anterior segments of thoracic axial region, with progressively denser ornamentation towards the back of each thoracic segment; thoracic pleural region ornamentation of limited to few granules; an inflated pygidial axial region; pygidial axial rings with a broad *m*-shape and moderately incised paired marginal pits; distinct pustules on pygidial axial rings; absent postaxial lobe; and pygidial border is weak.

Gerastos emmetus also differs from *G. lisanrasus* in that the former has the following traits: anterior and lateral borders are convex; glabella has shallow convexity; glabellar shape is ovoid; few pustules ornament the occipital ring; and the pygidium is in the shape of a segment of a circle.

The other species within the clade is *G. taqus*, which when contrasted with *G. emmetus,* displays two of differing traits: the presence of larger pustules encircling ocular platform and finer granules adorning remainder of genal field, and granules adorning the whole pygidial border.

Gerastos emmetus differs from *G. raribus* in the following: glabellar shape is ovoid; glabellar furrows S1, S2 & S3 are evident; palpebral lobes are adorned with posterolateral ridges/granules; ocular platform is present; ocular platform is surrounded by pustules and remainder of genal field with minor fine granules; lateral border furrows are moderately incised; lateral border prosopon consists of fine granules; genal angle is rounded; occipital ring is incised by posterolaterally hooking lateral occipital furrows; thoracic axial region has limited ornamentation anteriorly which grades into more abundant granules posteriorly; pleural region of thorax has a limited number of pustules; pygidium has the shape of a segment of a circle; pygidial axial region is convex in lateral profile; axis of pygidium consists of seven rings plus a terminal piece with no postaxial lobe; and pygidial axial rings are adorned with abundant and large pustules.

GERASTOS IZIUS new species

Figure 3-18.5, 3-30.1 – 3-30.13

Diagnosis.— Cephalon has shape of semi-circle; genal angle is rounded; lateral and anterior border lack prosopon; ocular platform is absent; glabellar ornamentation (anterior to S0) grades anteriorly from pointed tubercles to granules and then disappears; pygidial axial rings are *m*-shaped.

Description.— Exoskeleton is inflated, except glabella which is not arched strongly transversely. Cephalon length (sag.) is 0.34-0.35 length of entire exoskeleton (sag.). Anterior border is inflated (sag.), has smooth texture dorsally and at least 4 fine ridges skirting entire anterior and lateral margins of cephalon. Facial sutures from anterior to posterior display following pattern: from α sutures diverge obliquely abaxially towards β at shallow angle, from β to γ converge distinctly, from γ sutures diverge and then converge minimally in a semicircular pattern through δ to ε (straighter around front and back of palpebral lobes than at δ), from ε to ξ sutures display vertical descent posteriorly, then after ξ they diverge strongly backward, to ω. Confined, deep axial furrows flank ovoid glabella that displays weak convexity. Glabella slightly overhangs anterior border furrow, which is deeply incised with no preglabellar field. Glabellar maximum width (K, tr.) is approximately equal to length of glabella (A_1, sag.): 0.96-1.1. Prosopon upon glabella consists of small to medium sized pustules posteriorly, that are rounded to pointed, and it diminishes in size and amount forward S0 as to be absent on front of glabella. Glabellar furrows are shallow, defined by a lack of pustules, and consist of S1, S2, and S3. S1 commences to axial furrow opposite δ, and runs inward and curves slightly backward adaxially. S2 is close to axial furrow posteromedial to γ, and is directed posteromedially about 25% of width of glabella. S3 is subcircular, located medially opposite γ. Palpebral lobes slope inward slightly until close to axial furrows, and display little to no ornamentation (fine granules close to margin posteriorly and scattered very low, obscure granules elsewhere). Palpebral lobes (δ-δ, tr.) approximately 0.98-1.05 times length of cephalon (sag.). Front of fixed cheek has a granular prosopon. Occipital ring (A_4) approximates posterior width of glabella (A_1): 0.86-1.04. Lateral occipital furrows marginally incise anterolaterally therefore lateral occipital lobes are distinguishable but not well defined. Prosopon of occipital ring consists of abundant pustules with a small and defined median node situated near back of L0.

Free cheeks are ornamented with small pointed pustules that decrease in number and eventually disappear approaching genal angle. Lateral border furrow is moderately incised (deep forward and shallower near genal angle), and lateral border is smooth. Posterior border is transverse to fulcrum then gently angles posteriorly while subtly flaring (exsag.). Lateral border furrow and posterior border furrow converge to form a near 90° angle. Prosopon of posterior border is smooth lateral to facial suture but scattered with small pustules adaxially. Eye socle is slightly depressed, and surrounded by shallow furrow. Genal field (from lateral border to eye socle furrow) is most constricted opposite and in front of δ: 0.14-0.18 in relation to δ-δ. Genal angle is rounded in mature specimens (short genal spine present in small free cheeks).

Hypostome is unknown.

Thorax is approximately 0.38-0.41 of total sagittal length of exoskeleton. Axis tapers 20.4-26.7% from first thoracic segment to tenth. Thorax is composed of 10 thoracic segments that have abundant small, low pustules on axial rings and limited pustules on posterior pleural ribs. Axial region is inflated and defined by deep axial furrows. Pleural region has deeply incised and short (exsag.) pleural furrows that terminate just beyond fulcrum on articulating facets. Medial aspect of pleural region is horizontal up until fulcrum, with lateral portion directed ventrolaterally at an abrupt angle. Thoracic segments take on appearance presented by Lütke (1980) of *Gerastos cuvieri*, showing pointed projection at anterolateral corner of flange and subrounded anterodistal and subangular to pointed posterodistal terminations. Anterior pleural bands are shorter than posterior pleural bands. Short (sag.) preannulus is smooth, short and lenticular.

Pygidium is slightly micropygous. Overall shape of pygidium is segment of circle. Pygidial length (Z) is 0.24 - 0.27 total length of exoskeleton (sag.). Z (sag.) is 0.56 - 0.60 to maximum width (W, tr.), while maximum axial width (X, tr.) is 0.33 - 0.41 to W (tr.); and axial length (Y, sag.) is 0.70 - 0.83 of Z (sag.). Convexity of axial rings is inflated; and they are sculpted with abundant and relatively large pustules. Axis has seven rings plus terminal piece. Axial taper from first to seventh axial ring is 40-50% (tr.). Axial rings display broad *m*-shape, with shallow grooves near margins posterolaterally. Axial furrows are deep. Articulating facet is angled approximately at 80° to articulating flange, and lacks prosopon. Articulating flange is clearly defined with moderately incising anterior (first) pleural furrow (adaxially, tr.) that extinguishes to a fine, short and shallow furrow adaxial to pygidial border. Second and third pleural furrows are shallow, fourth furrow is faint and fifth is very weak. Four nearly indiscernible interpleural furrows become even less decipherable backward. Both pleural and interpleural furrows terminate at pygidial border. Region of pleural and interpleural furrows lacks prosopon. Pygidial border is broad and shallow, and finely granulated in texture. Postaxial lobe is weak. At least three fine ridges encompass lateral and posterior margins of pygidium.

Etymology.— The Berbers working the *couches* refer to proetids as 'flies' because they are extraordinarily common. Therefore, the Berber term was used: *izi* = fly.

Types.— Holotype, complete exoskeleton UA13473. Paratype, complete exoskeleton UA13474.

Occurrence.— '2cc horizon', Bou Dib Formation, Givetian, Jbel El Mrakib, Ma'der Region, southern Morocco.

Discussion.— Due to the lack of published species that demonstrate any similarities to *Gerastos izius*, only the two highest stratigraphic species of *Gerastos*, from the same region (*G. raribus* and *G. emmetus*) and the next most derived species upon the phylogenetic tree, *G. aintawilus,* are contrasted with this species.

Gerastos raribus is the stratigraphically older than *G. izius*, and *G. emmetus* slightly younger than *G. raribus*. Once again, to reduce repetition, these two species shall be addressed as one, and then specifically addressed with regard to any remaining differences demonstrated by *G. izius*. *G. izius* portrays the following character traits in contrast to *G. raribus* and *G. emmetus*: anterior border lacks any sculpture; glabellar prosopon is more tightly packed and displays more ornamentation throughout, though grading to smaller and less granules more anteriorly; palpebral lobes are laterally encircled with a row of fine granules; eye socle is depressed; genal field is completely covered with fine tubercles or granules; occipital ring is adorned

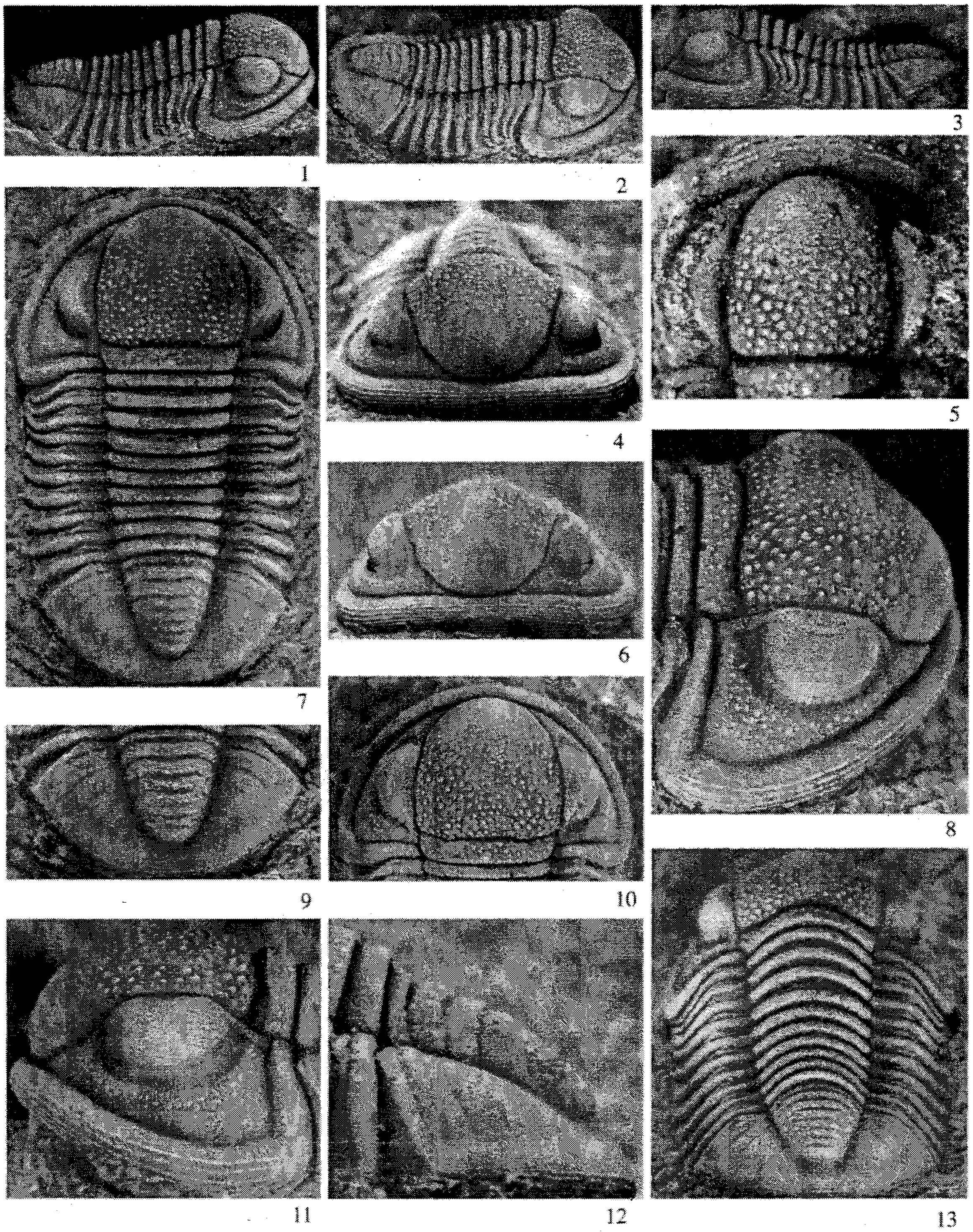

FIGURE 3-30—*1-13*, *Gerastos izius* new species from the '2cc horizon', Bou Dib Formation, Mrakib, Ma'der region, southern Morocco. *1-4, 6-13* (UA13473) (complete specimen). *1*, lateral view X2.8; *2*, dorsolateral view X2.5; *3*, lateral view X2.9; *4*, anterior view X4.3; *6*, anterior view X4.3; *7*, dorsal view X4.2; *8*, dorsolateral view X6.7; *9*, dorsal view X4.6; *10*, dorsal view X4.2; *11*, lateral view X7.3; *12*, lateral view X10.0; *13*, posterodorsal view X4.1. *5*, (UA13474) (meraspid cranidium) dorsal view X16.8.

with continuous and abundant fine pustules; axial region of thorax is sculpted by abundant small pustules; pleural region of thorax has a limited number of low pustules; weak pygidial postaxial lobe is present; and pygidium displays a shallow border.

Gerastos izius differs from *G. raribus* in: glabella is convex in lateral view; glabellar shape is ovoid; glabellar furrows S1, S2 and S3 are present; lateral border furrow is moderately incised; genal angle is rounded; pygidium has shape of a segment of a circle; pygidium has seven axial rings plus a terminal piece; and abundant fine pustules upon the pygidial axial rings.

Gerastos izius differs from *G. emmetus* in the following: an ocular platform is absent; lateral border is smooth; and lateral occipital furrows only marginally incise the occipital ring at a posterolateral angle.

The closest species upon the phylogenetic tree, *G. aintawilus*, is the second oldest species, within the ingroup. *G. izius* differs from *G. aintawilus* in: anterior and lateral cephalic borders are smooth; convexity of glabella in lateral profile is shallow; glabellar ornamentation (anterior to S0) is comprised of pointed small tubercles posteriorly, that grade into smaller tubercles and granules more anteriorly; eye socle is depressed; genal angle is rounded; pygidial axis in lateral profile is inflated; and pygidial border is shallow.

CONCLUSIONS

Through collection and analysis of new Moroccan specimens, the following new species/subspecies have been proposed: *Gerastos tuberculatus marocensis, G. aintawilus, G. lisanrasus, G. ainrasifus, G. discombobulatus, G. cuvieri malisus, G.*

taqus, G. malisjildus, G. raribus, G. emmetus, and G. izius. A phylogenetic analysis of these species and some other species from Europe and Laurentia produced a single tree. This tree helped to illuminate relationships among this large group of rather similar species. However, it did not appear to group the species particularly in relationship to their stratigraphic or geographic positions. It also did not seem to group species that appear to show the same grades in their morphological traits that, before the analysis, seemed to have some biostratigraphic utility. These characters are K/δ–δ, a reduction of the genal spine and the disappearance of tuberculose ornament on the front of the glabella. If one observes a histogram of K/δ–δ ratios it can be seen that as the species become younger stratigraphically, the K/δ–δ increases and approaches 1.0; therefore, the palpebral lobe width (tr.) is getting smaller and/or the glabella width (tr.) wider. The one contradiction to this trend is *G. raribus*, but this species appears to be demonstrating a number of traits not expected of a younger specimen (smaller K/δ–δ ratio and pygidial axial ring count of eight plus a terminal piece, similar to one of the Silurian outgroup members, *G. mellishae)*. Another trait that appears homoplasious on the phylogenetic tree is reduction of the genal spine, from a pointed to a rounded genal angle. The last trait, stratigraphically, that appears unimportant according to the cladistic analysis is a reduction of ornamentation on the glabella anterior to S0, in particular the reduction of ornamentation on the front of the glabella to minute granules or even total absence. Thus, if the phylogenetic analysis has provided a tree that illuminates the true relationships of these species, some external influences were forcing several clades to lose genal spines, form wider glabellas, and lose ornamentation on the front of the glabella at more or less the same time. This poses the question, are some homoplasous characteristics useful for biostratigraphy?

ACKNOWLEDGEMENTS

The assistance and knowledge provided by Hammi Ait Hssain within Morocco, to identify localities and trilobites was invaluable. The Moroccan Geological Survey provided much appreciated assistance. The stratigraphic measurements were done by Kevin Brett, unless otherwise noted. The majority of specimens illustrated were prepared by Allan Lindoe. Valued assistance in the field was provided by Jim Bohun, Allan Lindoe, Ryan McKellar, and Hammi Ait Hssain. NSERC operations grant to B.D.E. Chatterton has funded this invaluable research.

REFERENCES

ADRAIN, J. M. 1997. Proetid trilobites from the Silurian (Wenlock-Ludlow) of the Cape Phillips Formation, Canadian Arctic Archipelago. Palaeontographia Italica, 84:21-111.

AITKEN, S. A., C. J. COLLOM, C. M. HENDERSON, AND P. A. JOHNSTON. 2002. Stratigraphy, paleoecology, and origin of Lower Devonian (Emsian) carbonate mud buildups, Hamar Laghdad, eastern Anti-Atlas, Morocco, Africa. Bulletin of Canadian Petroleum Geology, 50(2):217-243.

ALBERTI, G. K. B. 1964. Neue Trilobiten aus dem marokkanischen und deutschen Unter- und Mitteldevon. Senckenbergiana lethaea, 45(1-4):115-133.

ALBERTI, G. K. B. 1966a. Note préliminaire sur quelques trilobites (en particulier des Proétidés) du Silurien, du Dévonien inférieur et du Dévonien moyen du Maroc. Notes du Service Géologique de Maroc, 26:55-68.

ALBERTI, G. K. B. 1966b. Über einige neue Trilobiten aus dem Silurium und Devon, besonders von Marokko. Senkenbergiana Lethaea, 47:111-121.

ALBERTI, G. K. B. 1967a. Neue obersilurische sowie unter- und mitteldevonische Trilobiten aus Marokko, Deutschland und einigen anderen europäischen Gebieten. 1. Senckenbergiana lethaea, 48(5):463-479.

ALBERTI, G. K. B. 1967b. Neue obersilurische sowie unter- und mitteldevonische Trilobiten aus Marokko, Deutschland und einigen anderen europäischen Gebieten. 2. Senckenbergiana lethaea, 48(6):481-509.

ALBERTI, G. K. B. 1969. Trilobiten des jüngeren Siluriums sowie des Unter- und Mitteldevons. I. Abhandlungen der Senckenbergischen Naturforschenden Gesellschaft, 520:1-692.

ALBERTI, G. K. B. 1970. Trilobiten des jüngeren Siluriums sowie des Unter- und Mitteldevons. II. Abhandlungen der Senckenbergischen Naturforschenden Gesellschaft, 525:1-233.

ALBERTI, G. K. B. 1980. Neue Daten zur Grenze Unter-/Mittel-Devon, vornehmlich aufgrund der Tentaculiten und Trilobiten im Tafilalt (SE-Marokko). Neues Jahrbuch fuer Geologie und Palaeontologie. Monatshefte, 39:581-594.

ALBERTI, G. K. B. 1981. Beziehungen zwischen "herzynischen" Trilobiten-Faunen aus NW-Marokko und Deutschland (Unter- und Mittel-Devon). Natur und Museum, 111(11):362-369.

ALBERTI, G. K. B. 1982. Der Hamar-Laghdad (Tafilalt, SE-Marokko), eine bedeutende Fundstätte devonischer Trilobiten. Natur und Museum, 112(6):172-182.

BARRANDE, J. 1846. Notice préliminaire sur le Système silurien et les trilobites de Bohême. Hirschfeld, Lipzig, 97 p.

BASSE, M. 1996. Trilobiten aus Mittlerem Devon des Rhenohercynikums: I. Corynexochida und Proetida (1). Palaeontographica Abteilung A, 239(4-6):89-182.

BASSE, M. 1998. Trilobiten aus Mittlerem Devon des Rhenohercynikums: III. Proetida (3), Phacopida (2), Lichida (Lichoidea, Odontopleuroidea) und ergänzende Daten. Palaeontographica Abteilung A, 249(1-6):1-162.

BECKER, G., N. LAZREQ, AND K. WEDDIGE. 2003. Ostracods of Thuringian provenance in the Lower Devonian of Eurasia and North Africa with special reference to the Emsian of Morocco. Courier Forschungsinstitut Senckenburg, 242:39-49.

BECKER, R. T., AND M. R. HOUSE. 1994. International Devonian goniatite zonation, Emsian to Givetian, with new records from Morocco. Courier Forschungsinstitut Senckenburg, 169:79-135.

BECKER, T. R., U. JANSEN, G. PLODOWSKI, E. SCHINDLER, S. Z. ABZOUSSALAM, AND K. WEDDIGE. 2004. Devonian litho- and biostratigraphy of the Dra Valley area -- an overview. Devonian Neritic-Pelagic Correlation and Events in the Dra Valley (Western Anti-Atlas, Morocco). Documents de l'Institut Scientifique(19):3-18.

BELKA, Z., B. KAUFMANN, AND P. BULTYNCK. 1997. Conodont-based quantitative biostratigraphy for the Eifelian of the eastern Anti-Atlas, Morocco. Geological Society of America Bulletin, 109(6):643-651.

BENSAID, M., P. BULTYNCK, P. SARTENAER, O. H. WALLISER, AND W. ZIEGLER. 1985. The Givetian-Frasnian Boundary in pre-Sahara Morocco. Courier Forschungsinstitut Senckenburg, 75:287-300.

BERGSTRÖM, J. 1977. Proetida -- a disorderly order of trilobites. Lethaia, 10:95-105.

BULTYNCK, P. 1985. Lower Devonian (Emsian) -- Middle Devonian (Eifelian and lowermost Givetian) conodont successions from the Ma'der and the Tafilalt, southern Morocco. Courier Forschungsinstitut Senckenberg, 75:261-286.

BULTYNCK, P. 1987. Pelagic and neritic conodont successions from the Givetian of pre-Sahara Morocco and the Ardennes. Bulletin de l'institut Royal des sciences naturelles de Belgique, Sciences de la Terre, 57:149-181.

BULTYNCK, P. 1989. Conodonts from a potential Eifelian-Givetian Global Boundary Stratotype at Jbel Ou Driss, southern Ma'der, Morocco. Bulletin de l'institut Royal des sciences naturelles de Belgique, Sciences de la Terre, 59:95-03.

BULTYNCK, P., AND H. HOLLARD. 1980. Distribution comparée de Conodontes et Goniatites dévoniens de plaines du Dra, de Ma'der et du Tafilalt (Maroc). Leuven University Press, 1, 73 p.

BULTYNCK, P., AND L. JACOBS. 1981. Conodontes et sédimentologie des couches de passage du Givetien au Frasnien dans le Nord du Tafilalt et dans le Ma'der (Maroc Présaharien). Bulletin de l'Institut Royal des Sciences Naturelles de Belgique. Sciences de la Terre, 53(2):1-23, pl.10, fig.23.

BULTYNCK, P., AND O. H. WALLISER. 2000. Devonian Boundaries in the Moroccan Anti-Atlas. Courier Forschungsinstitut Senckenburg, 225:211-226.

CAMPBELL, K. S. W., R. E. BARWICK, B. D. E. CHATTERTON, AND T. R. SMITHSON. 2002. A new Middle Devonian dipnoan from Morocco: structure and histology of the dental plates. Records of the Western Australian Museum, 21:39-61.

CAVET, P., AND J. PILLET. 1958. Les Trilobites des Calcaires a Polypiers siliceux (Eifélien) du synclinal de Villefranche-de-Conflent (Pyrénées-Orientales). Bulletin de la Societe Geologique de France, 8:21-37.

CHARPENTIER, R. R. 1984. Conodonts through time and space, p. 11-32. *In* D. L. Clark (ed.), Conodont Biofacies and Provincialism. Special Paper 196. The Geological Society of America, Inc., Boulder.

CHATTERTON, B.D.E., FORTEY, R., BRETT, K., GIBB, S., MCKELLAR, R. Submitted. Trilobites from the upper Lower to Middle Devonian Timrhanrhart Formation, Jbel Gara el Zguilma, southern Morocco. Palaeontographica Canadiana, 158p, 3 figs, 54 pls.

DALMAN, J.W. 1827. Om Palaeaderna eller de så kallade Trilobiterna. Kongliga Svenska Vetenskaps-Akademiens Handlingar 1828: 134-135.

ELLERMANN, I. 1992. Trilobiten aus dem Unterdevon der Karnischen Alpen/Oesterreich. Palaeontographica. Abteilung A; Palaeozoologie-Stratigraphie, 221(1-3):1-62.

FEIST, R., AND B. ORTH. 2000. Trilobites de la limite Eifélien/Givétien de la région stratotypique (Tafilalt, Maider, Maroc), p. 78-91. *In* A. Tahiri and A. El Hassani (eds.), Proceedings of the Subcommission on Devonian Stratigraphy (SDS) -- IGCP 421 Morocco Meeting. Volume 20. Travaux de L'Institut Scientifique Série Géologie & Géographie Physique, Rabat, Morocco.

FETAH, S. E. M., M. BENSAÏD, AND M. DAHMANI. 1986. Carte Géologique de Maroc: Tafilalt - Taouz. Editions du Service Géologique de Maroc, Notes et Mémoires No. 244. Royaume du Maroc. Ministère de l'Énergie et des Mines. Direction de la Géologie, Rabat.

FETAH, S. E. M., M. BENSAÏD, AND M. DAHMANI. 1988. Carte Géologique de Maroc: Todrha-Ma'der (Anti-Atlas oriental, zones axiale et périphérique Nord et Sud). Editions du Service Géologique du Maroc, Notes et Mémoires No. 243. Royaume du Maroc. Ministére de l'Énergie et des Mines, Rabat.

FORTEY, R. A., AND R. M. OWENS. 1975. Proetida -- a new order of trilobites. Fossils and Strata, 4:227-239.

GOLDFUSS. 1843. Systematische bersichte der trilobiten und beschreibung einiger neuen arten derselben. Neues Jahrbuch für Mineralogie, Geognosie, Geologie und Pegrefaktenkunde:537-567.

HECKEL, P. H., AND B. J. WITZKE. 1979. Devonian world palaeogeography determined from distribution of carbonates and related lithic palaeoclimatic indicators, p. 99-123. *In* M. R. House, C. T. Scrutton, and M. G. Bassett (eds.), The Devonian System: A Palaeontological Association International Symposium. Special Papers in Palaeontology No. 23. The Palaeontological Association, London.

HOLLARD, H. 1967. Le Dévonien de Maroc et du Sahara Nord-Occidental, p. 203-244. *In* D. H. Oswald (ed.), International Symposium on the Devonian System. Volume 1. Alberta Society of Petroleum Geologists, Calgary, Alberta.

HOLLARD, H. 1974. Recherches sur la stratigraphie des Formations du Dévonien Moyen, de l'Emsien Supérieur au Fransien, dans le Sud du Tafilalt et dans le Ma'der (Anti-Atlas oriental). Notes du Service Géologique de Maroc, 36(264):7-68.

HOLLARD, H. 1978. Corrélations entre niveaux á brachiopodes et á goniatites au voisinage de la limite Dévonien inférieur -- Dévonien moyen dans les plaines du Dra (Maroc présaharien). Newsletter of Stratigraphy, 7(1):8-25.

HOLLARD, H. 1981. Principaux caractères des formations dévoniennes de l'Anti-Atlas. Notes du Service Géologique de Maroc, 42(308):15-22.

HOLZAPFEL, E. 1895. Das obere Mitteldevon (Schichten mit *Stringocephalus burtini* and *Maeaneceras terebratum*) in Rheinischen Gebirge. Abhandlungen der Preussischen Geologischen Landesanstalt, 16:1-459.

JAÏDI, S. E. M., A. BENCHEQROUN, M. DIOURI, AND Y. ENNADIFI. 1970. Carte géologique de l'Anti-Atlas Central et de la Zone Synclinale de Ouarzazate. Feuilles Ouarzazate, Alougoum et Telouet Sud. Editions du Service Géologique du Maroc, Notes et Mémoires No. 138. Royaume du Maroc. Direction des Mines et de la Géologie, Rabat.

JAÏDI, S. E. M., M. DOUÏEB, M. DIOURI, M. SAÂDI, AND Y. ENNADIFI. 1971. Carte géologique des Plaines du Dra au sud de l'Anti-Atlas Central: Agadir Tissinnt - Oued Zemoul. Éditions de Service Géologique de Maroc, Notes et Mémoires No. 219. Royaume du Maroc. Ministère du Commerce, de l'Industrie, des Mines et de la Marine Marchande: Direction des Mines et de la Géologie division de la Géologie, Rabat.

KIELAN, Z. 1954. Les Trilobites Mésodévoniens des Monts de Sainte-Croix. Palaeontologia Polonica, 6:1-64.

KOWALSKI, V. H. 1990. Trilobiten aus dem Devon der Eifel. Der Aufschluss, 33:11-63.

LIEBERMAN, B. S. 1994. Evolution of the trilobite Subfamily Proetinae SALTER, 1864, and the origin, diversification, evolutionary affinity, and extinction of the Middle Devonian Proetid fauna of Eastern North America. Bulletin of the American Museum of Natural History, 223:1-176.

LÜTKE, F. 1977. Neue Proetidae (Trilobita) aus dem herzynischen Unter-Devon des Harzes. Senckenbergiana Lethaea, 58(1-3):99-111.

LÜTKE, F. 1980. Zur Evolution der altpaläozoischen Proetina (Trilobita). Senkenbergiana Lethaea, 61:73-144.

LÜTKE, F. 1990. Contributions to a phylogenetical classification of the subfamily Proetinae SALTER, 1864 (Trilobita). Senkenbergiana Lethaea, 71:1-83.

MADDISON, D. R., AND W. P. MADDISON. 2001. MacClade 4: Analysis of Phylogeny and Character Evolution. Version 4.06. Sinauer Associates, Sunderland, Massachusetts.

MAKSIMOVA, Z. A. 1978. Nekotoryye novyye devonskiye trilobity. Ezhegodnik Vsesoyuznogo Paleontologicheskogo Obshchestva, 21:94-106.

MAYR, E., AND P. D. ASHLOCK. 1991. Principles of Systematic Zoology. McGraw-Hill, Inc., New York, 475 p.

MORZADEC, P. 1983. Trilobites du Devonien (Emsien-Famennien) de la rade de Brest (Massif Armoricain). Palaeontographica Abt. A, 181(4-6):103-184.

MORZADEC, P. 2001. Asteropyginae trilobites from the Devonian of the Anti-Atlas (Morocco). Palaeontographica Abt. A, 262:53-85.

MULLER, K. J., AND M. BENSAID. 1969. Devonian conodonts from Morocco, p. 523-534. *In* R. Said, J. P. Beckmann, M. A. Ghorab, S. El Ansary, C. Viotti, and M. T. Kerdany (eds.), Proceedings of the Third African Micropaleontological Colloquium (Cairo, March 4-10, 1968). The National Information and Documentation Centre, Cairo.

OWENS, R. M. 1973. British Ordovician and Silurian Proetidae (Trilobita). Palaeontographical Society Monographs:1-98, 15 pls.

PILLET, J. 1972. Les Trilobites du Dévonien inférieur et du Dévonien moyen du Sud-Est du Massif armoricain. Société d'Études scientifiques de L'Anjou. Mémoire, 1:1-307.

PIQUE, A., J.-J. CORNEE, J. MULLER, AND J. ROUSSEL. 1991. The Moroccan Hercynides, p. 229-263. *In* R. D. Dallmeyer and J. P. Lécorché (eds.), The West African orogens and Circum-Atlantic correlatives. Springer-Verlag, New York.

PIQUE, A., AND A. MICHARD. 1989. Moroccan Hercynides: A synopsis. The Paleozoic sedimentary and tectonic evolution at the northern margin of West Africa. American Journal of Science, 289:286-330.

PLODOWSKI, G., G. BECKER, R. BROCKE, U. JANSEN, N. LAZREQ, E. SCHINDLER, G. SCHRAUT, O. H. WALLISER, K. WEDDIGE, AND W. ZIEGLER. 1999. The section at Jebel Issimour (NW Maïder, Early to Early Middle Devonian) First results with respect to lithology and biostratigraphy. Notes du Service Géologique de Maroc, 399:43-48.

PŘIBYL, A. 1960. Nove poznatky o stredoceskych trilobitech z nadceledi Proetacea. Rozpravy Ustredniho Ustavu Geologickeho:177-221.

RICHTER, R. 1909. Beiträge zur Paläontologie des Thuringer Waldes. Die Grauwacke des Bohlens und des Pfaffenbergs bei Saalfeld. Dresden & Leipzig, 48p, 6pls.

RICHTER, R., AND E. RICHTER. 1918. Neue Proetus-Arten aus dem Eifler Mitteldevon (Vorläntige Mitteilung). Centralblatt fuer Mineralogie, Geologie, und Palaeontologie, 3/4:64-70.

RICHTER, R., AND E. RICHTER. 1943. Studiem im Palaeozoikum der Mittelmeer-Laender; 4a, Trilobiten aus dem Devon von Marokko, mit einem Anhand über Arten des Rheinlands. Senckenbergiana, 26(1-3):116-199.

RICHTER, R., AND E. RICHTER. 1956. Annular-Teilung bei Trilobiten am Beispiel besonders von *Proetus (Pr.) cuvieri* und *prox*. Senckenbergiana Lethaea, 37(3-4):343-381.

SALTER, J. W. 1864. A Monograph of British Trilobites from the Cambrian, Silurian, and Devonian Formations. The Palaeontographical Society, London, 1-224 p.

SCHÖNE, B. R., M. BASSE, AND A. MAY. 1998. Korrelationen des Eifelium/Givetium-Grenzbereichs im Rheinischen Schiefergebirge. Senckenbergiana lethaea, 77(1/2):233-242.

SCHRANK, V. E. 1972. Proetacea, Encrinuridae und Phacopina (Trilobita) aus silurischen Geschieben. Geologie, 21(76):1-117.

SCHRAUT, G. 2000. Trilobiten aus dem Unter-Devon des südöstlichen Anti-Atlas, Süd-Marokko. Senkenbergiana Lethaea, 79(2):361-433.

SCHUH, R. T. 2000. Biological Systematics: Principles and Applications. Cornell University Press, Ithaca, 236 p.

SCOTESE, C. R. 2001. Paleogeographic Atlas, PALEOMAP Progress Report 90-0497. Department of Geology, University of Texas at Arlington, Arlington, Texas, 45 p.

ŠNAJDR, M. 1980. Bohemian Silurian and Devonian Proetidae (Trilobita). Vydal Ústrední ústav geologick'y, Praha, 324 p.

STEININGER, J. 1831. Bemerkungen über die Versteinerungen, welche in dem Übergangs-Kalkgebirge der Eifel gefunden werden. Beilage zum Gymnasial-Programmschrift zu Trier, Blattau, 46p.

STRØMER, L. 1980. Sculpture and microstructure of the exoskeleton in Chasmopinid and Phacopid trilobites. Palaeontology, 23(2):237-271.

SWINNERTON, H.H. 1915. Suggestions for a revised classification of trilobites. Geological Magazine, 52:487-496, 538-545.

SWOFFORD, D. 2002. PAUP* 4.0 Beta: Phylogenetic Analysis Using Parsimony. Sinauer Associates, Inc.

Tönebõhn, R. 1991. Bildungsbedingungen epikontinentaler Cephalopodenkalke (Devon, SE-Marokko). Göttinger Arbeiten zur Geologie und Paläontologie, 47:1-131.
Whittington, H. B., and S. R. A. Kelly. 1997. Morphological terms applied to Trilobita, p. 313-329. *In* R. C. Moore and R. L. Kaesler (eds.), Treatise on Invertebrate Paleontology, Part O, Arthropoda 1, Trilobita, Revised. Volume 1. The Geological Society of America, Inc. and The University of Kansas, Boulder, Colorado and Lawrence, Kansas.

CHAPTER 4: CONCLUSIONS

Synthesis

A number of exciting and new ideas, a new genus and thirteen new species/subspecies are the result of this thesis. Correlations among trilobites found throughout Morocco, especially in the older strata, were recognized by the similarity of species/subspecies, which also carried into Germany (*Timsaloproetus haasi* (Alberiti, 1971) and *Gerastos cuvieri cuvieri* (Steininger, 1831)) and the Czech Republic (*Gerastos tuberculatus tuberculatus* (Barrande, 1846)).

The new genus of *Timsaloproetus* was erected to recognize the distinct differences between it and *Sculptoproetus*. With the introduction of *Timsaloproetus*, Alberti's (1971) *Cornuproetus (Sculptoproetus) haasi* was designated the holotype (Mbg. 2076), and is now *Timsaloproetus haasi* (Alberti, 1971). This species was also found at Zguilma (within the Dra Valley), more specifically the ZGEE3 horizon and 'Near Zguilma', and at the bou Dib locality – '*Harpes/Thysanopeltis* horizon', and correlated to be lower Eifelian. Two other species within this genus were described, discussed and illustrated: *T. elguerrouji* and *T. dibbanus*. The former is from the ZGEE3 horizon and the latter from the lower horizon at Zguilma, referred to as ZGEE1.

The work on *Gerastos* produced many interesting results, both in the cladistic analysis and the correlation of two subspecies. The cladistic analysis produced a single tree (cladogram) for *Gerastos*, using an outgroup from the Silurian of Arctic Canada. When the type species for *Longiproetus* – *Longiproetus tenuimargo* – was introduced into the cladistic analysis, it too was placed within the *Gerastos* tree, thus confirming Owens' (1973) suggestion that *Longiproetus* is a synonym of *Gerastos* was correct.

One subspecies of *Gerastos*, *G. tuberculatus marocensis,* was found in three different regions of southern Morocco (Dra Valley at Zguilma; Ma'der region at Taharajat; and Tafilalt region at Merzouga). A closely related subspecies, *G. tuberculatus tuberculatus*, occurs in the Czech Republic. Thus this species and its subspecies demonstrates that *Gerastos* may be valuable for correlating strata of Devonian age. However, most of the new species that are described here are known at present from a single locality, and their value for correlation is in doubt. It is possible that some *Gerastos* species were so restricted in distribution (geographically or ecologically) that they have limited value for biostratigraphy.

All other specimens of *Gerastos* discussed are new species. Though an intensive literature search was done, no common species could be identified. Therefore the following new species of *Gerastos* were defined: *G. aintawilus, G. lisanrasus, G. ainrasifus, G. discombobulatus, G. taqus, G, malisjildus, G. raribus, G. emmetus* and *G. izius*.

Admittedly, the results of the cladistic analysis were not expected. The final tree suggests that cladistics can effectively demonstrate evolutionary processes involving numerous reversals and mosaic evolution.

Future Work

> "God is not dead but alive and well and working on a much less ambitious project" (Anonymous).

Throughout this thesis a number of tasks were undertaken which were often time consuming and tangential to the final product. An overly ambitious approach does, however, lead to an awareness of possibilities for future work. Much remains to be done on Moroccan proetids, and needs to be completed for the Order to be established properly. Areas requiring further study include the analysis of the remaining proetids from the Lower-Middle Devonian of Morocco, more comprehensive treatment of the micro- and macrofauna found within the horizons and correlation to formations and other horizons both in Morocco and throughout the world, and more thorough stratigraphic measurements for each locality, with detailed lithological and biological data followed up with extensive acid digestion to retrieve more microfaunal information and establish definitive correlations worldwide. The determination of the environmental setting for each locality, and if possible, each horizon, will provide a better understanding of the Lower-Middle Devonian environment of Morocco. Biogeography is a captivating area of research and it is unfortunate that more could not be undertaken within this thesis.

> Einstein's axiom: "All our science, measured against reality, is primitive and childlike -- and yet it is the most precious thing we have."

Literature Cited

ALBERTI, G. K. B. 1971. *Cornuproetus* (*Sculptoproetus*) *haasi* n. sp. (Trilobiten, Proetidae) aus dem Devon des Rheinischen Schiefergebirges. Senckenbergiana Lethaea, 52(4):371-375.

ANONYMOUS. Michael Moncur's (Cynical) Quotations. http://www.quotationspage.com/quote/54.html.

BARRANDE, J. 1846. Notice préliminaire sur le Système silurien et les trilobites de Bohême. Hirschfeld, Lipzig, 97 p.

OWENS, R. M. 1973. British Ordovician and Silurian Proetidae (Trilobita). Palaeontographical Society Monographs:1-98, 15 pls.

STEININGER, J. 1831. Bemerkungen über die Versteinerungen, welche in dem Übergangs-Kalkgebirge der Eifel gefunden werden. Beilage zum Gymnasial-Programmschrift zu Trier, Blattau, 46p.

APPENDIX 1:

Phylogenetic tree including both *Proetus morinensis* and *Longiproetus tenuimargo*.

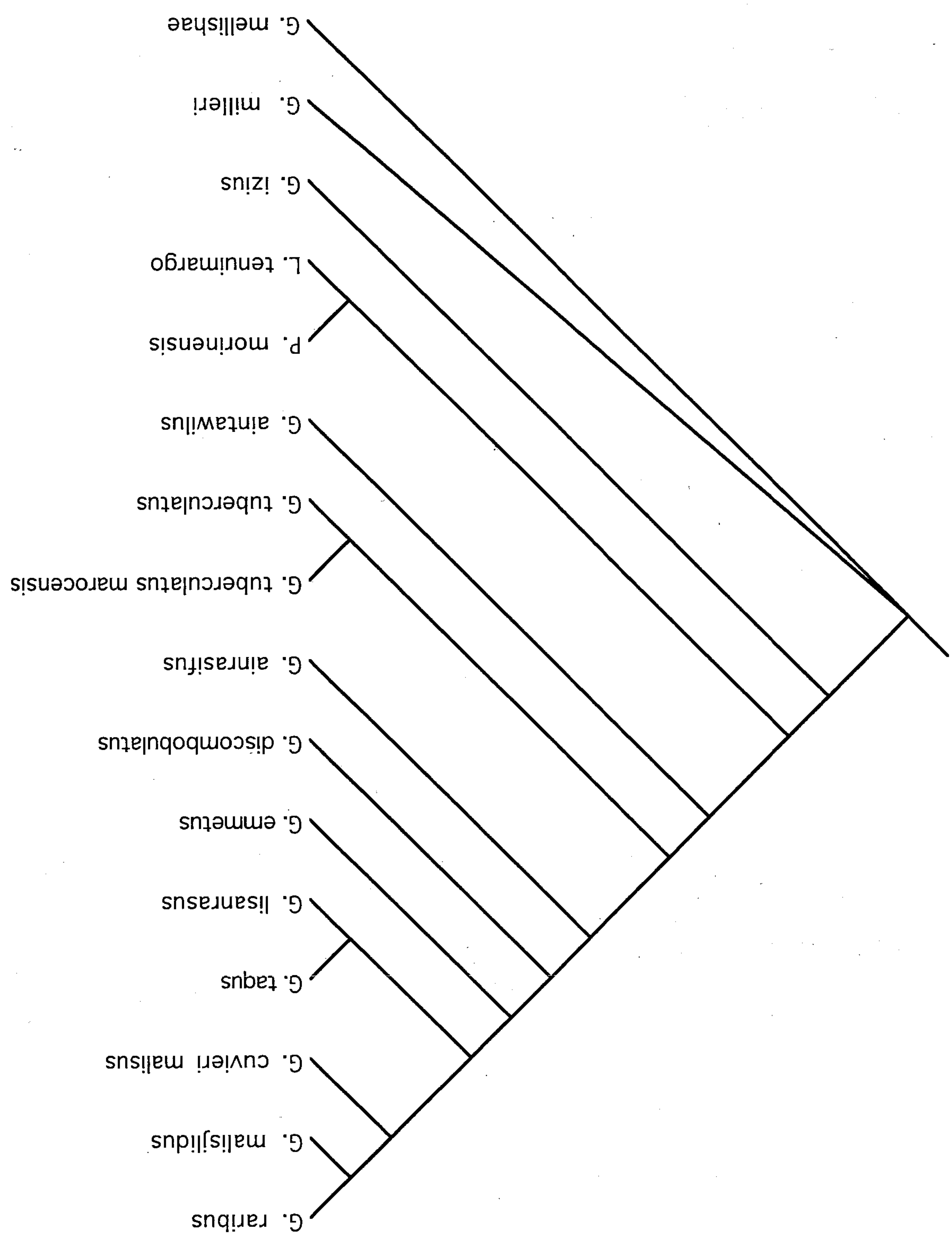
G. mellishae
G. milleri
G. izius
L. tenuimargo
P. morinensis
G. aintawilus
G. tuberculatus
G. tuberculatus marocensis
G. ainrasifus
G. discombobulatus
G. emmetus
G. lisanrasus
G. taqus
G. cuvieri malisus
G. malisjilidus
G. raribus

APPENDIX 2:

Numerical calculations and ratios for all specimens of *Gerastos*.

Specimen	Total Specimen Length (if intact) mm	A (Cephalon/ Cranidium Length) mm	A (as ratio of max length)	Thoracic Length mm	Thoracic Ratio (of max length)	Z (Pygidim Length) mm	Z (as ratio of max length)	A1 (mm)	A1 (ratio to A)	A2+A3 (mm)	A2+A3 (ratio to A)	A4 (mm)	A4 (ratio to A)	δ–δ (mm)	k (mm)	Width of Posterior aspect of Glabella	k (in ratio to δ δ)	Width of L0 (occipital ring)	L0 (in ratio to δ – δ)	L0 (in ratio to k)	L0 (in ratio to width of posterior Glabella	Thoracic Length	# Thoracic Segments	Z (Pygidium Length – mm)	X (mm)	X (in ratio with W)	Last axial segment width (mm)	% change from X to last axial segment	Y (mm)
ZG4-1	15.93	5.45	0.342122	7.09	0.4450722	3.39	0.212806	4.23	0.7761	0.95	0.174312	0.76	0.139	6.74	4.51	3.93	0.669139	4.17	0.618694	0.924612	1.0610687	7.09	10	3.39	2.72	0.382022	1.23	45.22059	2.97
ZG4-2	19.14	6.38	0.333333	8.08	0.4221526	4.63	0.241902	5.09	0.7978	0.63	0.098746	0.97	0.152	8.32	5.66	5.19	0.680288	5.07	0.609375	0.89576	0.9768786	8.08	10	4.63	3.33	0.41625	2.01	60.36036	3.65
ZG1-6	15.84	5.03	0.317551	7.45	0.4703283	3.36	0.212121	3.78	0.7515	0.39	0.077535	1.06	0.211	6.42	4.57	4.16	0.711838	4.01	0.624611	0.877462	0.9639423	7.45	10	3.36	2.75	0.403226	1.37	49.81818	2.85
Zg Lower Bed 2001 -3	20.1	6.43	0.3199	9.17	0.4562189	4.5	0.223881	5.41	0.8414	0.28	0.043546	1.21	0.188	8.66	5.6	5.19	0.646651	5.11	0.590069	0.9125	0.9845857	9.17	10	4.5	3.39	0.417488	1.77	52.21239	3.42
Zguilma 1	23.03	7.48	0.324794	10.02	0.4350847	5.53	0.240122	5.6	0.7487	0.53	0.070856	1.07	0.143	9.34	6.42	5.79	0.687366	5.54	0.593148	0.862928	0.9568221	10.02	10	5.53	3.65	0.398037	2.1	57.53425	4.37
ZGE2-1	n/a	n/a	n/a	n/a	n/a	n/a	n/a	n/a	n/a	n/a	n/a	1.18	n/a	8.94	5.91		0.661074	5.4	0.604027	0.913706	#DIV/0!	n/a	n/a	n/a	n/a	n/a	n/a	n/a	n/a
ZGE2-3	21.87	7.4	0.338363	10.49	0.4796525	4.6	0.210334	5.58	0.7541	1.4	0.189189	1.23	0.166	8.81	5.9	5.34	0.669694	5.36	0.6084	0.908475	1.0037453	10.49	10	4.6	3.52	0.386389	1.9	53.97727	3.69
Zga-1	n/a	6.33	n/a	12.61	n/a	n/a	n/a	4.35	0.6872	0.66	0.104265	1	0.158	6.84	4.67	4.05	0.682749	4.05	0.592105	0.867238	1	12.61	10	n/a	n/a	n/a	n/a	n/a	n/a
ZGH-2	22.92	7.86	0.342932	9.81	0.4280105	5.25	0.229058	6.05	0.77	1.02	0.13	1.18	0.15	9.87	6.53	6.13	0.661601	6.12	0.620061	0.937213	0.9983687	9.81	10	5.25	4.67	0.483437	1.97	42.18415	4.71
Zgl-9	14.62	4.96	0.339261	6.96	0.4760602	2.7	0.184679	3.92	0.7903	0.54	0.108871	0.73	0.147	5.32	3.62	3.27	0.680451	3.21	0.603383	0.88674	0.9816514	6.96	10	2.7	1.9	0.365385	1.09	57.36842	2.21
Zguilma 2003-1	18.84	5.15	0.273355	10.28	0.5456476	2.75	0.145966	3.58	0.6951	0.37	0.071845	0.81	0.157	5.72	3.86	3.44	0.674825	3.45	0.603147	0.893782	1.002907	10.28	10	2.75	2.03	0.377323	1.21	59.60591	2.35
Zguilma 2003-2	16.45	4.38	0.266261	9.31	0.5659574	2.76	0.167781	3.43	0.7831	0.71	0.1621	0.79	0.18	5.38	3.41	3.13	0.633829	3.1	0.576208	0.909091	0.9904153	9.31	10	2.76	1.87	0.341241	1.14	60.96257	2.22
MKP-1	24.29	7.98	0.32853	10.17	0.4186908	6.14	0.252779	5.68	0.7118	0.76	0.095238	1.65	0.207	9.6	7.01	6.21	0.730208	6.31	0.657292	0.900143	1.0161031	10.17	10	6.14	4.44	0.417686	2.61	58.78378	5.01
MKP-6	33.65	11.61	0.345022	13.71	0.4074294	8.33	0.247548	9.08	0.7821	0.66	0.056848	1.42	0.122	13.19	9.44	8.68	0.715694	8.47	0.642153	0.897246	0.9758065	13.71	10	8.33	5.71	0.415575	2.83	49.56217	6.68
MKP-7	31.97	11.91	0.372537	12.04	0.3766031	8.02	0.25086	9.57	0.8035	0.76	0.063812	1.82	0.153	12.52	9.09	8.43	0.726038	9	0.71885	0.990099	1.0676157	12.04	10	8.02	5.71	0.418622	3.12	54.64098	6.25
MKP-8	30.68	9.65	0.314537	14.2	0.4628422	6.83	0.222621	7.53	0.7803	0.84	0.087047	1.35	0.14	10.4	7.48	6.97	0.719231	6.9	0.663462	0.92246	0.989957	14.2	10	6.83	4.67	0.421861	2.42	51.82013	5.3
MKP-10	30.38	11.71	0.385451	11.18	0.3680053	7.49	0.246544	9.19	0.7848	0.96	0.081981	1.32	0.113	12.3	9.04	8.36	0.734959	8.22	0.668293	0.909292	0.9832536	11.18	10	7.49	5.32	0.422558	3.08	57.89474	6.04
MKP-11	30.51	9.99	0.327434	13.34	0.4372337	7.18	0.235333	8.04	0.8048	0.39	0.039039	1.5	0.15	11.58	8.11	7.47	0.700345	7.42	0.64076	0.91492	0.9933066	13.34	10	7.18	4.63	0.400519	2.69	58.09935	5.64
MKP-12	19.69	7.5	0.380904	7.42	0.376841	4.77	0.242255	5.9	0.7867	0.64	0.085333	1.24	0.165	8.14	5.76	5.21	0.707617	5.21	0.640049	0.904514	1	7.42	10	4.77	3.43	0.424505	2.08	60.6414	3.72
MM1-3	25.4	9.61	0.378346	9.11	0.3586614	6.68	0.262992	7.75	0.8065	0.99	0.103018	1.27	0.132	10.54	7.55	7.1	0.716319	6.92	0.656546	0.916556	0.9746479	9.11	10	6.68	4.48	0.421846	2.11	47.09821	5.21
MM1-6	30.62	11.3	0.36904	11.55	0.3772044	7.77	0.253756	9.14	0.8088	0.44	0.038938	1.62	0.143	12.45	8.95	8.28	0.718876	8.28	0.66506	0.92514	1	11.55	10	7.77	5.77	0.430276	3.18	55.11265	6.5
MM1-10	44.4	13.44	0.302703	21.54	0.4851351	9.42	0.212162	11.8	0.878	0.75	0.055804	1.73	0.129	13.48	10.3	9.06	0.761869	8.41	0.623887	0.81889	0.9282561	21.54	10	9.42	5.97	0.430425	3.49	58.45896	7.62
MM1-16	38.97	11.65	0.298948	18.95	0.4862715	8.37	0.214781	9.49	0.8146	0.84	0.072103	1.63	0.14	12.75	9.45	8.8	0.741176	8.73	0.684706	0.92381	0.9920455	18.95	10	8.37	5.59	0.38157	3.32	59.39177	6.9
MM1-17	31.04	11.75	0.378544	11.38	0.3666237	7.91	0.254832	9.41	0.8009	0.47	0.04	1.63	0.139	12.9	10	9.57	0.776744	9.35	0.724806	0.933134	0.9770115	11.38	10	7.91	6.07	0.437005	3.55	58.48435	6.78
MM1-21	29.96	10.31	0.344126	12.78	0.4265688	6.87	0.229306	8.52	0.8264	0.85	0.082444	1.54	0.149	10.8	7.87	7.51	0.728704	7.3	0.675926	0.927573	0.9720373	12.78	10	6.87	4.71	0.396465	2.46	52.2293	5.83
MOB3-9	25.92	8.43	0.325231	12.17	0.4695216	5.32	0.205247	6.23	0.739	1.2	0.142349	1.48	0.176	9.66	6.68	6.25	0.691511	6.16	0.637681	0.922156	0.9856	12.17	10	5.32	3.79	0.371205	2.03	53.56201	4.52
MOD1-2	25.23	9.91	0.392786	9.23	0.3658343	6.09	0.241379	7.35	0.7417	0.49	0.049445	1.61	0.162	10.29	7.91	7.38	0.768707	7.33	0.712342	0.926675	0.9932249	9.23	10	6.09	4.68	0.441509	2.97	63.46154	4.94
MOD1-4	26.23	9.49	0.361799	10.76	0.4102173	5.98	0.227983	7.31	0.7703	0.86	0.090622	1.64	0.173	9.58	7.19	7.03	0.750522	6.81	0.710856	0.947149	0.9687055	10.76	10	5.98	4.48	0.465696	2.6	58.03571	4.62
Mrkib 2-prong *Cyphasphis* Layer -1	19.69	6.95	0.352971	7.42	0.376841	5.32	0.270188	5.36	0.7712	0.54	0.077698	1.01	0.145	7.28	5.98	5.95	0.821429	5.14	0.706044	0.859532	0.8638655	7.42	10	5.32	3.84	0.408511	1.87	48.69792	4.41
2 prong-03-1-A	23.75	8.12	0.341895	9.23	0.3886316	6.4	0.269474	6.1	0.7512	0.46	0.05665	1.04	0.128	8.16	6.33	5.93	0.775735	6.18	0.757353	0.976303	1.0421585	9.23	10	6.4	3.54	0.332083	2.16	61.01695	4.45
2 prong-03-1-B	21.22	7.51	0.353911	7.96	0.3751178	5.75	0.270971	5.9	0.7856	0.3	0.039947	1.05	0.14	7.38	5.66	5.58	0.766938	5.69	0.771003	1.0053	1.0197133	7.96	10	5.75	3.67	0.365174	1.89	51.49864	3.98
2 prong-03-2	21.33	7.37	0.345523	8.79	0.4120956	5.17	0.242382	5.3	0.7191	0.7	0.09498	1.16	0.157	7.33	5.35	5.13	0.729877	5.14	0.701228	0.960748	1.0019493	8.79	10	5.17	3.54	0.381055	1.73	48.87006	4.23
2cc-1a		6.24						4.55	0.7292	0.8	0.128205	0.78	0.125	5.81	4.58	4.24	0.788296	4.06	0.698795	0.886463	0.9575472								
2cc-1c		2.81						1.82	0.6477	0.42	0.149466	0.38	0.135	2.32	1.77	1.54	0.762931	1.53	0.659483	0.864407	0.9935065								
2cc-4	16.59	5.9	0.355636	6.73	0.4056661	3.96	0.238698	4.41	0.7475	0.67	0.113559	0.76	0.129	5.66	4.41	4.06	0.779152	3.9	0.689046	0.884354	0.9605911	6.73	10	3.96	2.75	0.388967	1.43	52	3.43
2cc-5	n/a	7.1						5.45	0.7676	0.73	0.102817	0.86	0.121	6.83	5.4	4.89	0.79063	4.98	0.729136	0.922222	1.0184049								
Mrkib *Proetus Couche*-1	27.97	9.28	0.331784	12.11	0.4329639	6.58	0.235252	7.38	0.7953	0.64	0.068966	1.25	0.135	10.36	7.52	7.15	0.725869	7.14	0.689189	0.949468	0.9986014	12.11	10	6.58	4.74	0.425112	2.63	55.48523	5
Mrkib *Proetus Couche*-3	24.88	9.07	0.36455	9.48	0.3810289	6.33	0.254421	6.48	0.7144	0.94	0.103638	1.21	0.133	10.01	7.09	6.1	0.708292	6.47	0.646354	0.912553	1.0606557	9.48	10	6.33	4.16	0.391714	2.48	59.61538	4.96
Mrkib *Proetus Couche*-	13.25	5.78	0.436226	4.41	0.3328302	3.06	0.230943	3.97	0.6869	0.61	0.105536	0.7	0.121	5.41	3.93	3.5	0.726433	3.28	0.606285	0.834606	0.9371429	4.41	10	3.06	2.26	0.383051	1.27	56.19469	2.67
Mrkib-02 Level 2 - 6 (not necessarily pygidium for cephalon)	n/a	5.53	n/a	n/a	n/a	3.56	n/a	4.23	0.7649	0.47	0.084991	0.91	0.165	6.47	4.46	4.03	0.689335	4	0.618238	0.896861	0.9925558	n/a	n/a	3.56	2.51	0.406807	1.41	56.1753	2.85
Mrkib *Proetus Couche*-	31.82	11.52	0.362036	12.39	0.3893777	7.91	0.248586	8.36	0.7257	0.89	0.077257	1.5	0.13	12.7	9.13	8.57	0.718898	8.84	0.696063	0.968237	1.0315053	12.39	10	7.91	5.54	0.402032	3.14	56.6787	6.41
MPC-03-1	24	9.09	0.37875	9.37	0.3904167	5.54	0.230833	6.69	0.736	0.32	0.035204	1.29	0.142	8.52	6.53	5.88	0.766432	6.14	0.720657	0.940276	1.0442177	9.37	10	5.54	3.72	0.37998	1.83	49.19355	4.03
MPC-03-2	30.03	9.17	0.305361	14.2	0.4728605	6.66	0.221778	6.11	0.6663	1.01	0.110142	1.74	0.19	8.65	6.19	5.64	0.715607	6	0.693642	0.969305	1.0638298	14.2	10	6.66	3.78	0.344891	2.09	55.29101	4.96
ODC-02-2	35.86	11.31	0.315393	15.95	0.4447853	8.6	0.239822	8.89	0.786	0.8	0.070734	1.45	0.128	11.96	9.12	8.4	0.762542	8.25	0.689799	0.904605	0.9821429	15.95	10	8.6	5.97	0.534467	3.67	61.47404	6.58
ODC-02-7	not complete	9.04	n/a	n/a	n/a	n/a	n/a	6.96	0.7699	0.69	0.076327	1.18	0.131	9	6.46	6.1	0.717778	6.02	0.668889	0.931889	0.9868852	n/a	n/a	n/a	n/a	n/a	n/a	n/a	n/a
ODC-02-8	19.38	7.17	0.369969	7.91	0.4081527	4.3	0.221878	5.26	0.7336	0.59	0.082287	1.14	0.159	7.26	5.08	4.87	0.699725	4.86	0.669421	0.956693	0.9979466	7.91	10	4.3	3.21	0.433198	1.89	58.8785	3.36
Box 29-2	31.62	10.06	0.831531	14.9	0.4712207	6.66	0.210626	7.57	0.7525	0.69	0.068588	1.38	0.137	10.94	8.23	7.68	0.752285	7.53	0.6883	0.914945	0.9804688	14.9	10	6.66	5.1	0.463215	3.03	59.41176	5.16
MM2-1	21.17	8.21	0.387813	8.94	0.4222957	5.46	0.257912	6.24	0.76	0.76	0.09257	1.23	0.15	8.8	6.31	5.61	0.717045	5.6	0.636364	0.88748	0.9982175	8.94	10	5.46	3.86	0.422782	2.36	61.1399	4.57
Tt-4	29.07	10.58	0.363949	11.98	0.4121087	6.51	0.223942	7.15	0.6758	0.69	0.065217	1.82	0.172	11.96	8.36	7.89	0.698997	7.81	0.65301	0.934211	0.9898606	11.98	10	6.51	5.24	0.415543	2.51	47.90076	5.52
Tt-6	27.69	9.51	0.343445	11.74	0.4239798	6.44	0.232575	6.56	0.6898	0.9	0.094637	1.5	0.158	9.88	6.8	6.37	0.688259	6.55	0.662955	0.963235	1.0282575	11.74	10	6.44	3.95	0.36106	2.22	56.20253	4.98
Tt-7	32.26	11.23	0.348109	13.19	0.4088655	7.84	0.243025	8.56	0.7622	1.11	0.098842	1.75	0.156	13.2	8.98	8.29	0.680303	8.6	0.651515	0.957684	1.0373945	13.19	10	7.84	5.7	0.39888	2.83	49.64912	6.12
Tt-8	22.78	8.01	0.351624	8.61	0.3779631	6.16	0.270413	5.99	0.7478	0.82	0.102372	1.14	0.142	8.79	6.15	5.69	0.699659	5.64	0.641638	0.917073	0.9912127	8.61	10	6.16	3.86	0.397528	1.92	49.74093	3.94
Tt-02-10	n/a	9.38						6.38	0.6802	0.94	0.100213	1.28	0.136	10.14	6.78	6.57	0.668639												
Zireg C Layer -1	23.25	8.31	0.357419	9.77	0.4202151	5.17	0.222366	6.19	0.7449	0.65	0.078219	1.23	0.148	7.5	5.64	5.42	0.752	5.3	0.706667	0.939716	0.9778598	9.77	10	5.17	3.3	0.379747	1.99	60.30303	4.05
Zireg T Layer -1	16.92	5.99	0.354019	7.97	0.4710402	2.96	0.174941	4.49	0.7496	0.58	0.096828	0.96	0.16	6.04	4.4	4.14	0.728477	3.97	0.657285	0.902273	0.9589372	7.97	10	2.96	2.45	0.432862	1.69	68.97959	2.42
OH - 1	25.09	9.76	0.389	9.53	0.3798326	5.8	0.231168	7.29	0.7469	1.18	0.120902	1.37	0.14	10.04	6.92	6.76	0.689243	6.85	0.682271	0.989884	1.0133136	9.53	10	5.8	4.46	0.392606	2.26	50.67265	4.78
?-1 A	20.8	8.17	0.392788	7.59	0.3649038	5.04	0.242308	6.05	0.7405	0.7	0.085679	1.41	0.173	8.2	5.91	5.61	0.720732	5.25	0.640244	0.888325	0.9358289	7.59	10	5.04	3.19	0.36836	1.72	53.9185	3.88
?-1 B	22.17	7.55	0.34055	9.3	0.4194858	5.32	0.239964	6.12	0.8106	0.85	0.112583	1.1	0.146	8.47	5.85	5.45	0.690673	5.48	0.646989	0.936752	1.0055046	9.3	10	5.32	3.37	0.374444	1.86	55.19288	4
?-1 C	20.19	8.25	0.408618	7.04	0.3486875	4.9	0.242694	5.92	0.7176	0.7	0.084848	0.9	0.109	8.23	5.7	5.67	0.692588	5.55	0.674362	0.973684	0.978836	7.04	10	4.9	3.61	0.431302	1.71	47.36842	4.04
MOC2-2	26.37	10.54	0.399697	9.27	0.3515358	6.56	0.248768	8.19	0.777	1.21	0.114801	1.61	0.153	10.55	8.02	7.68	0.76019	7.3	0.691943	0.910224	0.9505208	9.27	10	6.56	4.89	0.444545	3	61.34969	6.49
KPE Upper-2	19.35	6.8	0.351421	7.16	0.3700258	5.39	0.278553	5.34	0.7853	1.02	0.15	0.99	0.146	6.91	4.44	3.92	0.642547	3.96	0.573082	0.891892	1.0102041	7.16	10	5.39	2.6	0.283533	1.57	60.38462	4.13
KPE Upper-1	18.37	6.57	0.357648	7.01	0.3816004	4.79	0.260751	4.89	0.7443	1.03	0.156773	0.94	0.143	6.53	4.44	4	0.679939	3.91	0.598775	0.880631	0.9775	7.01	10	4.79	2.74	0.295896	1.78	64.9635	3.79
Tab-1	20.14	7.14	0.354518	8.17	0.4056604	4.83	0.239821	5.87	0.8221	0.61	0.085434	1.09	0.153	7.77	5.38	5.13	0.692407	5.09	0.655084	0.946097	0.9922027	8.17	10	4.83	3.52	0.44898	1.93	54.82955	4.37
MKD-1 (actually TAB)	n/a	7.22						5.55	0.7687	1.14	0.157895	0.87	0.12	8.52	6.3	5.32	0.739437	5.78	0.678404	0.91746	1.0864662								
MKD-2	20.94	7.89	0.376791	7.01	0.334766	6.04	0.288443	5.85	0.7414	0.91	0.115336	1.22	0.155	8.31	6.3	5.87	0.758123	5.85	0.703971	0.928571	0.9965928	7.01	10	6.04	3.89	0.385149	2.27	58.35476	4.53
BD5-30	12.31	4.52	0.367181	5.06	0.4110479	2.73	0.221771	3.43	0.7588	0.54	0.119469	0.51	0.113	4.68	3.34	2.76	0.713675	2.69	0.574786	0.805389	0.9746377	5.06	10	2.73	1.71	0.392202	1.05	61.40351	1.98
MRZP-1	13.06	5.11	0.391271	5.15	0.3943338	2.8	0.214395	3.91	0.7652	0.74	0.144814	0.49	0.096	5.11	3.44	3.07	0.67319	3.07	0.600783	0.892442	1	5.15	10	2.8	1.93	0.378431	1.23	63.73057	2.18

Numerical calculations and ratios for all specimens of *Gerastos*.

Y (in ratio with Z)	W (mm)	W (in ratio with δ–δ)	# Axial Segments in Pygidium	Glabella (length [A1]:width [k])	Genal Field (from eye [adjacent to δ] to lateral border) (mm)	Ratio of Genal Field to δ	Length of Eye (mm)	Length of Eye: Length of Glabella (A1)	δ–δ:A ratio (δ δ/A) [Campbell 1967 in description]	Pygidial Width/Length Ratio (from Campbell 1967)	Width (tr.) of 1st thoracic segment axial region (mm)	Width (tr.) of last thoracic segment axial region (mm)	% Taper of Axial region of Thorax	Pygidial Length/ Width Ratio	Specimen
0.876106	7.12	1.05638	7+1	0.9379157	0.73	0.108309	2.17	0.513002	1.236697248	2.100294985	3.8	2.8	73.68421	0.476124	ZG4-1
0.788337	8	0.961538	7+1	0.8992933	n/a	n/a	2.84	0.557957	1.304075235	1.727861771	4.55	3.5	76.92308	0.57875	ZG4-2
0.848214	6.82	1.062305	7+1	0.8271335	0.61	0.095016	2.25	0.595238	1.276341948	2.029761905	3.8	2.88	75.78947	0.492669	ZG1-6
0.76	8.12	0.937644	7+1	0.9660714	0.52	0.060046	2.67	0.49353	1.34681182	1.804444444	4.63	3.61	77.96976	0.554187	Zg Lower Bed 2001 -3
0.790235	9.17	0.981799	7+1	0.8722741	1.07	0.114561	2.98	0.532143	1.248663102	1.658227848	5.09	4.09	80.35363	0.603053	Zguilma 1
n/a	n/a	n/a	n/a	n/a		0		#VALUE!					#DIV/0!		ZGE2-1
0.802174	9.11	1.034052	7+1	0.9457627	0.71	0.08059	2.69	0.482079	1.190540541	1.980434783	5.06	3.73	73.71542	0.50494	ZGE2-3
n/a	n/a	n/a	n/a	0.9314775	0.62	0.090643	2.11	0.485057	1.08056872		n/a	n/a	n/a		Zga-1
0.897143	9.66	0.978723	7+1	0.9264931	1.16	0.117528	2.98	0.492562	1.255725191	1.84	5.46	4.27	78.20513	0.543478	ZGH-2
0.818519	5.2	0.977444	7+1	1.0828729	n/a	n/a	n/a	n/a	1.072580645	1.925925926	2.94	2.45	83.33333	0.519231	Zgl-9
0.854545	5.38	0.940559	7+1	0.9274611	0.52	0.090909	2.16	0.603352	1.110679612	1.956363636	3.27	2.39	73.08869	0.511152	Zguilma 2003-1
0.804348	5.48	1.018587	7+1	1.0058651	0.3	0.055762	1.86	0.542274	1.228310502	1.985507246	2.87	2.04	71.08014	0.50365	Zguilma 2003-2
0.815961	10.63	1.107292	7+1	0.810271	1.23	0.128125	3.01	0.52993	1.203007519	1.731270358	5.63	4.68	83.12611	0.577611	MKP-1
0.801921	13.74	1.041698	7+1	0.9618644	2.1	0.159212	3.94	0.433921	1.136089578	1.649459784	7.96	6.02	75.62814	0.606259	MKP-6
0.779302	13.64	1.089457	7+1	1.0528053		0		0	1.051217464	1.70074813			#DIV/0!	0.587977	MKP-7
0.775988	11.07	1.064423	7+1	1.0066845	1.35	0.129808	3.49	0.463479	1.077720207	1.62079063	6.1	4.98	81.63934	0.616983	MKP-8
0.806409	12.59	1.023577	7+1	1.0165929	1.85	0.150407	3.46	0.376496	1.050384287	1.680907877	7.49	5.73	76.502	0.594917	MKP-10
0.785515	11.56	0.998273	7+1	0.9913687	1.62	0.139896	3.23	0.401741	1.159159159	1.610027855	6.63	5.15	77.67722	0.621107	MKP-11
0.779874	8.08	0.992629	7+1	1.0243056	1.15	0.141278	2.67	0.452542	1.085333333	1.693920335	4.66	3.59	77.03863	0.590347	MKP-12
0.77994	10.62	1.00759	7+1	1.0264901	1.48	0.140417	3.33	0.429677	1.096774194	1.589820359	6.19	4.75	76.73667	0.629002	MM1-3
0.836551	13.41	1.077108	7+1	1.0212291	1.35	0.108434	3.53	0.386214	1.101769912	1.725868726	7.6	5.82	76.57895	0.579418	MM1-6
0.808917	13.87	1.028932	7+1	1.1489776	2.23	0.16543	4.03	0.341525	1.00297619	1.472399151	7.78	6.22	79.94859	0.679164	MM1-10
0.824373	14.65	1.14902	7+1	1.0042328	1.7	0.133333	3.69	0.38883	1.094420601	1.750298686	7.64	6.04	79.05759	0.571331	MM1-16
0.857143	13.89	1.076744	7+1	0.9391218	1.77	0.137209	3.76	0.399575	1.09787234	1.756005057	8.33	6.55	78.63145	0.569474	MM1-17
0.848617	11.88	1.1	7+1	1.0825921	1.74	0.161111	3.43	0.402582	1.047526673	1.729257642	6.56	5.18	78.96341	0.578283	MM1-21
0.849624	10.21	1.056936	7+1	0.9326347	0.94	0.097308	2.99	0.479936	1.145907473	1.919172932	5.57	4.18	75.04488	0.521058	MOB3-9
0.811166	10.6	1.030126	7+1	0.9292035		0		0	1.038345106	1.740558292				0.574528	MOD1-2
0.772575	9.62	1.004175	7+1	1.0166898	0.89	0.092902	3.34	0.456908	1.009483667	1.608695652	6.2	4.77	76.93548	0.621622	MOD1-4
0.828947	9.4	1.291209	7+1	0.8963211	1.25	0.171703	2.97	0.554104	1.047482014	1.766917293	4.92	3.92	79.6748	0.565957	Mrkib 2-prong *Cyphasphis* Layer -1
0.695313	10.66	1.306373	damaged	0.9636651	1.47	0.180147	3.24	0.531148	1.004926108	1.665625	5.55	4.37	78.73874	0.600375	2 prong-03-1-A
0.692174	10.05	1.361789	7+1	1.0424028	1.19	0.161247	3.11	0.527119	0.982689747	1.747826087	5.4	3.96	73.33333	0.572139	2 prong-03-1-B
0.818182	9.29	1.267394	7+1	0.9906542	1.04	0.141883	3.27	0.616981	0.994572592	1.796905222	5.11	3.8	74.36399	0.556512	2 prong-03-2
				0.9934498	1.16	0.199656	2.54	0.558242	0.931089744						2cc-1a
				1.0282486											2cc-1c
0.866162	7.07	1.249117	7+1	1	1.33	0.234982	2.45	0.555556	0.959322034	1.785353535	3.67	2.96	80.65395	0.560113	2cc-4
				1.0092593	1.12	0.163982	2.69	0.493578	0.961971831						2cc-5
0.759878	11.15	1.076255	7+1	0.981383	1.35	0.130309	3.1	0.420054	1.11637931	1.694528875	6.39	4.96	77.62128	0.590135	Mrkib *Proetus Couche*-1
0.78357	10.62	1.060939	7+1	0.9139633	1.1	0.10989	3.09	0.476852	1.103638368	1.677725118	5	3.76	75.2	0.596045	Mrkib *Proetus Couche*-3
0.872549	5.9	1.090573	7+1	1.0101781	0.41	0.075786	2.14	0.539043	0.935986159	1.928104575	2.95	2.43	82.37288	0.518644	Mrkib *Proetus Couche*-5
0.800562	6.17	0.953632	7+1	0.9484305	0.61	0.094281	2.44	0.576832	1.169981917	1.733146067	3.51	n/a	n/a	0.576985	Mrkib-02 Level 2 - 6 (not necessarily pygidium for cephalon)
0.810367	13.78	1.085039	7+1	0.9156627	1.59	0.125197	3.82	0.456938	1.102430556	1.742098609	7.77	6.02	77.47748	0.57402	Mrkib *Proetus Couche*-7
0.727437	9.79	1.149061	7+1	1.0245023	1.08	0.126761	2.78	0.415546	0.937293729	1.767148014	5.9	4.48	75.9322	0.565884	MPC-03-1
0.744745	10.96	1.267052	7+1	0.9870759	0.73	0.084393	3.08	0.504092	0.943293348	1.645645646	5.76	4.43	76.90972	0.607664	MPC-03-2
0.765116	11.17	0.933946	7+1	0.9747807		0		0	1.057471264	1.298837209			n/a	0.769919	ODC-02-2
n/a	n/a	n/a	n/a	1.0773994	0.78	0.086667	3.06	0.439655	0.995575221	n/a	5.44	n/a	n/a		ODC-02-7
0.781395	7.41	1.020661	7+1	1.0354331	0.48	0.066116	2.72	0.51711	1.012552301	1.723255814	4.31	3.36	77.95824	0.580297	ODC-02-8
0.774775	11.01	1.006399	7+1	0.9198056	1.25	0.11426	3.36	0.443857	1.087475149	1.653153153	7.02	5.45	77.63533	0.604905	Box 29-2
0.836996	9.13	1.0375	7+1	0.9889065	1.18	0.134091	2.95	0.472756	1.071863581	1.672161172	5.09	4.18	82.12181	0.598028	MM2-1
0.847926	12.61	1.054348	7+1	0.8552632	1.48	0.123746	3.21	0.448951	1.130434783	1.937019969	7.34	5.6	76.29428	0.516257	Tt-4
0.773292	10.94	1.107287	7+1	0.9647059	1.27	0.128543	2.9	0.442073	1.038906414	1.698757764	6.41	4.65	72.5429	0.588665	Tt-6
0.780612	14.29	1.082576	7+1	0.9532294	1.97	0.149242	3.63	0.424065	1.175422974	1.822704082	7.97	6.35	79.67378	0.548635	Tt-7
0.63961	9.71	1.104664	7+1	0.9739837	0.81	0.09215	2.84	0.474124	1.097378277	1.576298701	5.09	3.89	76.42436	0.634398	Tt-8
				0.9410029	0.92	0.09073	3.18	0.498433	1.081023454		n/a	n/a	n/a		Tt-02-10
0.783366	8.69	1.158667	7+1	1.0975177	0.89	0.118667	2.55	0.411955	0.902527076	1.680851064	4.58	3.49	76.20087	0.594937	Zireg C Layer -1
0.817568	5.66	0.937086	7+1	1.0204545	0.39	0.06457	2.33	0.518931	1.008347245	1.912162162	3.58	2.7	75.41899	0.522968	Zireg T Layer -1
0.824138	11.36	1.131474	7+1	1.0534682	1	0.099602	3.35	0.459534	1.028688525	1.95862069	6.13	4.76	77.6509	0.510563	OH - 1
0.769841	8.66	1.056098	7+1	1.0236887	0.84	0.102439	2.58	0.426446	1.003671971	1.718253968	4.99	3.49	69.93988	0.581986	?-1 A
0.75188	9	1.062574	7+1	1.0461538	0.8	0.094451	2.78	0.454248	1.121854305	1.691729323	5.14	3.82	74.31907	0.591111	?-1 B
0.82449	8.37	1.017011	7+1	1.0385965	0.59	0.071689	2.59	0.4375	0.997575758	1.708163265	5.19	3.99	76.87861	0.585424	?-1 C
0.989329	11	1.042654	7+1	1.021197	1.27	0.120379	3.36	0.410256	1.000948767	1.676829268	6.74	5.01	74.33234	0.596364	MOC2-2
0.766234	9.17	1.327062	8+1	1.2027027	n/a	n/a	n/a	n/a	1.016176471	1.701298701	3.55	2.82	79.43662	0.587786	KPE Upper-2
0.791232	9.26	1.41807	8+1	1.1013514	1.7	0.260337	2.53	0.517382	0.99391172	1.933194154	3.69	3.05	82.65583	0.517279	KPE Upper-1
0.904762	7.84	1.009009	7+1	1.0910781	0.66	0.084942	2.93	0.499148	1.088235294	1.623188406	4.61	3.68	79.82646	0.616071	Tab-1
				0.8809524	0.96	0.112676	2.75	0.495495	1.180055402						MKD-1 (actually TAB)
0.75	10.1	1.215403	7+1	0.9285714	1.47	0.176895	2.96	0.505983	1.053231939	1.67218543	5.52	4.09	74.0942	0.59802	MKD-2
0.725275	4.36	0.931624	7+1	1.0269461	0.67	0.143162	1.84	0.536443	1.03539823	1.597069597	2.51	1.88	74.9004	0.626147	BD5-30
0.778571	5.1	0.998043	7+1	1.1366279	0.63	0.123288	1.92	0.491049	1	1.821428571	2.73	2.14	78.38828	0.54902	MRZP-1

Numerical calculations and ratios for all specimens of *Gerastos*.

APPENDIX 3:

MacClade 4.06 (Maddison and Maddison, 2001) derived data matrix for *Gerastos*.

	1	2	3	4	5	6	7	8	9	10	11	12	13	14	15	16	17	18	19	20	21
G. tuberculatus marocensis	1	0	1	0	0	1	0	1	0	0	0	0	0	1	1	1	1	1	0	1	0
G. aintawilus	1	0	1	0	1	1	1	1	1	2	0	0	0	1	1	1	1	1	0	1	0
G. lisanrasus	1	1	1	2	1	1	0	1	1	3	1	0	0	1	1	1	0	2	0	1	1
G. ainrasifus	0	0	1	0	0	1	0	1	0	2	0	0	0	1	1	1	0	0	0	1	1
G. discombobulatus	1	1	1	2	0	1	0	2	0	1	0	0	0	1	1	1	0	1	0	1	1
G. cuvieri malisus	2	0	0	2	0	1	0	0	1	3	?	0	1	1	1	1	0	0	1	1	1
G. taqus	1	0	1	2	1	1	0	2	1	3	3	0	1	1	1	?	0	?	0	1	1
G. malisjildus	1	0	0	2	0	0	1	0	1	3	3	0	1	1	0	3	0	0	?	1	1
G. raribus	2	1	0	2	1	0	1	2	1	2	2	1	1	1	1	0	0	0	0	1	0
G. emmetus	0	0	1	2	0	1	0	2	1	2	0	0	1	0	1	1	1	2	1	1	2
G. izius	0	0	1	1	1	1	1	1	2	1	0	0	1	0	0	0	1	1	0	1	2
G. tuberculatus	1	0	1	0	0	1	0	1	0	0	0	0	0	1	?	1	1	1	1	1	0
G. mellishae	1	0	0	0	1	1	1	1	0	2	1	1	1	1	2	2	?	?	1	0	2
G. milleri	0	0	0	0	1	1	1	1	0	0	1	0	1	1	2	?	?	?	1	0	2

MacClade 4.06 (Maddison and Maddison, 2001) derived data matrix for *Gerastos*